University of São Paulo
"Luiz de Queiroz" College of Agriculture

Crop modeling for understanding yield-gap causes and the potential for sustainable intensification of soybean in Brazil

Evandro Henrique Figueiredo Moura da Silva

Thesis presented to obtain the degree of Doctor in Science.
Area: Agricultural Systems Engineering

Piracicaba
2022

Evandro Henrique Figueiredo Moura da Silva
Agronomist

Crop modeling for understanding yield-gap causes and the potential for sustainable intensification of soybean in Brazil

versão revisada de acordo com a resolução CoPGr 6018 de 2011

Advisor
Prof. Dr. **FÁBIO RICARDO MARIN**

Thesis presented to obtain the degree of Doctor in Science.
Area: Agricultural Systems Engineering

Piracicaba
2022

Dados Internacionais de Catalogação na Publicação
DIVISÃO DE BIBLIOTECA – DIBD/ESALQ/USP

Silva, Evandro Henrique Figueiredo Moura da

Crop modeling for understanding yield-gap causes and the potential for sustainable intensification of soybean in Brazil / Evandro Henrique Figueiredo Moura da Silva. - -versão revisada de acordo com a resolução CoPGr 6018 de 2011. - - Piracicaba, 2022.

194 p.

Tese (Doutorado) - - USP / Escola Superior de Agricultura “Luiz de Queiroz”.

1. *Glycine max* L. 2. Fertilização nitrogenada 3. Uso da água 4. Produtividade potencial 5. Lacuna de produtividade 6. Modelagem agrícola I. Título

ACKNOWLEDGMENTS

The successful completion of this work would not have been possible without the support of many people over the years that I have been thinking, researching, and writing. I would first like to thank my adviser, Dr. Fábio Ricardo Marin, for everything you have done to make this thesis happen. Working with Fábio opened the door to an exceptional network of researchers and has provided me with invaluable experience. He helped me navigate my first rocky steps in crop modeling and has always been an incredible adviser to me. Thank you for your enormous guidance, support, and encouragement that played an essential role in this research; you took me on as a graduate student and from there helped shape my ideas with very enthusiasm into this thesis. I am eternally grateful for his mentorship.

I am extremely thankful to Dr. Kenneth Boote and Dr. Gerrit Hoogenboom of the University of Florida for teaching me and providing me the opportunity to learn from you both how to be a meticulous researcher. Additionally, I am also thankful to them for always taking some time out of their busy schedule to read my manuscripts and hold meetings to discuss my scientific progress during my time in Gainesville, as well as, after my return to Piracicaba.

I am thankful for all funding of Coordination for the Improvement of Higher Education Personnel (CAPES)- Ministry of Education of Brazil (MEC) through the Ph.D. scholarship (3 months) and São Paulo Research Foundation (FAPESP) through the Ph.D. scholarship and technical reserve [Process 2017/23468-9 (33 months)] and intern scholarship and technical reserve [Process 2019/18303-6 (12 months)] at University of Florida. I am also so thankful to the Department of Biosystems Engineering from Luiz de Queiroz College of Agriculture, University of São Paulo (LEB/ESALQ/USP) for all its excellent infrastructure provided over the years.

I wish to express appreciation to: (i) Dr. Aderson Soares Andrade Junior, Dr. Henrique Antunes de Souza, and whole team of Brazilian Agricultural Research Corporation (EMBRAPA) Mid-North for conducted experiments in Teresina/PI; (ii) Dr. Alencar Junior Zanon and whole team of Field Crops from Federal University of Santa Maria (UFSM) for conducted experiments in Cruz Alta/RS and Tupanciretã/RS; (iii) Dr. Kassio dos Santos Carvalho and whole team of Federal Institute of Mato Grosso for conducted experiments in Sorriso/MT; (iv) Dr. Patricio Grassini, Dr. Juan Ignacio Rattalino Edreira, Dr. Nicolas Cafaro La Menza from University of Nebraska–Lincoln, Dr. José Francisco Andrade from University of Buenos Aires, and Juan Pablo Monzon from Universidad Nacional de Mar del Plata for all

comments during Global Yield Gap Atlas (GYGA) meetings; (v) Dr. Edson Lazarini (FEIS/UNESP), Dr. Felipe Gustavo Pilau (ESALQ/USP), and Dr. Rafael Battisti (EA/UFG) for all suggestions in my PhD' qualification exam; (vi) Ana Carolina Melo (GAPE/ESALQ/USP) for the help in fertilization protocol, (vii) MSc Welinton Yoshio Hirai the help in statistics analysis, (viii) Ricardo Cunha, Lagoa Bonita Sementes Company, for soybean seeds donation; (ix) Leonardo Gorgen, Yara International Company, for fertilizer donation; (x) Daniel Medeiros, BASF Company, for fungicides, insecticides, and herbicides donation; (xi) Mariana Coleti and Levy Lobato, Irrigabras Irrigação do Brasil Company, for all the technical assistance for maintenance of the central pivot at ESALQ/USP.

My sincere appreciation also extends to Angela Márcia Derigi Silva, Agnaldo Ferraz Degaspari, Áureo Santana de Oliveira, Beatriz Regina Duarte Novaes, Davilmar Aparecida Domingues Collevatti, Edivaldo Modesto de Abreu, Erreinaldo Donizeti Bortolazzo, Fernanda Barbosa Neves da Silva, Francisco Bernardo Dias, Francisco de Oliveira, Gilmar Batista Grigolon, José Geraldo Gomes, Juarez Renó do Amaral, Lino Stênico, Luis Custódio Camargo, Luis Fernando Sanglade Marchiori, Luiz Fernando Novello, and Rodrigo Fray da Silva from ESALQ for their help in bureaucracies and field experiments conduction during various stages of the project.

My huge thanks to the whole GEPEMA/AGRIMET team, especially to the soybeans Field Coordinators: Raul Murigi Regiani, Vitor Cavalcante Botter, Izael Martins Fattori Júnior, Lucas Barbato Sallum, Vivian Ribeiro Blasig for help me in the soybean experiments in Piracicaba. Also, thank you Stephanie do Carmo for helping me in the scientific partnerships; and for undergraduate students Maria Carolina Melo Sciencia, Álex Júnior Zanchet Bordignon, Stefany Quilles Fava, Juliana Vogelaar Girardi, Giulia Vitória Simioni Dias, Leonardo Medici Ceregato, Rudy Gomes Pereira de Godoi, Renan Baraldi de Moraes, and Luiza Mucci de Oliveira for participating in scientific meetings.

I also would like to thank graduate colleges Dr. Alexandre Ortega Gonçalves, MSc. Juliano Mantellatto Rosa, MSc. Letícia Gonçalves Gasparotto, MSc. Luís Alberto Silva Antolin, Dr. Luiz Ricardo Sobenko, Dr. Murilo dos Santos Vianna, MSc. Nilson Aparecido Vieira Júnior, and MSc. Rodolfo Armando de Almeida Pereira for providing enormous support throughout the whole process of graduate school.

Finally, I cannot fully express gratitude toward my loving wife, Stefany Amanda Quilles Fava, I thank you for being my forever family, and for adding untold depth and richness to my life. Mom and Dad, Sonia Maria Figueiredo Moura da Silva and José Antônio Moura da Silva, I am so thankful to you both who helped me build a foundation that has withstood the

winds of life. To my brother and sister, Ewerton Luiz Figueiredo Moura da Silva and Giulia Carolina Figueiredo Moura da Silva, thank you for your empathy and encouragement. I also thank my niece, Olivia Figueiredo Moura Sena, for her joy and energy.

TABLE OF CONTENTS

RESUMO

O uso da modelagem agrícola para o entendimento das causas da lacuna de produtividade e quantificação do potencial de intensificação sustentável da soja no Brasil

As projeções de demanda de alimentos apontam para a necessidade de aumento substancial na oferta de soja (*Glycine max* L.). A soja é a principal fonte de proteína alimentar, e o Brasil corresponde a 37% (com base na safra 2020/2021) da produção mundial; sendo o maior produtor e exportador da cultura. A produção brasileira de soja é distribuída em ambientes tropicais (60%) e subtropicais (40%). Espera-se que a intensificação agrícola propicie aumentos substanciais na produção de alimentos nas áreas produtivas já existentes, com os menores custos ambientais globais possíveis. Esta tese de doutorado estimou a produtividade potencial da soja em ambientes tropicais e subtropicais associados ao manejo de água e nitrogênio (N), usando análise de dados de campo e modelagem agrícola. No Capítulo 1, uma estrutura conceitual foi desenvolvida para compreender os fatores de produtividade potencial da cultura para os sistemas de cultivo de soja no Brasil. Prospectou-se os fatores hídricos no Capítulo 2, usando dados de campo e modelagem agrícola para avaliar o balanço hídrico do solo, métodos de evapotranspiração e evaporação da água do solo e produtividade da água. Cenários de longo prazo foram simulados para determinar o impacto do manejo sustentável da água, sob diferentes regimes de irrigação, textura do solo e práticas de cultivo no desenvolvimento da soja. O Capítulo 3 focou nos efeitos da fertilização nitrogenada no crescimento da soja, produtividade de grão e concentração de proteína e óleo usando doses de nitrogênio (N) em condições de escassez e com pleno suprimento hídrico, em treze experimentos conduzidos em importantes regiões produtoras do Brasil. Também foi explorado cenários de longo prazo para avaliar o manejo de N na soja. As principais descobertas nos Capítulos 2 e 3 foram: (i) o modelo CROPGRO-Soybean foi uma ferramenta útil para analisar o manejo da água e do N na soja em ambientes tropicais e subtropicais; (ii) o método de evapotranspiração de FAO- 56 Penman-Monteith (PM) combinado com o método de Ritchie de evaporação da água do solo em dois estágios forneceram simulações mais acuradas; e (iii) a fertilização com N proporcionou aumentos substanciais na concentração de proteína da semente, apesar de ter apresentado resposta marginal ou nula em relação a produtividade. No Capítulo 4 estimou-se a produtividade potencial limitada por água ($Y_{P\text{-}W}$) e a produtividade potencial (Y_P) usando a calibração de cultivares e as configurações do modelo obtidas nos Capítulos 2 e 3; definindo-se dezesseis zonas agroclimáticas (CZs) estrategicamente selecionadas para representar a produção brasileira de soja. Também se estimou a lacuna de produtividade (Y_G), eficiência climática (E_C) e eficiência agrícola (E_A) para todos os CZs. Quantificou-se um $Y_{P\text{-}W}$ médio de 4.684 kg ha^{-1}, Y_P de 5.441 kg ha^{-1}, Y_G de 3.092 kg ha^{-1}, E_C de 78% e E_A de 50%. Em 26% da área de soja no Brasil a E_C < 95%, para esta área, melhorias na distribuição da densidade do comprimento da raiz e práticas de plantio direto podem contribuir para a redução média de 20% no consumo de água irrigada. Esta tese destacou a importância de melhorar o manejo agrícola da soja em condições tropicais e subtropicais para atender à segurança alimentar com sustentabilidade ambiental.

Palavras-chave: *Glycine max* L., Fertilização nitrogenada, Uso agrícola da água, Produtividade potencial, Lacuna de produtividade, Modelagem agrícola

ABSTRACT

Crop modeling for understanding yield-gap causes and the potential for sustainable intensification of soybean in Brazil

In the next decades, the population is expected to rise by more than two billion people, and food demand projections point to the need to substantially increase soybean (*Glycine max* L.) supply for food, livestock feed, and biofuel. Soybean is the most important food protein source, and Brazil accounts for 37% (based on the 2020/2021 harvest) of the world's soybean. The country is the largest soybean producer and exporter, with 60% and 40% of its soybean production is in tropical and subtropical environments. It is expected that the intensification of agricultural management will allow substantial increases in food production on existing agricultural lands, with lowest possible global environmental costs. This Ph.D. thesis explored the estimating of soybean potential yield under tropical and subtropical environments associated with agricultural water and nitrogen (N) management using field data analysis and crop modeling. In Chapter 1, we developed the conceptual framework for understanding the crop yield potential factors for soybean cropping systems in Brazil. We prospected water factors on Chapter 2, using field data and crop modeling to evaluate the soil water balance, evapotranspiration and soil water evaporation methods and crop water productivity. We also examined long-term scenarios to determine the impact of sustainable crop water management under different irrigation regimes, soil texture, and tillage practices on soybean growth and development. Chapter 3 focused on the effects of N-fertilization on soybean growth, crop yield, and protein and oil concentration using several doses of N under limited and non-limiting water conditions across thirteen soybean experiments in major soybean Brazilian producing regions. We also explored long-term scenarios to evaluate N management on soybean. The major findings in Chapters 2 and 3 were: (i) CROPGRO-Soybean model is a useful tool to analyze water and N management on soybean under tropical and subtropical environments; (ii) FAO-56 Penman-Monteith evapotranspiration combined with Ritchie-Two-Stage soil water evaporation methods provided more accurate simulations; and (iii) N-fertilization provided substantially increases on seed protein concentration, despite that showed marginal or no response on soybean crop yield. Chapter 4 estimated the water-limited crop yield potential (Y_{P-W}) and crop yield potential (Y_P) using the cultivar calibration and model settings obtained in Chapter 2 and 3, and defined sixteen strategically selected agroclimatic zones (CZs) to represent Brazilian production. We also estimated the crop yield gap (Y_G), climate efficiency (E_C), and agricultural efficiency (E_A) for all CZs. We quantify an average Y_{P-W} of 4,684 kg ha^{-1}, Y_P of 5,441 kg ha^{-1}, Y_G of 3,092 kg ha^{-1}, E_C of 78%, and E_A of 50%. We also identified that 26% of soybean area in Brazil with E_C < 95%, for this area improvements on root length density distribution with no-tillage practices can contribute to irrigated water savings by 20%. This Ph.D. thesis highlighted the importance of improving agricultural management across the soybean sowed in tropical and subtropical conditions to meet food security with environmental sustainability.

Keywords: *Glycine max* L., N-fertilization, Water use, Crop yield potential, Yield gap, Crop modeling

LIST OF FIGURES

LIST OF TABLES

1. CONCEPTUAL FRAMEWORK FOR UNDERSTANDING THE YIELD POTENTIAL FACTORS FOR SOYBEAN CROPPING SYSTEMS UNDER TROPICAL AND SUBTROPICAL CONDITIONS

Ensuring global food security constitutes one of the main challenges for future decades, mainly due to the projected population increase to 9.7 billion by 2050 and the rise of the middle class (Godfray *et al*., 2010; Mueller *et al*., 2012; Pradhan *et al*., 2015, United Nations, 2019). In order to attain food security, the agricultural sector will need to play a strategic role (Tscharntke *et al*., 2012; Tschirley *et al*., 2015). Soybean [*Glycine max* (L.) Merr.] production is a key component of global food security as a main dietary source of protein for humans and feed for livestock, as well as oil for cooking (Smárason *et al*., 2019; Wajid *et al*., 2020; Parisi *et al*., 2020). Soybean is the most important legume globally, with a harvested area of 123 million ha and total production of 337 million Mg in 2020 (USDA, 2020), accounting for 53% of the total global oilseed production (Beta and Isaak, 2016). Brazil is the largest soybean producer in the world, with over 38.5 million hectares of soybean production area (USDA, 2021) in tropical and subtropical environments.

With a view to responding to the increased demand for food, many scientists point to sustainable intensification of agriculture as a prominent need, which, in the broadest sense, would increase agricultural production and economic returns without negative impacts on soil and water resources or on the integrity of ecosystems and biodiversity (Tilman *et al*., 2011; Godfray and Garnett., 2014; Pretty *et al*., 2018; Kropp *et al*., 2019; Cassman and Grassini, 2020). In this context, the concept of crop yield potential (Y_P) has been used in the literature to estimate the maximum yield of a crop cultivar grown in the environment. It is determined by solar radiation and temperature, *i.e*., water and nutrients are non-limiting, and biotic stresses are effectively controlled. The water-limited crop yield potential ($Y_{P\text{-}W}$) is the Y_P estimated considering water deficit as a limiting factor, and the climate efficiency (E_C) is the ratio between $Y_{P\text{-}W}$ and Y_P (Evans, 1999; van Ittersum and Rabbinge, 1997; Passioura, 2006; Passioura and Angus, 2010; van Ittersum *et al*., 2013). Knowledge regarding crop yield potential is very useful for investigating production levels and for determining the magnitude yield gap (Y_G) and agricultural efficiency (E_A) in a wide range of environments. The Y_G is the difference between Y_P and actual crop yields (Y_A), *i.e*., crop yields achieved by farmers (Lobell *et al*., 2009; Edreira *et al*., 2017), and E_A is the ratio between Y_A and $Y_{P\text{-}W}$, considering that major soybean fields are cultivated under rainfed conditions in Brazil. Thus, estimates of Y_G can contribute to

sustainable agricultural intensification (i) to estimate the potential of sustainably exploitable land, (ii) to elucidate opportunities for increasing crop yield, (iii) to compute water productivity and nitrogen (N)-use efficiency, and (iv) to identify and correct inappropriate management that generates crop yield losses.

This Ph.D. thesis sought to investigate the Y_P of soybean under tropical and subtropical conditions, focusing on water and N factors. Tropical and subtropical environments are subject to frequent dry spells, which are supposedly the main factor limiting crop yield (Battisti *et al*., 2016; Multsch *et al*., 2020). This occurs because most tropical rainfall is characterized by irregularity and high intensity, while crop water needs are generally large due to high temperatures and intense solar radiation (Nieuwolt, 1989). Furthermore, the process of sustainable intensification of agriculture often raises the debate on N-fertilization of soybean, with the focus on increasing yield in already highly productive environments (*e.g*., Ray *et al*., 2006; Salvagiotti *et al*., 2009; Cafaro La Menza *et al*., 2017; Zhou *et al*., 2019; Cafaro La Menza *et al*., 2020) or the use of N-fertilization combined with higher N-fixing bacteria doses to increase the soybean yield in unfavorable environments (Cordeiro and Echer, 2019). In previous studies on soybean N-fertilization, the focuses were (i) N-increase in protein grain concentration (Nakasathien *et al*., 2000); (ii) N supply interaction with different atmospheric carbon dioxide concentrations [CO_2] (Sims *et al*., 1998); and (iii) increasing the crop yield (Sinclair and Wit, 1976; Hayati and Crafts-Brandner, 1995; Barker and Sawyer, 2005; Ray *et al*., 2006). Despite the considerable number of studies on N-fertilization of soybean, the results are not yet conclusive and sometimes contradictory; and a little is known about the effects of N-fertilization on soybean under tropical and subtropical environments. Thus, improvements in water management and better understanding of N use on soybeans can be useful in Y_G estimates under tropical and subtropical conditions.

For Y_P or $Y_{P\text{-}W}$ estimates, dynamic crop simulation models have great relevance because they can quantify the impact of weather and crop management on plant growth and development. The physiological processes incorporated into models include photosynthesis, transpiration, respiration, organ development, and transport assimilation (Boote and Pickering, 1994; Kim and Hsiao, 2020), making these models an excellent support tool for research and decision making (*e.g*., Soler *et al*., 2007; Popp, *et al*., 2016). Also, models can support systematic analysis, discussion, and presentation of the interaction between crops with weather, soil, irrigation management (Boote *et al*. 1998; Jones *et al*., 2003), water-limited production (Araya *et al*., 2017; Wu *et al*., 2019; Soltani *et al*., 2020), crop water productivity (Timsina *et al*., 2008; Edreira *et al*., 2018; Er-Raki *et al*., 2020), crop residue management (Andales *et al*.,

2000; Corbeels *et al*., 2016; Liben *et al*., 2020), and nitrogen fertilization (Negm *et al*., 2017; Prasad *et al*., 2018).

The Cropping System Model (CSM) CROPGRO-Soybean (Boote *et al*., 1998) is a robust and widely used soybean process-based crop model that is part of the Decision Support System for Agrotechnology Transfer (DSSAT; www.DSSAT.net) (Jones *et al*., 2003; Hoogenboom *et al*., 2019a, Hoogenboom *et al*., 2019b). The model simulates soybean growth, aboveground biomass, and the timing of phenological events and ultimately predicts the final yield across a wide range of environments and for different management scenarios. This model was used in this study because it achieved results with greater accuracy when compared to field data and other crop models (Battisti *et al*., 2017; Kothari *et al*., 2021).

In this research, we hypothesized that there is a yield gap in the current management system adopted by soybean farmers in Brazil. Thus, given the importance of tropical and subtropical soybean to world food security, we used field experiments and crop modeling simulations to explore the roles of water and nitrogen as limiting factors for soybean yield. The research questions behind our study are (i) what are the soybean Y_P, $Y_{P\text{-}W}$, and Y_G in tropical and subtropical environments? and (ii) to what extent can such crop yield be maximized by improving water and nitrogen management?

1.1. Research goals

The main goal of the present research was to estimate the yield potential and yield gap for soybean in tropical and subtropical environments in Brazil. To summarize, the main objectives of the present research were (i) to conduct well-managed soybean experiments to achieve the yield potential (Chapters 2 and 3); (ii) to determine the effects of the different evapotranspiration approaches for improving irrigation management in soybean (Chapter 2); (iii) to calibrate and evaluate the CROPGRO-Soybean using a data set from field experiments (Chapters 2 and 3); (iv) to elevate our understanding regarding soybean growth and development, evapotranspiration demand, soil water balance, water management, conservation tillage, and crop water productivity, using CROPGRO-Soybean as a tool (Chapter 2); (v) to evaluate the soybean response to N-fertilization in experiments conducted under tropical and subtropical conditions (Chapter 3); (vi) to augment our understanding regarding soybean growth and development, soil and plant N balance, and N-fertilization using CROPGRO-Soybean as a tool (Chapter 3); and (vii) to simulate the Y_P, $Y_{P\text{-}W}$, E_C, E_A, and Y_G for soybean

under tropical and subtropical conditions (Chapter 4). Finally, Chapter 5 summarizes the main findings of this research.

References

Andales, A. A., Batchelor, W. D., Anderson, C. E., Farnham, D. E., Whigham, D. K., 2000. Incorporating tillage effects into a soybean model. Agricultural Systems, 66 (2), 69–98.

Araya, A., Kisekka, I., Gowda, P. H., Prasad, P. V. V., 2017. Evaluation of water-limited cropping systems in a semi-arid climate using DSSAT-CSM. Agricultural Systems, 150, 86–98.

Boote, K. J., Pickering, N. B., 1994. Modeling photosynthesis of row crop canopies. HortScience, 29(12), 1423-1434.

Boote, K. J., Jones, J. W., Hoogenboom, G., Pickering, N. B., 1998. The CROPGRO model for grain legumes. In: p. 99-128 [G. Y. Tsuji, G. Hoogenboom, and P. K. Thornton (Eds.)], Understanding options for agricultural production. Kluwer Academic Publishers, London, United Kingdom.

Barker, D. W., Sawyer, J. E., 2005. Nitrogen application to soybean at early reproductive development. Agronomy Journal, 97(2), 615-619.

Battisti, R., 2016. Calibration, uncertainties and use of soybean crop simulation models for evaluating strategies to mitigate the effects of climate change in Southern Brazil (Doctoral dissertation, Universidade de São Paulo).

Battisti, R., Sentelhas, P. C., 2017. Improvement of soybean resilience to drought through deep root system in Brazil. Agronomy Journal, 109(4), 1612-1622.

Beta, T., Isaak, C., 2016. Grain production and consumption: Overview. In: p. 349-428 [C. Wrigley, H. Corke, K. Seetharaman, J. Faubion (Eds.)], Encyclopedia of Food Grains – the World of Food Grains, V.1, Elsevier, Oxford, United Kingdom.

Cafaro La Menza, N., Monzon, J. P., Specht, J. E., Grassini, P., 2017. Is soybean yield limited by nitrogen supply?. Field Crops Research, v. 213, p. 204-212.

Cafaro La Menza, N., Monzon, J. P., Lindquist, J. L., Arkebauer, T. J., Knops, J. M., Unkovich, M., Specht, J.E., Grassini, P., 2020. Insufficient nitrogen supply from symbiotic fixation reduces seasonal crop growth and nitrogen mobilization to seed in highly productive soybean crops. Plant, Cell & Environment, 43(8), 1958-1972.

Cassman, K. G., Grassini, P., 2020. A global perspective on sustainable intensification research. Nature Sustainability, 3(4), 262-268.

Corbeels, M., Chirat, G., Messad, S., Thierfelder, C., 2016. Performance and sensitivity of the DSSAT crop growth model in simulating maize yield under conservation agriculture. European Journal of Agronomy, 76, 41-53.

Cordeiro, C. F.S., Echer, F. R., 2019. Interactive effects of nitrogen-fixing bacteria inoculation and nitrogen fertilization on soybean yield in unfavorable edaphoclimatic environments. Scientific Reports, 9(1), 1-11.

Edreira, J. I. R., Guilpart, N., Sadras, V., Cassman, K. G., van Ittersum, M. K., Schils, R. L., Grassini, P., 2018. Water productivity of rainfed maize and wheat: a local to global perspective. Agricultural and Forest Meteorology, 259, 364-373.

Edreira, J. I. R., Mourtzinis, S., Conley, S. P., Roth, A. C., Ciampitti, I. A., Licht, M. A., Kandel, H., Kyveryga, P.M., Lindsey, L.E., Muller, D.S., Naeve, S.L., Nafziger, E., Specht, J.E., Stanley, J., Staton, M., Grassini, P., 2017. Assessing causes of yield gaps in agricultural areas with diversity in climate and soils. Agricultural and forest meteorology, 247, 170-180.

Evans, L.T., Fischer, R.A., 1999. Yield potential: its definition, measurement, and significance. Crop Sci. 39:1544–1551.

Er-Raki, S., Bouras, E., Rodriguez, J. C., Watts, C. J., Lizarraga-Celaya, C., Chehbouni, A., 2020. Parameterization of the AquaCrop model for simulating table grapes growth and water productivity in an arid region of Mexico. Agricultural Water Management, 106585.

Godfray, H. C. J., Beddington, J. R., Crute, I. R., Haddad, L., Lawrence, D., Muir, J. F., Pretty, J., Robinson, S., Thomas, S.M., Toulmin, C., 2010. Food security: the challenge of feeding 9 billion people. Science, 327(5967), 812-818.

Godfray, H.C.J, Garnett T., 2014 Food security and sustainable intensification. Philosophical Transactions of the Royal Society B. 369: 20120273.

Hayati, R., Egli, D. B., Crafts-Brandner, S. J., 1995. Carbon and nitrogen supply during seed filling and leaf senescence in soybean. Crop science, 35(4), 1063-1069.

Hoogenboom, G., Porter, C.H., Boote, K.J., Shelia, V., Wilkens, P.W., Singh, U., White, J.W., Asseng, S., Lizaso, J.I., Moreno, L.P., Pavan, W., Ogoshi, R., Hunt, L.A., Tsuji, G.Y., Jones, J.W., 2019a. The DSSAT crop modeling ecosystem. In: p.173-216 [K.J. Boote, (Eds.)] Advances in Crop Modeling for a Sustainable Agriculture. Burleigh Dodds Science Publishing, Cambridge, United Kingdom.

Hoogenboom, G., Porter, C.H., Shelia, V., Boote, K.J., Singh, U., White, J.W., Hunt, L.A., R. Ogoshi, J.I. Lizaso, J. Koo, S. Asseng, A. Singels, L.P. Moreno, Jones, J.W., 2019b. Decision Support System for Agrotechnology Transfer (DSSAT) Version 4.7 (www.DSSAT.net). DSSAT Foundation, Gainesville, Florida, USA.

Jones, J. W., Hoogenboom, G., Porter, C. H., Boote, K. J., Batchelor, W. D., Hunt, L. A., Wilkens, P.W., Singh, U., Gijsman, A.J., Ritchie, J. T., 2003. The DSSAT cropping system model. European Journal of Agronomy, 18(3), 235–265.

Kothari, K., Battisti, R., Boote, K., Archontoulis, S., Confalone, A., Constantin, J., Cuadra, S. V., Debaeke, P., Faye, B., Grant, B., Hoogenboom, G., Jing, Q., van der Laan, M., Macena, F. A., Marin, F. R., Nehbandani, A., Nendel, C., Purcell, L. C., Qian, B., Ruane, A. C., Silva, E. H. F. M., Smith, W., Soltani, A., Srivastava, A., Vieira Jr., N. A., Slone, S., Salmerón, M., 2021. Are soybean models ready for climate change food impact assessments?. European Journal of Agronomy (under review).

Kim, J., Schultz HK, S., 2020. Advances and improvements in modeling plant processes. In Advances in crop modelling for a sustainable agriculture (pp. 3–43). Dublin: Burleigh Dodds Science.

Kropp, I., Nejadhashemi, A. P., Deb, K., Abouali, M., Roy, P. C., Adhikari, U., Hoogenboom, G., 2019. A multi-objective approach to water and nutrient efficiency for sustainable agricultural intensification. Agricultural Systems, 173, 289-302.

Liben, F. M., Wortmann, C. S., Tirfessa, A., 2020. Geospatial modeling of conservation tillage and nitrogen timing effects on yield and soil properties. Agricultural Systems, 177, 102720.

Lobell, D. B., Cassman, K. G., Field, C. B., 2009. Crop yield gaps: their importance, magnitudes, and causes. Annual review of environment and resources, 34, 179-204.

Mueller, N. D., Gerber, J. S., Johnston, M., Ray, D. K., Ramankutty, N., Foley, J. A., 2012. Closing yield gaps through nutrient and water management. Nature, 490(7419), 254-257.

Multsch, S., Krol, M. S., Pahlow, M., Assunção, A. L. C., Barretto, A. G. O. P., de Jong van Lier, Q., Breuer, L., 2020. Assessment of potential implications of agricultural irrigation policy on surface water scarcity in Brazil. Hydrol. Earth Syst. Sci., 24(1), 307-324.

Nakasathien, S., Israel, D. W., Wilson, R. F., Kwanyuen, P., 2000. Regulation of seed protein concentration in soybean by supra-optimal nitrogen supply. Crop Science, 40(5), 1277-1284.

Negm, L. M., Youssef, M. A., Jaynes, D. B., 2017. Evaluation of DRAINMOD-DSSAT simulated effects of controlled drainage on crop yield, water balance, and water quality for a corn-soybean cropping system in central Iowa. Agricultural Water Management, 187, 57-68.

Nieuwolt, S., 1989. Estimating the agricultural risks of tropical rainfall. Agricultural and Forest Meteorology, 45(3–4), 251–263.

Parisi, G., Tulli, F., Fortina, R., Marino, R., Bani, P., Dalle Zotte, A., Angelis, A., Piccolo, G., Pinotti, L., Schiavone, A., Terova, G., Prandini, A., Gasco, L., Roncarati, A., Danieli, P. P., 2020. Protein hunger of the feed sector: the alternatives offered by the plant world. Italian Journal of Animal Science, 19(1), 1204-1225.

Passioura, J., 2006. Increasing crop productivity when water is scarce—from breeding to field management. Agricultural Water Management, 80(1-3), 176-196.

Passioura, J., Angus, J.F., 2010. Improving productivity of crops in water-limited environments. In: p. 37-75 [D.L. Sparks (Ed.)], Advances in Agronomy. Elsevier, Oxford, United Kingdom.

Popp, M., Purcell, L., Salmerón, M., 2016. Decision support software for soybean growers: Analyzing maturity group and planting date tradeoffs for the US midsouth. Crop, Forage & Turfgrass Management, 2(1), 1-9.

Pradhan, P., Fischer, G., van Velthuizen, H., Reusser, D. E., Kropp, J. P., 2015. Closing yield gaps: How sustainable can we be?. Plos One, 10(6), e0129487.

Prasad, L. R. V., Mailapalli, D. R., 2018. Evaluation of nitrogen fertilization patterns using DSSAT for enhancing grain yield and nitrogen use efficiency in rice. Communications in Soil Science and Plant Analysis, 49(12), 1401-1417.

Pretty, J., Benton, T. G., Bharucha, Z. P., Dicks, L. V., Flora, C. B., Godfray, H. C. J., Goulson, D., Hartley, S., Lampkin, N., Morris, C., Pierzynski, G., Prasad, P.V.V., Reganold, J.R., Smith, P., Thorne, P., Wratten, S., 2018. Global assessment of agricultural system redesign for sustainable intensification. Nature Sustainability, 1(8), 441-446.

Ray, J. D., Heatherly, L. G., Fritschi, F. B., 2006. Influence of large amounts of nitrogen on nonirrigated and irrigated soybean. Crop Science, 46(1), 52-60.

Salvagiotti, F., Specht, J. E., Cassman, K. G., Walters, D. T., Weiss, A., Dobermann, A., 2009. Growth and nitrogen fixation in high-yielding soybean: Impact of nitrogen fertilization. Agronomy Journal, 101(4), 958-970.

Sims, D. A., Luo, Y., Seemann, J. R., 1998. Comparison of photosynthetic acclimation to elevated CO_2 and limited nitrogen supply in soybean. Plant, Cell & Environment, 21(9), 945-952.

Sinclair, T. R., De Wit, C. T., 1976. Analysis of the carbon and nitrogen limitations to soybean yield 1. Agronomy Journal, 68(2), 319-324.

Soltani, A., Alimagham, S. M., Nehbandani, A., Torabi, B., Zeinali, E., Dadrasi, A., Zand, E., Ghassemi, S., Pourshirazi, S., Alasti, O., Hosseini, R.S., Zahed, M., Arabameri, R., Mohammadzadeh, Z., Rahban, S., Kamari, H., Fayazi, S., Mohammadi, S., Keramat, S., Vadez, V., van Ittersum, M.K., Sinclair, T.R., 2020. SSM-iCrop2: A simple model for diverse crop species over large areas. Agricultural Systems, 182, 102855.

Smárason, B. Ö., Alriksson, B., Jóhannsson, R., 2019. Safe and sustainable protein sources from the forest industry–The case of fish feed. Trends in Food Science & Technology, 84, 12–14.

Soler, C. M. T., Sentelhas, P. C., Hoogenboom, G., 2007. Application of the CSM-CERES-Maize model for planting date evaluation and yield forecasting for maize grown off-season in a subtropical environment. European Journal of Agronomy, 27(2-4), 165-177.

Tilman, D., Balzer, C., Hill, J., Befort, B. L., 2011. Global food demand and the sustainable intensification of agriculture. Proceedings of the National Academy of Sciences, 108(50), 20260-20264.

Timsina, J., Godwin, D., Humphreys, E., Kukal, S. S., Smith, D., 2008. Evaluation of options for increasing yield and water productivity of wheat in Punjab, India using the DSSAT-CERES-Wheat model. Agricultural Water Management, 95(9), 1099–1110.

Tscharntke, T., Clough, Y., Wanger, T. C., Jackson, L., Motzke, I., Perfecto, I., Vandermeer, J., Whitbread, A., 2012. Global food security, biodiversity conservation and the future of agricultural intensification. Biological Conservation, 151(1), 53-59.

Tschirley, D., Reardon, T., Dolislager, M., Snyder, J., 2015. The rise of a middle class in East and Southern Africa: Implications for food system transformation. Journal of International Development, 27(5), 628-646

United Nations, 2019. Growing at a slower pace, world population is expected to reach 9.7 billion in 2050 and could peak at nearly 11 billion around 2100. UN Department of Economic and Social Affairs, New York, USA.

USDA., 2021. Foreign Agricultural Service. April 2021 Oilseeds and Products Annual report, U.S. Department of Agriculture, Washington, DC, USA.

Van Ittersum, M.K., Rabbinge, R., 1997. Concepts in production ecology for analysis and quantification of agricultural input-output combinations. Field Crops Res. 52,197-208.

Van Ittersum, M. K., Cassman, K. G., Grassini, P., Wolf, J., Tittonell, P., Hochman, Z., 2013. Yield gap analysis with local to global relevance—a review. Field Crops Research, 143, 4-17.

Wajid, A. L. I., Ahmad, M. M., İftakhar, F., Qureshi, M., Ceyhan, A., 2020. Nutritive potentials of Soybean and its significance for humans' health and animal production: A Review. Eurasian Journal of Food Science and Technology, 4(1), 41-53.

Wu, R., Lawes, R., Oliver, Y., Fletcher, A., Chen, C., 2019. How well do we need to estimate plant-available water capacity to simulate water-limited yield potential? Agricultural Water Management, 212, 441-447.

Zhou, H., Yao, X., Zhao, Q., Zhang, W., Zhang, B., Xie, F., 2019. Rapid effect of nitrogen supply for soybean at the beginning flowering stage on biomass and sucrose metabolism. Scientific Reports, 9(1), 1-13.

2. PERFORMANCE OF THE CSM-CROPGRO-SOYBEAN IN SIMULATING SOYBEAN GROWTH AND DEVELOPMENT, EVAPOTRANSPIRATION, SOIL WATER BALANCE AND CROP WATER PRODUCTIVITY UNDER TROPICAL AND SUBTROPICAL ENVIRONMENTS[1]

Abstract

Crop water management is a key-factor for reaching sustainable cropping systems. The main goal of this chapter was to use the Cropping System Model (CSM) CROPGRO-Soybean model, in conjunction with field data, to determine the impact of different irrigation regimes, soil texture, and tillage practices on soybean growth, development, and crop yield in tropical and subtropical conditions. The model was evaluated for simulating soil water content (SWC), evapotranspiration (ET) and crop water productivity. Field experiments were conducted at: (i) Piracicaba with conventional tillage, and no-tillage practices, under full water requirements conditions; and (ii) Teresina under conventional tillage under full and 50% of water requirements conditions. In both sites, the SWC was measured for all experiments using an electromagnetic probe installed at several depths. The results showed that the model was able to simulate soybean growth and development for both sites, with good agreement (D > 0.8). In addition, the SWC was simulated with satisfactory accuracy (D > 0.5). For experiments conducted in Piracicaba, we evaluate CROPGRO-Soybean using either the Priestley–Taylor (PT) or FAO-56 Penman–Monteith (PM) methods for potential ET combined with either the Ritchie-Two-Stage (R-2) or Suleiman–Ritchie (S-R) soil water evaporation methods. These ET simulations were confronted with measured data obtained by the Bowen Ratio Energy Balance method. The model provided excellent predictions of daily (D > 0.7) and cumulative evapotranspiration (RMSE ranged from 8 to 64 mm). PM with R-2 methods provided the best fit when compared with measured data. Simulations of long-term scenarios showed that the use of no-tillage could reduce the average amount of irrigation in Piracicaba by 30% and in Teresina by 17%.

Keywords: Tillage practices; Irrigated agriculture; Drought stress; Soil moisture; DSSAT

2.1. Introduction

Water scarcity is the most limiting abiotic stress in agricultural systems. Evaluating the soil-crop water balance is a proven approach for understanding drought stress effects during

[1] Part of this chapter previously published as:

(i) Silva, E. H. F. M., Boote, K. J., Hoogenboom, G., Gonçalves, A. O., Junior, A. S. A., Marin, F. R., 2021. Performance of the CSM-CROPGRO-soybean in simulating soybean growth and development and the soil water balance for a tropical environment. Agricultural Water Management, 252, 106929;

(ii) Silva, E. H. F. M., Hoogenboom, G., Boote, K. J., Gonçalves, A. O., Marin, F. R., 2021. Predicting soybean evapotranspiration and crop water productivity for a tropical environment using the CSM-CROPGRO-Soybean model. Agricultural and Forest Meteorology (under review).

the growing season (Brisson *et al*., 1992; Ritchie, 1998; Candogan *et al*., 2013; Zhou and Zhi Zhao, 2019). Cropping System Models (CSM) are useful tools for simulating the soil water balance, plant growth, and development, for quantifying crop yield, and for exploring alternate options for water management (Tsuiji *et al*., 1998; Alagarswamy *et al*., 2000; Sau *et al*., 2004; Soldevilla-Martinez *et al*., 2014; Battisti and Sentelhas, 2017). The soil water balance can estimate the amount of water available for root uptake along with water loss quantification (evaporation and drainage), which are important to design effective management strategies for soil water conservation (Hoogenboom *et al*., 1991; Heinemann *et al*., 2000, Nijbroek *et al*., 2003).

Evapotranspiration (ET) is a critical component of soil water balance and for irrigation management, because ET determines the amount of water to be applied (Zeleke and Wade, 2012). In this sense, crop water consumption mensuration can be obtained by the product of the reference evapotranspiration (ETo) and the crop coefficient (Kc), resulting in estimated crop evapotranspiration (ETc) (Allen *et al*., 1998). This approach has been universally adopted for scheduling and quantifying the water amount to be applied to the crops and has been supported by long-term data.

Still, evapotranspiration is an essential process for the estimation of crop water productivity (CWP) and it is, therefore, very important for efficient water management of cropping systems. Accurate crop evapotranspiration estimates could help improve water use efficiency (Jassal *et al*., 2009; Hussain *et al*., 2019; Qubaja *et al*., 2020), sustainable crop intensification (Rosa *et al*., 2017; Bhatt et.al, 2019), and irrigation efficiency (Qiu *et al*., 2008; Valentín *et al*., 2020). However, simulations of crop evapotranspiration should be tested against a robust set of experimental data. We are unaware of any published study that has evaluated CROPGRO-Soybean simulations of evapotranspiration with observed data using the Bowen Ratio Energy Balance (BREB) method (Bowen, 1926) under subtropical conditions.

To simulate ETo the CROPGRO-Soybean has two methods: Priestley-Taylor (PT) (Priestley and Taylor, 1972) and FAO-56 Penman-Monteith (PM) model (Allen *et al*., 1998). The model computes the ETc as the product of the ETo and the crop coefficient, resulting in estimated crop evapotranspiration (Allen *et al*., 1998). DSSAT uses an asymptotic function of daily leaf area index (LAI) with a crop energy-extinction coefficient (Kep) (Sau *et al*., 2004, Boote *et al*., 2008a); and partitions reference evapotranspiration separately to soil water evaporation and crop transpiration as described by Boote *et al*. (2008b).

The soil water evaporation can be calculated by two methods for CROPGRO-Soybean: Ritchie Two-Stage (R-2) (Ritchie, 1972) and Suleiman–Ritchie (S-R) (Suleiman and Ritchie,

2003; Suleiman and Ritchie, 2004; Richie *et al*., 2009). The R-2 method is calculated in two stages: (i) constant rate stage during which soil is sufficiently wet for the water to be transported to the surface, in this stage the soil water evaporation is limited only by supply of energy to the soil surface; and (ii) falling rate stage, the soil water content (SWC) on surface has decreased below a threshold value; during this stage the soil water evaporation is controlled by unsaturated soil hydraulic properties (Ritchie, 1972). In the R-2 method, soil water is only lost from the top 0.05 m of the soil profile (Boote *et al*., 2008b). The S-R method assumes there is no clear distinction between those stages of soil water evaporation (Ritchie *et al*., 2009), as S-R simulates the soil water redistribution from deeper to shallower soil layers to contribute to soil water evaporation (energy demand) considering all soil layers based on the diffusivity theory for the simulation of soil water dynamics (Ritchie *et al*., 2009).

Furthermore, the soil water movement is simulated by CROPGRO-Soybean using a tipping bucket (Ritchie, 1998) and the United States Department of Agriculture (USDA) SCS curve number approach (Williams, 1991) to represent soil water redistribution, infiltration, and runoff. The time step for soil water balance is daily, and the model considers root water uptake from each individual soil horizon or layer (homogeneous horizontally), and drainage of water through the profile and below the root zone (Boote *et al*., 2008b). The functional soil water balance model used in CROPGRO-Soybean requires inputs for soil water holding characteristics: (i) permanent wilting point or lower limit of plant extractable soil water (LL), (ii) field capacity or drained upper limit (DUL), and (iii) field saturation or saturated soil water content (SAT) (Ritchie, 1998). The soil water holding traits can be estimated using the SBUILD tool available in the DSSAT software (Hoogenboom *et al*., 2019), based on soil texture, bulk density, and organic carbon content data, as well as soil surface and general soil profile characteristics. However, few studies were carried out aiming to evaluate the soil water balance and associated crop growth and development with the CROPGRO-Soybean model with experimental data from tropical and subtropical environments.

In this chapter, we conducted field experiments and explored this robust data set in conjunction with model simulations during soybean seasons under tropical and subtropical conditions. Thus, we sought to achieve a better understanding of the processes controlling the evapotranspiration and soil water content and to explore sustainable alternatives for long-term water management to increase soybean crop yield.

2.1.1. Research goals

The main goal of this chapter was to elevate understanding regarding soybean growth and development, evapotranspiration demand, soil water balance, water management, conservation tillage, and crop water productivity using CROPGRO-Soybean as a tool.

To summarize, the main objectives of the present chapter are: (i) to calibrate CROPGRO-Soybean model; (ii) to evaluate the performance of the model for simulating soybean growth and development; (iii) to evaluate the performance of the model to simulate soil water content; (iv) to evaluate the performance of the model for simulating daily and cumulative evapotranspiration and crop water productivity using two different evapotranspiration methods each paired with two different soil water evaporation methods for irrigated soybean under subtropical conditions, and (v) to apply hypothetical scenarios using different water management and conservation tillage options for tropical and subtropical environments.

2.2. Materials and Methods

2.2.1. Description of field experiments

We conducted irrigated experiments in Piracicaba (22°43′S, 47°38′W, 524 m a.s.l), SP, Cwa (high-altitude tropical climate) (Koeppen, 1948) during two crop seasons: (i) 2016/2017 season (PI_1-100), and (ii) 2017/2018 (PI_2-100); and in Teresina (05°05′S, 42°48′W, 74 m a.s.l), PI, Aw (tropical savanna climate) (Koeppen, 1948), during 2019 season. Daily weather data for Piracicaba were obtained from the Luiz de Queiroz College of Agriculture (ESALQ) on-site automatic weather station, University of São Paulo (http://www.leb.esalq.usp.br/posto/) (Appendix A), and for Teresina were obtained from the Teresina-A312 on-site automatic weather station managed by *Instituto Nacional de Meteorologia* (INMET) (http://www.inmet.gov.br/portal/index.php?r=estacoes/estacoes Automaticas) (Appendix B). For both automatic weather stations, the following daily variables were measured: (i) total solar radiation (MJ m^{-2} day^{-1}); (ii) maximum and minimum air temperatures (ºC); (iii) rainfall (mm); (iv) dewpoint temperature (ºC); (v) wind speed (m s^{-1}).

Soil was classified as Eutric Rhodic Ferralic Nitisol and experiments were conducted under conventional tillage for PI_1-100, with subsoiling and grid leveling operations, and no-tillage practices for PI_2-100 sown in wheat crop residue (4,000 kg ha^{-1}), with cultivar BRS399,

a maturity group (MG) 6.0, under full water requirements in Piracicaba (Table 2.1). For Teresina, the trial was sowed on a Dystrophic Red Yellow Acrisol soil under conventional tillage, with subsoiling (0.45 m deep) and grid leveling operations, and two irrigation treatments: 50% (TE-50) of full water requirements and full (TE-100), with cultivar 8579RSF (MG 8.0) (Table 2.1).

Table 2.1 Description of field experiments conducted in Piracicaba (PI_1-100 and PI_2-100) and Teresina (TE-50 and TE-100), Brazil.

Exp.	Crop season	Effective irrigation (mm)	Tillage practices	Sowing date	Sowing density (plants m^{-2})
PI_1-100	2016/2017	177.6	Conventional tillage	Nov 14	35.5
PI_2-100	2017/2018	242.4	No-tillage	Dec 16	35.5
TE-50	2019	271.6	Conventional tillage	Jul 26	22.0
TE-100	2019	418.3	Conventional tillage	Jul 26	22.0

The seeds were inoculated with *Bradyrhizobium elkanii* (strains SEMIA 587 and SEMIA 5019) at a concentration of $5x10^9$ CFU mL^{-1} (colony forming units). Pesticides management was performed with the goal of minimizing potential damage due to pests and diseases, maintaining the crop under weekly monitoring for pests and diseases to evaluate the effectiveness of pest control (Appendix C). We considered the crop phenological stages (Fehr and Caviness, 1977) and soil analysis (Appendix D) for performing the fertilization management (Appendix E).

The Piracicaba experiments were irrigated by center pivot sprinklers Senninger Model i-Wob-UP3, while at Teresina a sprinkler line-source technique, using sprinklers Fabrimar Model A232. The irrigation amounts were scheduled by potential evapotranspiration (ETo) determined, for both sites, with the Priestley-Taylor (PT) method (Priestley and Taylor, 1972) based on solar radiation and air temperature variables measured with sensors properly calibrated and checked weather data daily at the on-site weather station. The PT method was applied under minimum advection conditions, using empirical parameter α=1.26 (Pereira and Villa Nova, 1992). The PT method showed close performance when compared to the Penman-Monteith method for Piracicaba (Vila Nova and Pereira, 2006) and Teresina (Andrade Junior *et al.*, 2018). Subsequently the crop evapotranspiration was computed by multiplying ETo by the crop coefficient (Kc) as described in FAO-56 (Allen, 1998). The triggering irrigation when 80% water available remained in the top 0.2 m of the soil profile.

Field observations and measurements for each experiment included daily phenology observations with recorded dates of emergence: (i) beginning flowering (R1), (ii) beginning pod (R3), (iii) beginning seed (R5), and (iv) physiological maturity (R7), when 50% of the plants were at each stage (Fehr and Caviness, 1977). Leaf area index (LAI), using plant canopy analyzer LI-COR Model LAI-2200C, and following the recommendations proposed by Gonçalves *et al.* (2020). Biomass samples were collected for a 1-m of row, row spacing of 0.5 m, from four replications (54 m^2 each plot) at approximately 10-day intervals. Biomass samples were separated into leaf dry matter, stem dry matter, aboveground biomass, and grain weight and were weighed after oven drying to constant weight at 70 ± 5ºC. At final harvest, crop yield was collected from three center rows (9 m^2) from each replication. LAI measurements were conducted at approximate 10-day intervals between V3 and R7 with four replications.

For experiments conducted in Piracicaba, the crop water productivity for total biomass (CWPt, kg m^{-3}) was calculated as the ratio between aboveground biomass (kg ha^{-1}) and seasonal evapotranspiration (mm). The crop water productivity for grain yield (CWPg, kg m^{-3}) was given by the ratio between grain yield (kg ha^{-1}) and seasonal evapotranspiration (mm).

2.2.2. Soil water content measurements

Volumetric soil water content measurements were made using a previously calibrated electromagnetic probe according to Topp *et al*. (1980) [Decagon Devices Model GS3 (PI_1-100 and PI_2-100), and Campbell Scientific Model CS650 (TE-100 and TE-50)] at 30-min time intervals and then converted to a daily value. The electromagnetic probe was installed in the center of the irrigated area, with the sensors installed both in the row and between the rows, at an average depth of 0.20 m (0.18-0.23 m) and 0.50 m (0.48-0.53 m) in Piracicaba, and at 0.20 m (0.18-0.23 m), 0.30 m (0.28-0.33 m) and 0.40 m (0.38-0.43 m) in Teresina; both sites had four replications for each depth. The measurements were initiated at 13 days after sowing (DAS) for a total of 104 observations for PI_1-100, and at 8 DAS for a total of 91 daily observations in PI_2-100. TE-100 and TE-50 measurements were started at 31 DAS for a total of 32 values for each experiment.

2.2.3. Crop model

The CROPGRO-Soybean model v.4.7.5 (Jones *et al*., 2003; Hoogenboom *et al*., 2019) simulates growth, development, yield, and soil water content during the crop season using a modular crop model structure described by Jones *et al*. (2001). The model computes the hourly distribution of temperatures (see Parton and Logan, 1981; Kimball and Bellamy, 1986), solar radiation, and photosynthesis photon flux density, considering photosynthetic irradiance split into direct and diffuse components (see Erbs *et al*., 1982; Spitters, 1986). Simulated hourly canopy photosynthesis approach is integrated to daily photosynthesis following the light interception and leaf to canopy assimilation method described by Boote and Pickering (1994) and Boote *et al*. (1998). Growth and maintenance respiration depend on temperature, crop photosynthesis rate, and current crop biomass (see Wilkerson *et al*., 1983; Jones *et al*., 1989); phenological development is calculated using linear-plateau functions that describe soybean cultivars sensitivity to both photoperiod and temperature (see Grimm *et al*.,1993; Grimm *et al*.,1994).

The model computes evapotranspiration by two approaches: the Priestley-Taylor method (Priestley and Taylor, 1972), which is the default option, and the FAO-56 Penman-Monteith method (Allen *et al*., 1998). The potential transpiration (crop water demand) is computed as the product of the reference evapotranspiration of either ET method and a model-computed crop coefficient that depends on daily leaf area index (LAI). The DSSAT approach for crop models uses an asymptotic function of daily LAI to compute a dynamic crop coefficient, with solar energy extinction equal to 0.68 (Sau *et al*., 2004, Boote *et al.*, 2008a). This coefficient partitions reference evapotranspiration to either soil water evaporation or crop transpiration based on a crop energy extinction coefficient as described by Sau *et al.* (2004) and Boote *et al.* (2008a). The soil water evaporation can be calculated by two methods in DSSAT: the Suleiman–Ritchie method is currently the default option (Suleiman and Ritchie, 2003), while the Ritchie Two-Stage method (Ritchie, 1972) is an older version that was previously used in DSSAT.

The soil water balance simulates the daily processes that directly affect soil water content: rainfall, irrigation, plant transpiration, soil water evaporation, infiltration, runoff, and drainage (Porter, 2004). Infiltration is calculated as the difference between water entry (rainfall and/or irrigation); and surface runoff, calculated using the USDA runoff curve number approach (Williams, 1991). Downward flow controls the rate of water movement between layers with a tipping bucket concept, using a drainage coefficient that is defined for the entire soil profile. Thus, drainage from one layer to the next occurs when soil water content exceeds

the field-capacity water holding capacity in each layer. Potential root water uptake is a function of root length density and fraction available soil water content in each soil layer and is integrated over all soil layers where roots are present (Boote *et al*., 2008b). Actual root water uptake is the minimum of potential root water uptake and potential transpiration (water) demand. Under soil water limitations when potential root water uptake is less than the transpiration demand, both photosynthesis (growth) and transpiration are reduced by a ratio, *i.e*., the actual daily root water uptake divided by the daily transpiration demand.

The simulations for Teresina and Piracicaba were conducted using the Priestley-Taylor potential evapotranspiration method (Priestley and Taylor, 1972), the Suleiman–Ritchie soil water evaporation method (Suleiman and Ritchie, 2003); and the Century soil organic matter method (Parton *et al*., 1992; Gijsman *et al*., 2002). We set the initial soil moisture to 50% of available soil water to start soil water balance of the model at 30 days prior to sowing.

The soil profiles data were created using the soil granulometry (texture) obtained on site for Piracicaba (PI_1-100 and PI_2-100) and for Teresina (TE-50 and TE-100). The soil water holding characteristics including LL, DUL, and SAT for each soil layer as well as bulk density and drainage rate were computed with the SBUILD program of DSSAT (Uryasev *et al*., 2004), which uses a pedo-transfer function to convert soil texture into soil water holding traits (Appendix F). For both soils, these initial soil water-holding traits were subsequently calibrated following four steps: (i) the first step was simulating the soil water content for different depths and adjusting the LL and SAT traits; (ii) step 2, adjusting only DUL; (iii) step 3, adjusting only soil root growth factor (SRGF); (iv) step 4, re-calibration of LL, DUL, and SAT. The calibration procedures, in all steps, were conducted by trial-and-error method against observed soil water content values, using data set from PI_1-100 for Piracicaba and from TE-100 for Teresina to improve on the statistics computed with the graphics program. Subsequently the soil water content was evaluated using data set from PI_2-100 for Piracicaba and from TE-50 for Teresina.

We also simulated daily soil water evaporation, root water uptake (equivalent to crop transpiration), extractable water, cumulative runoff, drainage, and mulch evaporation to analyze the water balance performance simulated by the model. For soil water content, we simulated the 0.20 m (0.15-0.20 m) and 0.50 m (0.40-0.50 m) soil depths for Piracicaba, and the 0.20 (0.15-0.20 m), 0.30 (0.20-0.30 m), and 0.40 m (0.30-0.40) soil depths for Teresina. Although the root length and depth were not measured in this study, the soil depths were chosen to represent well the root system of soybean in tropical conditions, which have a higher root density in the layer of 0.10 to 0.50 m, and the maximum depth of around 0.60 m for typical Brazilian soybean fields (Pivetta *et al*, 2011; Battisti and Sentelhas, 2017; Balbinot Junior *et*

al., 2018). The SRGF in Appendix F describes the fractional hospitality of successive soil layers to root length growth. The daily distribution of root mass to root length in each layer follows this SRGF, but is also dependent on soil water status of soil layers (reduced if too dry or saturated) and whether the rooting front has reached that depth (see Boote *et al*., 2008). In addition, allocation to root growth ceases when rapid seed growth begins.

The cultivar coefficients for BRS399 (MG 6.0) for Piracicaba and 8579RSF (MG 8.0) for Teresina, were estimated following the procedures developed by Boote (1999), as summarized in three phases: (i) during the first phase, the goal was to evaluate the efficiency of simulations with the default cultivar parameters (M GROUP 6 for BRS399 and M GROUP 8 for 8579RSF) using observed weather, soil, and management; (ii) during the second phase, only the coefficients associated with crop phenology were calibrated, including the following development stages (compared to observed data for R1, R3, R5, and R7); and (iii) during the third phase, the calibration of other crop growth coefficients was also considered, by comparison to measured data on LAI, leaf dry matter, total tops dry matter, and grain weight (Appendix G). Specifically for TE-100, it was necessary to change the PPSEN to mimic the soybean cultivar types grown in low latitude regions, such as northeastern Brazil that has a short-day length to make the cultivar less sensitive to photoperiod. The soybean cultivars recommended for this region were developed to have a very low sensitivity to photoperiod through the use of the long juvenile trait (Campelo *et al*., 1998; Carpentieri-Pípolo *et al*. 2002; Viana *et al*., 2013; Abrahão and Costa, 2018). The calibration of the MG 6.0 was evaluated for PI_2-100, while the calibration of MG 8.0 cultivar was evaluated for TE-50. For both cultivars, we evaluated the model capacity to predict: (i) phenology, (ii) LAI, (iii) leaf dry matter, (iv) stem dry matter, (v) total tops dry matter, (vi) grain weight, (vii) soil water content. Furthermore, we evaluated the model capacity to simulate evapotranspiration only for BRS 399RR cultivar; this is presented in the section 2.2.5.

2.2.4. Evapotranspiration measurements

For PI_1-100 and PI_2-100, we collected daily crop evapotranspiration measurements during each growing season using the BREB method (Bowen, 1926). The BREB system was

installed in the center of the field that was approximately 3.0 ha, with an extensive fetch over a homogeneous surface with fetch/height ratios in the order of 1:100 (Heilman and Brittin, 1989; Garratt, 1994; Stannard, 1997). For experiments conducted in Teresina were no fetch/height enough to collect BREB data. The BREB system recorded the following measurements: (i) net radiation (Rn) (Kipp and Zone Model NR-Lite2); (ii) soil heat flux (G) (Hukeseflux Model HFP01) measured at two depths at 0.05 m below soil surface; and (iii) vertical gradients of air temperature and partial vapor pressure (Vaisala Model HMP155) measured 0.80 m between the sensors and 0.20 m above the canopy, the sensors were moved up periodically as the canopy grew taller. For assessment of the reliability of the BREB database, we applied the criteria proposed by Perez *et al*. (1999) to reject any physically inconsistent data. The BREB measurements were collected during the main soybean development phase, defined as the time from the third node (V3) to physiological maturity (R7) (Fehr and Caviness, 1977). The measurements were recorded every 15-minutes and summarized to daily values starting at 13 days after planting (DAP) for PI_1-100 and at 9 DAP for PI_2-100. The Eqs. 1 to 3 were used to estimate evapotranspiration by the BREB method.

$$e_s = \left(0.6108\, e^{\frac{17.3\,T}{273.3\,T}}\right) RH \quad (1)$$

$$\beta = \gamma \frac{\Delta T}{\Delta e_a} \quad (2)$$

$$ET_C = \frac{R_n - G}{\lambda\,(\beta+1)} \quad (3)$$

where e_a is the current water vapor pressure (kPa), T is the air temperature (°C), RH is the relative humidity (decimals), β is the Bowen ratio, γ is the psychrometric constant (kPa $°C^{-1}$), ΔT and Δea are air temperature (°C) and partial vapor pressure difference (kPa) between two heights, respectively, ETc is the crop evapotranspiration (mm d^{-1}), Rn is the surface radiation balance (MJ m^{-2} d^{-1}), G is the soil heat flux (MJ m^{-2} d^{-1}) and λ is the latent heat of vaporization (MJ m^{-2} d^{-1}).

2.2.5. Simulation of evapotranspiration

We confronted the BREB measurements with CROPGRO-Soybean ET simulated values using either Priestley-Taylor or FAO-56 Penman-Monteith evapotranspiration methods combined with the Suleiman-Ritchie or Ritchie Two-Stage soil water evaporation methods. The PT method requires air temperature and solar radiation (Priestley and Taylor, 1972), whereas PM requires air temperature, solar radiation, windspeed and relative humidity or dewpoint

temperature as input (Allen *et al*., 1998). The PT is defined in Eq. 4 and PM is defined in Eq. 5:

$$ETo_{PT} = \alpha\ 23.923\ Q_g\ (2\ 10^{-4} - 1.83\ 10^{-4}\ a)(T + 29) \quad (4)$$

$$ETo_{PM} = \frac{0.408\ s\ (R_N - G) + \gamma\left(\frac{900}{T+273}\right) u_2\ (e_s - e_a)}{s + \gamma\ (1 + 0.34\ u_2)} \quad (5)$$

where, α is the empirical parameter [using default α = 1.1 for maximum air temperature (T_M, ºC) between 5 and 35ºC, for $T_M \leq 5$ ºC α = 0.01 exp[0.18 (T_M+20)], for $T_M \geq 35$ ºC α = 0.05 [(T_M -35) +1.1], Q_g is the global solar radiation (MJ m^{-2} day^{-1}), a is the surface albedo, T is the average daily air temperature (ºC), s is the slope of the saturation vapor pressure (kPa $ºC^{-1}$), γ is the psychrometric constant (kPa $ºC^{-1}$), R_N is the net radiation MJ m^{-2} day^{-1}) proportional to solar radiation, G is the soil heat flux (MJ m^{-2} day^{-1}), T is the mean daily temperature (ºC), e_s is the saturation partial pressure of water vapor T (kPa), e_a is the partial pressure of water vapor in the air (kPa), u_2 is the mean daily wind speed at 2-m height (m s^{-1}).

The evapotranspiration simulated by CROPGRO-Soybean model is partitioned on ETo to potential plant transpiration (EPo) and potential soil evaporation (ESo) (Eqs. 6 and 7). This partition considers that the energy not absorbed by canopy is transmitted to the soil surface which drives ESo, using the LAI and crop energy-extinction coefficient (Kep) with default value of 0.68 (Sau *et al*., 2004; Boote *et al*, 2008a).

$$EPo = ETo - ESo \quad (6)$$

$$ESo = ETo\ \{\exp[-Kep\ (LAI)]\} \quad (7)$$

For soil water evaporation, the model uses either the R-2 (Ritchie, 1972) or S-R (Ritchie *et al.*, 2009) method; the S-R method is currently the default option of the model. For both methods the actual soil evaporation is calculated daily and limited by (cannot exceed) ESo. The R-2 method calculates the soil water evaporation (mm day^{-1}) in two stages for soil layer thickness [d_z (cm)]: (i) ES_1 for soil water evaporation in the constant rate stage (Eq. 8), and (ii) ES_2 for soil water evaporation in the falling rate stage (Eq.10). The model starts soil water evaporation computation when the SWC in top is less or equal to DUL. When the soil water deficit below DUL and LL [SWC_d (cm^3 cm^{-3})] is less or equal to the evaporation limit [U (cm^3)], only ES_1 (Eq. 8) occurs and ES_2 is zero. On the other hand, when $SWC_d \geq U$ both evaporation stages occur (Eq. 9 and 10), where d_z is the soil thickness for each layer (cm).

$$ES_1 = 10\ (DUL - SW)\ d_z, \text{ when } SWC_d \geq U \quad (8)$$

$$ES_1 = U, \text{ when } SWC_d \geq U \quad (9)$$

$$ES_2 = [10\ (DUL - SWC)\ d_z] - U, \text{ when } SWC_d \geq U \quad (10)$$

The algorithm for R-2 method has adjustments based on soil water infiltration and conditions that the soil evaporation cannot be larger than the current extractable soil water in the top layer. If available soil water is less than soil evaporation, the first and second evaporation stages are adjusted by the algorithm.

The S-R method was developed using diffusivity theory and algorithms for soil water redistribution and soil water evaporation (Suleiman and Ritchie, 2003). However, S-R is appropriate only for the falling rate stage, when the SWC is below the drained upper limit (θ_{DUL}). Ritchie *et al.* (2009) improved the S-R original method to consider the soil water contents higher than θ_{DUL}; these modifications were incorporated into the DSSAT and represents the current S-R method (Eq. 11 and 12). The model for the S-R method considers three soil profile types conditions: (i) wet, when SWC is greater than DUL in at least one layer in the top 1 m; (ii) intermediate, when SWC is less than the SWC threshold in the top layer; and (iii) dry, when SWC is less than DUL in all layers in the top 1 m.

$$ES_{z,t} = 10\left(\theta'_{z,t} - \theta_{ADz}\right)F_z\ d_z \quad (11)$$

$$ES_{SR} = MIN\{ES_O, \sum_z ES_{z,t} d_z\} \quad (12)$$

where $ES_{z,t}$ is the daily variation in soil water content at depth z due to soil water evaporation (mm day^{-1}), $\theta'_{z,t}$ is the soil water content at depth z on day t, θ_{ADz} is the air-dry volumetric water content (using default value equal to 0.3 LL) at depth z (cm^3 cm^{-3}), z is the mean depth of soil layer (cm), F_z is the transfer coefficient for soil at depth z for each soil profile types condition (see more details in Ritchie *et al.*, 2009), ES_{SR} is the total daily evaporation accounting layer thickness d_z.

2.2.6. Hypothetical scenarios of agricultural water management

We applied the CROPGRO-Soybean after calibration and evaluation of the model, to explore water and tillage practices to ask what-if questions (Tsuji *et al.*, 1998; Thornton and Hoogenboom, 1994) by conducting virtual simulation experiments in Piracicaba (PI) and Teresina (TE). This included (i) conventional tillage versus no-tillage practices with 4,000 kg ha^{-1} of crop surface residue in the initial conditions; (ii) rainfed versus irrigation triggered at 30, 40, 50, 60, 70, or 80% water soil available in the 0.30 m of the soil profile, and (iii) irrigation

application rates at 10, 20, and 30 mm. For these simulations we used the planting date and initial soil water conditions from the PI_1-100 experiment for Piracicaba and from the TE-100 experiment for Teresina. The simulations were repeated for 30 seasons using long-term historical weather data from 1989 to 2020 for both sites (Appendix H).

2.2.7. Statistics for model evaluation

To determine the degree of model predictability for daily evapotranspiration simulations, we computed the root mean square error (RMSE) (Loague and Green, 1991) and index of agreement (D) (Willmott *et al*., 1985). For the final values for cumulative evapotranspiration and crop water productivity, we computed the bias variation (B) for final values. The following equations were used for the calculations:

$$\mathrm{RMSE} = \sqrt{\frac{\sum_{i=1}^{n}(s_i - o_i)}{n}} \tag{13}$$

$$\mathrm{D} = 1 - \left[\frac{\sum_{i=1}^{n}(s_i - o_i)^2}{\sum_{i=1}^{n}|(s_i - \bar{o}| + |o_i - \bar{o}|)^2}\right], 0 \leq \mathrm{D} \leq 1 \tag{14}$$

$$\mathrm{B} = 100\frac{s_i - o_i}{o_i} \tag{15}$$

where n is number of observations; s_i is simulated, value corresponding to measurement i on each date; o_i is observed value for measurement i; and $\bar{o}$ is the average of observed values.

The D, RMSE and B were used to assess the simulation error in relation to measured daily and cumulative evapotranspiration and crop water productivity. The D is the degree to which the simulated model values are approached by the measured values; it ranges from 0 to 1, with 0 indicating no agreement between the observed and simulated values and 1 indicating perfect agreement. The B measures the variation between simulated and observed values (%), if the model under-predicts, the B is negative or if the model overpredicts the B is positive, and values near zero indicate small model errors. A high value for the D, a low value for RMSE, and B near zero would imply better model performance.

2.3. Results and Discussion

2.3.1. Simulated phenology, growth and development for BRS-399 and 8579RSF

We used PI_1-100 and TE-100 treatments for model calibration based on the Priestley-Taylor method for evapotranspiration and the Suleiman-Ritchie method for soil water evaporation. After the second phase of calibration, the model showed a correct prediction of the R1, R3, R5, and R7 for both experiments (Table 2.2). The PI_2-100 and TE-50 treatments were then used for evaluation. We observed good accuracy in simulation for the BRS-399 and 8579RSF across the phenological stages; the maximum difference was 5 days between the simulated and the observed values.

Table 2.2 Soybean crop phenology observed and simulated for cultivar BRS399 and 8579RSF with the CROPGRO-Soybean model, after cultivar and soil calibration. Experiments were conducted in Piracicaba during two growing seasons (PI_1-100 and PI_2-100) and in Teresina for two water management treatments (TE-100 and TE-50) during one growing season.

Cultivar	Phenology	Observed	Simulated
		day after sowing (DAS)	
Model calibration			
BRS399 (PI_1-100)	R1, Beginning flowering	39	39
	R3, Beginning pod	54	54
	R5, Beginning seed	64	64
	R7, Physiological maturity	104	104
8579RSF (TE-100)	R1, Beginning flowering	30	30
	R3, Beginning pod	41	41
	R5, Beginning seed	48	48
	R7, Physiological maturity	83	83
Model evaluation			
BRS399 (PI_2-100)	R1, Beginning flowering	36	36
	R3, Beginning pod	51	49
	R5, Beginning seed	58	57
	R7, Physiological maturity	91	89
8579RSF (TE-50)	R1, Beginning flowering	30	30
	R3, Beginning pod	41	41
	R5, Beginning seed	48	49
	R7, Physiological maturity	83	78

The evaluation of the CROPGRO-Soybean model for predicting phenology for TE-50 showed identical results for simulated and observed R1 and R3, but with simulated R7 earlier than observed R7 (Table 2.2). A shorter simulated cycle (time between planting to physiological maturity) for TE-50 than observed would possibly be an indication that the real crop did not experience as much drought stress as the simulated crop. There was a reduction in the simulated

cycle for TE-50 because the model simulates reproductive development as a function of photoperiod and temperature and soil water and nitrogen deficits (Boote *et al*., 1998). In this case, the difference was caused by the prediction of drought stress, which uses the water stress factor for photosynthesis to account for water deficit effects on plant physiological processes (Boote *et al*., 2008a), resulting in an acceleration to maturity after R5. This index indicates the daily severity of drought stress during the cropping season and ranges from a value of zero (well-watered conditions) to one (maximum stress) (Fig.2.1).

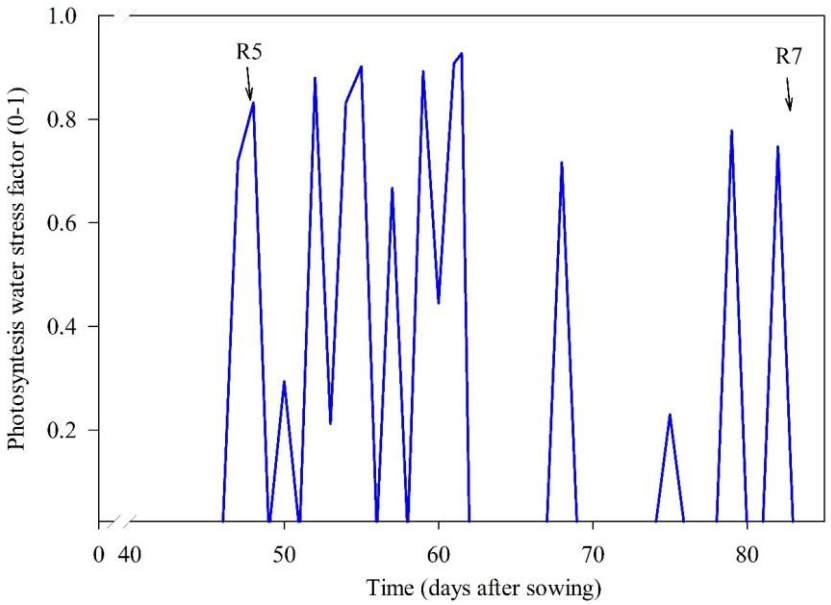

Fig. 2.1. Simulated photosynthesis water stress factor during 2019 season at Teresina (TE-50), after cultivar and soil calibration. Observed phenological stages during the drought period are beginning seed (R5) and physiological maturity (R7).

The experiment PI_2-100 showed identical results for evaluation of R1, but it was less accurate for the simulation of the R3, R5, and R7 stages. The crop model simulated a cycle slightly shorter than was observed in the field experiment, with a difference between simulated and observed data that ranged from 1 to 2 days between R3 and R7. The model was able to show a similar shortening of cycle length between PI_1-100 and PI_2-100. In PI_2-100, with later planting and successively shorter days, flowering and all stages were earlier compared to PI_1-100. Phenology affects dry matter accumulation and partitioning, ultimately affecting seed yield (Boote *et al*., 1998; Kim and Schultz, 2020; Salmerón and Purcell, 2016; Soltani and Thomas, 2012). Thus, the simulated and observed shorter cycle caused the grain yield in PI_2-100 to be almost 20% lower than PI_1-100 (Fig.2.2). The model successfully simulated this lower yield

associated with a shorter duration from planting to physiological maturity due to a later planting.

The full water requirements treatments (PI_1-100, PI_2-100, TE-100) did not show any drought stress because the irrigation management was sufficient to supply the evapotranspiration demand throughout the growing season (Fig. 2.2). In TE-50 periodic drought stresses was simulated between R5 and R7 (Fig.2.1) which resulted in a reduction in total crop and grain weight compared to TE-100. Drought during the R5-R7 phase induces a decrease of the grain-filling period by stimulating the acceleration of senescence (Souza, Egli, and Bruening, 1997) (Fig.2.1). The water supply for TE-100 resulted in a grain yield of 3,290 kg ha^{-1}, while for TE-50 the grain yield was 1,379 kg ha^{-1}; the model was able to successfully simulate a similar response to water deficit with a decrease in total crop weight and grain yield (Fig.2.2).

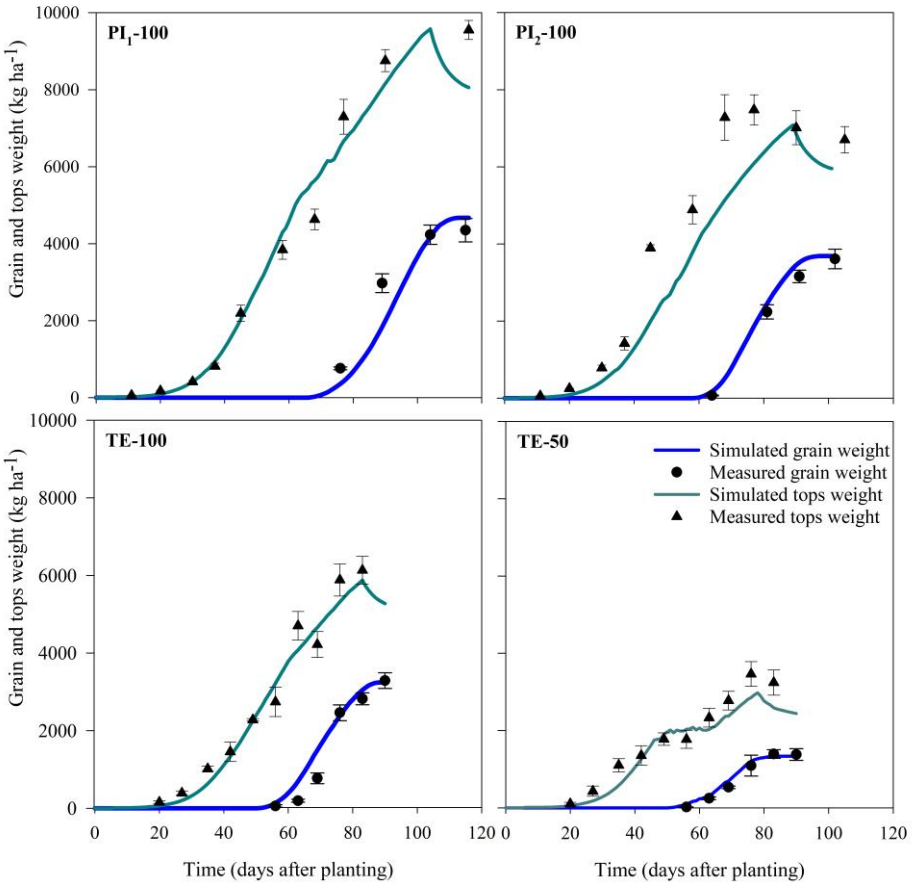

Fig. 2.2. Grain and total crop (tops) weight (kg ha^{-1}), simulated and observed and standard deviation of observed data for the experiments conducted in Piracicaba (PI_1-100 and PI_2-100) and Teresina (TE-100 and TE-50), after soil and cultivar calibration.

For our calibration procedure for PI_1-100 and TE-100, we minimized the RMSE, maximized the D, and visually evaluated whether the cultivar coefficient adjustments were able

to provide a better description of the observed growth variables. Based on these indicators, we obtained the best possible adjustment and the calibrated model was able to correctly simulate LAI, leaf dry matter, stem dry matter, total top dry matter, and grain weight over time compared to the observed data (Table 2.3). We evaluated the CROPGRO-Soybean simulations, and found that all evaluated variables were well simulated, with values for the D that were above 0.90 for all variables, except for the leaf and stem components that had values for the D that were greater than 0.80 (Table 2.3).

Table 2.3. Statistical analysis for the crop growth variables over time simulated with the CROPGRO-Soybean model following cultivar and soil calibration. The experiments were conducted in Piracicaba (PI_1-100 and PI_2-100) and Teresina (TE-100 and TE-50).

Treatment	Variable	Unit	RMSE	D
Model calibration				
BRS399 (PI_1-100)	Leaf area index	—	0.397	0.983
	Leaf dry matter	kg ha^{-1}	120	0.994
	Stem dry matter	kg ha^{-1}	485	0.964
	Total tops dry matter	kg ha^{-1}	667	0.992
	Grain weight	kg ha^{-1}	625	0.960
8579RSF (TE-100)	Leaf area index	—	0.418	0.927
	Leaf dry matter	kg ha^{-1}	204	0.874
	Stem dry matter	kg ha^{-1}	480	0.819
	Total tops dry matter	kg ha^{-1}	394	0.990
	Grain weight	kg ha^{-1}	373	0.977
Model evaluation				
BRS399 (PI_2-100)	Leaf area index	—	0.273	0.984
	Leaf dry matter	kg ha^{-1}	392	0.889
	Stem dry matter	kg ha^{-1}	495	0.918
	Total tops dry matter	kg ha^{-1}	625	0.988
	Grain weight	kg ha^{-1}	200	0.994
8579RSF (TE-50)	Leaf area index	—	0.413	0.947
	Leaf dry matter	kg ha^{-1}	257	0.823
	Stem dry matter	kg ha^{-1}	130	0.954
	Total tops dry matter	kg ha^{-1}	385	0.964
	Grain weight	kg ha^{-1}	94	0.992

2.3.2. Simulation of soil water dynamics

The soil water content in Piracicaba was satisfactorily simulated, as the D values for both depths, *i.e.*, 0.20 m and 0.50 m, ranged from 0.579 to 0.835 and the RMSE ranged from 0.011 to 0.020 cm^3 cm^{-3}, although the model tended to overestimate soil water content in both experiments (Fig. 2.3). For the Teresina site, the soil water content was satisfactorily simulated, with D values for 0.20, 0.30, and 0.50 m depths ranging from 0.535 to 0.984 and RMSE values ranging from 0.005 to 0.027 cm^3 cm^{-3} (Fig.2.4); the soil water content was overestimated in TE-100 and underestimated in TE-50. The underestimation of simulated soil water content in TE-50 corroborates with the previous arguments that the model overestimated drought stress (Fig. 2.1).

The different soil textures at Piracicaba and Teresina resulted in considerable differences in the amount of water retained under no drought stress conditions (PI_1-100, PI_2-100, TE-100). We observed a higher soil water content for the soil with the higher clay content, *i.e*., the soil at Piracicaba, since the clay fraction contributes to the formation of micropores (Dexter, 2004; Zaffar and Sheng-Gao, 2015).

The soil at Piracicaba was a clay loam soil, and showed large soil water content fluctuation for the 0.20 m soil depth, whereas the 0.50 m soil depth had a less variable and higher soil water content, especially at the beginning of the soybean cycle (Fig.2.3). The soil water content for the 0.50 m depth remained close to the DUL; the model simulated a similar response by smaller amount of soil water extraction by the soybean roots during this phase. The cumulative value for rainfall was 947.0 mm with 177.6 mm of effective irrigation for PI_1-100, while PI_2-100 the rainfall was 703.5 mm with 242.4 mm of effective irrigation.

The soil at Teresina was a sandy loam soil, and for both treatments (TE-100 and TE-50) there was a large soil water content oscillation for the 0.20 m soil depth, and a moderate oscillation for the 0.30 and 0.40 m soil depths in TE-100 during the growing season, with satisfactory simulated soil water content evaluation for the deeper layers at 60 days after planting (Fig. 2.4). In TE-50 there was a slow decrease of the soil water content from 40 days after planting for the 0.30 and 0.40 m depths. This could indicate that the roots of the soybeans penetrated more deeply when the surface layers dried out due to soil water evaporation. In these two deeper layers, the soil water content declined and approached LL later during the growing season, which is reflected in a high Photosynthesis Water Stress Factor (Fig. 2.1) and reduced biomass growth and yield for this treatment (Fig. 2.2).

The CROPGRO-Soybean simulated a large amount of total extractable water in the soil profile during the harvest period in Piracicaba (PI_1-100 and PI_2-100) with runoff and drainage values increasing during tropical storms (Fig. 2.5). For the drought periods between 80 and 100 days after planting in PI_1-100, which was supplemented with irrigation, the runoff was stabilized and the drainage was less. The cumulative mulch evaporation in PI_2-100 was computed as described by Porter *et al*. (2010) and the reduced soil-plus-mulch evaporation allowed the model to simulate the practice of conservation of soil water by maintaining more constant levels of extractable water and a smoother runoff curve. The inclusion of crop residue in the initial conditions of the PI_2-100 simulation was helpful to improve the statistical indicators for both the evaluation of soil water content and for soybean growth and development.

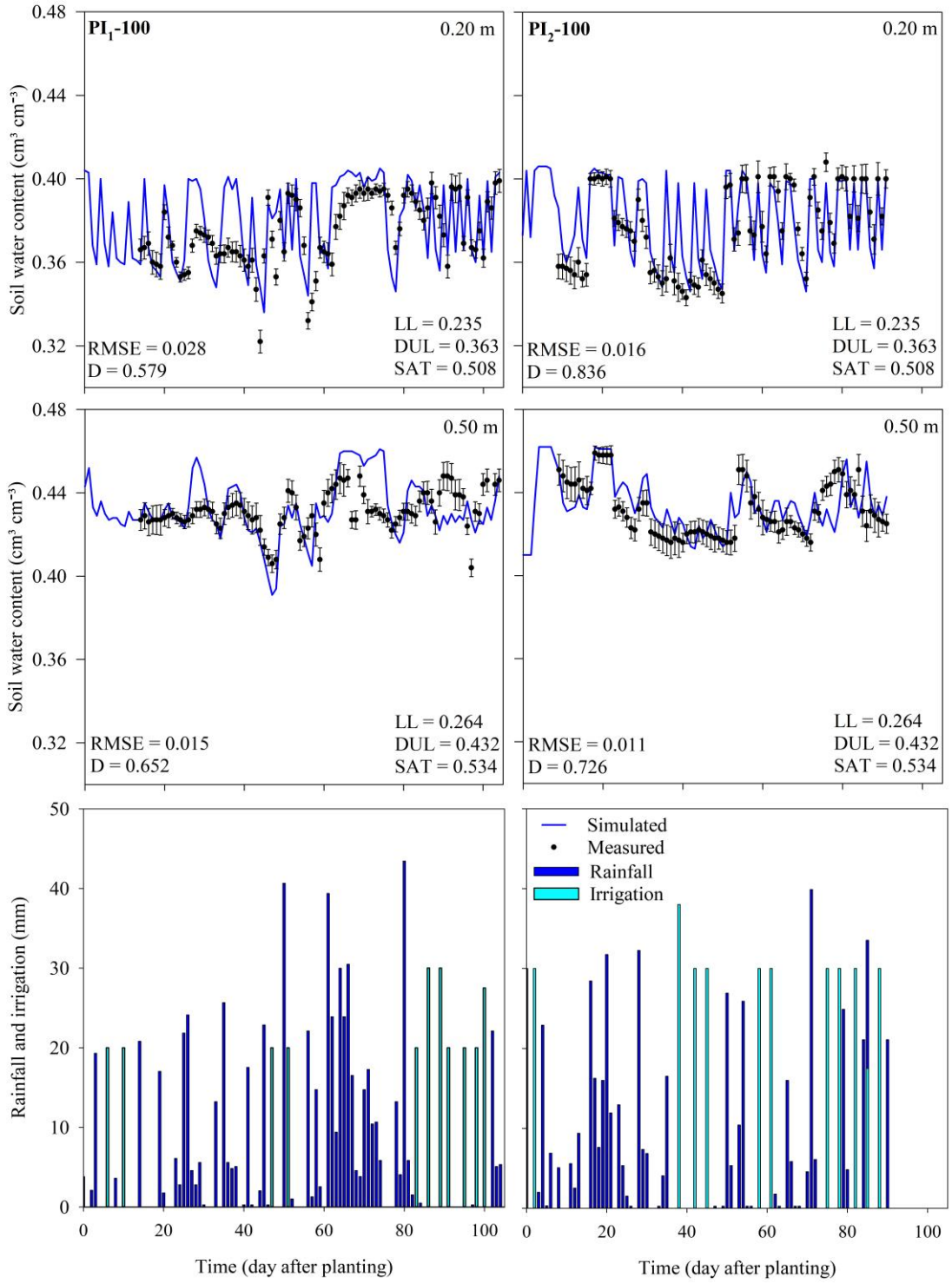

Fig 2.3. Simulated and observed soil water content for Piracicaba (PI_1-100 and PI_2-100) for the 0.20 and 0.50 m soil depths and the rainfall and irrigation events. The soil water holding characteristics are shown: lower limit of plant extractable soil water (LL), drained upper limit (DUL), and saturated soil water content (SAT).

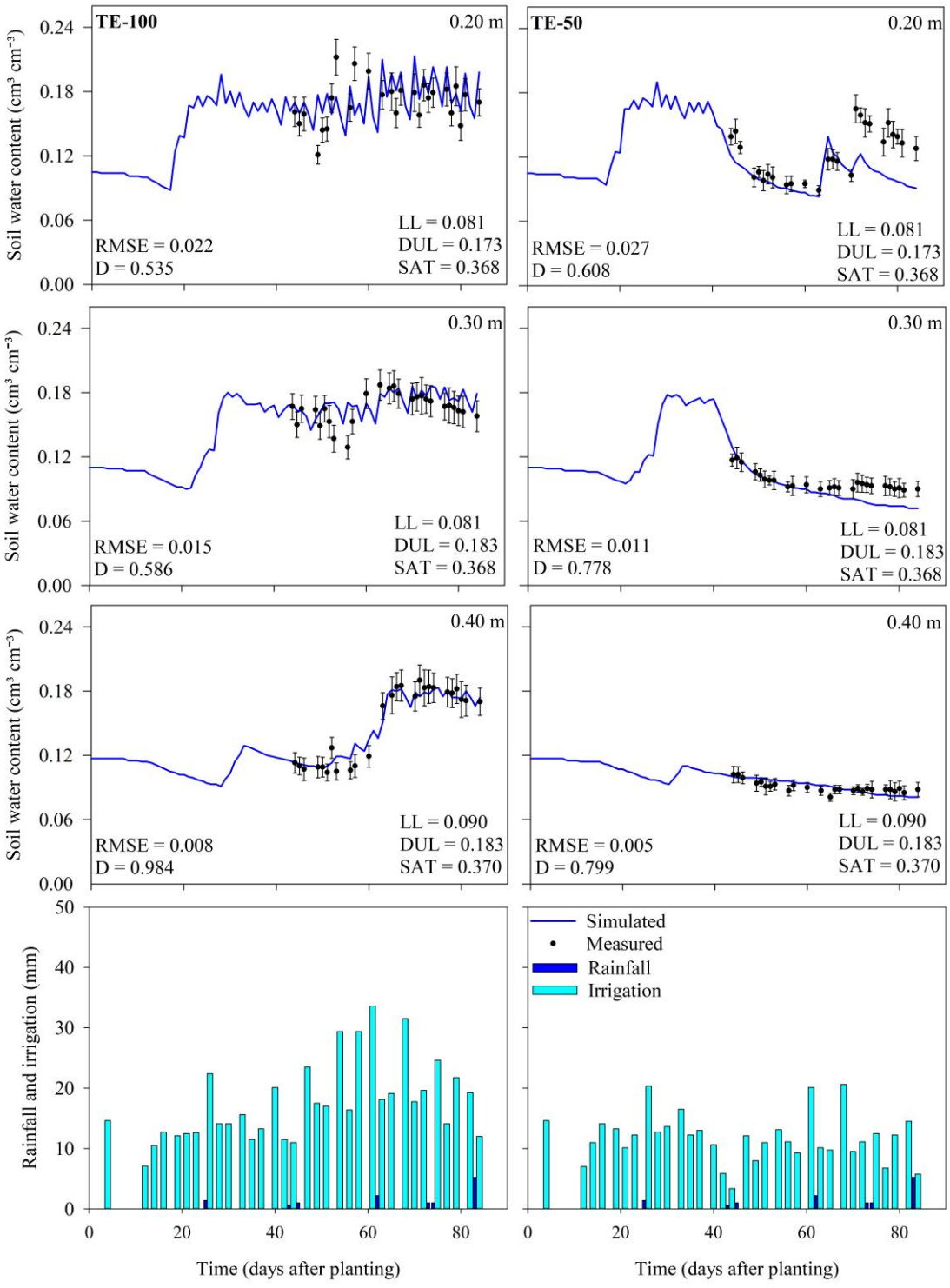

Fig 2.4. Simulated and observed soil water content for Teresina (TE-100 and TE-50) for the 0.20, 0.30 and 0.40 m soil depths and the rainfall and irrigation events. The soil water holding characteristics are shown: lower limit of plant extractable soil water (LL), drained upper limit (DUL), and saturated soil water content (SAT).

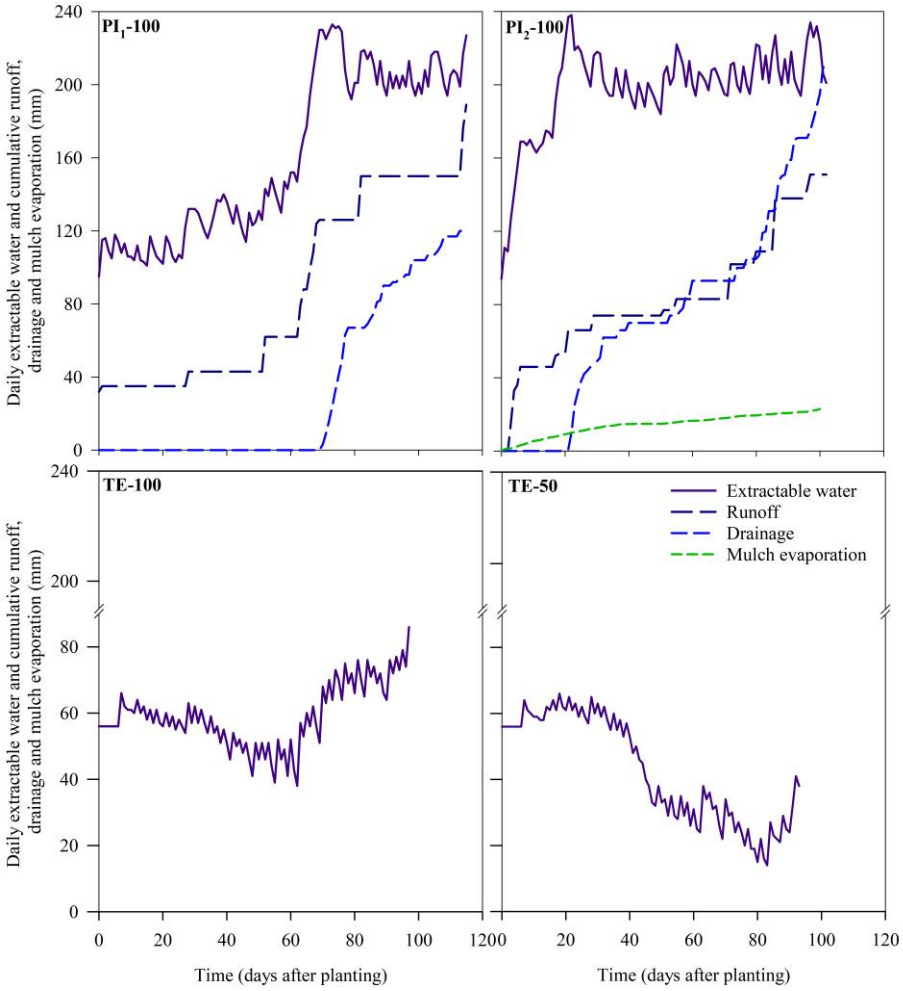

Fig 2.5. CROPGRO-Soybean simulations for daily extractable water (mm), cumulative runoff, drainage, and mulch evaporation (mm) in the soil profile for experiments conducted in Piracicaba (PI_1-100 and PI_2-100), and Teresina (TE-100 and TE-50), after cultivar and soil calibration. The mulch evaporation in PI_1-100, TE-100, and TE-50 was less than 5 mm (data not shown).

The experiments in Teresina (TE-100 and TE-50) were conducted under high average temperature (28.4 ºC) and dry weather, with only a total of 15.4 mm of rainfall (Appendix B). The irrigation management was then responsible for practically supplying all the soybean water requirements, since the effective irrigation amounts were 418.3 mm for TE-100 and 271.6 mm for TE-50. The model did not simulate runoff or drainage during the season, while the cumulative mulch evaporation was less than 5 mm (Fig. 2.5). This happened because the irrigation management was carried out with a small amount of water per irrigation application. The average irrigation amount was 17.6 mm for TE-100 and 11.7 mm for TE-50, with 2- or 3-days irrigation intervals. Simulated drainage is calculated by a 'cascading' approach, in which excess water above DUL from an upper layer cascades to lower layers (Ritchie, 1985; Shelia *et al*., 2018). The soil from Teresina is deeper (1.8 m depth) and we did not observe a soil water

content above DUL in the deepest measured layer 0.4 m depth (Fig. 2.4). Therefore, there was no drainage.

2.3.3. Simulation of soil water evaporation and root water uptake

PI_1-100 had a higher soil water evaporation rate during the early stages of the growing season than PI_2-100 (Fig. 2.6). The model simulated less soil water evaporation during the PI_2-100 season because the soil surface water dynamics were modified by the presence of crop residue under no-tillage practices. Other studies also have found a satisfactory performance of the CSM model for the simulation of the impact of tillage and residue on soil water dynamics (Andales *et al.*, 2000; Liu *et al.*, 2011; Corbeels *et al.*, 2016; Adhikari *et al*., 2016). The higher soil water evaporation rate was obtained for PI_1-100 within the first 20 days after planting, under bare soil conditions with a high soil water content. For the experiments conducted in Piracicaba and Teresina, the soil water evaporation rate decreased during the growing season until rising again near physiological maturity, when the reduction in canopy coverage due to leaf senescence and abscission increased solar radiation to the soil surface and increased soil water evaporation rate (Fig. 2.6).

The LAI is a very important trait for the simulation of the soil water balance by CROPGRO-Soybean, because the amount of solar radiation (MJ m^{-2}) that reaches the soil is a function of the LAI, thus impacting soil water evaporation and plant transpiration (Boote *et al.*, 2008a; Sau *et al.*, 1999). The root water uptake is calculated using a law of the limiting approach whereby soil water and root resistance, or atmospheric demand control root water uptake (Ritchie, 1981), which depends on the available soil water and root length density of each soil layer or horizon. Potential root water uptake must be computed before actual plant transpiration is computed, featuring an upward flow closely related to soil water evaporation and plant transpiration (Shelia *et al*., 2018). As expected, we observed a strong relationship between the highest LAI values and the highest root water uptake rates (Fig. 2.6).

A good LAI calibration is relevant to obtain a satisfactory performance for predicting yield (Richetti *et al.*, 2019) and soil water balance simulation. The TE-50 simulation of LAI suggests that the model simulated more drought stress than was observed in the field experiment (Fig. 2.6), which corroborates with the slightly lower simulated tops and grain weight (Fig. 2.2) compared with the observed data. The greater severity of the simulated drought stress may

explain the 5 days gap (Table 2.2) in phenological maturity between the simulated and the observed data.

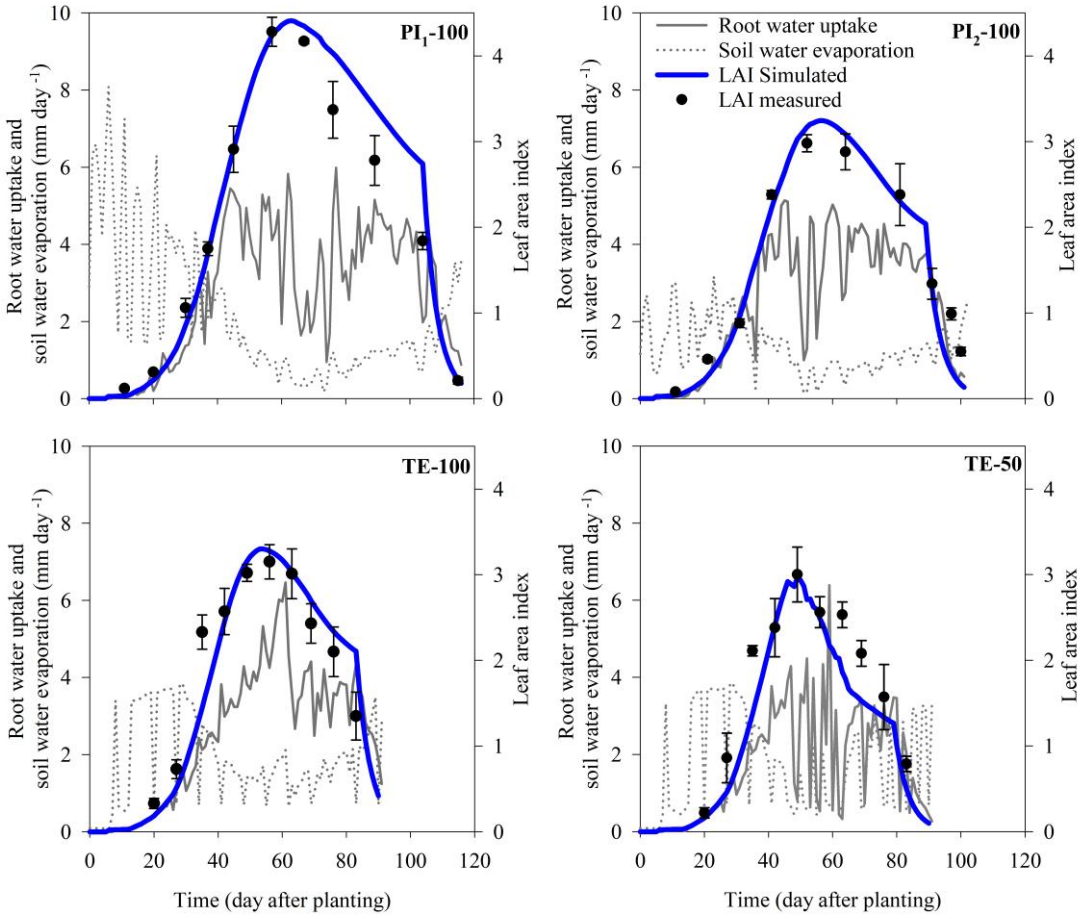

Fig 2.6. Simulated and observed leaf area index (LAI; average and standard deviation), and simulated soybean root water uptake and soil water evaporation rate for the experiments conducted in Piracicaba (full crop water requirements, PI_1-100 and PI_2-100), and Teresina [TE-100 (full crop water requirements) and TE-50 (50% crop water requirements)] following cultivar and soil calibration.

2.3.4. Simulations of daily and seasonal evapotranspiration

For PI_1-100, the daily ET rates for PT and PM methods showed rising ET values during the first 50 days after planting (DAP) (Fig. 2.7). During this period for conventional tillage practices, the S-R had higher rates of soil water evaporation compared to R-2 for both ET methods, thus contributing to a higher ET with both methods for the first 50 days. The PT method simulated higher ET values than PM for the same 50-day period. After 50 DAP, the S-R and R-2 methods showed little difference in ET rates, although the PT method had a tendency

for higher values than the PM method (Fig. 2.7). PI_2-100 confirmed the tendency of PT to estimate higher ET values in relation to PM, but the soil water evaporation difference between the R-2 and S-R methods was much smaller compared to PI_1-100 until 50 DAP (Fig. 2.7). The mulch presence on the soil surface in PI_2-100 under no-tillage practice, seemed to compensate for the difference in soil water evaporation rates between the R-2 and S-R methods.

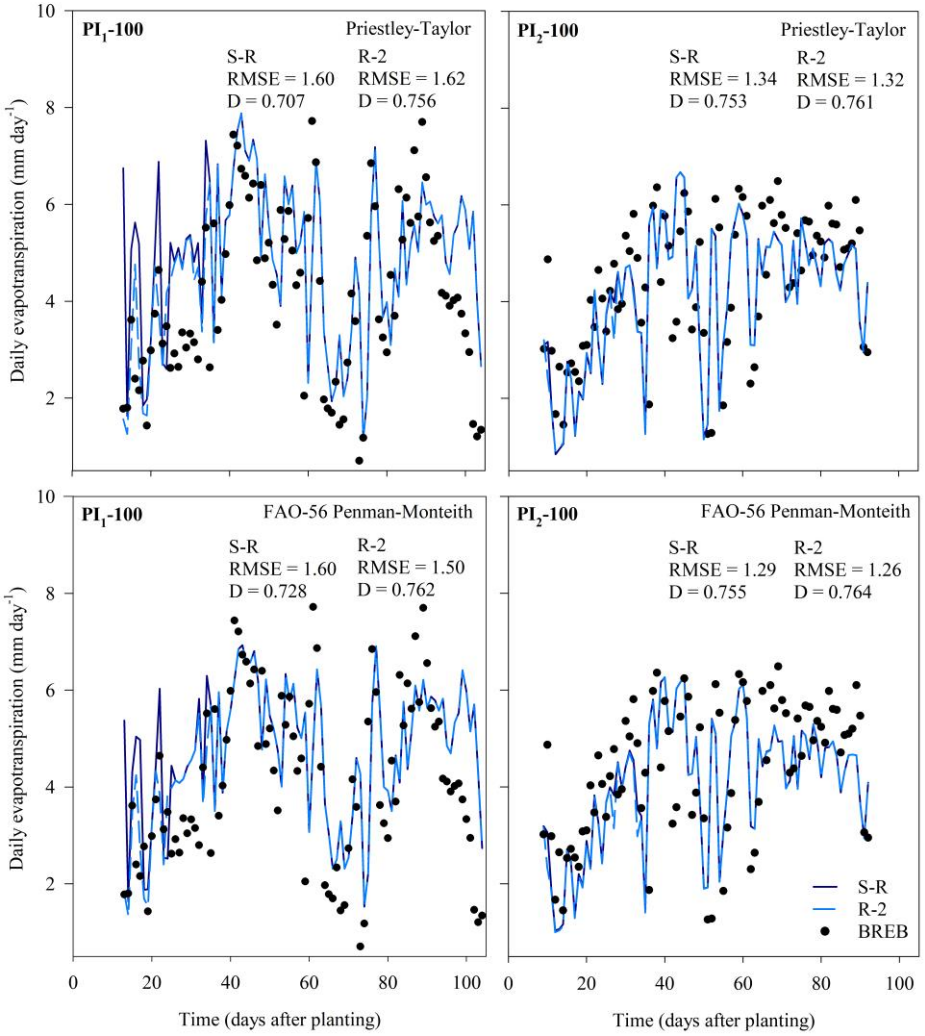

Fig. 2.7. Simulated daily evapotranspiration (mm day^{-1}) using either Priestley-Taylor (PT) or FAO-56 Penman-Monteith (PM) evapotranspiration methods combined with the Suleiman-Ritchie (S-R) or Ritchie Two-Stage (R-2) soil water evaporation methods and observed daily evapotranspiration with Bowen Ratio-Energy Balance (BREB) method for irrigated soybean during 2016-2017 (PI_1-100) and 2017-2018 (PI_2-100) seasons.

For both PI_1-100 and PI_2-100, visual comparison showed that the dynamics of the time-course simulation were similar to the measured ET rates, for either the PT and PM methods combined with the S-R and R-2 methods, with excellent statistical performance, with RMSE

ranging from 1.26 to 1.60 mm and the D ranging from 0.707 to 0.764 (Fig. 2.7). However, we observed an overestimation in ET for PI_1-100 up 40 DAP when the S-R soil evaporation method was used for either of the PT and PM potential ET methods in relation to the BREB measurements. This period corresponds to the incomplete canopy phase when soil water evaporation is the dominant portion of the daily ET. For the daily ET, as expected the PM provided better performance than PT, as already reported for other environments (Sau *et al*., 2004; Boote *et al*., 2008b; Akumaga and Alderman, 2019). However, the results of the soil water evaporation method were surprising, revealing that an older method, R-2 (Ritchie, 1972), outperformed the newer and default evaporation method, S-R (Ritchie *et al*., 2009). In the prior soil water content simulations for the same field experiments, in previous sections reported that the model using PM with S-R caused a slight overestimation of soil water depletion for 0.2 and 0.5 m depth layers when compared with time-series of observed soil water content values. Thus, the PM method combined with the R-2 method provided a better performance in relation to other combinations for both PI_1-100 and PI_2-100 (Fig. 2.7).

The CROPGRO-Soybean model somewhat overestimated the cumulative evapotranspiration in PI_1-100 for all four combinations, with the B between simulated and measured ranging from 11.5 to 16.8% (or 44 to 64 mm) (Fig. 2.8). For PI_2-100, there was also a slight overestimation, with B ranging from 2.7 to 14. 8% (or 8 to 54 mm) (Fig. 2.8). We reported in previous section that the same dataset, that the traditional FAO-56 Penman-Monteith method with engineered equations in which reference evapotranspiration (ETo) is multiplied by Kc, overestimated the seasonal crop water use by nearly 20% in relation to the measured BREB values. Thus, the cumulative ET simulated by CROPGRO-Soybean using PM combined with R-2 method provided a better simulation when compared with the BREB for both experiments, with an overestimation of 11.5% (or 44 mm) for PI_1-100 and 2.7 % (or 8 mm) for PI_2-100 (Fig. 2.8). The CROPGRO-Soybean crop model uses LAI and the Kep (Boote *et al*., 2008b; Sau *et al*., 2004) during the growing season to predict a dynamic Kc, which is a slightly different approach from the traditional FAO-56 Penman-Monteith method. This explicit use of simulated LAI with Kep could explain the better performance of the model in relation to the traditional FAO-56 method.

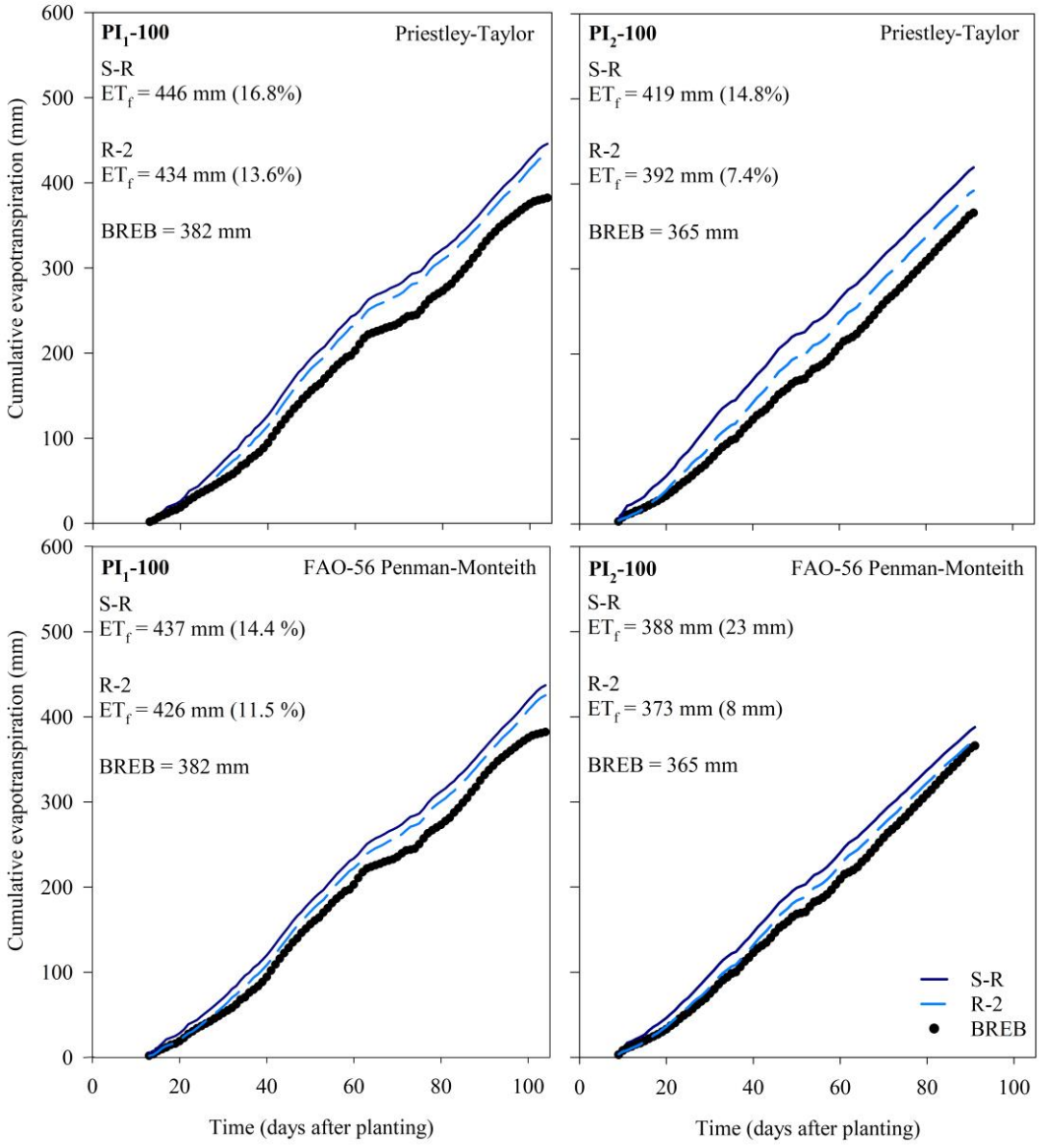

Fig. 2.8. Simulated cumulative evapotranspiration (mm) using either the Priestley-Taylor (PT) or FAO-56 Penman-Monteith (PM) evapotranspiration method combined with the Suleiman-Ritchie (S-R) or Ritchie Two-Stage (R-2) soil water evaporation method, and observed cumulative evapotranspiration with the Bowen Ratio-Energy Balance (BREB) method for irrigated soybean during 2016-2017 (PI_1-100) and 2017-2018 (PI_2-100) seasons. Cumulative evapotranspiration final values (ET_f) are shown with variation between simulated and measured (%) in brackets.

In order to further understand the factors driving the simulated evapotranspiration rates, we analyzed the simulated soil water evaporation, transpiration, and LAI patterns (Fig.2.9). The daily simulated transpiration rate increases over time as the LAI increases throughout the development of the soybean plant (Fig 2.9). Under a fully closed canopy, the rate of soil water evaporation reached its lowest values. We confirmed that the tendency of

overprediction of ET early during the growing season could be attributed to higher than observed soil water evaporation for the S-R method (Fig. 2.9). On the other hand, the overprediction late during the growing season for PI_1-100 could be attributed to an overestimation of LAI between 60-100 DAP for both PT and PM evapotranspiration methods. However, it is also possible that the observed reduction of ET late during the growing season could be associated with a reduction in photosynthesis and a reduced stomatal conductance, which occur during the latter part of grain-filling, but the effect of declining stomatal conductance is not explicitly accounted for in the CROPGRO-Soybean model for either ET method. Yet, in PI_2-100 with no-tillage practices, the soil water evaporation simulations for S-R and R-2 were very close, and confirmed that the effects of mulching reduce soil water evaporation and thus overcome the limitations of the S-R method limitations (Fig. 2.9).

Separating the soybean life cycle into three phases: incomplete canopy (V3 to R1), full canopy (R1 to R5), and declining LAI phase (R5 to R7) is helpful to evaluate the ET methods (Fig. 2.10), particularly to understand the influence of daily variation in ET relative to daily weather. In the incomplete canopy phase, the ET rate is dominated by soil water evaporation (Ritchie, 1972), and the PM method combined with R-2 method had the best fit (D = 0.599) compared to the observed data (Fig. 2.10). During the full canopy phase, the canopy cover increases and the ET rate was influenced by LAI, and, thus, the simulation showed a very similar performance for all methods, with a satisfactory performance (D ranging from 0.677 to 0.679) (Fig. 2.10). There was good ET prediction (D ranging from 0.731 to 0.761) during the declining LAI phase, due to senescence. However, the reduction in photosynthesis and conductance during the declining LAI phase are not accounted for in either ET method. Our findings showed better performance for R-2 in the incomplete canopy phase, a result that agrees with results reported by Kimball *et al*. (2019), who tested the same DSSAT evapotranspiration methods for maize sown in Iowa. However, those authors obtained better performance using S-R than R-2 from 41 DAP to maturity; while we had an almost identical performance for both soil E methods in full canopy and declining LAI phase.

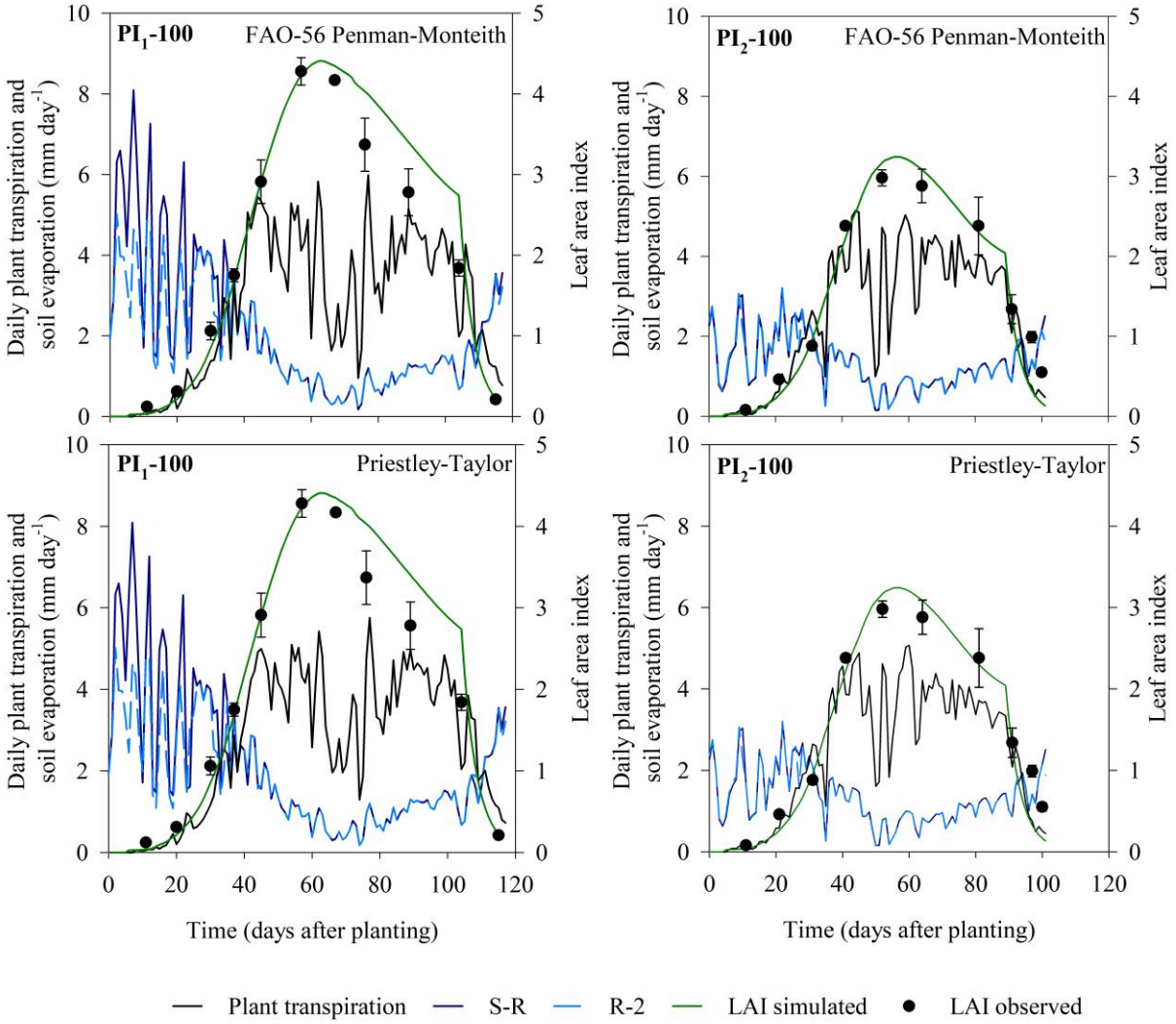

Fig. 2.9. Simulations of leaf area index (LAI), soybean transpiration using either Priestley-Taylor (PT) or FAO-56 Penman-Monteith (PM) evapotranspiration methods, and soil water evaporation using either the Suleiman-Ritchie (S-R) or Ritchie Two-Stage (R-2) methods; and observed LAI (average and standard deviation) for soybean grown at Piracicaba during the 2016-2017 (PI_1-100) and 2017-2018 (PI_2-100) seasons.

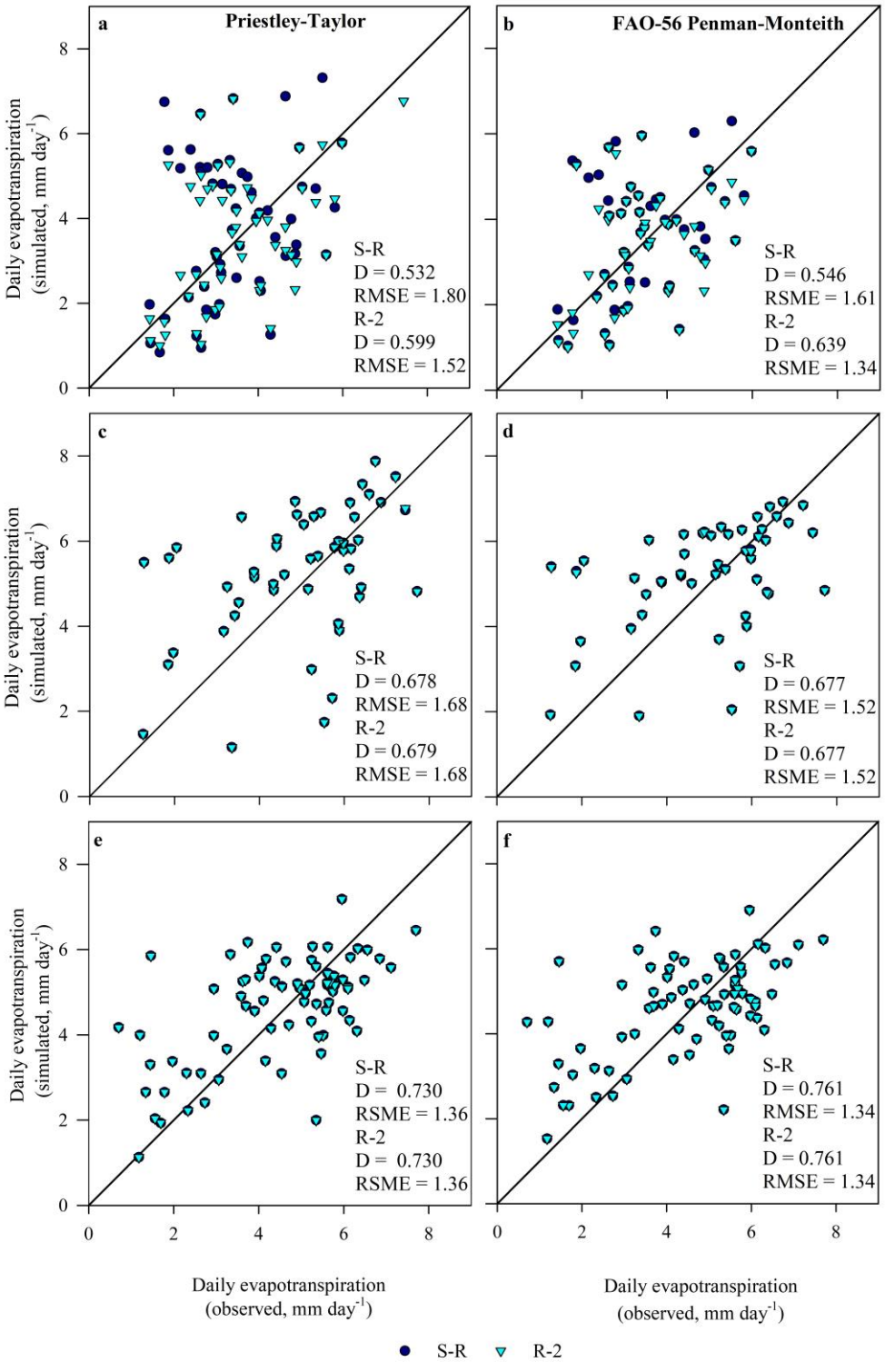

Fig. 2.10. Simulated daily evapotranspiration using either Priestley-Taylor or FAO-56 Penman-Monteith evapotranspiration methods combined with the Suleiman-Ritchie (S-R) or Ritchie Two-Stage (R-2) soil water evaporation methods versus obtained daily evapotranspiration with the Bowen Ratio-Energy Balance for soybean grown at Piracicaba during 2016-2017 (PI_1-100) and 2017-2018 (PI_2-100) seasons. Also shown are the evapotranspiration rates from (a,b) V3 to R1 for PI_1-100 (13 to 39 DAP) and for PI_2-100 (9 to 36 DAP), (c,d); R1 to R5 for PI_1-100 (40 to 64 DAP) and for PI_2-100 (37 to 58 DAP); and (e,f) R5 to R7 for PI_1-100 (65 to 104 DAP) and for PI_2-100 (59 to 88 DAP).

2.3.5. Crop water productivity for soybean

Following the evaluation of ET simulations, we analyzed the prediction of crop water productivity by CROPGRO-Soybean. The model had a good predictive capacity for CWPt and CWPg, although the model somewhat underestimated both. The B of simulated compared to observed CWPt ranged from -11.6 to -16.8 % for PI_1-100, and from -2.2 to -13.0 % in PI_2-100. The CWPg ranged from -10.8 to -14.4 %, for PI_1-100, and from -2.8 to -14.7 %, for PI_2-100 (Table 2.4). These underpredictions of CWP for the different methods are consistent with the slight overestimation of ET that was discussed previously. The best performance for the simulation of CWP was obtained using the PM method for potential ET and the R-2 methods for soil evaporation. There was a lower CWP for grain than for biomass; this is expected because grain yield is less than total crop biomass as expressed by the harvest index, which was 0.39 for PI_1-100 and 0.42 for PI_2-100.

Table 2.4. Simulated and observed crop water productivity (kg m^{-3}) for total biomass (CWPt), and grain yield (CWPg) using the Bowen Ratio-Energy Balance method for observed seasonal evapotranspiration and using either the Priestley-Taylor (PT) or FAO-56 Penman-Monteith (PM) evapotranspiration methods combined with the Suleiman-Ritchie (S-R) or Ritchie Two-Stage (R-2) soil evaporation methods for the simulations for soybean grown at Piracicaba during 2016-2017 (PI_1-100) and 2017-2018 (PI_2-100)) seasons. The variation between the simulated and measured values (%) is shown in parentheses.

Experiments		FAO-56 Penman-Monteith		Priestley-Taylor	
	BREB	S-R	R-2	S-R	R-2
CWPt			kg m^{-3}		
PI_1-100	25.0	21.9 (-12.4)	22.4 (-11.6)	21.4 (-16.8)	22.0 (-13.6)
PI_2-100	18.4	17.3 (-6.0)	18.0 (-2.2)	16.0 (-13.0)	17.1 (-7.6)
CWPg			kg m^{-3}		
PI_1-100	11.1	9.7 (-12.6)	9.9 (-10.8)	9.5 (-14.4)	9.8 (-13.3)
PI_2-100	10.9	10.2 (-6.4)	10.6 (-2.8)	9.5 (-14.7)	10.1 (-7.4)

2.3.6. Simulation of long-term of water management scenarios

Following the evaluation of the CROPGRO-Soybean model for simulation of soybean growth and development and the soil water balance, we conducted a seasonal analysis based on what-if scenarios for a tropical and subtropical environment. The long-term simulations for soybean yield and the impact of tillage practices on water management are presented in Fig. 2.11. The rainfed condition in Piracicaba presented the largest variation in the crop yield among

the 30 simulated seasons, and the no-tillage practices increased crop yield about 240 kg ha^{-1} on average (Fig. 2.11).

The simulations showed that the average yield increased by 564 kg ha^{-1} compared to PI-rainfed if irrigation was triggered when 50% available water remained. Among the PI-50 to PI-80 irrigation triggering scenarios, the difference in crop yield was only 50 kg ha^{-1}. The use of irrigation made it possible to reduce the production risk in relation to rainfed conditions, because the range between highest and lowest values in PI-rainfed was 3,020 kg ha^{-1} while the range was 1,400 kg ha^{-1} for the PI-50 irrigation scenarios. Conservation tillage practices reduced the irrigation amount on average by 43% for PI-30 and 27% for PI-80, while maintaining productivity levels very close to conventional tillage. The use of no-tillage reduced the number of irrigation applications on average by one application among the different scenarios.

The soybean grown in Teresina showed a lower yield potential than in Piracicaba because it was grown in a low latitude region during the winter with a shorter life cycle, along with less daily total solar radiation. For the Teresina winter environment with almost no rainfall, the average yield under rainfed conditions was less than 50 kg ha^{-1}. Yield response to irrigation was greatest at the first irrigation increments, 0 to 30, 30 to 40, or 40 to 50% triggering thresholds. The highest average crop yield was 3,532 kg ha^{-1} in TE-70, with 140 kg ha^{-1}more yield than TE-60 but required an additional 52 mm in seasonal applied irrigation.

Within a given irrigation scenario such as TE-40, yield was an average of 2,084 kg ha^{-1} under conventional tillage and 2,225 kg ha^{-1} with no-tillage practices, while saving 13 mm of water under no-tillage. Surface residue with no-tillage in Teresina resulted in increased yield for triggering supplemental irrigation at 30, 40, and 50%, but showed little to no yield benefit at higher triggering levels of 60, 70, or 80% (Fig. 2.11). However, no-tillage practices reduced the seasonal applied irrigation, on average, by 20 mm for TE-50 and 56 mm for TE-70 (Fig. 2.11).

The use of a relatively high amount of irrigation per application is common in Brazilian agricultural practices mainly due to a decrease in the energy costs associated with each irrigation event. However, in this case farmers might apply more water than is needed, thus both water and energy are wasted (Kamienski *et al*., 2019; Marin *et al*., 2019). In our findings with DSSAT as a water management tool for scheduling irrigation, decreasing the amount of water per irrigation application from 30 to 10 mm for PI-50 could save 38 mm for conventional tillage and 27 mm for the no-tillage practices. This represents almost 40% of water saved with an increase of three irrigation applications while maintaining the same yield level (Fig. 2.12).

The decreased irrigation application rate from 30 to 10 mm showed the largest reduction in the total amount of water applied for PI-80 with no-tillage practices at around 115 mm. However, as shown in Fig. 2.11, irrigation triggering above a 50% threshold level in Piracicaba does not result in a yield increase despite the increase in water consumption.

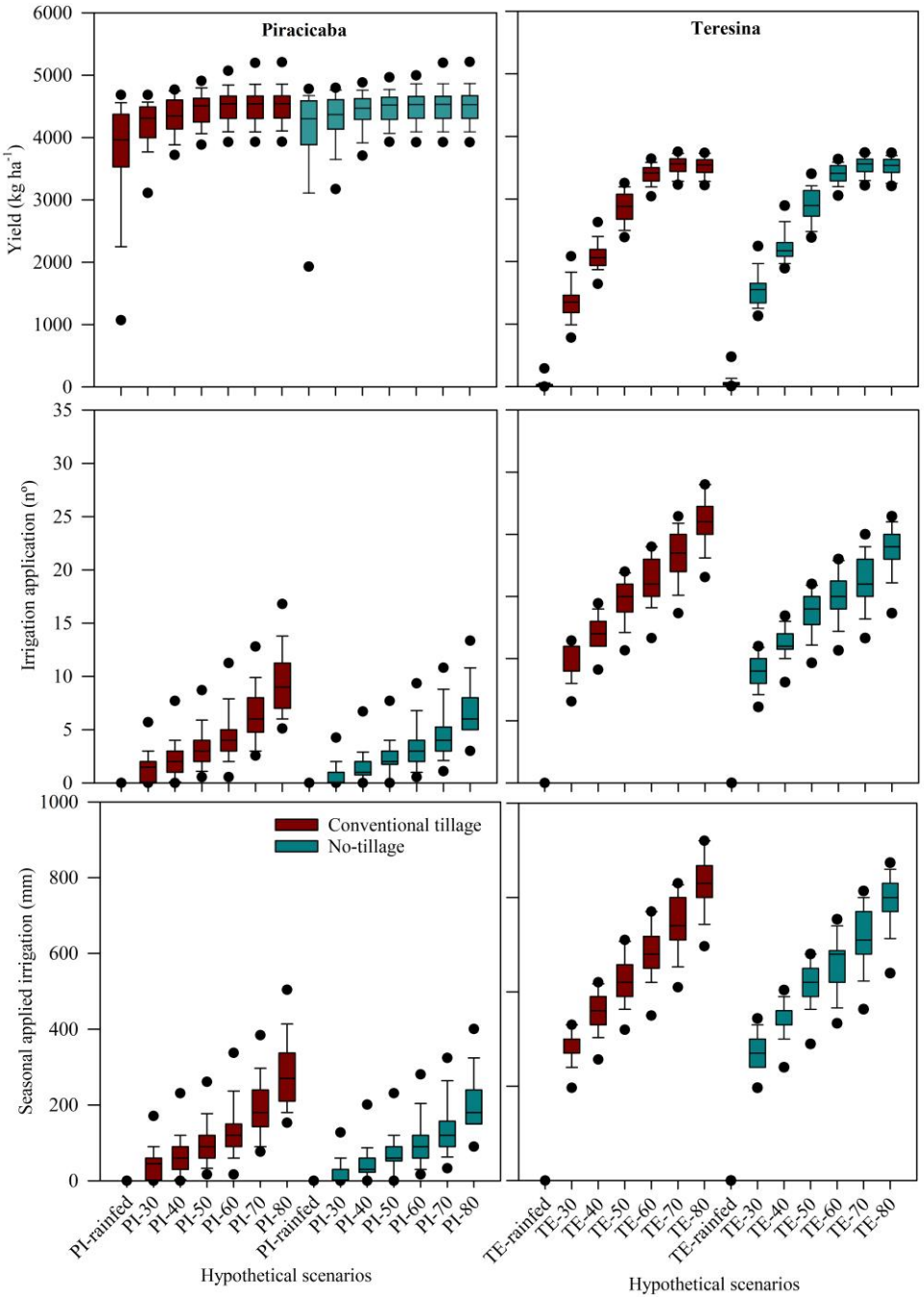

Fig 2.11. Simulated long-term scenarios for Piracicaba (PI) and for Teresina (TE) for rainfed and irrigation management scenarios, triggering irrigation based on 30 to 80% water remaining in the top 0.30 m of the soil profile for conventional tillage and no-tillage. Boxplots were set at 90th (upper whisker), 75th (upper quartile), 50th (median), 25th (lower quartile), and 10th (lower whisker) percentiles; outliers are shown as black dots.

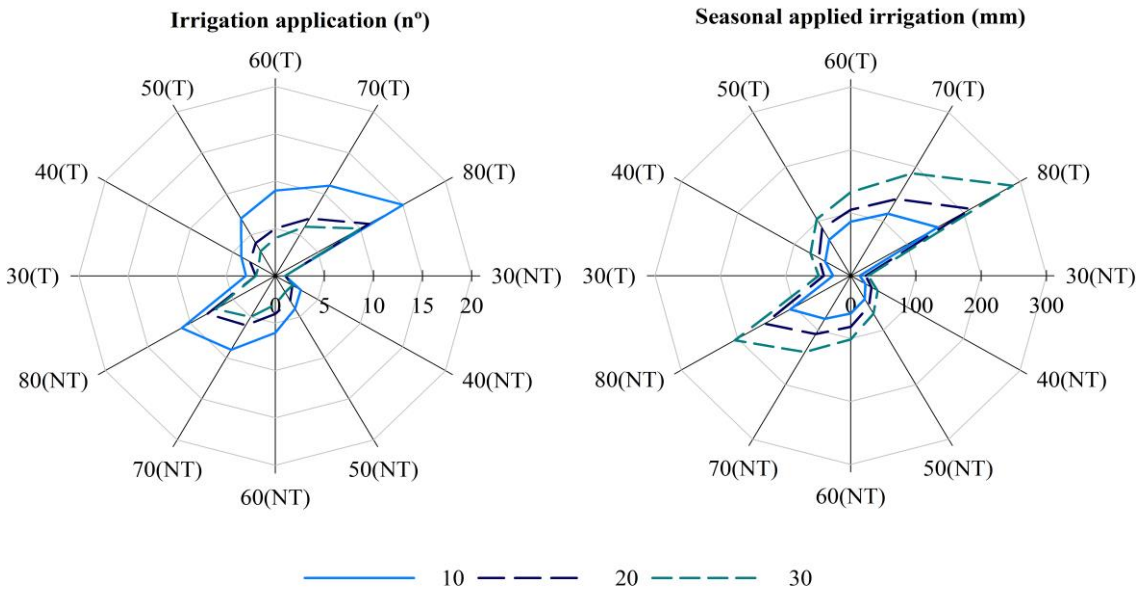

Fig 2.12. Total number of irrigation applications and total irrigation applied for the long-term scenarios for Piracicaba under rainfed and irrigated conditions for conventional tillage (T) and no-tillage (NT) and for three application rates, *i.e.* 10 mm, 20 mm and 30 mm, at triggers of 30, 40, 50, 60, 70, and 80% of water remaining.

The scenarios for Teresina showed that applying irrigation triggered at 60% water remaining is most efficient, showing a greater yield per seasonal applied irrigation (Fig. 2.11). However, reducing the irrigation amount per application from 30 to 20 mm decreased the total water requirement from 494 to 472 mm with conventional tillage and from 454 to 424 mm with no-tillage practices, at the expense of seven more irrigation applications (Fig. 2.13). Frequent light irrigations like this may work with drip irrigation, but from a realistic viewpoint, no farmer-producer would apply an irrigation amount of 10 or 20 mm per overhead application to save 20 or 30 mm with an increase in seven applications, so this argument of water-savings is somewhat artificial. Thus, the irrigation management of soybean in Teresina, during the winter with 30 mm of irrigation application rate with no-tillage practices is potentially more appropriate because this site has a deep soil with a good water-retention capacity and a small amount of water loss due to drainage and runoff (Appendix F, Fig. 2.9).

The simulations of the CROPGRO-Soybean model for both sites showed differences among tillage practices, soil texture, and irrigation amount. As discussed previously, the model was able to explore different scenarios combining tillage practices and water management using long-term historical weather data following successful calibration of the model for crop growth and development and soil moisture. Soil management with the maintenance of soil mulch can contribute to reducing the amount of water required for supplemental irrigation for soybean

production and contribute to sustainable intensification of agriculture in Brazil. However, for the agricultural system analysis in the long-term scenarios, it is important to consider that the model showed a slight tendency to overestimate the soil water content under fully irrigated conditions (PI_1-100, PI_2-100, TE-100); and to underestimate the soil water content in drought conditions (TE-50). This may suggest the need to improve several model features: (i) the simulated efficiency of applied irrigation that is infiltrating the soil, (ii) the soil evaporation method (which may cause excessive soil water depletion under drought), and (iii) the transpiration method (which may also cause too much soil water depletion under drought). Implications for scenario analyses, are that the model at present may overestimate drought-stress for drought conditions. This study demonstrates the potential of the CROPGRO-Soybean model as a tool for agricultural water management under tropical and subtropical conditions.

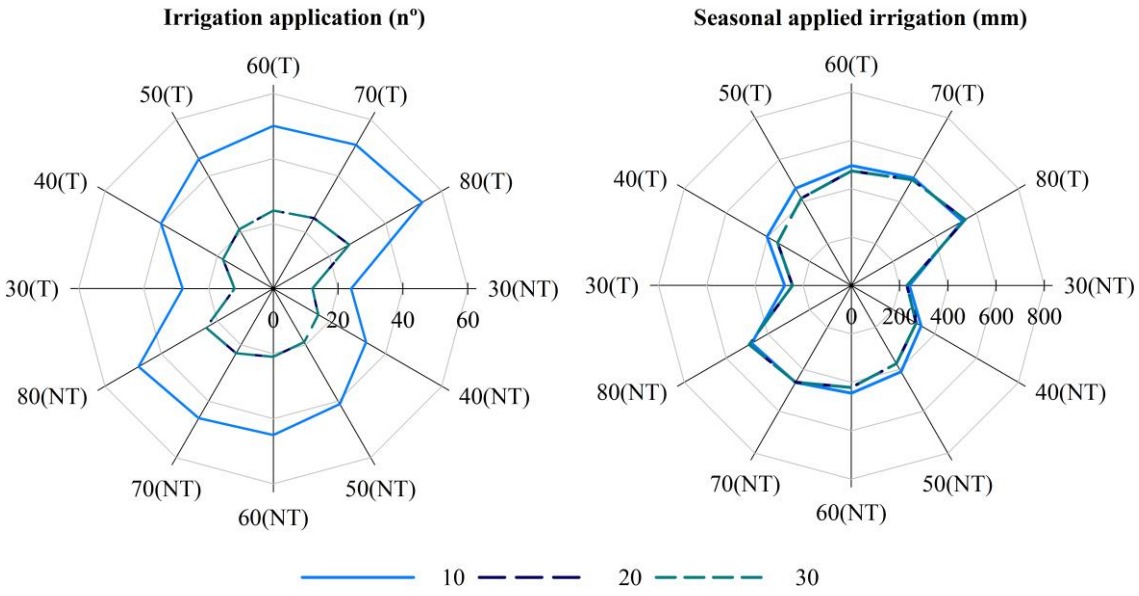

Fig 2.13. Total number of irrigation applications and total irrigation applied for the long-term scenarios for Teresina under rainfed and irrigated conditions for conventional tillage (T) and no-tillage (NT) and for three application rates, *i.e.* 10 mm, 20 mm and 30 mm, at triggers of 30, 40, 50, 60, 70, and 80% of water remaining.

2.3.7. Application of seasonal analyses of crop water productivity for soybean

Following the evaluation of crop water productivity simulated by CROPGRO-Soybean model, we conducted long-term simulations based on different management scenarios for a tropical and subtropical environment. The CWPg indicates how much grain yield (kg ha^{-1}) is produced per unit (mm) of water, and it can be affected by irrigation, tillage, and mulching (Arora *et al*., 2011, Humphreys *et al*., 2016, Li *et al.*, 2020). The long-term simulations for 30 years of daily weather showed that under rainfed conditions for conventional tillage, the CWPg ranged from 0.5 under extreme drought to 11.3 kg m^{-3} under a good water supply. The CWPg ranged from 5.6 to 11.3 kg m^{-3} when irrigation was triggered at 40% of available water, it ranged from 6.5 to 11.1 kg m^{-3} when irrigation was triggered at 60% of available water, and it ranged from 6.6 to 10.9 kg m^{-3} when irrigation was triggered at 80% of available water (Fig. 2.14). Variations in CWPg within a given management are caused by differential weather patterns of the 30 seasons simulated. The long-term simulations under no-tillage conditions showed an increase in CWPg compared to conventional tillage for both rainfed or irrigated conditions. Under rainfed conditions for no-tillage, the CWPg ranged from 0.5 to 12.1 kg m^{-3}; while for irrigated conditions triggered at different percentage of water available remaining, it ranged from: (i) 5.4 to 12.1 kg m^{-3} for 40% water available remaining, (ii) 7.6 to 12.0 kg m^{-3} for 60% of water available, and (iii) 7.6 to 11.7 kg m^{-3} for 80% of water available (Fig. 2.14). For both conventional and no-tillage conditions, irrigation at 60% of available water resulted in the highest values CWPg. Thus, this option was the most efficient water management practice for tropical and subtropical soybean and the most applicable for sustainable crop intensification practices.

The impact of insufficient soil water to meet transpiration demand reduced dry matter accumulation for the rainfed crop and, thus, affected final yield, showing a potential increase in production risk. Increasing water supply by irrigation scenarios up to 60% of available water contributed to an increase in grain yield and CWPg, while a further increase in irrigation did not result in a proportional increase in grain yield and CWPg. At a result, CWPg decreased slightly at high irrigation frequencies (Fig. 2.14). CWPg and CWPt can be enhanced with the adoption of no-till practices (Fig. 2.14); this is confirmed by several studies that have shown that a reduction in soil water evaporation is an effective way to improve soil water storage and can increase CWPg (Adeboye *et al*., 2010, Alfonso *et al*., 2020, Kader *et al*., 2020). Furthermore, we observed a decrease in CWPg for both very low or very high levels of irrigation, because a very small amount of seasonal irrigation did not provide a water supply that was sufficient to reduce drought stress and increase yield; while the opposite of a very large amount of seasonal irrigation did not result in an increase in yield despite the increase in water

supply. Thus, non-optimum use of irrigation does not contribute to efficient water management of soybean cropping systems.

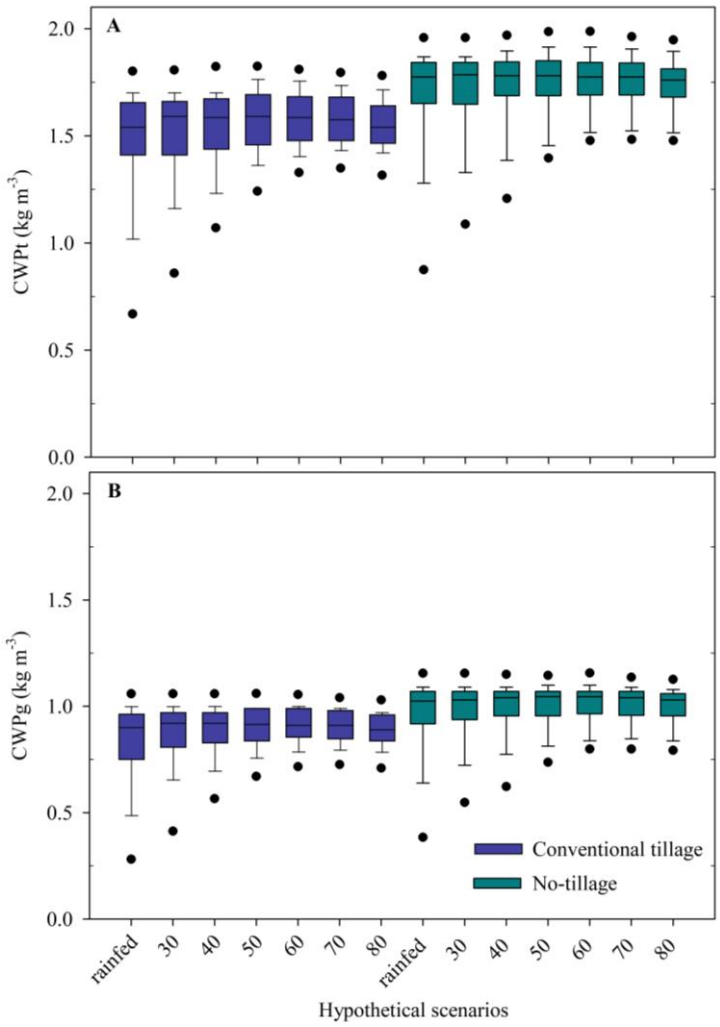

Fig. 2.14. Simulated long-term scenarios (1989 to 2020) for crop water productivity for aboveground biomass (CWPt) (a) and for grain yield (CWPg) (b) using the FAO-56 Penman-Monteith methods for potential evapotranspiration and the Ritchie Two-Stage methods for soil evaporation for rainfed, and irrigation conditions triggered at 30 to 80% of available water in the top 0.30 m of the soil profile. Boxplots were set at 90th (the upper whisker) and 75th (the upper quartile), outliers are shown as black dots.

Crop water productivity is an important indicator for quantifying the effect of proper and efficient water management. Thus, a good accuracy for simulating evapotranspiration is a critical aspect for a satisfactory prediction of crop water productivity. The CROPGRO-Soybean model showed excellent performance in predicting evapotranspiration and crop water productivity for the subtropical environment of this study. The model, therefore, has great

potential to be used as a tool for exploring efficient management strategies that are needed to improve sustainable water use in agriculture in tropical and subtropical environments.

2.4. Conclusions

The CROPGRO-Soybean model of DSSAT was successfully calibrated for cultivars BRS 399 and 8579RSF. For experiments conducted in Piracicaba, compared to the measured ET, FAO-56 Penman-Monteith potential ET method combined with the Ritchie Two-Stage soil water evaporation method, performed best for the simulating daily and cumulative ET. The model had a slight tendency for overestimating ET with consequent underestimation of CWP. The long-term scenarios showed that the amount of irrigation for a soybean crop in tropical and subtropical environments might be reduced with the use of no-tillage practices, therewithal no-tillage practices that leave crop residue on the soil surface may provide a higher soybean water productivity compared to conventional tillage practices. Thus, we conclude that the CROPGRO-Soybean model was able to accurately simulate the soybean growth, development, and yield as well as the soil water balance for different tropical and subtropical environments, as well as, simulating evapotranspiration and crop water productivity; and that DSSAT can be applied to evaluate different irrigation management options to help conserve water use.

References

Abrahão, G. M., Costa, M. H., 2018. Evolution of rain and photoperiod limitations on the soybean growing season in Brazil: The rise (and possible fall) of double-cropping systems. Agricultural and Forest Meteorology, 256, 32–45.

Adeboye, O. B., Schultz, B., Adekalu, K. O., Prasad, K. C., 2019. Performance evaluation of AquaCrop in simulating soil water storage, yield, and water productivity of rainfed soybeans (*Glycine max* L. Merr) in Ile-Ife, Nigeria. Agricultural Water Management, 213, 1130-1146.

Adhikari, P., N. Omani, S. Ale, P.B., DeLaune, K.R., Thorp, E.M. Barnes, Hoogenboom, G., 2017. Simulated effects of winter wheat cover crop on cotton production systems of the Texas rolling plains. Transactions of the ASABE 60(6):2083-2096.

Akumaga, U., Alderman, P. D., 2019. Comparison of Penman–Monteith and Priestley-Taylor evapotranspiration methods for crop modeling in Oklahoma. Agronomy Journal.

Alagarswamy, G., Singh, P., Hoogenboom, G., Wani, S. P., Pathak, P., Virmani, S. M., 2000. Evaluation and application of the CROPGRO-Soybean simulation model in a Vertic Inceptisol. Agricultural Systems, 63(1), 19-32.

Alfonso, C., Barbieri, P. A., Hernández, M. D., Lewczuk, N. A., Martínez, J. P., Echarte, M. M., Echarte, L., 2020. Water productivity in soybean following a cover crop in a humid environment. Agricultural Water Management, 232, 106045.

Allen, R. G., Pereira, L. S., Raes, D., Smith, M., 1998. Crop evapotranspiration-Guidelines for computing crop water requirements-FAO Irrigation and drainage paper 56. FAO, Rome, 300(9), D05109.

Andales, A. A., Batchelor, W. D., Anderson, C. E., Farnham, D. E., Whigham, D. K., 2000. Incorporating tillage effects into a soybean model. Agricultural Systems, 66(2), 69–98.

Andrade Junior, A. S., da Silva, C. O., de Sousa, V. F., Ribeiro, V. Q., 2018. Avaliação de métodos para estimativa da evapotranspiração de referência no estado do Piauí. Agrometeoros, 25(1).

Arora, V. K., Singh, C. B., Sidhu, A. S., Thind, S. S., 2011. Irrigation, tillage and mulching effects on soybean yield and water productivity in relation to soil texture. Agricultural Water Management, 98(4), 563-568.

Balbinot Junior, A.A., Debiasi, H., Franchini, J.C., Prieto, M. T.M, Moraes, M.T., Werner, F., Ferreira, A. S., 2018. Crescimento e distribuição de raízes de soja em diferentes densidades de plantas. Revista de Ciências Agroveterinárias, 17 (1), 12-22.

Battisti, R., Sentelhas, P. C., 2017. Improvement of Soybean Resilience to Drought through Deep Root System in Brazil. Agronomy Journal, 109(4), 1612-1622.

Bhatt, R., Hossain, A., Hasanuzzaman, M., 2019. Adaptation strategies to mitigate the evapotranspiration for sustainable crop production: A perspective of rice-wheat cropping system. In: p.559-581 [Hasanuzzaman, H. (Ed.)], Agronomic Crops, V.2, Springer, Singapore.

Boote, K. J., Pickering, N. B., 1994. Modeling photosynthesis of row crop canopies. HortScience, 29(12), 1423-1434.

Boote, K. J., Jones, J. W., Hoogenboom, G., Pickering, N. B., 1998. The CROPGRO model for grain legumes. In: pp. 99–128 [Tsuji, G. Y., Hoogenboom, G., and Thornton, P. K. (Eds.)], Understanding options for agricultural production, Kluwer Academic Publishers, London, UK.

Boote, K. J., 1999. Systematic approach and order for calibration. In: pp.185-191 [G. Hoogenboom, P.W. Wilkens, G.Y. Tsuji (Eds.)], Volume 4- DSSAT version 4: Concepts for calibrating crop growth models, IBSNAT, Honolulu, USA.

Boote, K. J., Sau, F., Hoogenboom, G., Jones, J. W., 2008a. Experience with water balance, evapotranspiration, and predictions of water stress effects in the CROPGRO model. In: 59-103 [L.R. Ahuja, V.R. Reddy, S.A. Saseendran, Qiang Yu (Eds.)], Response of Crops to Limited Water: Understanding and Modeling Water Stress Effects on Plant Growth Processes, V.1., Advances in Agricultural Systems Modeling - ASA-CSSA-SSSA, Madison, WI.

Boote, K.J., Jones, J.W., Hoogenboom, G., 2008b. Crop simulation models as tools for agro-advisories for weather and disease effects on production. Journal of Agrometeorology (Indian) 10 Special Issue Part 1:9-17.

Bowen, I. S., 1926. The ratio of heat losses by conduction and by evaporation from any water surface. Physical Review, 27(6), 779.

Brisson, N., Seguin, B., Bertuzzi, P., 1992. Agrometeorological soil water balance for crop simulation models. Agricultural and Forest Meteorology, 59(3–4), 267–287.

Campelo, G. J., Kiihl, R. A. S., Almeida, L. A., 1998. Soybean: development for low latitude regions. Teresina: Embrapa Meio-Norte, 36.

Candogan, B. N., Sincik, M., Buyukcangaz, H., Demirtas, C., Goksoy, A. T., Yazgan, S., 2013. Yield, quality and crop water stress index relationships for deficit-irrigated soybean [*Glycine max* (L.) Merr.] in sub-humid climatic conditions. Agricultural Water Management, 118, 113–121.

Carpentieri-Pípolo, V., Almeida, L. A. D., Kiihl, R. A. D. S., 2002. Inheritance of a long juvenile period under short-day conditions in soybean. Genetics and molecular biology, 25(4), 463-469.

Corbeels, M., Chirat, G., Messad, S., Thierfelder, C., 2016. Performance and sensitivity of the DSSAT crop growth model in simulating maize yield under conservation agriculture. European Journal of Agronomy, 76, 41–53.

Dexter, A. R., 2004. Soil physical quality: Part I. Theory, effects of soil texture, density, and organic matter, and effects on root growth. Geoderma, 120(3–4), 201–214.

Erbs, D. G., Klein, S. A., Duffie, J. A., 1982. Estimation of the diffuse radiation fraction for hourly, daily and monthly-average global radiation. Solar energy, 28(4), 293-302.

Fehr, W. R., Caviness, C. E., 1977. Stages of Soybean Development. Iowa State University Experimental Station Publications, Ames, Iowa, USA.

Garratt, J. R.,1994. The atmospheric boundary layer. Earth-Science Reviews, 37(1-2), 89-134.

Gijsman, A. J., Hoogenboom, G., Parton, W. J., Kerridge, P. C., 2002. Modifying DSSAT crop models for low-input agricultural systems using a soil organic matter–residue module from CENTURY. Agronomy Journal, 94(3), 462-474.

Gonçalves, A.O, Silva, E.H.F.M, Gasparotto, L.G, Mantelatto, J.R, Carmo, S., Fattori Júnior, I.M, Marin, F.R., 2020. Improving indirect measurements of the leaf area index using canopy height. Pesquisa Agropecuária Brasileira, 55, 1-9.

Grimm, S. S., Jones, J. W., Boote, K. J., Hesketh, J. D., 1993. Parameter estimation for predicting flowering date of soybean cultivars. Crop Science, 33(1), 137-144.

Grimm, S. S., Jones, J. W., Boote, K. J., Herzog, D. C., 1994. Modeling the occurrence of reproductive stages after flowering for four soybean cultivars. Agronomy Journal, 86(1), 31-38.

Heilman, J.L., Brittin, C.L., 1989. Fetch requirements for Bowen ratio measurements of latent and sensible heat fluxes. Agricultural and Forest Meteorology, 44, 261–273.

Heinemann, A.B., Hoogenboom, G., Georgiev, G.A. de Faria, R.T. and Frizzone, J.A., 2000. Center pivot irrigation management optimization of dry beans in humid areas. Transactions of the ASAE. 43(6):1507-1516.

Hoogenboom, G., J. W. Jones, K. J. Boote., 1991. A decision support system for prediction of crop yield, evapotranspiration, and irrigation management. In: p. 198-204. [W. F. Ritter (Ed.)] Irrigation and Drainage: Proceedings of the 1991 National Conference. American Society of Civil Engineers, New York, New York.

Hoogenboom, G., C.H. Porter, K.J. Boote, V. Shelia, P.W. Wilkens, U. Singh, J.W. White, S. Asseng, J.I. Lizaso, L.P. Moreno, W. Pavan, R. Ogoshi, L.A. Hunt, G.Y. Tsuji, Jones, J.W., 2019. The DSSAT crop modeling ecosystem. In: p.173-216 [K.J. Boote, editor] Advances in Crop Modeling for a Sustainable Agriculture. Burleigh Dodds Science Publishing, Cambridge, United Kingdom.

Humphreys, E., Kukal, S. S., Eberbach, P. L., 2016. Effects of tillage and mulch on the growth, yield and irrigation water productivity of a dry seeded rice-wheat cropping system in north-west India. Field Crops Research, 196, 219-236.

Hussain, M. Z., Hamilton, S. K., Bhardwaj, A. K., Basso, B., Thelen, K. D., Robertson, G. P., 2019. Evapotranspiration and water use efficiency of continuous maize and maize and soybean in rotation in the upper Midwest US. Agricultural Water Management, 221, 92-98.

Jassal, R. S., Black, T. A., Spittlehouse, D. L., Brümmer, C., Nesic, Z., 2009. Evapotranspiration and water use efficiency in different-aged Pacific Northwest Douglas-fir stands. Agricultural and Forest Meteorology, 149(6-7), 1168-1178.

Jones, J. W., Boote, K. J., Hoogenboom, G., Jagtap, S. S., Wilkerson, G. G., 1989. SOYGRO V5. 42, Soybean crop growth simulation model. User's guide. Florida Agricultural Experiment Station Journal, 8304, 83.

Jones, J. W., Keating, B. A., Porter, C. H., 2001. Approaches to modular model development. Agricultural Systems, 70(2-3), 421-443.

Jones, J. W., Hoogenboom, G., Porter, C. H., Boote, K. J., Batchelor, W. D., Hunt, L. A., Wilkens, P.W, Singh, U, Gijsman, A.J, Ritchie, J. T., 2003. The DSSAT cropping system model. European Journal of Agronomy, 18(3–4), 235–265.

Kader, M. A., Nakamura, K., Senge, M., Mojid, M. A., Kawashima, S., 2020. Effects of colored plastic mulch on soil hydrothermal characteristics, growth and water productivity of rainfed soybean. Irrigation and Drainage, 69(3), 483-494.

Kamienski, C., Soininen, J. P., Taumberger, M., Dantas, R., Toscano, A., Salmon Cinotti, T., Maia, R.F., Torre Neto, A., 2019. Smart water management platform: Iot-based precision irrigation for agriculture. Sensors, 19(2), 276.

Kim, J., Schultz HK, S., 2020. Advances and improvements in modeling plant processes. In: pP. 3–43 [Boote, K (Ed.)], Advances in crop modelling for a sustainable agriculture, Burleigh Dodds Science, London, UK.

Kimball, B. A., Bellamy, L. A., 1986. Generation of diurnal solar radiation, temperature, and humidity patterns. Energy in agriculture, 5(3), 185-197.

Kimball, B. A., Boote, K. J., Hatfield, J. L., Ahuja, L. R., Stockle, C., Archontoulis, S., Baron, C., Basso, B., Bertuzzi, P., Constantin, J., Deryng, D., Dumont, B., Durand, J.L, Ewert, F., Gaiser, T., Gayler, S., Hoffmann, M.P., Jiang, Q., Kim, S.H., Lizaso, J., Srivastava, A., Stella, T., Tao, F., Thorp, K.R., Timlin, D., Webber, H., Willaume, M., Williams, K., 2019. Simulation of maize evapotranspiration: an inter-comparison among 29 maize models. Agricultural and Forest Meteorology, 271, 264-284.

Koeppen, W., 1948. Climatologia: Con Un Estudio de Los Climas de La Tierra. Fondo de Cultura Econômica, Mexico City, Mexico, 478 p.

Li, C., Li, Y., Fu, G., Huang, M., Ma, C., Wang, H., Zhang, J., 2020. Cultivation and mulching materials strategies to enhance soil water status, net ecosystem and crop water productivity of winter wheat in semi-humid regions. Agricultural Water Management, 239, 106240.

Liu, H. L., Yang, J. Y., Tan, C. S., Drury, C. F., Reynolds, W. D., Zhang, T. Q., Bai, J.J, He, P., Hoogenboom, G., 2011. Simulating water content, crop yield and nitrate-N loss under free and controlled tile drainage with subsurface irrigation using the DSSAT model. Agricultural Water Management, 98(6), 1105-1111.

Loague, K., Green, R. E., 1991. Statistical and graphical methods for evaluating solute transport models: overview and application. Journal of Contaminant Hydrology, 7(1–2), 51–73.

Marin, F. R., Angelocci, L. R., Nassif, D. S., Vianna, M. S., Pilau, F. G., da Silva, E. H., Sobenko, L.R, Goncalves, A.O, Pereira, R.A., Carvalho, K. S., 2019. Revisiting the crop coefficient–reference evapotranspiration procedure for improving irrigation management. Theoretical and Applied Climatology, 138(3-4), 1785-1793.

Nijbroek, R., G. Hoogenboom, and J.W. Jones. 2003. Optimal irrigation strategy for a spatially variable soybean field: a modeling approach. Agricultural Systems 76(1):359-377.

Parton, W. J., and Logan, J. A., 1981. A model for diurnal variation in soil and air temperature. Agricultural Meteorology, 23, 205-216.

Parton, W. J., McKeown, B., Kirchner, V., Ojima, D., 1992. Century users manual. Natural Resource Ecology Laboratory, Colorado State University, Fort Collins.

Pereira, A. R., Nova, N. A. V., 1992. Analysis of the Priestley-Taylor parameter. Agricultural and Forest Meteorology, 61(1-2), 1-9.

Perez, P. J., Castellvi, F., Ibanez, M., Rosell, J. I., 1999. Assessment of reliability of Bowen ratio method for partitioning fluxes. Agricultural and Forest Meteorology, 97(3), 141-150.

Pivetta, L. A., Castoldi, G., Santos, G. P. D., Rosolem, C. A., 2011. Soybean root growth and activity as affected by the production system. Pesquisa Agropecuária Brasileira, 46(11), 1547-1554.

Porter, C. H., Jones, J. W., Hoogenboom, G., Wilkens, P. W., Ritchie, J. T., Pickering, N. B., Boote, K., Baer, B. 2004. DSSAT v4 soil water balance module. Decision Support System for Agrotechnology Transfer Version, 4, 1-23.

Porter, C. H., Jones, J. W., Adiku, S., Gijsman, A. J., Gargiulo, O., Naab, J. B. 2010. Modeling organic carbon and carbon-mediated soil processes in DSSAT v4. 5. Operational Research, 10(3), 247–278.

Priestley, C. H. B., Taylor, R. J., 1972. On the assessment of surface heat flux and evaporation using large-scale parameters. Monthly Weather Review, 100(2), 81–92.

Qiu, G. Y., Wang, L., He, X., Zhang, X., Chen, S., Chen, J., Yang, Y., 2008. Water use efficiency and evapotranspiration of winter wheat and its response to irrigation regime in the north China plain. Agricultural and Forest Meteorology, 148(11), 1848-1859.

Qubaja, R., Amer, M., Tatarinov, F., Rotenberg, E., Preisler, Y., Sprintsin, M., and Yakir, D., 2020. Partitioning evapotranspiration and its long-term evolution in a dry pine forest using measurement-based estimates of soil water evaporation. Agricultural and Forest Meteorology, 281, 107831.

Richetti, J., Boote, K. J., Hoogenboom, G., Judge, J., Johann, J. A., Uribe-Opazo, M. A. 2019. Remotely sensed vegetation index and LAI for parameter determination of the CSM-CROPGRO-Soybean model when in situ data are not available. International Journal of Applied Earth Observation and Geoinformation, 79, 110-115.

Ritchie, J. T., 1972. Model for predicting evaporation from a row crop with incomplete cover. Water Resources Research, 8(5), 1204–1213.

Ritchie, J. T., 1981. Water dynamics in the soil-plant-atmosphere system. Plant and Soil, 81-96.

Ritchie, J. T., 1985. A user-orientated model of the soil water balance in wheat. In Wheat growth and modelling. Boston: Springer, 293–305.

Ritchie, J. T., 1998. Soil water balance and plant water stress. In: 41-54 [G. Y. Tsuji, G. Hoogenboom, P. K. Thornton (Eds.)], Understanding Options for Agricultural Production. Kluwer Academic Publishers, London, United Kingdom.

Ritchie, J. T., Porter, C. H., Judge, J., Jones, J. W., Suleiman, A. A., 2009. Extension of an existing model for soil water evaporation and redistribution under high water content conditions. Soil Science Society of America Journal, 73(3), 792-801.

Rosa, M. F., Bonham, C. A., Dempewolf, J., Arakwiye, B., 2017. An integrated approach to monitoring ecosystem services and agriculture: implications for sustainable agricultural intensification in Rwanda. Environmental Monitoring and Assessment, 189(1), 15. https://doi.org/10.1007/s10661-016-5607-6.

Salmerón, M., Purcell, L. C., 2016. Simplifying the prediction of phenology with the DSSAT-CROPGRO-soybean model based on relative maturity group and determinacy. Agricultural Systems, 148, 178–187.

Sau, F., Boote, K. J., Ruíz-Nogueira, B., 1999. Evaluation and improvement of CROPGRO-soybean model for a cool environment in Galicia, northwest Spain. Field Crops Research, 61(3), 273–291.

Sau, F., Boote, K. J., Bostick, W. M., Jones, J. W., Mínguez, M. I., 2004. Testing and improving evapotranspiration and soil water balance of the DSSAT crop models. Agronomy Journal, 96(5), 1243–1257.

Shelia, V., Šimůnek, J., Boote, K., Hoogenbooom, G., 2018. Coupling DSSAT and HYDRUS-1D for simulations of soil water dynamics in the soil-plant-atmosphere system. Journal of Hydrology and Hydromechanics, 66(2), 232–245.

Soldevilla-Martinez, M., Quemada, M., López-Urrea, R., Munoz-Carpena, R., Lizaso, J. I., 2014. Soil water balance: Comparing two simulation models of different levels of complexity with lysimeter observations. Agricultural Water Management, 139, 53–63.

Soltani, A., Sinclair, T. R., 2012. Modeling physiology of crop development, growth and yield. Podicherry: CABi.

Souza, P. I., Egli, D. B., Bruening, W. P.,1997. Water stress during seed filling and leaf senescence in soybean. Agronomy Journal, 89(5), 807–812.

Spitters, C. J. T., 1986. Separating the diffuse and direct component of global radiation and its implications for modeling canopy photosynthesis Part II. Calculation of canopy photosynthesis. Agricultural and Forest meteorology, 38(1-3), 231-242.

Stannard, D.I., 1997. A theoretically based determination of Bowen ratio fetch requirements. Boundary-Layer Meteorology. 83, 375–406.

Suleiman, A. A., Ritchie, J. T., 2003. Modeling soil water redistribution during second-stage evaporation. Soil Science Society of America Journal, 67(2), 377–386.

Suleiman, A. A., Ritchie, J. T., 2004. Modifications to the DSSAT vertical drainage model for more accurate soil water dynamics estimation. Soil science, 169(11), 745-757.

Thornton, P. K., Hoogenboom, G., 1994. A computer program to analyze single-season crop model outputs. Agronomy Journal 86(5):860-868.

Topp, G. C., Davis, J. L., Annan, A. P., 1980. Electromagnetic determination of soil water content: Measurements in coaxial transmission lines. Water resources research, 16(3), 574-582.

Tsuji, G. Y., Hoogenboom, G., Thornton, P. K., 1998. Understanding Options for Agricultural Production. Systems Approaches for Sustainable Agricultural Development. Kluwer Academic Publishers, Dordrecht, the Netherlands. 400 pp.

Valentín, F., Nortes, P. A., Domínguez, A., Sánchez, J. M., Intrigliolo, D. S., Alarcón, J. J., and López-Urrea, R., 2020. Comparing evapotranspiration and yield performance of maize under sprinkler, superficial and subsurface drip irrigation in a semi-arid environment. Irrigation Science, 38(1), 105–115.

Viana, J. S., Gonçalves, E. P., Silva, A. C., Matos, V. P., 2013. Climatic conditions and production of soybean in northeastern Brazil. A Comprehensive Survey of International Soybean Research-Genetics, Physiology, Agronomy and Nitrogen Relationships. InTech, 377–392.

Uryasev, O., Gijsman, A. J., Jones, J. W., Hoogenboom, G., Wilkens, P. W., Porter, C. H., 2004. Soil data editing program (Sbuild). In: pp. 2-14 [P. W. Wilkens, G. Hoogenboom, Porter, C. H., J. W. Jones, O. Uryasev (Eds.)], Volume 2- DSSAT version 4: Concepts for calibrating crop growth models, IBSNAT, Honolulu, USA.

Villa Nova, N. A., Pereira, A. B., 2006. Ajuste do método de Priestley-Taylor às condições climáticas locais. Engenharia Agrícola, 26(2), 395-405.

Wilkerson, G. G., Jones, J. W., Boote, K. J., Ingram, K. T., Mishoe, J. W., 1983. Modeling soybean growth for crop management. Transactions of the ASAE, 26(1), 63-0073.

Williams, J. R.,1991. Runoff and water erosion. In Modeling Plant and Soil Systems. Wisconsin: ASA-CSSA-SSSA, 439–455.

Willmott, C. J., Ackleson, S. G., Davis, R. E., Feddema, J. J., Klink, K. M., Legates, D. R., O'Donnell, J., Rowe, C. M., 1985. Statistics for the evaluation and comparison of models. Journal of Geophysical Research: Oceans, 90(C5), 8995–9005.

Zaffar, M., Sheng-Gao, L. U., 2015. Pore size distribution of clayey soils and its correlation with soil organic matter. Pedosphere, 25(2), 240–249.

Zeleke, K. T., Wade, L. J., 2012. Evapotranspiration estimation using soil water balance, weather and crop data. Evapotranspiration: remote sensing and modeling, 1, 41-58.

Zhou, H., Zhi Zhao, W., 2019. Modeling soil water balance and irrigation strategies in a flood-irrigated wheat-maize rotation system. A case in dry climate, China. Agricultural Water Management, 221, 286–302.

3. PERFORMANCE OF THE CSM-CROPGRO-SOYBEAN IN SIMULATING SOYBEAN GROWTH AND DEVELOPMENT WITH N-FERTILIZATION UNDER TROPICAL CONDITIONS

Abstract

Nitrogen (N) is important to global food production and the nutrient most demanded by soybean. Soybean represents more than 60% of all plant protein produced in the world, being a key crop for food security, in this sense many studies have evaluated N fertilization in soybean agricultural systems. Cropping System Model (CSM)-CROPGRO-Soybean can be used for simulating the effects of high rates of N-fertilization in soybean. Our goal in this study was to evaluate the effect of N-fertilization in soybean crops under tropical and subtropical environments using nine well-managed field experiments and crop modeling. Furthermore, the experiments were conducted under different water availability, soils, and cultivars. Field experiments were conducted in Brazil: (i) Piracicaba over three seasons with TGM 7062 cultivar; (ii) Sorriso over two seasons with TMG 7063 cultivar and NS 7901 cultivar; (iii) Cruz Alta over one season with 65i65RSF cultivar; (iv) Tupanciretã over one season with 65i65RSF cultivar; and (v) Teresina, 8579RSF (one season). The results showed that the N-fertilization was not able to increase crop yield in experiments conducted under non-limiting water conditions. However, under water-limited conditions there were marginal or no response to N-fertilization, and we attributed these crop yield increases to unfavorable environmental conditions. N-fertilization provided consistently increasing on grain protein concentration under field experiments. Also, the results showed that the model was able to simulate soybean growth and development for the different sites and water availability, with good agreement for all sites (D > 0.80), except for Tupanciretã where the D was greater than 0.60. The yield gains from N fertilization were not proportional to the amount of N-fertilizer (1,000 kg ha^{-1}). The observed crop yield increases in field ranged from 19 to 626 kg ha^{-1}, and the simulated increase was 5 to 995 kg ha^{-1}. The model was able to predict the effects on N concentration in vegetative and seed tissues (D > 0.80). Simulations of soil inorganic N balance suggested very high losses of N by volatilization for urea-N-fertilization treatments. The long-term scenarios simulated for Piracicaba and Teresina showed that the use of doses higher than 600 kg ha^{-1} are potentially inappropriate.

Keywords: Nitrogen balance; High crop yield; Ammonium volatilization; Urea.

3.1. Introduction

The soybean yield increase is closely related to the total plant nitrogen (N) uptake because N is the nutrient most demanded by soybean. The soybean system in the world is mostly fed by both symbiotic fixation of atmospheric N_2 (SNF) and from soil minerals, not rely upon N-fertilizer application (Herridge *et al*., 2008; Reis *et al*., 2021). N is important in global food production, and impacts on the environment related to ammonia (NH_3) volatilization

(Erisman *et al*., 2008; Dari and Rogers, 2021). Although NH_3 itself is not a greenhouse gas, NH_3 volatilization and subsequent re-deposition indirectly cause nitrous oxide (N_2O) emissions, which have a 298 times higher global warming potential than carbon dioxide (CO_2) (Ferm, 1998; IPCC, 2013). In this sense, the SNF process on soybean crop systems plays an important role in climate preservation and agriculture sustainability. However, has recently been a concern whether biological N_2 fixation will be enough to meet the increased N needs for soybean high-yield (Cafaro La Menza *et al*., 2017, 2019, 2020).

That way, soybean yield increasing often raises the debate on nitrogen (N) fertilization has been resurrected, with the focus on increasing production in highly productive environments (*e.g*., Ray *et al*., 2006, Salvagiotti *et al*., 2009; Cafaro La Menza *et al*., 2017; Zhou *et al*., 2019; Cafaro La Menza *et al*., 2020) or using N-fertilization combined with high doses of inoculations with N-fixing bacteria for increasing soybean yield in unfavorable environments (Cordeiro and Echer, 2019). In older studies on N-fertilization of soybean, the focus was: (i) increasing in protein grain concentration (Nakasathien *et al*., 2000); (ii) N supply interaction with atmospheric carbon dioxide CO_2 concentrations (Sims *et al*., 1998) and (iii) increasing crop yield (Ojima *et al*., 1965; Sinclair and Wit, 1976; Hayati and Crafts-Brandner, 1995; Barker and Sawyer, 2005; Ray *et al*, 2006). Despite the considerable number of studies on N-fertilization of soybean, these are still not conclusive and sometimes contradictory to each other.

Crop modeling can contribute for interpreting studies of N-fertilization of the soybean crop. Soybean crop models have been available since the 1980s with the original version of SOYGRO V4.2 (Wilkerson *et al*., 1983). The model version described by Boote *et al*. (1998) was improved with the incorporation of water balance (Ritchie, 1985) and crop phenological modules (Grimm *et al*., 1994; Piper *et al*., 1996). After various improvements (see Jones *et al*., 1989), the SOYGRO model was the origin of the CROPGRO model, with improvements such as leaf-level, hedgerow canopy photosynthesis (Boote and Pickering, 1994; Boote *et al*., 1998), an N_2 fixation module (Boote *et al*, 2009), soil N balance, and N uptake features (Godwin and Jones, 1991; Godwin and Singh, 1998). We are not aware of any study that addressed crop modelling with the nitrogen use on soybeans under tropical and subtropical environments, and this chapter will also contribute to studies of soybean yield potential in Brazil (Chapter 4).

In this chapter, we sought to test the hypothesis that high N-fertilization can contribute for achieving high soybean yield, protein or oil concentration under tropical and subtropical conditions. Thus, we had 8,945 kg ha^{-1} as crop yield target, this value is based on the maximum

soybean yield obtained, until the season 2016/2017, in contest areas in Brazil (CESB, 2017 and later reported by Battisti *et al*, 2018).

3.1.1. Research goals

The goals of the present chapter were improving the understanding regards soybean growth, crop yield, seed protein and oil concentration, and N-fertilization under tropical and subtropical environments in Brazil. Specific objectives of this chapter were: (i) to conduct well-managed soybean experiments under tropical and subtropical conditions, (ii) to evaluate the effect of N-fertilizer on soybean growth, crop yield, seed protein and oil concentration under water-limited and non-limiting water conditions, (iii) to calibrate and evaluate the CROPGRO-Soybean, (iv) to drive to understand the relations between soybean growth and development, soil and plant N balance, and N-fertilization using CROPGRO-Soybean as tool.

3.2. Materials and Methods

3.2.1. Field experiments

The experiments were conducted with two-way treatment (environment x N-fertilization) structure in randomized complete block, design with four replications, each plot measuring 54 m^2, under water-limited or non-limiting water conditions. The environments were defined as the combination of locations, seasons, sowing dates, and cultivars: (i) Piracicaba (22°42′N, 47°30′W, 546 a.m.s.l), during three crop seasons [2017/2018 (PI-1), 2018/2019 (PI-2), and 2019/2020 (PI-3)], conducted under conventional tillage on a Eutric Rhodic Ferralic Nitisol, previous crop was maize (*Zea mays* L.) for P1-1 and PI-3, and wheat (*Triticum aestivum* L.) for PI-2; (ii) Sorriso (12°42′S, 55°48′W, 375 a.m.s.l), during two crop seasons [2018/2019 (SO-1) and 2019/2020 (SO-2)], conducted under conventional tillage on Dystrophic Red Yellow Ferrosol, where the crop prior to planting was degraded pasture area for SO-1, and maize for SO-2; (iii) Cruz Alta (28°38′S, 53°36′W, 476 a.m.s.l), during one crop season [2018/2019 (CA-1)], conducted under no-tillage practices on Dystrophic Red Acrisol, previous crop was wheat; (iv) Tupanciretã (28°48′S, 53°48′W, 466 a.m.s.l) during one crop season [2019/2020 (TU-1)], conducted under no-tillage on Dystrophic Red, previous crop was maize; and (v) Teresina (05°02′S, 42°47′W, 78 a.m.s.l) during one crop season [2019 (TE-1)],

conducted under conventional tillage on Dystrophic Red Yellow Acrisol, previous crop was cowpea (*Vigna unguiculata* L.) (Table 3.1).

The N-fertilizer treatments were: (i) no N-fertilizer (0N), the soybean only relied on indigenous soil N sources (inorganic soil N, mineralized N, and N fixed from biological symbiosis); and (ii) with N-fertilizer (1000N). For computing the amount of N-fertilizer we considered the yield target of 8,945 kg ha^{-1}, and that soybean crop accumulates is 79 kg N ha^{-1} in its aboveground biomass per each additional 1,000 kg of seed yield (Salvagiotti *et al*., 2008; Tamagno *et al*., 2017), with extra 40% on application to compensate N losses through ammonium volatilization (Cantarella *et al*., 2018), and plus 1.5% on application to compensate others N losses. Therefore, amounting 1,000 kg N ha^{-1}, using urea (45 00 00) as nitrogen source. The urea amount applied was split in several applications during the crop season following N supply and crop N demand reported by Thies *et al*. (1995) and Bender *et al*. (2015): (i) 10% in V2; (ii) 10% in V4; (iii) 20% in R2; (iv) 30% in R3; (v) 30% in R5. For both treatments, the seeds were inoculated with *Bradyrhizobium elkanii* (strains SEMIA 587 and SEMIA 5019) at a concentration of $5x10^9$ CFU mL^{-1} (colony forming units).

The experiments were conducted under water-limited or non-limiting water conditions. The water-limited experiments (total of 8), were conducted under rainfed conditions at Piracicaba (three crop seasons), Sorriso (two crop seasons), Cruz Alta (one crop season), Tupanciretã (one crop season). For one crop season at Teresina the crop was grown under irrigation to supply 50% of full crop water requirement. For non-limiting water treatment (total of 5), crops were irrigated at 100% of water requirements supplied by irrigation at Piracicaba (three crop seasons), Tupanciretã (one crop season) and Teresina (one crop season).

The irrigation amounts applied on non-limiting water conditions treatment were determined by the potential evapotranspiration determined by Priestley-Taylor method; computed using the daily weather data measured with well-calibrated sensors from the on-site weather station (see Appendix B, I, J, K, L). The Priestley-Taylor was applied under minimum advection conditions and using empirical parameter α=1.26 (Pereira and Villa Nova, 1992). The water amount required was applied with sprinkler irrigation by: (i) center pivot sprinklers Senninger Model i-Wob-UP3 at Piracicaba; (ii) center pivot sprinklers Plona KS 1500 at Tupanciretã, and (iii) line-source sprinkler technique, Fabrimar Model A232 at Teresina. The irrigation water amounts applied were: (i) 50 mm for PI-1, (ii) 260 mm for PI-2, (iii) 150 mm for PI-3, (iv) 270 mm for TU-1, and (v) 366 mm (R) and 529 mm (I) for TE-1 (see irrigation amounts distributions on Appendix B, I, J, K, L).

Table 3.1. Description of field experiments conducted in Piracicaba (PI-1, PI-2, and PI-3), Sorriso (SO-1 and SO-2), Cruz Alta (CA-1), Tupanciretã (TU-1), and Teresina (TE-1) under water-limited conditions (R) or non-limiting water conditions (I), with zero (0N) or 1,000 kg N ha^{-1} (1000N).

Sites	Experiments	Treatments	Crop season	Cultivar and maturity group (MG)	Sowing date	Harvest date	Sowing density (plant m^{-1})
Piracicaba	PI-1	R, I, 0 N,	2017/2018	TMG 7062	Dec 26	Apr 13	28
	PI-2	1000N	2018/2019	MG (6.0)	Nov 11	Mar 17	
	PI-3		2019/2020		Nov 27	Mar 23	28
Sorriso	SO-1	R, 0N,	2018/2019	TMG 7063	Nov 20	Mar 7	30
		1000N		MG (7.0)			
	SO-2	R, 0N,	2019/2020	NS 7901	Nov 01	Mar 3	30
		1000N		MG (8.0)			
Cruz Alta	CA-1	R, 0N,	2018/2019	65i65RSF	Nov 28	Mar 31	35
		1000N		MG (6.0)			
Tupanciretã	TU-1	R, I, 0 N,	2019/2020	65i65RSF	Dec 03	Apr 14	35
		1000N		MG (6.0)			
Teresina	TE-1	R, I, 0 N,	2019	8579RSF	Jul 23	Oct 21	22
		1000N		MG (8.0)			

Macronutrient fertilization was computed based on surface and subsurface soil analysis (Appendix M). Soil nutrient initial levels under all experiments were as follows: 0.9 to 3.1% of organic matter (Walkey-Black method), 0.7 to 27.0 mg P dm^{-3} (Melich-1 method), 0.2 to 5.4 K $mmol_c$ dm^{-3} (Melich-1 method), 4.0 to 19.0 Mg $mmol_c$ dm^{-3} (extracted by calcium acetate), 10.6 to 44.2 Ca $mmol_c$ dm^{-3} (extracted by calcium acetate), 3.0 to 15.0 mg S kg^{-1} (turbidimetry method) (Appendix D). The soil fertilization sought to reach: P > 26 mg dm^{-3}, K > 2.5 $mmol_c$ dm^{-3}, Mg > 13 mmol dm^{-3}, Ca > 26 $mmol_c$ dm^{-3}, S > 15 mmol dm^{-3}. The soybean micronutrients were supplied via foliar fertilization based on crop cycle and extraction and export of micronutrients (see fertilization management on Appendix E). Sowing density ranged from 22 to 35 plants m^{-1} (Table 3.1). Field observations and measurements for each experiment included: (i) daily phenology with recorded dates of emergence, beginning flowering (R1), beginning pod (R3), beginning seed (R5), and physiological maturity (R7), when 50% of the plants were at each stage (Fehr and Caviness, 1977); (ii) leaf area index (LAI) at approximate 10-day intervals between V3 and R7, using plant canopy analyzer LI-COR Model LAI-2200C following the recommendations proposed by Gonçalves *et al*. (2020); (iii) biomass samples collected for a single 1-m length of row (0.5 m^2 land area) from each replication at approximately 10-day intervals; (iv) seed protein concentration was determined by Kjeldahl procedure (described by Detmann *et al*., 2012a); and (v) oil seed concentration was determined by Goldfish procedure (described by Detmann *et al*., 2012b). The biomass was separated into

leaf, stem plus petiole, aboveground biomass [(ADM) defined as sum of total top dry matter (leaf, stem-petiole, pod and grain), fallen and senesced leaves were not included], (iii) seed yield (kg ha^{-1})], and grain, which were weighed after oven drying to constant weight at 70 ± 5ºC. For TE-1, we also determined the N concentration in leaf, stem and grain over time by Kjeldahl procedure (described by Detmann *et al*., 2012a) for all treatments. The final harvest grain yield determinations were made on three center rows (9 m^2) for four replications.

3.2.2. Crop model

The CROPGRO-Soybean model simulates crop growth and development, carbon balance, crop and soil N balance, and soil water balance (Boote *et al*., 1998, 2008, 2009). Crop growth and development processes depend on temperature, crop photosynthesis rate, and current crop state (see Wilkerson *et al.*, 1983; Jones *et al.*, 1989; Boote *et al*., 1998); those processes and environments influence dry-matter partitioning of soybean over time. The time step in the model is hourly to compute: (i) distribution of temperatures (see Parton and Logan, 1981; Kimball and Bellamy, 1986), (ii) solar radiation, (iii) photosynthetic photon flux density, considering photosynthetic irradiance split into direct and diffuse components (see Erbs *et al.*, 1982; Spitters, 1986; Spitters *et al.*, 1986), and (iv) leaf-level, hedgerow canopy photosynthesis (Boote and Pickering, 1994).

Daily inputs from photosynthesis, conversion of carbon (C) into crop tissues, C losses through senescence process and maintenance respiration are considered in crop C balance (Boote *et al*., 2009). The C balance in the model includes all carbohydrate use and mobilization processes that are related to vegetative tissue growth and senescence process (Boote *et al*., 2009). The crop N balance includes daily soil N uptake, N_2 fixation, mobilization and translocation of N from old vegetative tissues to new growth of vegetative or reproductive tissues, rate of N use for new tissue growth, and rate of N loss in abscised parts. Soil N balance processes are those described by Godwin and Jones (1991) and Godwin and Singh (1998). The soil N balance processes in CROPGRO-Soybean include root N uptake, mineralization, immobilization, nitrification, denitrification, and N leaching processes, with options of using either the Godwin or Century soil organic carbon modules (Gijsman *et al.*, 2002).

The Priestley-Taylor (Priestley and Taylor, 1972) is the default option for simulating potential evapotranspiration and Suleiman–Ritchie (Suleiman and Ritchie, 2003) method is currently the default option for simulating soil water evaporation. Nevertheless, we have conducted the simulation using the FAO-56 Penman-Monteith potential evapotranspiration

method (Allen *et al.*, 1998) combined with Ritchie Two-Stage soil water evaporation method (Ritchie, 1972) because we found better performance for those two methods for tropical and subtropical environment (see Chapter 2). Century (Parton *et al.*, 1992; Gijsman *et al.*, 2002) was chose as the soil organic matter method, using default organic carbon content being set by soil texture. The initial conditions of the simulations were set to soil moisture at 50% of available soil water to start soil water balance of the model at 30 days prior to sowing. The inorganic N soil concentration was obtained by soil analyses (see Appendix M). For all simulations, the symbiosis (N_2 fixation) option was turned on. The N fertilization treatments were simulated with real distribution of the N-fertilizer over time applied in the field experiments. The soil profiles data were computed with the SBUILD program of DSSAT (Uryasev *et al.*, 2004), using the soil granulometry (texture) obtained on each site (see Appendix F).

Calibration of cultivar coefficients for: (i) TMG 7062 was carried out using the experimental data from Piracicaba (PI-1), under fully-irrigated conditions for the 0N treatment, (ii) TMG 7063 was carried out using the experimental data from Sorriso (SO-1), under rainfed conditions for the 0N treatment; (iii) NS7901 was carried out using the experimental data from Sorriso (SO-2), under rainfed conditions for the 0N treatment; (iv) 65i65RSF was carried out using the experimental data from Cruz Alta (CA-1), under rainfed conditions for the 0N treatment; and (v) 8579RSF was previously calibrated for this cultivar and field, used fully-irrigated treatment for the 0N from season 2019 (see Chapter 2).

We estimated cultivar parameters following the calibration procedures developed by Boote (1999) as summarized in three phases: (i) first phase, simulations were evaluated using the default cultivar parameters (M GROUP 6 for TMG 7062 and 65i65RSF; M GROUP 7 for TMG 7063, and M GROUP 8 for NS7901) using weather variables measured on-site (Appendix B, I, J, K, L), soil (Appendix F), and management for each site; (ii) second phase, only the crop phenology coefficients were calibrated against observed phenological stages (R1, R3, R5, and R7); and (iii) third and final phase, crop growth coefficients were considered in the calibration against growth analysis and final yield data. After third phase of calibration, we calibrated the parameters SDPRO (fraction protein in seeds) and SDLIP (fraction oil in seeds) by trial-and-error method against observed seed oil and protein concentration values, using data from PI-1, SO-1, SO-2, CA-1, and TE-1. The cultivar traits obtained after final calibration are shown in Appendix G.

To evaluate the accuracy of CROPGRO-Soybean model for the R1, R3, R5, and R7 phenological stages (Fehr and Caviness, 1977), the simulations were compared with observed data for: (i) TMG 7062 using data set from PI-1 (R-0N), PI-2 (R-0N and I-0N), PI-3 (R-0N and I-0N); (ii) 65i65RSF using data set from TU-1 (R-0N and I-0N); and (iii) 8579RSF was previously evaluated using data set from TE-1 (R-0N). However, for cultivars TMG 7063 and NS7901, it was not possible to evaluate the performance of the model in relation to crop phenology, because these were conducted in one crop season with only one treatment of water availability.

Also, the accuracy of CROPGRO-Soybean model was evaluated for its capacity to simulate LAI, leaf and stem dry matter, aboveground biomass, grain weight, seed protein concentration [estimated by multiplying grain N concentration simulated by 6.25 (Mariotti, 2008)], and oil seed concentration for: (i) TMG 7062 using measured data obtained in PI-1, PI-2 and PI-3; (ii) TMG 7063 using measured data obtained in SO-1; (iii) NS7901 using measured data obtained in SO-2; (iv) 65i65RSF using measured data obtained in CA-1 and TU-1; and (v) 8579RSF using measured data obtained in TE-1.

For TE-1 we conducted a case study to illustrate simulated N concentration in leaf, stem, and grain over time compared with observed values over time. We chose the experiments conducted in Teresina because this is the most adverse environment for soybean cultivation among the experiments conducted in this study. TE-1 was conducted under sandy soil, less solar radiation availability during the crop season, and higher air temperatures (Appendix B).

After calibration and evaluation, the CROPGRO-soybean model was used to explore soil inorganic N balance that included simulated outputs of soil N state variables relative to N inputs and losses such as: (i) soil N initial; (ii) mineralized N; (iii) N-fertilizer, (iv) N-fixation; and N subtractions: (v) N immobilized; (vi) N leached; (vii) N uptake; (viii) ammonia (NH_3) loss; (ix) other losses, included nitrous oxide (N_2O), dinitrogen (N_2), and nitric oxide (NO); (x) soil N final. Also, we analyzed the simulated plant N balance that included N fixed (from biological fixation) and N uptake from soil.

3.2.3. Hypothetical scenarios of N-fertilizer of soybean

After calibration and evaluation of CROPGRO-Soybean using measured data obtained in several field experiments, we applied the model to explore different N-fertilization doses to

ask what-if questions (Thornton and Hoogenboom, 1994) by conducting virtual simulation experiments in Piracicaba and Teresina. Our objective with these hypothetical scenarios was to investigate if there is any N-fertilizer dose that contributes to sustainable increase of soybean yield under tropical and subtropical conditions. This included irrigated experiments (fully irrigated conditions, automatic when required option) under 0; 100; 200; 300; 400; 500; 600; 700; 900; 1,000 kg N ha^{-1}. The simulations were set using urea as N source, applied 40 days after planting using surface broadcast application method. We chose these simulation options to mimic the real situation in Brazilian agriculture: (i) urea is the most common N-fertilizer in Brazil (Mazzetto *et al*., 2020), and (ii) soybean crop is usually soil fertilized at planting and around 40 DAP [end of vegetative phase), usually with potassium sources], so this did not replicate the protocol of N-fertilization applied in the field experiments, with five splits doses. From a realistic viewpoint, no farmer-producer would apply high N doses at planting, so we applied the N-fertilizer at 40 DAP. For these simulations we used the planting date and initial soil water conditions from the PI-1 and from the TE-1. The simulations were repeated for 30 seasons using long-term historical weather data from 1989 to 2020 for both sites (Appendix H). It was not possible to simulate long-term scenarios for Sorriso, Cruz Alta, and Tupanciretã because we lacked available historical measured weather data for 30 seasons.

The long-term scenarios were evaluated for N-fertilizer effect on crop yield, crop N productivity (CNP) and ammonium volatilization during the growing season. The CNP has been defined as amount of biomass produced per unit of N uptake (Ågren and Igestad, 1987). Thus, we computed simulated CNP as the ratio between simulated crop yield (kg ha^{-1}) and sum of N uptake from soil and N fixed (kg ha^{-1}).

3.2.4. Statistical analysis

Bartlett test (Milliken and Johnson, 2009) was applied to investigate the homogeneity of variances, and we concluded that variances were equal (p-value > 0.05) for all field experiments. Once the homogeneity of within-environment variances was obtained, we conducted the combined analysis of variance (AOV) to determine the effect of environments and N treatments on LAI, ADM, to determine the effect of water and N treatments on final aboveground biomass, crop yield, seed protein concentration, and seed oil concentration; and the means were compared by the Tukey test considering the significance level of 5% (agricolae package, Team R Core, https://www.r-project.org).

The model performance was evaluated by comparing simulated values with observed data from Piracicaba, Sorriso, Cruz Alta, Tupanciretã, and Teresina. We used the root mean square error (RMSE) (Loague and Green, 1991), index of agreement (D) (Willmott *et al.*, 1985), and difference (B) as measures of goodness-of-fit. We used the RMSE to assess the error associated with simulation in relation to observed data. The D is an index of the extent to which the observed values are approached by the model simulated values; it ranges from 0 to 1, with 0 indicating no agreement between the observed and predicted values and 1 indicating perfect agreement. The B measures the difference between simulated and observed final values, if the model under-predicts, the B is negative or if the model overpredicts B is positive. Thus, a high value for the D, a low value for RMSE, and B near zero would imply better performance. The statistics were calculated using the following equations:

$$RMSE = \sqrt{\frac{\sum_{i=1}^{n}(s_i - o_i)^2}{n}} \quad (1)$$

$$D = 1 - \left[\frac{\sum_{i=1}^{n}(s_i - o_i)^2}{\sum_{i=1}^{n}|(s_i - \bar{o}| + |o_i - \bar{o}|)^2}\right], 0 \leq \mathrm{D} \leq 1 \quad (2)$$

$$\mathrm{B} = s_i - o_i \quad (3)$$

where n is number of observations; s_i is simulated, value corresponding to measurement i on each date; o_i is observed value for measurement i; and $\bar{o}$ is the average of observed values.

3.3. Results and Discussion

3.3.1. Analysis of field experiments

A statistically significant effect of the environment on all variables was observed in the AOV under experiments conducted in both water availability conditions (Table 3.2). Also, we observed a significant effect of N treatments on seed yield, seed protein and oil concentration. Variables LAI and ADM did not show significant effects for N-fertilization. There was interaction between environments and N-fertilization treatments for seed yield, seed protein, and seed oil under water-limited conditions, as well as for ADM and seed oil under non-limiting water conditions.

Table 3.2. Analysis of variance for effects of environments, N-fertilization treatment, and interaction between environments x N-fertilization in randomized complete block design structure in experiments with water-limited conditions.

Source of Variation		LAI	ADM	Crop yield	Seed protein	Seed oil
Water-limited experiments						
Design structure	df	F	F	F	F	F
Blocks	3	0.64	0.63	0.83	0.73	0.83
Treatment structure						
Environment	7	97.16***	114.89***	265.24***	97.10***	115.87***
N	2	0.06	2.07	17.23***	121.68***	3.87
Environment x N	6	1.90	1.70	3.55**	5.44***	10.74***
Error structure		MS	MS	MS	MS	MS
Block x treatments	45	0.22	567495	61467	1.39	0.18
Non-limiting water experiments						
Design structure	df	F	F	F	F	F
Blocks	3	0.11	1.36	0.10	1.52	2.06
Treatment structure						
Environment	4	67.77***	52.91***	47.59***	92.12***	367.06***
N	1	2.01	1.26	2.16	33.44***	2.82
Environment x N	4	1.96	4.56**	0.281	1.34	7.21***
Error structure		MS	MS	MS	MS	MS
Block x treatments	27	0.30	806237	2318131	1.45	0.144

df = degrees of freedom; F = F-statistic; LAI = maximum leaf area index; ADM = final aboveground biomass. Statistical significance was indicated by: * =p-value <0.05; ** = p-value <0.01; ***= p-value<0.001.

For testing the interaction effects, an analysis of variance was carried out for the effects of N-fertilization treatment for each environment (Table 3.3). We found a statistically significant effect due to the interaction of N-fertilization and environment, under water-limited water conditions for: (i) seed yield in CA-1, PI-1, PI-2, and SO-1; (ii) seed protein in PI-1, PI-2, PI-3, SO-1, SO-2, CA-1, and TU-1; and (iii) seed oil for PI-1, PI-3, SO-1, SO-2, CA-1, TU-1, and TE-1. For experiments conducted under non-limiting water conditions, we obtained interaction effects for: (iv) ADM in PI-2, PI-3; and (v) seed oil in TU-1, and TE-1.

The maximum leaf area index varied from 1.8 to 8.9 among all experiments because of variation in weather, soil, sowing date, and cultivar (Fig.3.1). The maximum LAI was obtained in CA-1 environment with 1000N treatment. The experiments conducted in the PI-2 environment were affected by drought. Under water-limited conditions the average LAI was 5.3 while under non-limiting water conditions it was 7.2. For Piracicaba and Sorriso, locations where the experiment was conducted for more than one season, the earliest sowing dates; PI-2 for Piracicaba and SO-2 for Sorriso reached a higher LAI compared to later sowing dates. Thus, sowing dates apparently influenced soybean growth (Fig. 3.1).

Diversity of environments resulted in a wide range of ADM from 2,193 to 13,448 kg ha-1 (Fig. 3.2). The ADM responded positively to N-fertilization in PI-1 and PI-3 under non-limiting water conditions. The average ADM increase between 0N and 1000N was 2,132 kg ha-1 for PI-2 and 1,641 kg ha-1 for PI-3.

Table 3.3. Analysis of variance for effects of N-fertilization for each environment.

Source of Variation		ADM	Seed Yield	Seed Protein	Seed oil
Water-limited experiments					
	df	F	F	F	F
N x PI-1	1	-	7.37**	13.14**	4.35*
N x PI-2	1	-	11.53**	4.65***	0.03
N x PI-3	1	-	0.01	7.11*	5.46*
N x SO-1	1	-	12.78***	54.78*	5.69*
N x SO-2	1	-	2.92	45.86***	11.14**
N x CA-1	1	-	6.64*	8.50**	35.19***
N x TU-1	1	-	0.17	25.31***	9.63**
N x TE-1	1	-	0.66	0.39	7.58**
Residual	45	-	-	-	-
Non-limiting water experiments					
N x PI-1	1	0.17	-	-	2.52
N x PI-2	1	11.28**	-	-	1.71
N x PI-3	1	6.68*	-	-	1.71
N x TU-1	1	1.29	-	-	20.31**
N x TE-1	1	0.21	-	-	5.44*
Residual	27	-	-	-	-

df = degrees of freedom; F = F-statistic; ADM = final aboveground biomass. Statistical significance was indicated by: * =p-value <0.05; ** = p-value <0.01; ***= p-value<0.001.

N-fertilization promoted seed yield increase at PI-1, PI-2, SO-1, and CA-1 under water-limited conditions (Fig. 3.3A). The seed yield increase obtained with 1000N was 476 kg ha^{-1} for PI-1, 596 kg ha^{-1} for PI-2, 627 kg ha^{-1} for SO-1, 452 kg ha^{-1} for CA-1 (Fig. 3.3A). There was also an unexpected result as the seed yield decreased with 1000N treatment for SO-2. We associated this yield decrease with the observed early leaf senescence from low canopy layers after R5 (Fehr and Caviness, 1977). We did not find any logical reason for soybean response to N-fertilization obtained in SO-2.

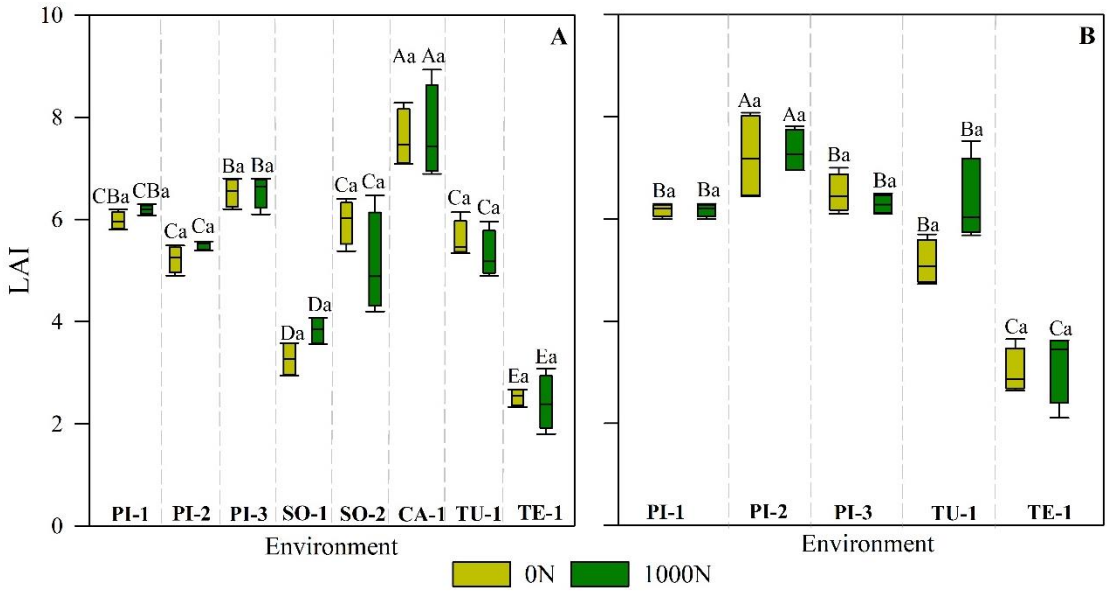

Fig. 3.1. Maximum leaf area index (LAI) under water-limited conditions (A) or non-limiting water conditions (B), with zero (0N) or 1,000 kg N ha^{-1} (1000N). For experiments conducted in Piracicaba (PI) under three seasons, Sorriso (SO) under two seasons, Cruz Alta (CA) under one season, Tupanciretã (TU) under one season, and Teresina (TE) under one season. Means followed by different letters, uppercase among environments and lowercase between N-treatment for each environment, differ by Tukey test ($p < 0.05$). Boxplots are set at 90th (the upper whisker) and 75th (the upper quartile), mean (black line inside the box).

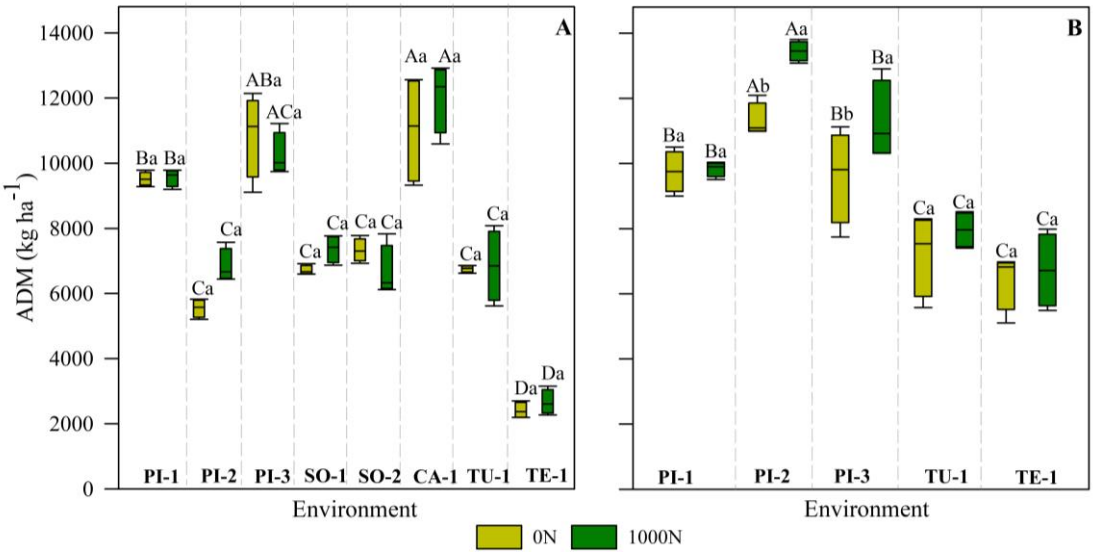

Fig. 3.2. Final aboveground biomass (ADM) under water-limited conditions (A) or non-limiting water conditions (B), with zero (0N) or 1,000 kg N ha^{-1} (1000N). For experiments conducted in Piracicaba (PI) under three seasons, Sorriso (SO) under two seasons, Cruz Alta (CA) under one season, Tupanciretã (TU) under one season, and Teresina (TE) under one season. Means followed by different letters, uppercase among environments and lowercase between N-treatment for each environment, differ by Tukey test ($p < 0.05$). Boxplots are set at 90th (the upper whisker) and 75th (the upper quartile), mean (black line inside the box).

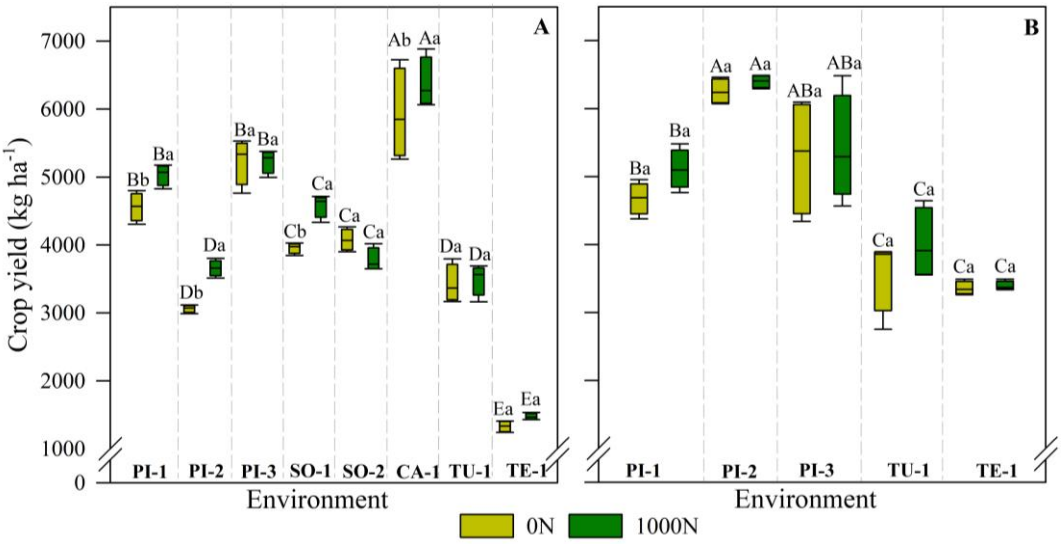

Fig. 3.3. Seed yield under water-limited conditions (A) or non-limiting water conditions (B), with zero (0N) or 1,000 kg N ha^{-1} (1000N). For experiments conducted in Piracicaba (PI) under three seasons, Sorriso (SO) under two seasons, Cruz Alta (CA) under one season, Tupanciretã (TU) under one season, and Teresina (TE) under one season. Means followed by different letters, uppercase among environments and lowercase between N-treatment for each environment, differ by Tukey test ($p < 0.05$). Boxplots are set at 90th (the upper whisker) and 75th (the upper quartile), mean (black line inside the box).

Crop yield in 9 of the 13 number needed soybean experiments failed to respond to N-fertilization on soybean. Only four positive responses for crop yield increase for N-fertilization were obtained in PI-1, PI-2, SO-1 and CA-1 under water-limited conditions. The greatest yield increase provided by N-fertilization was 627 kg ha^{-1} (13.3%) in SO-1 R-1000N (prior to planting it was degraded pasture area), because the environment seemingly was limited for SNF for two reasons: 1) the soil had no prior initial inoculum of N-fixing bacteria (no prior soybean crop), and 2) low initial soil phosphorus content (see Appendix D) may reduce root nodulation (Hungria *et al.*, 2006; Pavanelli and Araújo, 2009). Consistent with our results Carneiro and Echer (2019) obtained an increase in the soybean yield using N-fertilizer, in the first year of sowing in areas following degraded pasture. For PI-2, the 1000N treatment provided crop yield increase of 596 kg ha^{-1} (16.3%) in relation to 0N treatment. During this season there were one drought period between 25 and 40 DAP, and between 78 and 96 DAP, when the accumulated rainfall was only 54.3 mm, being almost 98% of rainfall concentrated from 77 to 84 DAP (see Appendix I). The drought occurred during a critical period for N accumulation, between R5 and R6 (Fehr and Caviness, 1977). Water stress affects survival and synthesis of leghemoglobin and nodule function (Sprent, 1971; Patterson and Hudak, 1996; Santachiara *et al.*, 2019). Similarly, several authors suggested that N uptake and assimilation from soil is less sensitive

to temporary water deficits than is SNF (Purcell and King, 1996; Ray *et al*., 2006; Purcell, 2014). Thus, drought can help explain the poor performance of the 0N treatment in PI-2, this result may suggest that under drought conditions the N-fertilizer can minimize yield losses. However, this was not observed in TE-1, under water deficit conditions, where N-fertilization had no beneficial effect. In this case, water limitation was more severe and restrictive, for crop yield attainable <2,000 kg ha^{-1} the amount of N available in both the 0N was sufficient to meet the N demand of the crop.

Cafaro La Menza *et al*. (2017, 2019, 2020) documented the existence of N limitation in highly productive environments in high-yield soybean trials in Argentina and USA, with N-fertilization and full-irrigated conditions. Their findings revealed productivity increases with the use of N-fertilizer under temperate environments. In that regard, among our experiments, only Piracicaba, Cruz Alta, and Tupanciretã were conducted in areas with a history of high-yield soybean [>4.5 Mg ha^{-1}, threshold established by Salvagiotti *et al*., 2008)]; however, there was no soybean yield response to N-fertilization in any of those sites. For PI-1 we obtained a crop yield increase of 476 kg ha^{-1} (10.4%) and of 452 kg ha^{-1} (7.6%) at CA-1 with 1000N when compared with 0N treatment, both under water-limited conditions.

The N-fertilization provided statistically significant increases in seed protein concentration for PI-1, PI-2, PI-3, SO-1, SO-2, CA-1 and TU-1 under water-limited water conditions (Fig. 3.4A) and for PI-2 under non-limiting water conditions (Fig. 3.4B). The average increase obtained in these experiments for 1000N treatment on seed protein concentration ranged from 2 to 16% in relation to the 0N treatment. Cafaro La Menza *et al*. (2017, 2019, 2020) documented positive responses for seed protein concentration under N-fertilization.

Seed oil concentration ranged from 13.0 to 22.9% under all experiments (Fig. 3.5). The higher levels of seed oil concentration were obtained in TE-1, under non-limiting water conditions. The seed oil concentration response to N-fertilizer was not clear: we observed a decrease in seed oil concentration with 1000N, under water-limited conditions for PI-1, SO-1, SO-2, TU-1, TE-1; and an increase for PI-3 and CA-1. Although the environments CA-1 and TU-1 were sown with the same 65i65RSF cultivar, they showed different responses. In CA-1 there was an increase in seed oil concentration in 1000N treatment while for TU-1 there was a decrease with 1000N under either water availability conditions. The average of seed oil obtained over all environments was 18.22% with 0N and 18.29% with 1000N.

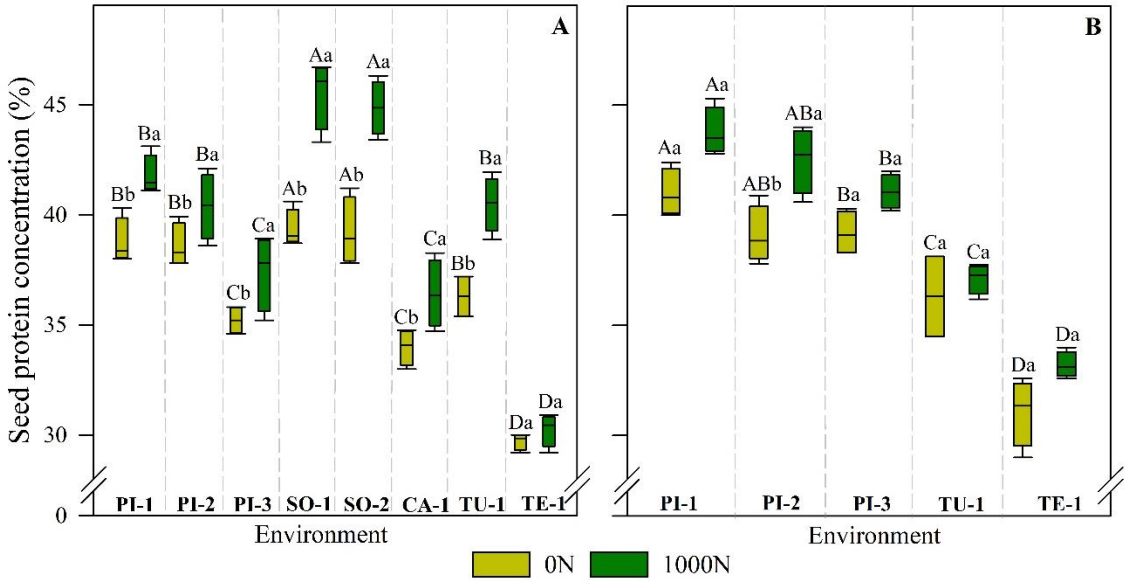

Fig 3.4. Seed protein concentration under water-limited conditions (A) or non-limiting water conditions (B), with zero (0N) or 1,000 kg N ha^{-1} (1000N). For experiments conducted in Piracicaba (PI) under three seasons, Sorriso (SO) under two seasons, Cruz Alta (CA) under one season, Tupanciretã (TU) under one season, and Teresina (TE) under one season. Means followed by different letters, uppercase among environments and lowercase between N-treatment for each environment, differ by Tukey test ($p < 0.05$). Boxplots are set at 90th (the upper whisker) and 75th (the upper quartile), mean (black line inside the box).

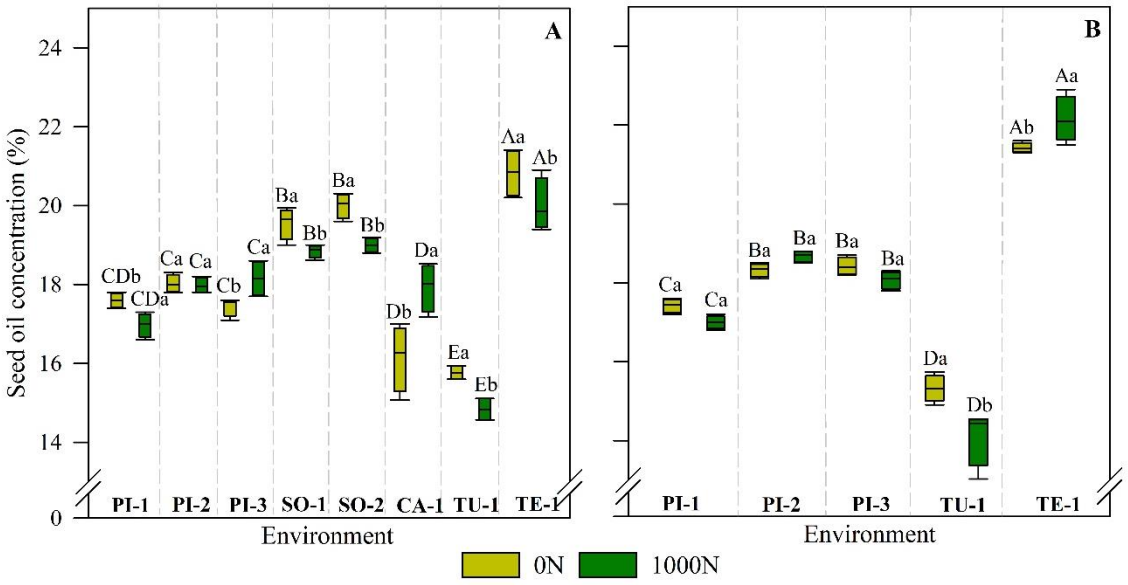

Fig 3.5. Seed oil concentration under water-limited conditions (A) or non-limiting water conditions (B), with zero (0N) or 1,000 kg N ha^{-1} (1000N). For experiments conducted in Piracicaba (PI) under three seasons, Sorriso (SO) under two seasons, Cruz Alta (CA) under one season, Tupanciretã (TU) under one season, and Teresina (TE) under one season. Means followed by different letters, uppercase among environments and lowercase between N-treatment for each environment, differ by Tukey test ($p < 0.05$). Boxplots are set at 90th (the upper whisker) and 75th (the upper quartile), mean (black line inside the box).

3.3.2. Simulated phenology, growth and development for TMG 7062, TMG 7063, NS7901, 65i65RSF, and 8579RSF

CROPGRO-Soybean was calibrated using experimental data set from: (i) PI-1 I-0N, for TMG 7062, (ii) SO-1 R-0N, for TMG 7063, (iii) SO-2 R-0N, for NS7901, (iv) CA-1 R-0N, for 65i65RSF, and (v) TE-1 using cultivar calibration for 8579RSF obtained in Chapter 2. After the second phase of calibration, the model showed correct simulation of the R1, R3, R5, and R7 (Fehr and Caviness, 1977), for all experiments used in calibration procedure (Figs. 3.6, 3.9, 3.10, 3.11, 3.13). The cultivars cycle (time between planting to physiological maturity) ranged from 83 to 130 days among the experiments used in the model calibration processes, with 8579RSF being a shorter cycle (TE-1) cultivar and 65i65RSF (CA-1) being a longer cycle cultivar (Figs. 3.11, 3.13).

During the model evaluation procedures, we observed variations in TMG 7062 cycle length over the successive seasons (PI-1, PI-2, and PI-3), under no drought stress conditions. The model was able to predict well the difference in cycle length according to the planting date, with longer cycles for earlier planting date (PI-2) and shorter cycle for later planting (PI-1) (Figs. 3.6, 3.7, 3.8). The same model response was observed for cultivar 65i65RSF, where the earliest planting in Cruz Alta (CA-1) resulted in a longer cycle when compared with later planting at Tupanciretã (TU-1), both under no drought stress conditions (Figs. 3.11, 3.12).

The CROPGRO-Soybean simulates crop phenology as a function of photoperiod, temperature, soil water, and N stress (Boote *et al.*, 1998). Neither the simulations (nor the observed data) showed any variation in phenological development between the zero-N and full-N treatments, because there was no severe N stress during the seasons. However, simulated phenology showed differences between water-limited and non-limiting water conditions in: (i) PI-2, there was a two-day increase in time from R1 to R3, and a one-day decrease to R7 (Fig. 3.7); (ii) TU-1, four-day decrease to R7 (Fig. 3.12); and (iii) TE-1, six-day decrease to R7 (Fig. 3.13). These differences were caused by the simulation of drought stress, based on the water stress factor for photosynthesis to account for water deficit effects on plant physiological processes (Boote *et al.*, 2008). The observed phenology was not affected by drought in all experiments, which is possibly an indication that the real crop did not experience as much drought stress as the simulated crop.

The evaluation of the CROPGRO-Soybean model for predicting phenology for TMG 7062 cultivar showed longer simulated cycle in PI-2 with one-day increased under rainfed conditions, and two-day increased under irrigated conditions, also we observed a delay of seven

days for anthesis, and a period of R3 to R5 seven days shorter than that observed, for both water conditions (Fig. 3.7). In PI-3 we observed the same tendency to overpredict cycle lengths; the model predicted a cycle 15 days longer than observed for TMG 7062, with delay of five days for the anthesis and a period of R3 to R5 nine days shorter than that observed, for both water conditions (Fig. 3.8). For 65i65RSF cultivar the model showed identical results for simulated and observed length of cycle in TU-1 under irrigated conditions, with anthesis three-day earlier, and a period of R3 to R5 eight-day shorter than that observed, for both water conditions (Fig. 3.12).

During the calibration procedure for TMG 7062, TMG 7063, NS 7901, and 65i65RSF our target was minimizing the RMSE, maximize the D, and visually evaluated whether cultivar trait adjustments were able to provide a better description of the observed growth traits for each cultivar. Based on these indicators, we obtained the best possible adjustment of the calibrated model, then simulations were compared with observed LAI, leaf dry matter, stem dry matter, aboveground biomass, and grain weight. The CROPGRO-Soybean was able to correctly simulate these variables over time (Figs. 3.6, 3.9, 3.10, 3.11, 3.13), with D >0.90 for all variables and cultivars.

In order to further understand response of the model to simulate soybean growth and development, the variable LAI is very important to explore, because it is directly related to the photosynthesis and evapotranspiration processes (see Boote and Pickering, 1994; Boote *et al*., 2008; Sau *et al*., 2004). We obtained a good adjustment of the LAI, in the final phase of the calibration procedure over the early season (defined as time between planting and R1), mid-season (defined as time between R1 and R5), and final season (defined as time between R5 and R7) in all experiments (Figs. 3.6, 3.9, 3.10, 3.11).

We evaluated the CROPGRO-Soybean simulations, and found that all variables evaluated over time were very well simulated, with values for the D that were greater or equal than 0.80 for almost all variables, except for: grain growth over time for TU-1, R-0N, R-1000N, and I-0N which had acceptable values for the D that were greater or equal than 0.68 (Fig. 3.12). For LAI, the RMSE ranged from 0.21 to 0.82, for grain weight RMSE ranged from 48 to 614 kg ha^{-1}, and for aboveground biomass from 231 to 1,536 kg ha^{-1}. In general, our results are close to simulations obtained in other sites and cultivars with CROPGRO-Soybean: (i) Boote *et al.* (1997) obtained D values ranged from 0.87 to 0.99 for grain and aboveground biomass variables, using Bragg and Williams cultivars from various locations in the USA; (ii) Wang *et al.* (2003) obtained RSME value ranged 0.30 to 1.24 for LAI simulations using Dekalb CX 420,

S46-44 RM, and Dekalb CX 420 cultivars in central Missouri, USA; (iii) Battisti *et al.* (2017) found D > 0.80 for cultivar BRS 284 in southern Brazil.

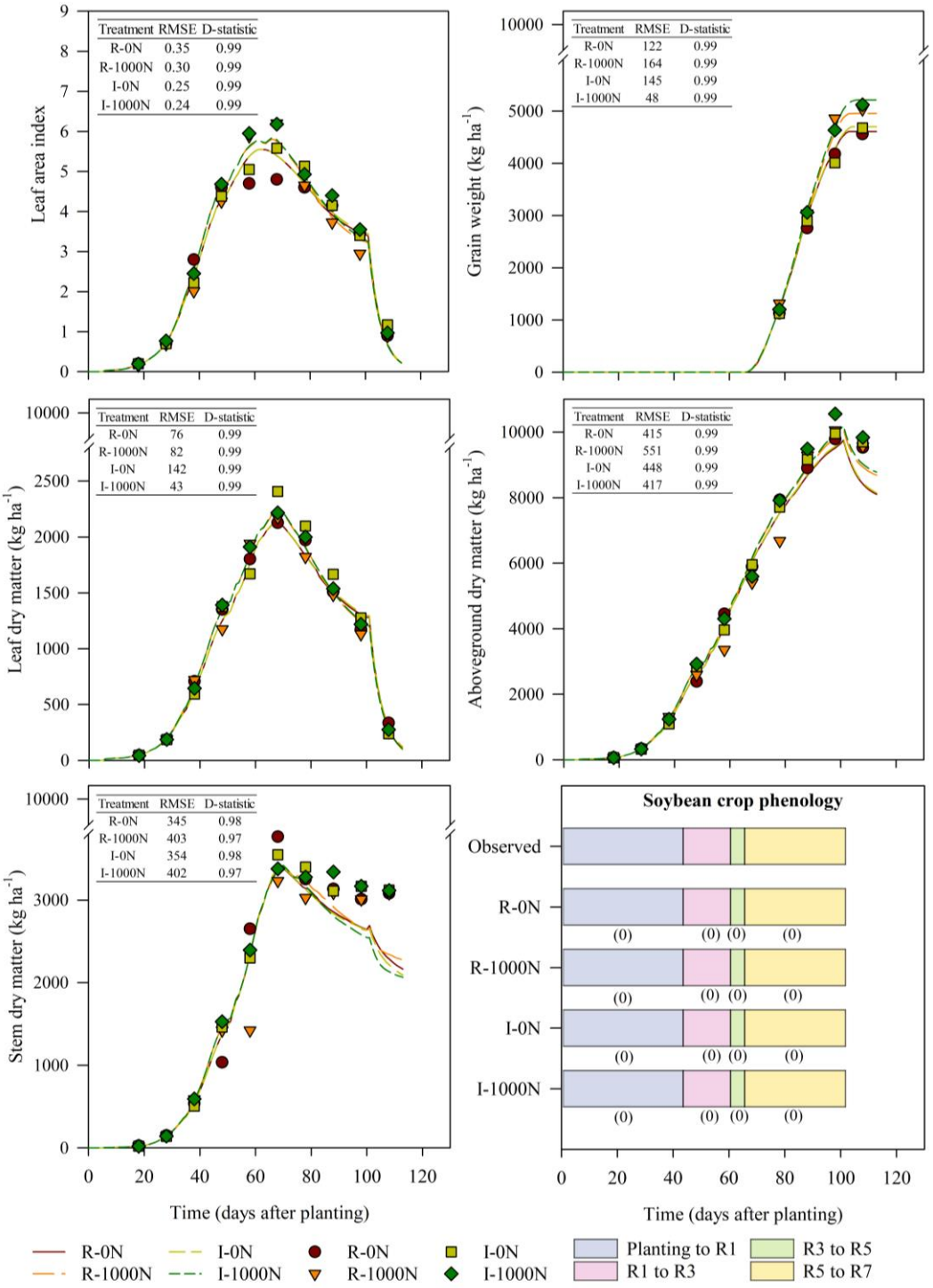

Fig. 3.6. Measured and simulated values for leaf area index, leaf dry matter, stem dry matter, grain weight, aboveground biomass over time; and crop phenology observed versus simulated values, with difference (B) between simulated and measured values in brackets. Experiment was conducted in Piracicaba during season 2017/2018 (PI-1) for cultivar TMG 7062 under water treatments [water-limited conditions (R) or non-limiting water conditions (I)] combined either with N treatments [with zero (0N) or fertilizer with 1,000 kg N ha^{-1} (1000N)].

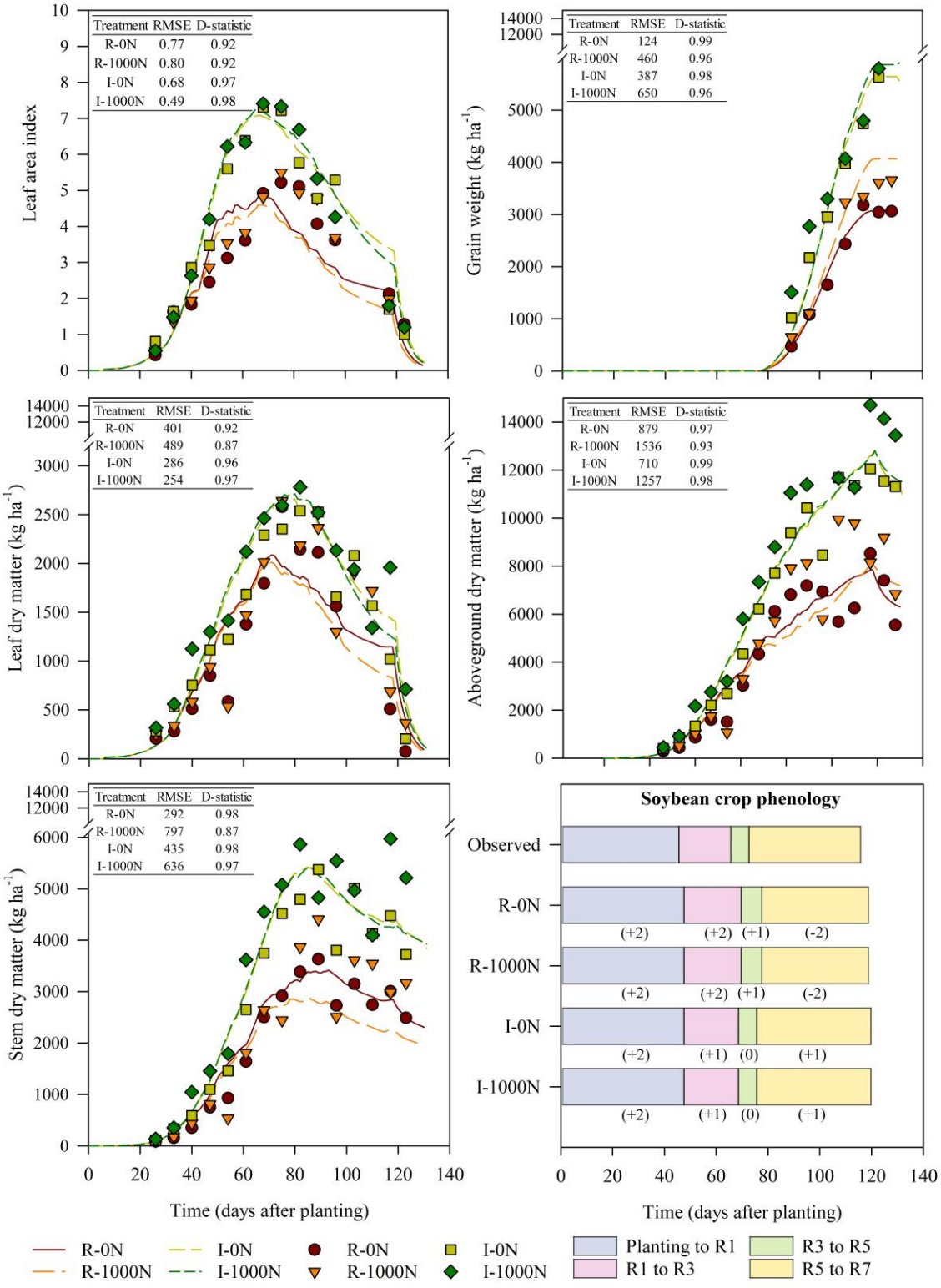

Fig. 3.7. Measured and simulated values for leaf area index, leaf dry matter, stem dry matter, grain weight, aboveground biomass over time; and crop phenology observed versus simulated values, with difference (B) between simulated and measured values in brackets. Experiment was conducted in Piracicaba during season 2018/2019 (PI-2) for cultivar TMG 7062 under water treatments [water-limited conditions (R) or non-limiting water conditions (I)] combined either with N treatments [with zero (0N) or fertilizer with 1,000 kg N ha^{-1} (1000N)].

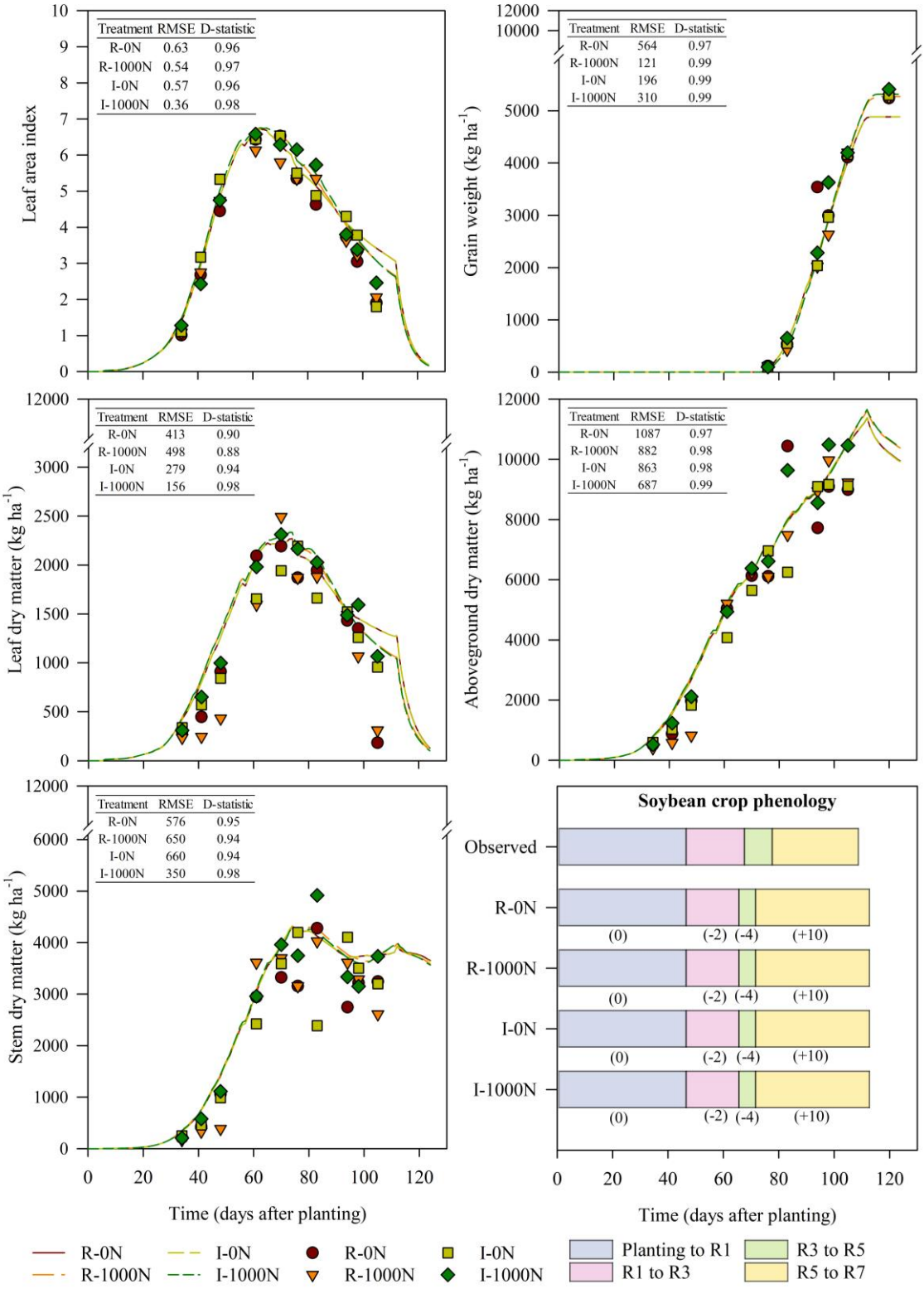

Fig. 3.8. Measured and simulated values for leaf area index, leaf dry matter, stem dry matter, grain weight, aboveground biomass over time; and crop phenology observed versus simulated values, with difference (B) between simulated and measured values in brackets. Experiment was conducted in Piracicaba during season 2019/2020 (PI-3) for cultivar TMG 7062 under water treatments [water-limited conditions (R) or non-limiting water conditions (I)] combined either with N treatments [with zero (0N) or fertilizer with 1,000 kg N ha^{-1} (1000N)].

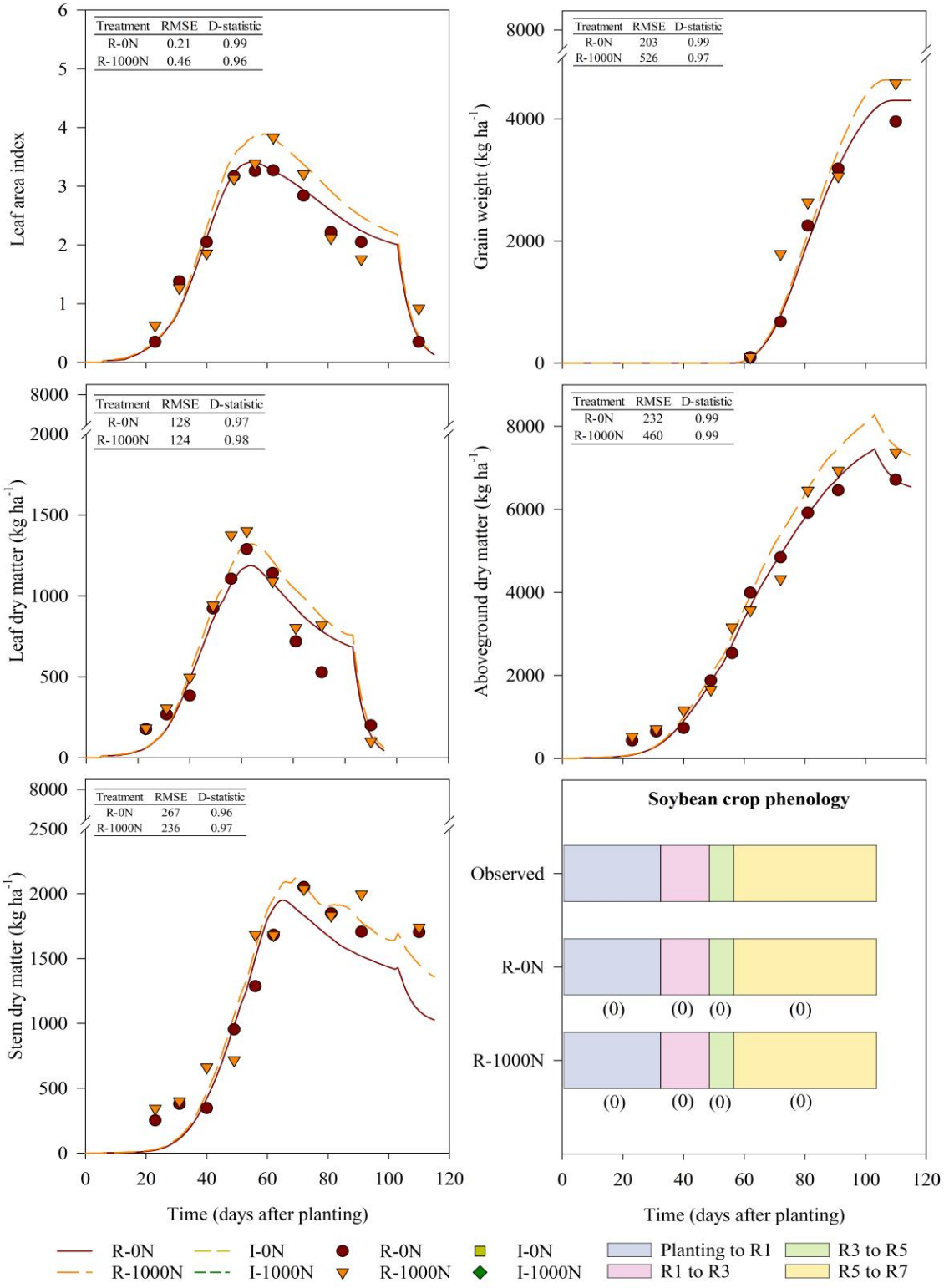

Fig. 3.9. Measured and simulated values for leaf area index, leaf dry matter, stem dry matter, grain weight, aboveground biomass over time; and crop phenology observed versus simulated values, with difference (B) between simulated and measured values in brackets. Experiment was conducted in Sorriso during season 2018/2019 (SO-1) for cultivar TMG 7063 under water treatments [water-limited conditions (R) or non-limiting water conditions (I)] combined either with N treatments [with zero (0N) or fertilizer with 1,000 kg N ha^{-1} (1000N)].

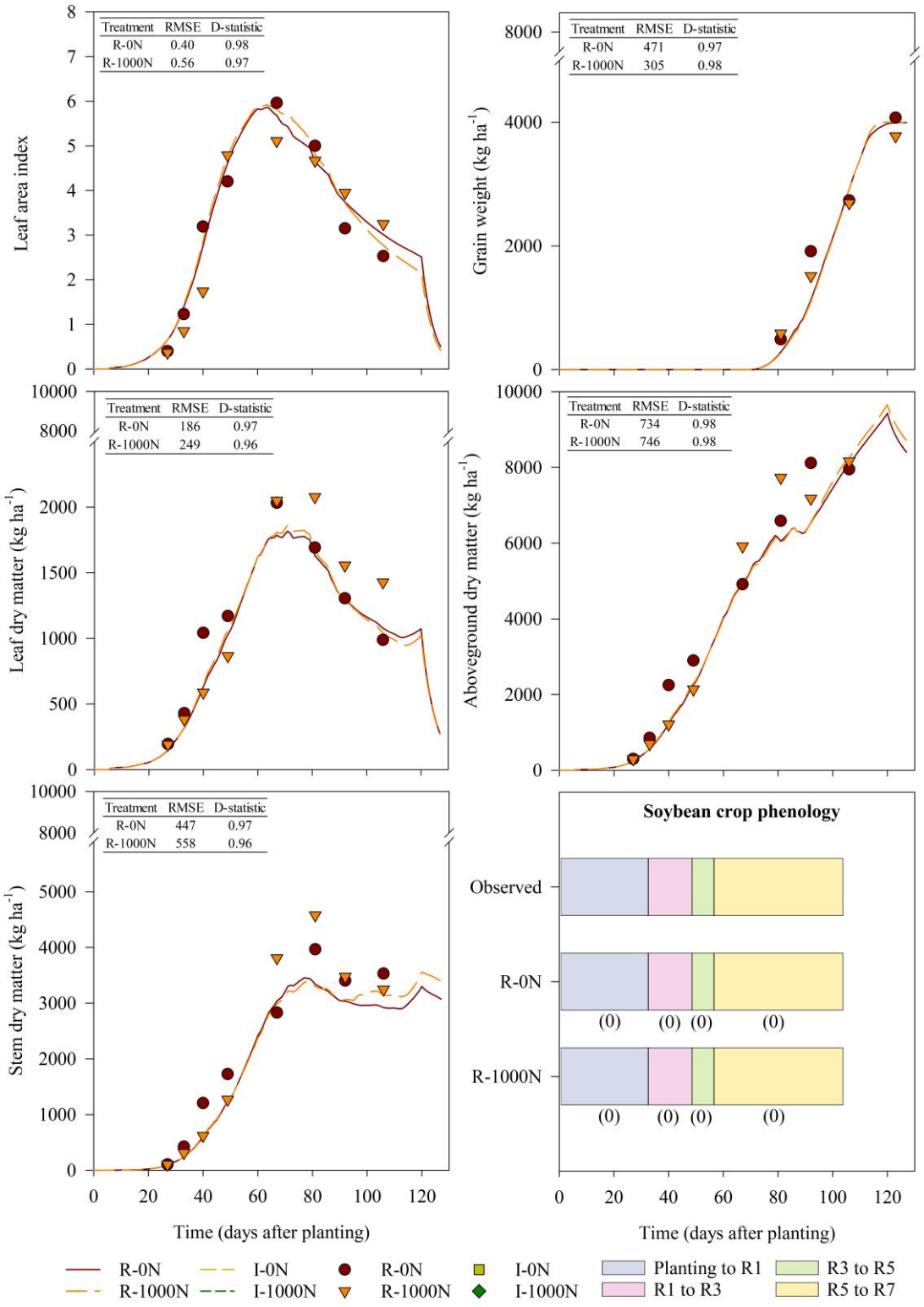

Fig. 3.10. Measured and simulated values for leaf area index, leaf dry matter, stem dry matter, grain weight, aboveground biomass over time; and crop phenology observed versus simulated values, with difference (B) between simulated and measured values in brackets. Experiment was conducted in Sorriso during season 2019/2020 (SO-2) for cultivar NS7901 under water treatments [water-limited conditions (R) or non-limiting water conditions (I)] combined either with N treatments [with zero (0N) or fertilizer with 1,000 kg N ha^{-1} (1000N)].

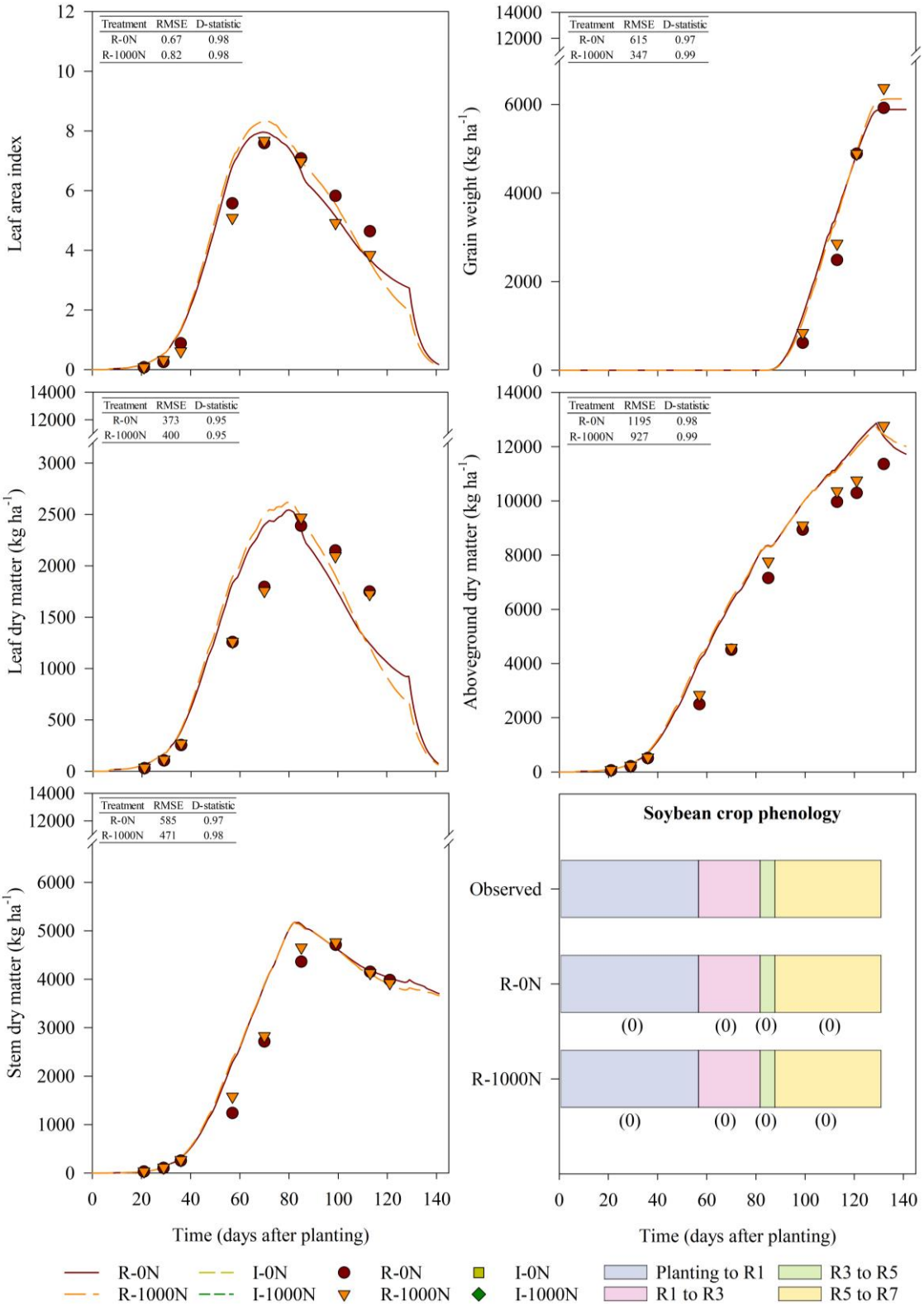

Fig. 3.11. Measured and simulated values for leaf area index, leaf dry matter, stem dry matter, grain weight, aboveground biomass over time; and crop phenology observed versus simulated values, with difference (B) between simulated and measured values in brackets. Experiment was conducted in Cruz Alta during season 2018/2019 (CA-1) for cultivar 65i65RSF under water treatments [water-limited conditions (R) or non-limiting water conditions (I)] combined either with N treatments [with zero (0N) or fertilizer with 1,000 kg N ha^{-1} (1000N)].

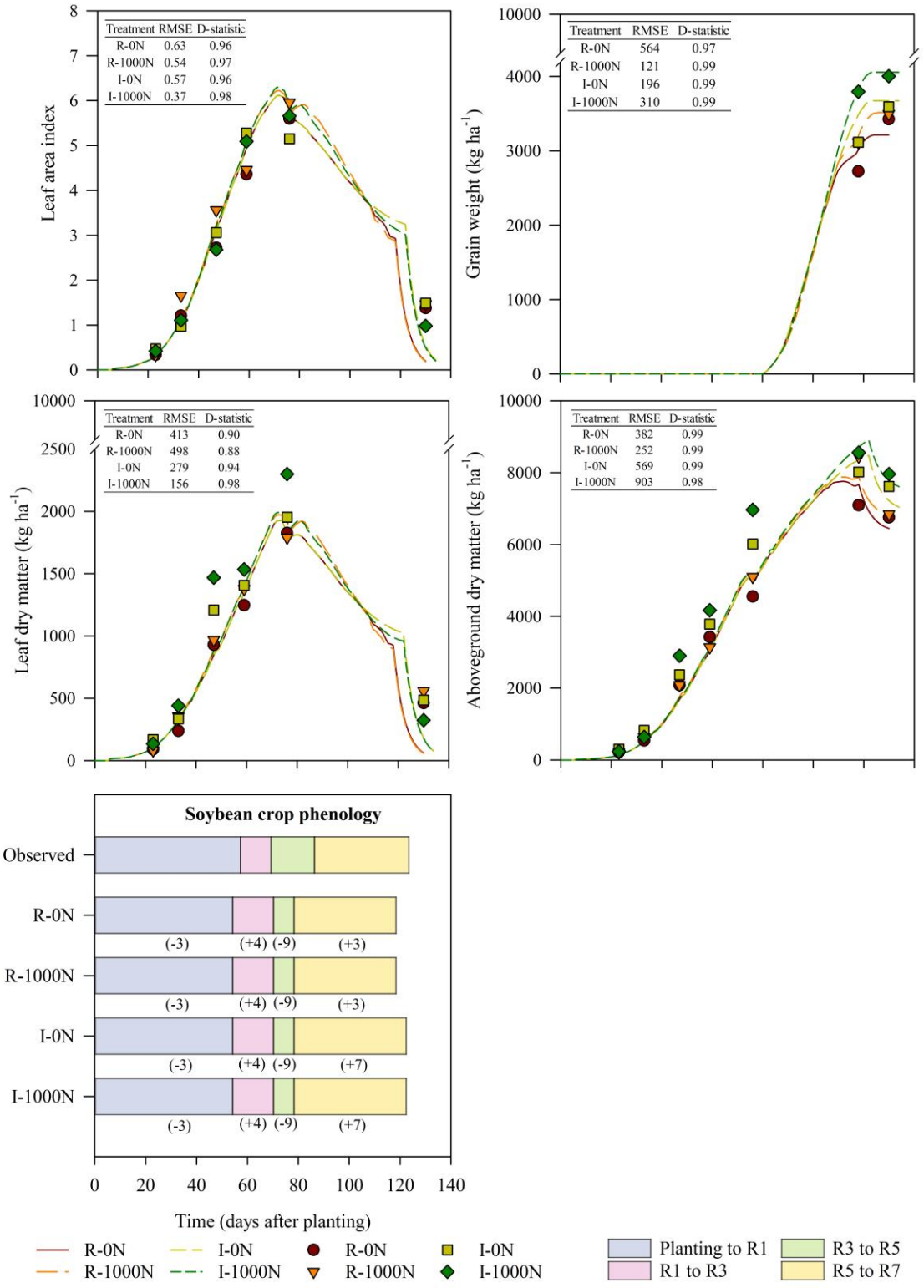

Fig. 3.12. Measured and simulated values for leaf area index, leaf dry matter, stem dry matter, grain weight, aboveground biomass over time; and crop phenology observed versus simulated values, with difference (B) between simulated and measured values in brackets. Experiment was conducted in Tupanciretã during season 2019/2020 (TU-1) for cultivar 65i65RSF under water treatments [water-limited conditions (R) or non-limiting water conditions (I)] combined either with N treatments [with zero (0N) or fertilizer with 1,000 kg N ha^{-1} (1000N)].

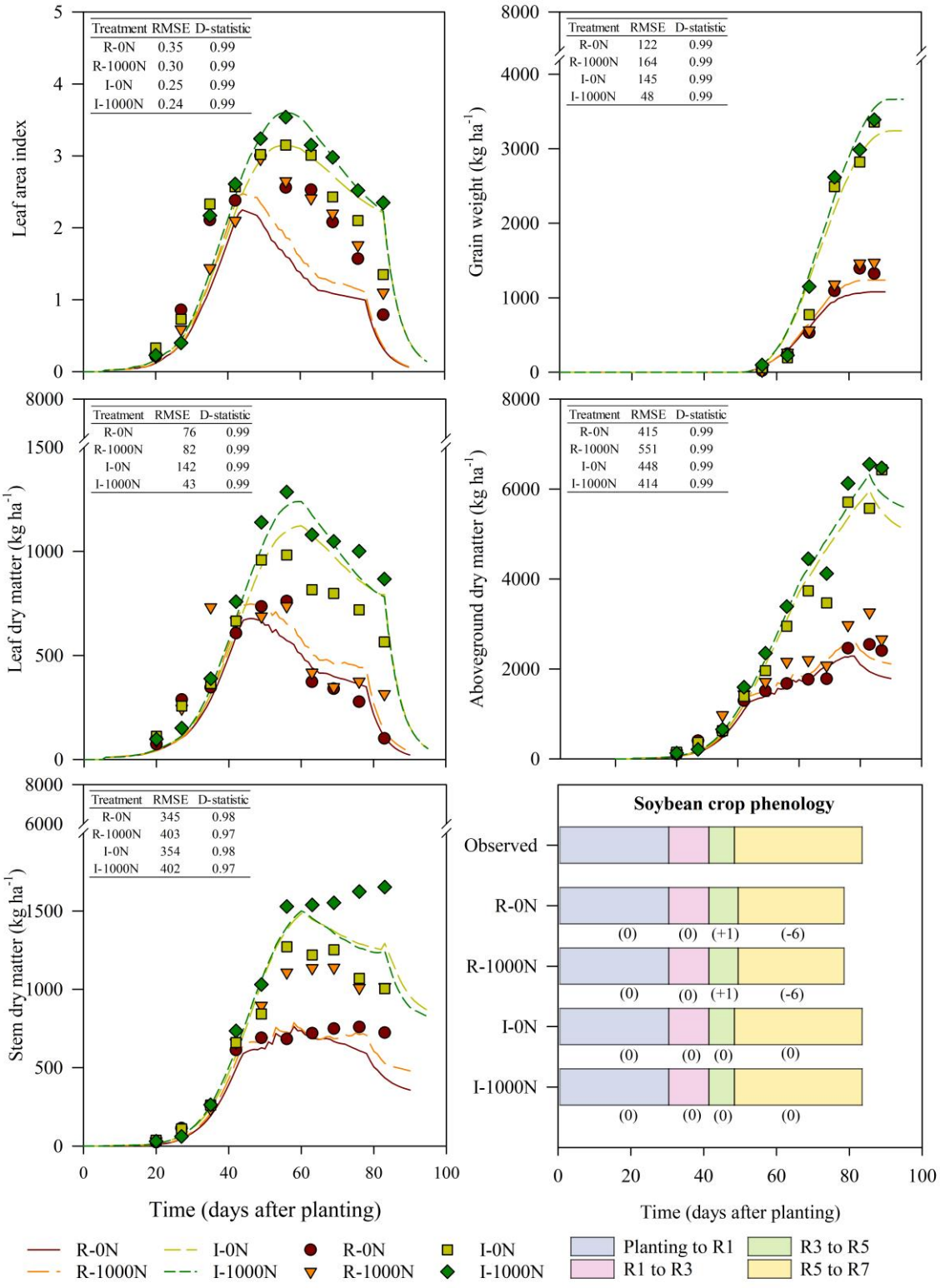

Fig. 3.13. Measured and simulated values for leaf area index, leaf dry matter, stem dry matter, grain weight, aboveground biomass over time; and crop phenology observed versus simulated values, with difference (B) between simulated and measured values in brackets. Experiment was conducted in Teresina during season 2019 (TE-1) for cultivar 8579RSF under water treatments [water-limited conditions (R) or non-limiting water conditions (I)] combined either with N treatments [with zero (0N) or fertilizer with 1,000 kg N ha^{-1} (1000N)].

During the CROPGRO-Soybean evaluation process, we observed a good visual adjustment for all cultivars, but with an overestimation of the LAI in PI-3 under all treatments, and underestimation in TU-1 under rainfed conditions at the final season. This was expected, because the cycle simulated in PI-3 was 15 days longer than observed, and in TU-1 it was 10 days shorter than observed. We also had a good fit for the full-N treatment, but LAI was slightly overestimated in PI-2 at the mid-final-season when compared with the observed LAI dataset.

In general, for aboveground biomass we obtained good simulations over time in all experiments (D > 0.95), we observed a slight overestimation during the season in CA-1 for 0N and 1000N treatment (Fig. 3.11). In the same way for TE-1, the model overestimated the aboveground biomass for R-0N and R-1000N treatments (Fig. 3.13). For grain weight the CROPGRO-Soybean also performed very well (D values between 0.52 and 0.99), we observed underestimation for: (i) final grain weight value in PI-2 R-0N and R-1000N (Fig. 3.7), PI-3 R-0N and R-1000N (Fig. 3.8); and TE-1I-0N and I-1000N (Fig. 3.13); and (ii) SO-2 at beginning of grain filling (between 80 and 100 DAP) for R-0N and R-100N (Fig. 3.10). In the opposite direction, we found overestimation for simulated final grain weight value in SO-1 R-0N (Fig. 3.9), SO-2 R-1000N (Fig. 3.10), TU-1 I-0N and I-1000N (Fig. 3.12).

3.3.3. Simulated N content in soybean: a case study for 8579RSF

During the grain-filling, which occurred after 60 DAP, the plant started to N remobilize from leaf and stem to grain tissues (Fig. 3.14). Despite the large amount of N fertilizer, it was not kept as leaf N during grain-filling and neither extend the life-span of leaf N in the field for R-1000N or I-1000N treatments. However, the greater N plant accumulation, as expected, resulted in an increase in field biomass [(leaf, stem, and grain), Figs. 3.13 and 3.14] and grains with higher protein concentration (Table 3.2); because the N plant concentration is strictly related to photosynthesis capacity (Kumar *et al.*, 2002; Zhou *et al.*, 2006), and protein formation in grains (Fabre and Planchon, 2000; Rontudo *et al.*, 2009).

We also realized in the field experiment a large N plant accumulation gap between water-limited and non-limiting water conditions (Fig. 3.13). The N plant accumulation amount was lower in R-0N and I-0N than R-1000N and I-1000N because drought stress plays an important role in physiological processes decreasing stomatal conductance (Liu *et al*., 2003; Earl, 2002); N fixation and leaf photosynthesis (Sinclair *et al.*, 1987; Ohashi *et al.*, 2006; Santachiara *et al*., 2019). Furthermore, the transport of dissolved urea-N across layers and

floodwater occurs via mass flow, then N transport simulation is dependent on water availability (Singh and Porter, 2019).

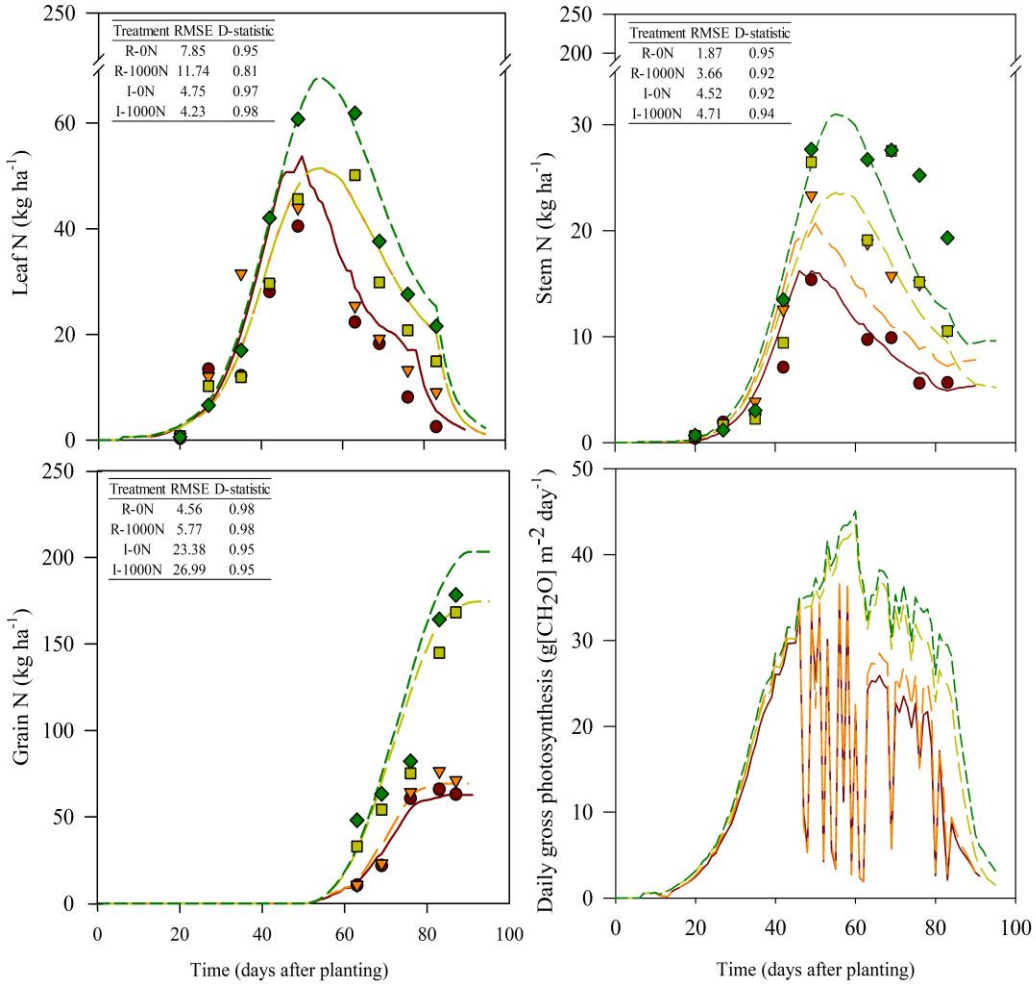

Fig. 3.14. Measured and simulated values for leaf N, stem N, and grain N over time; and simulated daily gross photosynthesis (g[CH_2O] m^{-2} day^{-1}). Experiment was conducted in Teresina during season 2019 for cultivar 8579RSF under water treatments [water-limited conditions (R) or non-limiting water conditions (I)] combined either with N treatments [non nitrogen fertilizer (0N) or fertilizer with 1,000 kg N ha^{-1} (1000N)].

The CROPGRO-Soybean was able to mimetic the remobilize N from vegetative dry matter (leaf and stem) to grain under different water availability. The model did a good job to associate N remobilization with gross photosynthesis in its simulation procedures: during seed-filling, we noticed a rapid linear decrease in simulated gross photosynthesis when leaf N was rapidly decreasing (Fig. 3.13). This movement of N from leaf to grain is associated with the decline of photosynthesis capacity and with leaf senescence observed in other researches (Boote

et al., 1978; Jiang *et al.*, 1993; Feng *et al.*, 2019). Thus, the model got excellent agreement between simulated and observed values (D > 0.81). For R-0N and R-1000N leaf N was overpredicted (kg ha^{-1}) and simulations well-agreed with observed data for I-0N and 0N (Fig. 3.13). This is in accordance with the overestimation for leaf dry matter for TE-1 R-0N and R-1000N (Fig. 3.13). The simulated stem N (kg ha^{-1}) for R-0N showed excellent visual agreement with observed values, therefore overestimated R-1000N treatment. For grain N (kg ha^{-1}) our findings showed good visual agreement, but with overprediction for I-1000N treatment (Fig. 3.13).

3.3.4. Simulated final crop yield, protein and oil concentration

The CROPGRO-Soybean showed excellent ability to predict the final grain yield in most treatments, in only 6 of the 26 combinations (N-fertilizer, environments, and water availability) were the |B| > 300 kg ha^{-1} (Table 3.2). For oil concentration, the bias in simulations ranged from -1.37 to 2.60 (absolute units) in relation to the observed data under all experiments. For grain protein concentration the bias in simulations ranged from -6.16 to 4.55 (absolute units) in relation to the observed data under all experiments.

The N-fertilization at 1,000 kg N ha^{-1} produced an increase in final crop yield that ranged from 19 to 627 kg ha^{-1} (4.2 to 13.3 %) in all field experiments. The model was able to simulate the increase in final crop yield that ranged from 5 to 995 kg ha^{-1}. There was one exception, in SO-2 high N fertilization caused a decrease in final grain yield of 300 kg ha^{-1}. As discussed previously, we suggested that yield decrease observed in the field was associated with the early leaf senescence from low canopy layers in the 1000N treatment for the cultivar NS 7901. As there was no logical reason to expect this response to N fertilization, the model was unable to simulate this atypical condition.

Although we hypothesized that the very high N fertilization (1,000 kg ha^{-1}) would result in a large yield increase, this was not observed in either the field or in the CROPGRO-Soybean simulations. The greatest yield increase observed by N-fertilization was 627 kg ha^{-1} in SO-1, and the largest model simulation increase was 995 kg ha^{-1} for the PI-2 case. The mean observed crop yield with 0N was 4,211 kg ha^{-1} and mean with 1000N was 4,478 kg ha^{-1}, which represented a yield increase of 6.34 % (Table 3.4) while the simulated mean yield increase was 8.21 %. This modest increase in the mean grain yield obtained from 1000 kg N ha^{-1} fertilization

indicates that for these planting conditions, the N demand of the crop could be met by N-fixation.

Table 3.4. Simulated and observed final values for grain yield, grain oil, and grain protein concentration. Experiments were conducted in Piracicaba over three crop seasons (PI-1, PI-2, PI-3), Sorriso over two crop seasons (SO-1, SO-2), Cruz Alta over one crop season (CA-1), Tupanciretã over one crop season (TU-1), and Teresina over one crop season (TE-1); under water-limited conditions (R) or non-limiting water conditions (I), with zero (0N) or 1,000 kg N ha^{-1} (1000N). Values in brackets are the difference between measured and simulated.

Experiments	Crop Yield (kg ha^{-1})		Grain oil concentration (%)		Grain protein concentration (%)	
	Obs.	Simul.	Obs.	Simul.	Obs.	Simul.
PI-1, R-0N	4560	4610 (50)	17.58	17.82 (0.24)	38.75	41.44 (2.69)
PI-1, R-1000N	5036	4957 (-79)	16.95	17.93 (0.98)	41.78	41.06 (-0.72)
PI-1, I-0N	4678	4703 (25)	17.48	17.94 (0.46)	41.00	41.06 (0.06)
PI-1, I-1000N	5121	5214 (93)	16.95	17.93 (0.98)	43.78	41.06 (-2.72)
PI-2, R-0N	3062	3074 (12)	18.02	18.21 (0.19)	38.58	39.75 (1.17)
PI-2, R-1000N	3658	4069 (411)	17.97	18.51 (0.54)	40.38	38.87 (-1.51)
PI-2, I-0N	6253	5642 (-611)	18.30	18.07 (-0.23)	39.10	40.25 (1.15)
PI-2, I-1000N	6399	5875 (-524)	18.68	18.11 (-0.57)	42.53	40.12 (-2.41)
PI-3, R-0N	5241	4883 (-358)	17.45	18.03 (0.58)	35.20	39.75 (4.55)
PI-3, R-1000N	5260	5273 (13)	18.15	18.73 (0.58)	37.40	37.69 (0.29)
PI-3, I-0N	5298	4883 (-415)	18.40	18.02 (-0.38)	39.20	39.81 (0.61)
PI-3, I-1000N	5410	5318 (-92)	17.98	18.84 (0.86)	40.55	37.31 (-3.24)
SO-1, R-0N	3956	4304 (348)	19.94	19.86 (-0.08)	39.35	40.88 (1.53)
SO-1, R-1000N	4582	4638 (56)	18.85	20.03 (1.18)	45.51	40.31 (-5.2)
SO-2, R-0N	4074	3995 (-79)	20.00	20.13 (0.13)	39.20	40.06 (0.86)
SO-2, R-1000N	3774	4000 (226)	19.00	20.6 (1.6)	44.85	38.69 (-6.16)
CA-1, R-0N	5921	5888 (-33)	16.15	16.54 (0.39)	33.97	35.31 (1.34)
CA -1, R-1000N	6373	6126 (-247)	17.93	16.56 (-1.37)	36.40	35.13 (-1.27)
TU-1, R-0N	3425	3213 (-212)	15.77	16.8 (1.03)	36.28	34.06 (-2.22)
TU-1, R-1000N	3496	3516 (20)	14.84	16.55 (1.71)	40.48	34.75 (-5.73)
TU-1, I-0N	3591	3674 (83)	15.32	16.41 (1.09)	36.31	35.19 (-1.12)
TU-1, I-1000N	4004	4056 (52)	14.12	16.72 (2.6)	37.13	34.19 (-2.94)
TE-1, R-0N	1324	1078 (-246)	20.90	22.26 (1.36)	29.74	29.75 (0.01)
TE-1, R-1000N	1471	1238 (-233)	20.02	21.46 (1.44)	30.25	32.19 (1.94)
TE-1, I-0N	3358	3242 (-116)	21.52	21.36 (-0.16)	32.05	32.50 (0.45)
TE-1, I-1000N	3390	3664 (274)	22.14	20.9 (-1.24)	33.19	33.94 (0.75)
Mean 0N	4211	4091 (-120)	18.22	18.57 (0.35)	36.82	36.67 (-0.15)
Mean 1000N	4478	4457 (-21)	18.29	18.68 (0.39)	39.55	37.33 (-2.22)

3.3.5. Simulation of soil and plant N balance

In order to understand the effects of N fertilization in agricultural systems we evaluated the simulated soil inorganic N balance. We found a very high simulated NH_3 loss, ranged from 463 to 801 N kg ha^{-1} (Fig. 3.15). This simulated NH_3-N volatilization is related to the urea being applied to the soil surfaces which is a function of temperature and soil water (Godwin and

Singh, 1998). This volatilization loss of N that can reach more than 50% under tropical and subtropical conditions, where there are no limitations of soil temperature and soil moisture (Gurgel *et al.*, 2016; Martins *et al.*, 2017; Cantarella *et al.*, 2018). The simulated N leaching losses were relatively small, ranged from 0 to 50 N kg ha^{-1}, the greater values were obtained in CA-1, SO-1, and SO-2 (Fig. 3.15), which seasons were characterized by high-intensity rainfall (Appendix J and K).

The simulated soil N uptake was substantially higher in full-N than zero-N treatment, as well as greater in non-limiting water compared to water-limited conditions (Fig. 3.16). Simulated N uptake by CROPGRO-Soybean depends on soil and root factors, but with the constraint that actual N uptake cannot exceed N demand (Boote *et al*., 2008). The model computes N demand based on the daily dry matter growth increment of each tissue multiplied by the N concentration of each tissue (non-limiting N conditions). Thus, if actual N uptake meets the N demand, there will be no N fixation, otherwise, N fixation occurs (Boote *et al*., 2008). The large difference between the 0N and 1000N treatments for soil N uptake (Fig. 3.15), and the relatively small difference in crop yield showed that N_2 fixation makes up the difference to meet N crop demand (Fig. 3.16). In addition, under severe drought stress conditions in TE-1 (see Chapter 2) R-0N and R-1000N, N uptake fell down dramatically and the final inorganic soil N remaining increased substantially (Fig. 3.15).

In general, for all experiments, the simulated crop yield gains were shown to be very consistent, matching observed yield gains under the N fertilization cases. The yield gains from N fertilization (both observed and simulated) were modestly small, and were not proportional to the very large amount of N-fertilization (1,000 kg N ha^{-1}). The simulation of the CROPGRO-Soybean soil inorganic N balance alerted us to a considerable chance of increasing environmental losses under tropical and subtropical conditions by high rates of the volatilization of N-NH_3 associated with urea application (Liu *et al.*, 2019; Ti *et al.*, 2020). On the other hand, if the volatilization is less than simulated (which could be the case, as there was no verification of volatilization) and the applied N did reach the roots, then it indicates that soybean truly does not respond to that large amount of N fertilization, but rather balances demand by N_2 fixation.

The simulated plant N balance showed that simulated N fixed fell down dramatically when N-fertilizer was applied in all experiments, and the total N input to the system was very close between treatments 0N and 1000N. This reinforces the argument that N fertilization can limit the N_2 fixation as already been observed in the field, where the fertilization of N in

soybeans limited the biological fixation by up to 70% (Salvagiotti *et al*., 2008; Santachiara *et al*., 2019); and that soybean does not respond to that large N fertilizer amount.

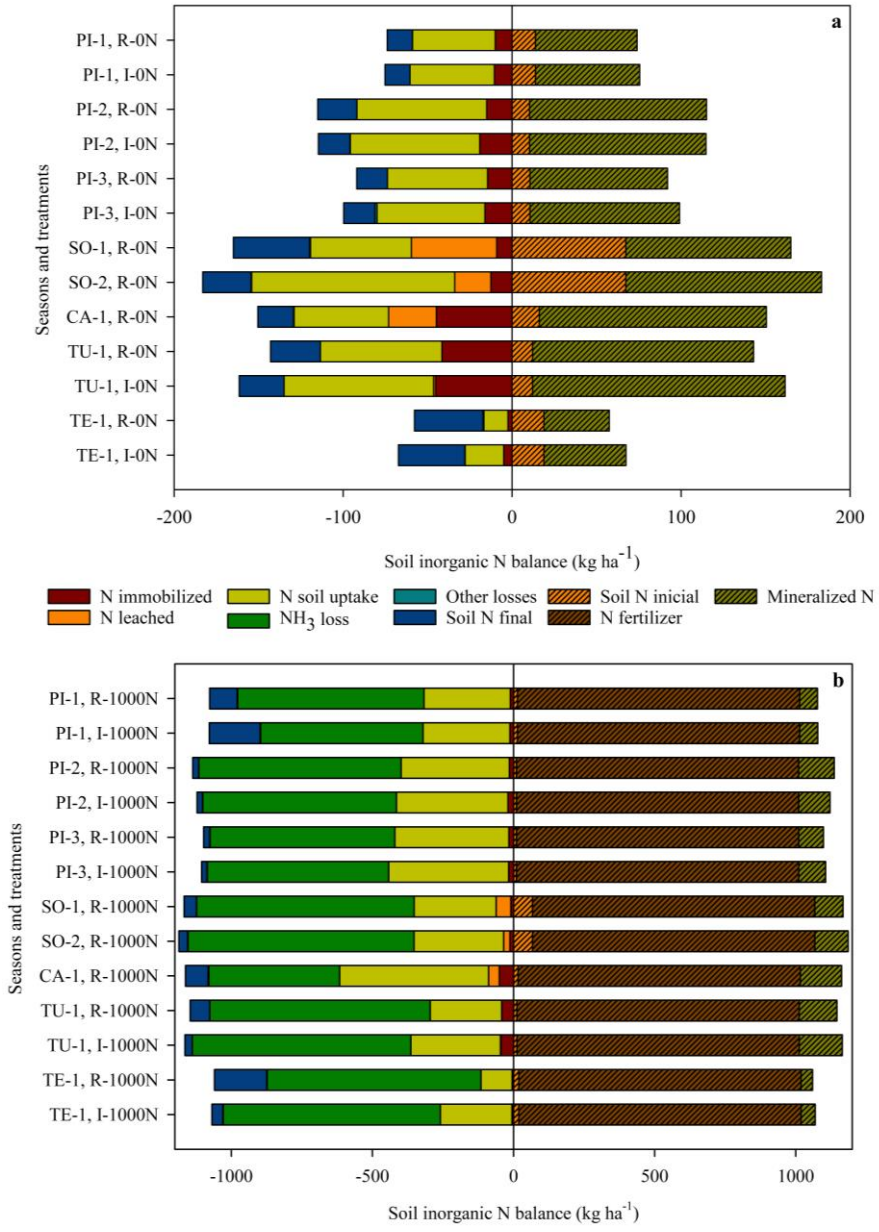

Fig. 3.15. Simulated soil inorganic N balance at Piracicaba over three crop seasons (PI-1, PI-2, PI-3), Sorriso over two crop seasons (SO-1, SO-2), Cruz Alta over one crop season (CA-1), Tupanciretã over one crop season (TU-1), and Teresina over one crop season (TE-1). a: for treatments water-limited combined with zero-N (R-0N), and non-limiting water combined with zero-N (I-0N); and b: water-limited combined with full-N (R-1000N), and non-limiting water combined with full-N [(I-1000N)]. The left side was shown N subtractions, and the right side was soil N state variables and N additions. Warning: the abscissas axis is quite different between plot a and b.

Furthermore, the biological N fixation can also be limited by drought stress, as there was a reduction in the simulated N2 fixation for the water-limited condition in relation to the non-limiting water condition in PI-1, PI-2, PI-3, TU-1 and TE-1. This is in line with what is recorded in the scientific literature, since drought stress can penalize N2 fixation by up to 40% (Santachiara et al., 2019).

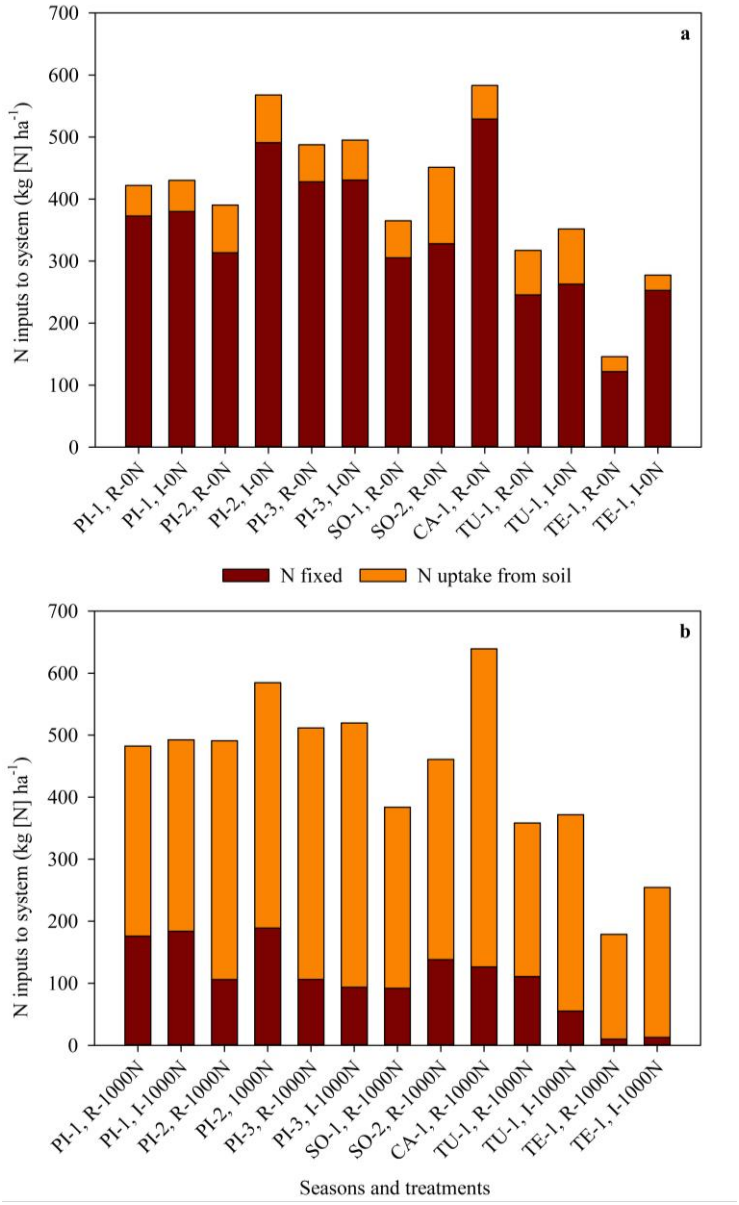

Fig. 3.16. Simulated plant N balance with 0N (a) versus 1000N (b), for treatments at Piracicaba in three crop seasons (PI-1, PI-2, PI-3), Sorriso in two crop seasons (SO-1, SO-2), Cruz Alta in one crop season (CA-1), Tupanciretã in one crop season (TU-1), and Teresina in one crop season (TE-1); under water-limited conditions (R) or non-limiting water conditions (I), with zero (0N) or 1,000 kg N ha^{-1} (1000N).

3.3.6. Simulation of long-term of N-fertilizer management scenarios

Following the evaluation of the CROPGRO-Soybean model for simulation of soybean growth and crop yield and the simulated soil and plant N balance, we conducted a what-if scenario analysis of N-fertilization for a tropical and subtropical condition. The long-term simulations over 30 years of weather for soybean yield and the impact of N-fertilizer using N fertilization rates are presented in Fig. 3.17. Soybean sown at Teresina had a lower yield potential than soybean at Piracicaba, because it was grown in a low latitude region during winter with less daily total solar radiation and a shorter life cycle. The simulated crop yield increased very gradually as N-fertilizer was increased from 0 to 1,000 kg N ha^{-1}, at which average crop yield reached 4,431 kg $ha^{-1}$for Piracicaba and 3,248 kg ha^{-1} for Teresina (Fig. 3.17).

Within a given location, there was no further yield increase from 600 to 1,000 kg N ha^{-1} for both long-term scenarios (Fig. 3.17). The simulated crop yield increase with 600 kg N ha^{-1} was 606 kg ha^{-1} (or 15%) for Piracicaba and 428 kg ha^{-1} (or 13%) for Teresina. However, despite the crop yield increase, this increase would not be cost-effective or environmentally appropriate. In conclusion, N fertilization with doses higher than 600 kg ha^{-1} would give no yield increase, and even fertilizing with 600 kg ha^{-1} would not be cost-effective or environmentally appropriate.

The CNP is modeled based on the concept of crop yield per plant N uptake amount (from soil and N_2 fixation) and the CROPGRO-Soybean simulations for both sites showed that higher CNP was obtained with no N fertilizer. This means that the N fertilization did not reflect a proportional increase in grain yield, because CNP is smaller for higher doses of N. Thus, model simulations revealed that the use of N-fertilizer decreases CNP for soybean yield.

The long-term simulations showed that the average NH_3 losses exceed 100 kg N ha^{-1} when the N-fertilizer applied is greater than 500 kg N ha^{-1} for Piracicaba and 400 kg N ha^{-1} for Teresina. The ammonia emissions are associated with environmental hazards because greenhouse gases (GHG) emissions cause climate change and put extra-pressure on food production. Thus, if N-fertilizer is used in tropical and subtropical soybean production, it is recommended that mitigation measures for ammonia volatilization are adopted, such as: (i) incorporation of urea into the soil (Rochette *et al.*, 2009, 2013; Fontoura *et al.*, 2010, Cantarella *et al*, 2018); and (ii) use of N fertilization with urease inhibitors (Mira *et al.*, 2017; Afshar *et al.*, 2018; Krol *et al.*, 2020; Cantarella *et al*, 2018).

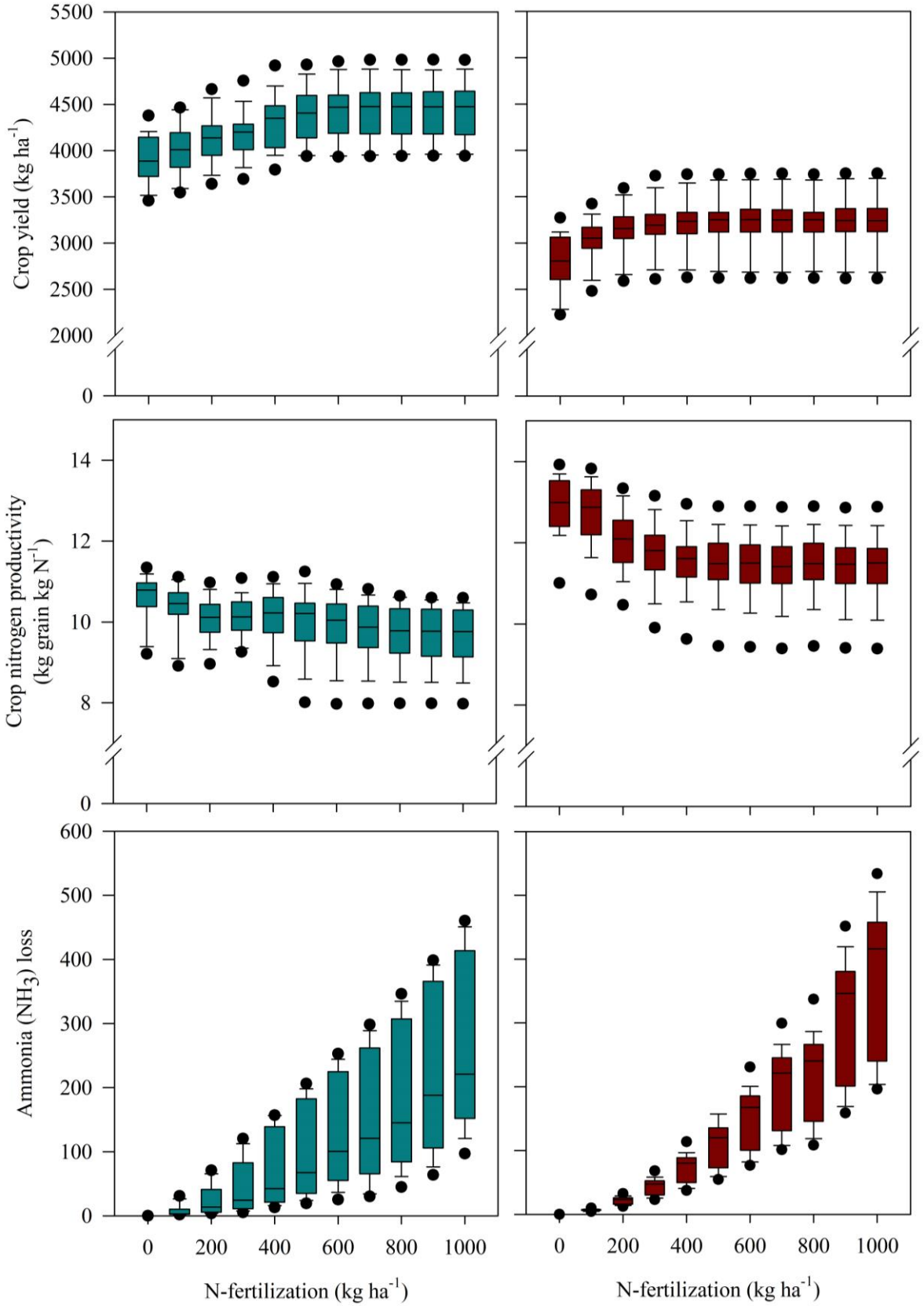

Fig. 3.17. Simulated long-term scenarios (1989 to 2020) for grain weight, crop N productivity, and ammonia loss under N-fertilization doses of 0 to 1,000 kg ha^{-1} under irrigated condition. Boxplots were set at 90^{th} (the upper whisker) and 75^{th} (the upper quartile), outliers are shown as black dots.

Still, the yield target of 8,945 kg ha^{-1} was not reached in any field or modelling experiment, the maximum average observed crop yield was 6,373 kg ha^{-1} in CA-1 (I-100N); that is 71.2% of the expected yield. It means that sowing data maybe have been a limiting factor to reach higher yield; because for the Southern Hemisphere, sowing between late September and mid-October may be more ideal for the soybean crop to reach its peak of development (between R5 and R6) in December (greatest solar energy availability), therefore soybeans could accumulate more carbohydrates and require N via fixation or fertilization.

Farmers should not consider very high doses of fertilizer N applied to soil on soybean under tropical and subtropical conditions, as our field data and the crop model simulations showed this practice to be inconsistent with the principles of sustainable intensification of agriculture and clearly not cost-effective. However, this study can be the basis for prospecting for crop yield potential and crop yield gaps (see Chapter 4), using the CROPGRO-Soybean model, which showed an excellent predictive capacity of soybean across tropical and subtropical conditions for different water conditions and N-fertilization cases.

3.4. Conclusions

Well-management soybean experiments were conducted under water-limited and non-limiting water conditions without N fertilizer and with 1,000 kg N ha^{-1} in several sites in Brazil. The yield target of 8,945 kg ha^{-1} was not reached in any experiment or treatment. N-fertilization showed marginal or no effect on soybean crop yield under tropical and subtropical conditions; however high rates of N-fertilization consistently increased seed protein concentration. This chapter showed that the CROPGRO-Soybean model of DSSAT was able to simulate plant and soil N balance, soybean growth and yield under high N-fertilization rates and different water availability under tropical and subtropical conditions. We found excellent agreement between simulated and observed values over time under different soils, water requirements, and N-fertilization under tropical and subtropical conditions in Brazil. We thus conclude that the model was able to accurately simulate N fertilization effects on N accumulation in vegetative tissues, soybean growth, development, crop yield, and oil seed concentration under different tropical and subtropical conditions.

References

Afshar, R. K., Lin, R., Mohammed, Y. A., Chen, C., 2018. Agronomic effects of urease and nitrification inhibitors on ammonia volatilization and nitrogen utilization in a dryland farming system: field and laboratory investigation. Journal of Cleaner Production, 172, 4130-4139.

Ågren, G. I., Ingestad, T., 1987. Root: shoot ratio as a balance between nitrogen productivity and photosynthesis. Plant, Cell & Environment, 10(7), 579-586.

Allen, R. G., Pereira, L. S., Raes, D., Smith, M., 1998. Crop evapotranspiration-Guidelines for computing crop water requirements-FAO Irrigation and drainage paper 56. FAO, Rome, 300(9), D05109.

Barker, D. W., Sawyer, J. E., 2005. Nitrogen application to soybean at early reproductive development. Agronomy Journal, 97(2), 615-619.

Battisti, R., Sentelhas, P. C., Boote, K. J., 2017. Inter-comparison of performance of soybean crop simulation models and their ensemble in southern Brazil. Field Crops Research, 200, 28-37.

Battisti, R., Sentelhas, P. C., Pascoalino, J. A. L., Sako, H., de Sá Dantas, J. P., Moraes, M. F., 2018. Soybean yield gap in the areas of yield contest in Brazil. International Journal of Plant Production, 12(3), 159-168.

Bender, R. R., Haegele, J. W., Below, F. E., 2015. Nutrient uptake, partitioning, and remobilization in modern soybean varieties. Agronomy Journal, 107(2), 563-573.

Boote, K. J., Gallaher, R. N., Robertson, W. K., Hinson, K., Hammond, L. C., 1978. Effect of foliar fertilization on photosynthesis, leaf nutrition, and yield of soybeans 1. Agronomy Journal, 70(5), 787-791.

Boote, K. J., Pickering, N. B., 1994. Modeling photosynthesis of row crop canopies. HortScience, 29(12), 1423-1434.

Boote, K. J., Jones, J. W., Hoogenboom, G., Wilkerson, G. G., 1997. Evaluation of the CROPGRO-Soybean model over a wide range of experiments. In: p.113-133 [M. J. Kropff, P. S. Teng, P. K. Aggarwal, J. Bouma, B. A. M. Bouman, J. W. Jones, H. H. van Laar (Eds.)], Applications of systems approaches at the field level, V.2. Springer-Science+Business Media, Wageningen, Netherlands.

Boote, K. J., Jones, J. W., Hoogenboom, G., Pickering, N. B., 1998. The CROPGRO model for grain legumes. In: p. 99-128 [G. Y. Tsuji, G. Hoogenboom, and P. K. Thornton (Eds.)], Understanding options for agricultural production. Kluwer Academic Publishers, London, United Kingdom.

Boote, K. J., 1999. Concepts for calibrating crop growth models. DSSAT Version, 3(4). Concepts for calibrating crop growth models. In: p.79-200 [G.Hoogenboom, P.W.Wilkens, G.Y. Tsuji (Eds.)], DSSAT Version 3, vol. 4, University of Hawaii, Honolulu, USA.

Boote, K. J., Sau, F., Hoogenboom, G., Jones, J. W., 2008. Experience with water balance, evapotranspiration, and predictions of water stress effects in the CROPGRO model. In: 59-103 [L.R. Ahuja, V.R. Reddy, S.A. Saseendran, Qiang Yu (Eds.)], Response of crops to limited water: understanding and modeling water stress effects on plant growth processes, vol.1.Advances in Agricultural Systems Modeling - ASA-CSSA-SSSA, Madison, WI.

Boote, K. J., Hoogenboom, G., Jones, J. W., Ingram, K. T., 2009. Modeling nitrogen fixation and its relationship to nitrogen uptake in the CROPGRO model. In: 13-46 [L. Ma, L.R. Ahuja, T. Bruulsema (Eds.)], Quantifying and Understanding Plant Nitrogen Uptake for Systems Modeling. CRC Press, Florence, USA.

Cafaro La Menza, N., Monzon, J. P., Specht, J. E., Grassini, P., 2017. Is soybean yield limited by nitrogen supply?. Field Crops Research, v. 213, p. 204-212.

Cafaro La Menza, N. C., Monzon, J. P., Specht, J. E., Lindquist, J. L., Arkebauer, T. J., Graef, G., Grassini, P., 2019. Nitrogen limitation in high-yield soybean: Seed yield, N accumulation, and N-use efficiency. Field Crops Research, 237, 74-81.

Cafaro La Menza, N.C., Monzon, J. P., Lindquist, J. L., Arkebauer, T. J., Knops, J. M., Unkovich, M., Specht, J.E., Grassini, P., 2020. Insufficient nitrogen supply from symbiotic fixation reduces seasonal crop growth and nitrogen mobilization to seed in highly productive soybean crops. Plant, Cell & Environment, 43(8), 1958-1972.

Cantarella, H., Otto, R., Soares, J. R., de Brito Silva, A. G., 2018. Agronomic efficiency of NBPT as a urease inhibitor: A review. Journal of advanced research, 13, 19-27.

Cassman, K. G., Grassini, P., 2020. A global perspective on sustainable intensification research. Nature Sustainability, 3(4), 262-268.

CESB., 2017. National challenge of maximum productivity. Brazilian Soybean Strategic Committee (accessed 28 September 2017). http://www.cesbrasil.org.br/desafio-da-soja.

Cordeiro, C. F.S., Echer, F. R., 2019. Interactive effects of nitrogen-fixing bacteria inoculation and nitrogen fertilization on soybean yield in unfavorable edaphoclimatic environments. Scientific Reports, 9(1), 1-11.

Dari, B., Rogers, C. W., 2021. Ammonia volatilization from fertilizer sources on a loam soil in Idaho. Agrosystems, Geosciences & Environment, 4(3), e20192.

Detmann, E., Queiroz, A.C., Cabral, L.S., 2012a. Avaliação do nitrogênio total (proteína bruta) pelo método Kjeldahl. In: 51-61 [E. Detmann, M.A. Souza, S.C. Valdares Filho, A.C. Queiróz, T.T. Berchielli, Saliba, E.O.S, Cabral, L.S., D.S. Pina, M.M, Ladeira, J.A.G, Azevedo (Eds.)], Métodos para Análise de Alimentos. INCT- Ciência Animal, Suprema, MG, Brazil.

Detmann, E., Souza, M.A., Valdares Filho, S.C., 2012b. Avaliação da gordura bruta ou extrato etério. In: 77-92 [E. Detmann, M.A. Souza, S.C. Valdares Filho, A.C. Queiróz, T.T. Berchielli, Saliba, E.O.S, Cabral, L.S., D.S. Pina, M.M, Ladeira, J.A.G, Azevedo (Eds.)], Métodos para Análise de Alimentos. INCT- Ciência Animal, Suprema, MG, Brazil.

Earl, H. J., 2002. Stomatal and non-stomatal restrictions to carbon assimilation in soybean (*Glycine max*) lines differing in water use efficiency. Environmental and Experimental Botany, 48(3), 237-246.

Erbs, D. G., Klein, S. A., Duffie, J. A., 1982. Estimation of the diffuse radiation fraction for hourly, daily and monthly-average global radiation. Solar energy, 28(4), 293-302.

Erisman, J. W., Sutton, M. A., Galloway, J., Klimont, Z., Winiwarter, W., 2008. How a century of ammonia synthesis changed the world. Nature Geoscience, 1(10), 636-639. Ferm, M., 1998. Atmospheric ammonia and ammonium transport in Europe and critical loads: a review. Nutrient Cycling in Agroecosystems, 51(1), 5-17.

Fabre, F., Planchon, C. 2000. Nitrogen nutrition, yield and protein content in soybean. Plant Science, 152(1), 51-58.

Fehr, W. R., Caviness, C. E., 1977. Stages of soybean development. Iowa State University Experimental Station Publications, Ames, Iowa, USA.

Feng, L., Raza, M. A., Li, Z., Chen, Y., Khalid, M. H. B., Du, J., Liu, W., Wu, X., W., Song, C., Liang, Y., Zhang, Z., Yuan, S., Yang, W, Yang, F., 2019. The influence of light intensity and leaf movement on photosynthesis characteristics and carbon balance of soybean. Frontiers in Plant Science, 9, 1952.

Ferm, M., 1998. Atmospheric ammonia and ammonium transport in Europe and critical loads: a review. Nutrient Cycling in Agroecosystems, 51(1), 5-17.

Fontoura, S. M. V., Bayer, C. 2010. Ammonia volatilization in no-till system in the south-central region of the State of Paraná, Brazil. Revista Brasileira de Ciência do Solo, 34(5), 1677-1684.

Gijsman, A. J., Hoogenboom, G., Parton, W. J., Kerridge, P. C., 2002. Modifying DSSAT crop models for low-input agricultural systems using a soil organic matter–residue module from CENTURY. Agronomy Journal, 94(3), 462-474.

Godwin, D. C., Jones, C.A., 1991. Nitrogen Dynamics in Soil-Plant Systems. Modeling Plant and Soil Systems, 31, 287-321.

Godwin, D. C.; Singh, U., 1998. Nitrogen balance and crop response to nitrogen in upland and lowland cropping systems. In: 55-77 [G. Y. Tsuji, G. Hoogenboom, and P. K. Thornton (Eds.)], Understanding options for agricultural production. Kluwer Academic Publishers, London, United Kingdom.

Gonçalves, A.O, Silva, E.H.F.M, Gasparotto, L.G, Mantelatto, J.R, Carmo, S., Fattori Júnior, I.M, Marin, F.R., 2020. Improving indirect measurements of the leaf area index using canopy height. Pesquisa Agropecuária Brasileira, 55, 1-9.

Grimm, S. S., J. W. Jones, K. J. Boote, J. D. Hesketh. 1993. Parameter estimation for predicting flowering date of soybean cultivars. Crop Science. 33:137-144.

Grimm, S. S., Jones, J. W., Boote, K.J., Herzog, D. C., 1994. Modeling the occurrence of reproductive stages after flowering for four soybean cultivars. Agronomy Journal, v. 86 (1), 31-38.

Gurgel, G. C.S., Ferrari, A. C., Fontana, A., Polidoro, J. C., Coelho, L. D. A. M., Zonta, E., 2016. Volatilização de amônia proveniente de fertilizantes minerais mistos contendo ureia. Pesquisa Agropecuária Brasileira, 51(9), 1686-1694.

Hayati, R., Egli, D. B., Crafts-Brandner, S. J., 1995. Carbon and nitrogen supply during seed filling and leaf senescence in soybean. Crop science, 35(4), 1063-1069.

Herridge, D. F., Peoples, M. B., Boddey, R. M., 2008. Global inputs of biological nitrogen fixation in agricultural systems. Plant and Soil, 311(1), 1-18.

Hungria, M., Franchini, J. C., Campo, R. J., Crispino, C. C., Moraes, J. Z., Sibaldelli, R. N., Mendes, I., Arihara, J., 2006. Nitrogen nutrition of soybean in Brazil: contributions of biological N_2 fixation and N fertilizer to grain yield. Canadian Journal of Plant Science, 86(4), 927-939.

Jiang, C. Z., Rodermel, S. R., Shibles, R. M., 1993. Photosynthesis, rubisco activity and amount, and their regulation by transcription in senescing soybean leaves. Plant Physiology, 101(1), 105-112.

Jones, J. W., Boote, K. J., Hoogenboom, G., Jagtap, S. S., Wilkerson, G. G., 1989. SOYGRO V5. 42, Soybean crop growth simulation model. User's guide. Florida Agricultural Experiment Station Journal, 8304, 83.

Kimball, B. A., Bellamy, L. A., 1986. Generation of diurnal solar radiation, temperature, and humidity patterns. Energy in agriculture, 5(3), 185-197.

Koeppen, W., 1948. Climatologia: con un estudio de los climas de la tierra. Mexico, DF: Fondo de Cultura Econômica, 478 p.

Krol, D. J., Forrestal, P. J., Wall, D., Lanigan, G. J., Sanz-Gomez, J., Richards, K. G., 2020. Nitrogen fertilisers with urease inhibitors reduce nitrous oxide and ammonia losses, while retaining yield in temperate grassland. Science of the Total Environment, 725, 138329.

Kumar, P. A., Parry, M. A., Mitchell, R. A., Ahmad, A., Abrol, Y. P., 2002. Photosynthesis and nitrogen-use efficiency. In: p.23-34 [C.H, Foyer, G, Noctor (Eds.)] Photosynthetic nitrogen assimilation and associated carbon and respiratory metabolism. Springer, Dordrecht, Netherlands.

Loague, K., Green, R. E., 1991. Statistical and graphical methods for evaluating solute transport models: overview and application. Journal of Contaminant Hydrology, 7(1–2), 51–73.

Liu, F., Jensen, C. R., Andersen, M. N., 2003. Hydraulic and chemical signals in the control of leaf expansion and stomatal conductance in soybean exposed to drought stress. Functional Plant Biology, 30(1), 65-73.

Liu, Q., Liu, B., Zhang, Y., Hu, T., Lin, Z., Liu, G., Wang, X., Ma, J., Wang, H., Jin, H. Ambus, P., Amonette, J., Xie, Z., 2019. Biochar application as a tool to decrease soil nitrogen losses (NH_3 volatilization, N_2O emissions, and N leaching) from croplands: Options and mitigation strength in a global perspective. Global Change Biology, 25(6), 2077-2093.

Mariotti, F., Tomé, D., Mirand, P. P., 2008. Converting nitrogen into protein—beyond 6.25 and Jones' factors. Critical reviews in food science and nutrition, 48(2), 177-184.

Martins, M. R., Sant'Anna, S. A. C., Zaman, M., Santos, R. C., Monteiro, R. C., Alves, B. J. R., Alvesa, B.J.R., Jantalia, C.P., Urquiaga, S., 2017. Strategies for the use of urease and nitrification inhibitors with urea: Impact on N_2O and NH_3 emissions, fertilizer-15N recovery and maize yield in a tropical soil. Agriculture, Ecosystems & Environment, 247, 54-62.

Mazzetto, A. M., Styles, D., Gibbons, J., Arndt, C., Misselbrook, T., Chadwick, D., 2020. Region-specific emission factors for Brazil increase the estimate of nitrous oxide emissions from nitrogen fertilizer application by 21%. Atmospheric Environment, 117506.

Milliken, G.A., Johnson, D.E., 2009. One-Way Treatment Structure in a Completely Randomized Design Structure with Heterogeneous Errors. In: p.21-39 [G.A. Milliken, Johnson, D.E. (Eds)], Analysis of Messy Data. CRC Press, New York, USA.

Mira, A. B., Cantarella, H., Souza-Netto, G. J. M., Moreira, L. A., Kamogawa, M. Y., & Otto, R. 2017. Optimizing urease inhibitor usage to reduce ammonia emission following urea application over crop residues. Agriculture, Ecosystems & Environment, 248, 105-112.

Mourtzinis, S., Kaur, G., Orlowski, J. M., Shapiro, C. A., Lee, C. D., Wortmann, C., Holshouser, D., Nafziger, E.D., Kandel, H., Niekamp, J., Ross, W.J., Lofton, J., Roozemboom, K.L., Thelen, K.D., Lindsey, L.E., Staton, M., Naeve, S.L., Casteel, S.N., Wiebold, W.J., Conley, S. P., 2018. Soybean response to nitrogen application across the United States: A synthesis-analysis. Field Crops Research, 215, 74-82.

Nakasathien, S., Israel, D. W., Wilson, R. F., Kwanyuen, P., 2000. Regulation of seed protein concentration in soybean by supra-optimal nitrogen supply. Crop Science, 40(5), 1277-1284.

Ohashi, Y., Nakayama, N., Saneoka, H., Fujita, K., 2006. Effects of drought stress on photosynthetic gas exchange, chlorophyll fluorescence and stem diameter of soybean plants. Biologia Plantarum, 50(1), 138-141.

Ojima, M., Fukui, J., Watanabe, I., 1965. Studies on the Seed Production of Soybean: II. Effect of three major nutrient elements supply and leaf age on the photosynthetic activity and diurnal changes in photosynthesis of soybean under constant temperature and light intensity. Japanese Journal of Crop Science, 33(4), 437-442.

Parton, W. J., and Logan, J. A., 1981. A model for diurnal variation in soil and air temperature. Agricultural Meteorology, 23, 205-216.

Parton, W. J., McKeown, B., Kirchner, V., Ojima, D., 1992. Century users manual. Natural Resource Ecology Laboratory, Colorado State University, Fort Collins, Colorado, USA.

Patterson, R. P., Hudak, C. M., 1996. Drought-avoidant soybean germplasm maintains nitrogen-fixation capacity under water stress. In: p.39-43 [Elkan, G.H., Upchurch, R.G. (Eds.)]. Current Issues in Symbiotic Nitrogen Fixation. Springer, Dordrecht.

Pavanelli, L. E., Araújo, F. F., 2009. Fixação biológica de nitrogênio em soja em solos arenosos cultivados com pastagem e culturas anuais do Oeste Paulista. Biosci. J. 25, 21–29.

Pereira, A. R., Nova, N. A. V., 1992. Analysis of the Priestley-Taylor parameter. Agricultural and Forest Meteorology, 61(1-2), 1-9.

Piper, E. L., Boote, K. J., Jones, J. W., Grimm, S. S., 1996. Comparison of two phenology models for predicting flowering and maturity date of soybean. Crop Science, 36(6), 1606-1614.

Priestley, C. H. B., and Taylor, R. J., 1972. On the assessment of surface heat flux and evaporation using large-scale parameters. Monthly Weather Review, 100(2), 81–92.

Purcell, L. C., King, C. A., 1996. Drought and nitrogen source effects on nitrogen nutrition, seed growth, and yield in soybean. Journal of Plant Nutrition, 19(6), 969-993.

Purcell, L. C., Serraj, R., Sinclair, T. R., De, A., 2004. Soybean N_2 fixation estimates, ureide concentration, and yield responses to drought. Crop Science, 44(2), 484-492.

Ray, J. D., Heatherly, L. G., Fritschi, F. B., 2006. Influence of large amounts of nitrogen on nonirrigated and irrigated soybean. Crop Science, 46(1), 52-60.

Reis, A. F.B., Rosso, L.M., Purcell, L. C., Naeve, S., Casteel, S. N., Kovacs, P., Archontoulis, S., Davidson, D. Ciampitti, I. A., 2021. Environmental factors associated with nitrogen fixation prediction in soybean. Frontiers in Plant Science, 12, 1013.

Ritchie, J.T., 1972. Model for predicting evaporation from a row crop with incomplete cover. Water Resources Research, 8(5), 1204–1213.

Ritchie, J. T., 1985. A user-orientated model of the soil water balance in wheat. In: 293-305 [W. Day, R. K. Atkin (Eds.)], Wheat growth and modelling. Springer, Boston, USA.

Rotundo, J. L., Borrás, L., Westgate, M. E., Orf, J. H., 2009. Relationship between assimilate supply per seed during seed filling and soybean seed composition. Field Crops Research, 112(1), 90-96.

Rochette, P., MacDonald, J. D., Angers, D. A., Chantigny, M. H., Gasser, M. O., Bertrand, N. 2009. Banding of urea increased ammonia volatilization in a dry acidic soil. Journal of Environmental Quality, 38(4), 1383-1390.

Rochette, P., Angers, D. A., Chantigny, M. H., Gasser, M. O., MacDonald, J. D., Pelster, D. E., Bertrand, N. 2013. Ammonia volatilization and nitrogen retention: how deep to incorporate urea?. Journal of Environmental Quality, 42(6), 1635-1642.

Salvagiotti, F., Cassman, K. G., Specht, J. E., Walters, D. T., Weiss, A., Dobermann, A., 2008. Nitrogen uptake, fixation and response to fertilizer N in soybeans: A review. Field Crops Research, 108(1), 1-13.

Salvagiotti, F., Specht, J. E., Cassman, K. G., Walters, D. T., Weiss, A., Dobermann, A., 2009. Growth and nitrogen fixation in high-yielding soybean: Impact of nitrogen fertilization. Agronomy Journal, 101(4), 958-970.

Santachiara, G., Salvagiotti, F., Rotundo, J. L., 2019. Nutritional and environmental effects on biological nitrogen fixation in soybean: A meta-analysis. Field Crops Research, 240, 106-115.

Sau, F., Boote, K. J., Bostick, W. M., Jones, J. W., Mínguez, M. I., 2004. Testing and improving evapotranspiration and soil water balance of the DSSAT crop models. Agronomy Journal, 96(5), 1243–1257.

Sims, D. A., Luo, Y., Seemann, J. R., 1998. Comparison of photosynthetic acclimation to elevated CO_2 and limited nitrogen supply in soybean. Plant, Cell & Environment, 21(9), 945-952.

Sinclair, T. R., De Wit, C. T., 1976. Analysis of the carbon and nitrogen limitations to soybean yield 1. Agronomy Journal, 68(2), 319-324.

Sinclair, T. R., Muchow, R. C., Bennett, J. M., Hammond, L. C., 1987. Relative sensitivity of nitrogen and biomass accumulation to drought in field-grown soybean. Agronomy Journal, 79(6), 986-991.

Singh, U., Porter, C., 2019. Improving modeling of nutrient cycles in crop cultivation. In: p.69-99 [K.J. Boote (Ed.)] Advances in Crop Modeling for a Sustainable Agriculture. Burleigh Dodds Science Publishing, Cambridge, United Kingdom.

Spitters, C. J. T., 1986. Separating the diffuse and direct component of global radiation and its implications for modeling canopy photosynthesis Part II. Calculation of canopy photosynthesis. Agricultural and Forest meteorology, 38(1-3), 231-242.

Spitters, C. J. T., Toussaint, H. A. J. M., Goudriaan, J., 1986. Separating the diffuse and direct component of global radiation and its implications for modeling canopy photosynthesis Part I. Components of incoming radiation. Agricultural and Forest Meteorology, 38(1-3), 217-229.

Sprent, J. I., 1971. Effects of water stress on nitrogen fixation in root nodules. Plant and Soil, 35(1), 225-228.

Suleiman, A. A., Ritchie, J. T., 2003. Modeling soil water redistribution during second-stage evaporation. Soil Science Society of America Journal, 67(2), 377–386.

Tamagno, S., Balboa, G. R., Assefa, Y., Kovács, P., Casteel, S. N., Salvagiotti, F., García, F.O., Stewart, W.M., Ciampitti, I. A., 2017. Nutrient partitioning and stoichiometry in soybean: A synthesis-analysis. Field Crops Research, 200, 18-27.

Thies, J. E., Singleton, P. W., Bohlool, B. B., 1995. Phenology, growth, and yield of field-grown soybean and bush bean as a function of varying modes of N nutrition. Soil Biology and Biochemistry, 27(4-5), 575-583.

Thornton, P. K., Hoogenboom, G., 1994. A computer program to analyze single-season crop model outputs. Agronomy Journal 86(5):860-868.

Ti, C., Ma, S., Peng, L., Tao, L., Wang, X., Dong, W., Wang, L., Yan, X., 2020. Changes of δ15N values during the volatilization process after applying urea on soil. Environmental Pollution, 270, 116204.

Uryasev, O., Gijsman, A. J., Jones, J. W., Hoogenboom, G., Wilkens, P. W., Porter, C. H., 2004. DSSAT v4 Soil data editing program [SBUILD]. Decision Support System for Agrotechnology Transfer Version, 4, 2-14.

Wang, F., Fraisse, C. W., Kitchen, N. R., Sudduth, K. A., 2003. Site-specific evaluation of the CROPGRO-soybean model on Missouri claypan soils. Agricultural Systems, 76(3), 985-1005.

Wilkerson, G. G., Jones, J. W., Boote, K. J., Ingram, K. T., Mishoe, J. W., 1983. Modeling soybean growth for crop management. Transactions of the ASAE, 26(1), 63-73.

Wilkerson, G. G., Jones, J. W., Boote, K. J., Mishoe, J. W., 1985. SOYGRO V5.0. Soybean crop growth and yield model. Technical documentation. Agricultural Engineering Department, University of Florida, Gainesville, USA.

Willmott, C. J., Ackleson, S. G., Davis, R. E., Feddema, J. J., Klink, K. M., Legates, D. R., O'Donnell, J., Rowe, C. M., 1985. Statistics for the evaluation and comparison of models. Journal of Geophysical Research: Oceans, 90(C5), 8995–9005.

Zhou, X. J., Liang, Y., Chen, H., Shen, S. H., Jing, Y. X., 2006. Effects of rhizobia inoculation and nitrogen fertilization on photosynthetic physiology of soybean. Photosynthetica, 44(4), 530-535.

Zhou, H., Yao, X., Zhao, Q., Zhang, W., Zhang, B., Xie, F., 2019. Rapid effect of nitrogen supply for soybean at the beginning flowering stage on biomass and sucrose metabolism. Scientific Reports, 9(1), 1-13.

4. YIELD POTENTIAL OF SOYBEAN IN TROPICAL ENVIRONMENTS: AN APPROACH REGARDS SUSTAINABLE AGRICULTURAL INTENSIFICATION

ABSTRACT

Brazil accounts for 37% (based on the 2020/2021 harvest) of the world's soybean [*Glycine max* (L.) Merr.] harvest. The quantification of Brazilian soybean yield potential (Y_P), water-limited crop yield potential (Y_{P-W}), and crop yield gap (Y_G) can contribute to agricultural intensification procedures and food security studies. We performed long-term simulations to investigate the effects of nitrogen (N)-fertilizer on soybean yield using several planting dates, two water availability conditions, four cultivars, and three N-fertilizer rates. N-fertilization provided marginal or no effect on soybean crop yield, and the soybean yield decreased with a late planting date, mainly in regions at higher latitudes. Sequentially, we simulated Y_P, Y_{P-W}, Y_G, climate efficiency (E_C), and agricultural efficiency (E_A) for 16 strategically selected agroclimatic zones (CZs) to represent Brazilian production. Calibrations obtained with well-managed experiments conducted throughout the country were used in all simulations. The Y_P and Y_{P-W} were estimated by crop simulation using CROPGRO-Soybean, and the Y_G was estimated as the difference between the Y_P and the actual crop yield. Across CZs, Y_{P-W} ranged from 3,133 kg ha^{-1} to 5,186, Y_P ranged from 3,952 to 6,084 kg ha^{-1}, and Y_G ranged from 589 to 4,401 kg ha^{-1}. The E_C ranged from 67 to 97%, and 14% of Y_P, on average, was penalized by drought stress. The E_A ranged from 26 to 88%, and represented 35% of Y_{P-W}, on average; it was mainly depleted by fertilization, planting date, or biotic stresses. We also found that 26% of the soybean production areas in Brazil had an $E_C < 95\%$, and for this area supplementary irrigation was required; moreover, it was possible to save around 20% of water through conservative soil practices, such as no-tillage, and through improvements in the soil root growth.

Keywords: Sustainable intensification; Climate efficiency; Agricultural efficiency; Crop water management; Planting dates.

4.1. Introduction

In the past 20 years, Brazil has had one of the most significant expansions of agricultural land (Zalles *et al*., 2019) and has established itself as the world's largest soybean exporter. Since 2020, Brazil has become a global leader in soybean production, with a harvested area of 38.5 million ha and total production of 134 million tons in the 2020/2021 season (USDA, 2021). Soybean production provides a basis for global food security because it is one of the most important vegetable oil and protein sources, widely used in food and feed products (Beta and Isaak, 2016; Smárason *et al*., 2019; Wajid *et al*., 2020; Parisi *et al*., 2020). Despite expressive soybean production, Cassaman and Grassini (2020) warn that expansion of the harvest area from 2002 to 2014 contributed an 85% increase in global production of soybean, a result of a combination of the impact of slowing yield and rapid expansion of the crop production area. These trends point to the need for sustainable agricultural intensification

studies due to the need to increase food production under conditions of agricultural land scarcity.

The sustainable intensification of agriculture depends on crops receiving adequate amounts of water and essential nutrients from the atmosphere and soil. Some researchers assert that water deficit is the greatest limiting factor in crop production, and agriculture accounts for 70% of global freshwater withdrawals (Hoogeveen *et al*., 2009; Armengot *et al*., 2021; Siyal *et al*., 2021); therefore, improved water management is an important component of sustainable cropping. Fertilizers are also a critical component of food security, as they are responsible for at least half of all global food production (Erisman *et al*., 2008). Among the most studied nutrients is nitrogen (N), given its importance in global food production and its impact on the environment related to ammonia (NH_3) volatilization. Most of the world's soybean crop systems do not use N-fertilizer application, but its use often raises the debate on N fertilization of soybean to increase crop yields, because N is the nutrient most required by soybean, as discussed in Chapter 3.

Evaluating the yield potential (Y_P, kg ha^{-1}), water-limited crop yield potential ($Y_{P\text{-}W}$, kg ha^{-1}), yield gap (Y_G, kg ha^{-1}), climate efficiency (E_C), and agricultural efficiency (E_A) (see definitions in Chapter 1) of soybean provides insight into ways to optimize agricultural processes to contribute to sustainable agricultural intensification. Previous studies on soybean yield gap analysis have been conducted for some countries around the world (Rattalino Edreira *et al*., 2017; Van Vugt *et al*., 2017; Di Mauro *et al*., 2018, Rizzo *et al*., 2021). In Brazil, efforts have been made by some researchers to estimate the yield gap: (i) Sentelhas *et al*. (2015) used only crop yield and phenology collected under 17 sites in southern Brazil to calibrate a simple crop model (FAO Agroecological Zone model); (ii) Battisti *et al*. (2018) used a dataset from soybean yield contest areas and adaptation of the FAO Agroecological Zone model for crop yield simulations; (iii) Nóia Júnior and Sentelhas (2020) used an ensemble of three crop models with only one cultivar calibration obtained by Battisti *et al*. (2017) from experiments conducted in southern Brazil; (iv) for soybean sown in the *Cerrado* biome, Santos *et al*. (2021) used a simple crop model adaptation of the FAO Agroecological Zone model with only one cultivar calibration obtained by Battisti *et al*. (2017); and (v) for soybean sown in the subtropics of Brazil, Tagliapietra *et al*. (2021) used CROPGRO-Soybean with cultivar parameters obtained by Mercau (2007) and Monzon (2007) from experiments conducted in Argentina. However, a thorough assessment of Y_P, $Y_{P\text{-}W}$, Y_G, E_C, and E_A across the whole Brazilian soybean-producing area, using a well-managed field experiment conducted with a single protocol and consistent crop model, calibrated and evaluated for tropical and subtropical environments, using various

planting dates, along with different water availability and N-fertilization conditions is still lacking and could contribute to studies regarding sustainable intensification of soybean in Brazil.

Thus, an assessment of soybean potential intensification in tropical and subtropical environments requires robust estimates of Y_P or Y_{P-W}. Here, we followed data-rich field experiments conducted with a consistent protocol in tropical and subtropical environments across Brazil, which were used to calibrate and evaluate the CROPGRO-Soybean (see details in Chapters 2 and 3). The calibrated crop model was coupled with good available sources of weather, soil, and production data, to determine the available capacity to increase soybean yield in the Brazilian production area.

4.1.1. Research goals

The main aims of the present chapter were (i) to assess the impact of different planting dates, the use of a soybean cropping system with N-fertilization, and the use of only indigenous soil N sources on crop yield and (ii) to estimate the Y_P, Y_{P-W}, and Y_G for soybean under a consolidated soybean production area in Brazil. The specific objectives of this chapter were to conduct long-term simulations (i) using several nitrogen doses under rainfed and irrigated conditions and various planting dates, (ii) to determine the best planting date to maximize the crop yield, (iii) to determine the amount of water applied per season to reach the yield potential under tropical and subtropical environments, (iv) to determine the effects (simulated) of N-fertilizer on crop yield, (v) to define agroclimatic zones representing the whole soybean sowing area, and (vi) to apply hypothetical scenarios using different crop water management for CZs with E_C <95%.

4.2. Materials and Methods

4.2.1. Long-term scenarios for agricultural practices

Several field experiments well conducted under tropical and subtropical environments in Brazil were used to calibrate and evaluate the CROPGRO-Soybean (see Chapter 3 for more details). We obtained excellent agreement between simulated and observed values for leaf area index, leaf dry matter, stem dry matter, grain weight, and aboveground dry matter for the

following cultivars: (i) TMG 7062 sown in Piracicaba [PI-1 (22°42′N, 47°30′W, 546 a.m.s.l.)], over three seasons (2017/2018, 2018/2019, 2019/2020); (ii) TMG 7063 sown in Sorriso [SO-1 (12°42′S, 55°48′W, 375 a.m.s.l.)], over one season (2018/2019); (iii) NS 7901 sown in Sorriso [SO-2 (12°42′S, 55°48′W, 375 a.m.s.l.)], over one season (2019/2020); (iv) 65i65RSF, sown in Cruz Alta [CA-1 (28°38′S, 53°36′W, 476 a.m.s.l.)], over one season (2018/2019) and in Tupanciretã [TU-1 (28°48′S, 53°48′W, 466 a.m.s.l.); and (v) 8579RSF, sown in Teresina [TE-1 (05°02′S, 42°47′W, 78 a.m.s.l.)] over one season.

We performed long-term simulations using the settings defined in Chapter 3: (i) the FAO-56 Penman-Monteith potential evapotranspiration method (Allen et al., 1998) combined with the Ritchie Two-Stage soil water evaporation method (Ritchie, 1972) (see more details in Chapter 2), (ii) Century (Parton et al., 1992; Gijsman et al., 2002) as the soil organic matter method, (iii) 50% of available soil water to start soil water balance of the model at 30 days prior to planting, (iv) soil profile data were computed with the SBUILD program of DSSAT (Uryasev et al., 2004), using the soil granulometry (texture) obtained on each site (Appendix F), (v) cultivar traits calibrated previously (Appendix G), and (iv) no-tillage practices with 8,500 kg ha^{-1} of crop surface residue (maize) under the initial conditions. The climatic datasets were obtained from NASA [National Aeronautics and Space Administration, NASA POWER API Client (Sparks, 2018)], for the period 1989–2020 (see Appendix H). The NASA dataset showed good accuracy when compared with weather data measured in Brazil (Monteiro et al., 2017; Valeriano et al., 2019; Duarte and Sentelhas, 2020). The climate datasets contained daily data on solar radiation (MJ m^{-2} day^{-1}), maximum and minimum air temperature (ºC), precipitation (mm), wind speed (m s^{-1}), and relative humidity (%); for Piracicaba, Sorriso, Cruz Alta, and Teresina from 1989 to 2020. The climatic dataset from Cruz Alta and Tupanciretã was the same, because these two locations are very close together; thus, we kept only Cruz Alta for the long-term simulations. To represent the soybean cropping systems for each site, we simulated various planting date sets based on the planting window officially recommended by Ministry of Agriculture in Brazil over 5-day intervals, as follows: (i) PI-1 was sown between September 8 and December 31; (ii) SO-1 and SO-2 was sown between September 30 and December 25; (iii) CA-1 was sown between September 17 and December 31; and (iv) TE-1 was sown between November 30 and February 28.

We applied the CROPGRO-Soybean for long-term simulations, to explore the crop yield potential and water-limited soybean yield potential of soybeans sown in tropical and subtropical environments, to ask what-if questions (Tsuji et al., 1998; Thornton and Hoogenboom, 1994) by conducting virtual simulation experiments in Piracicaba, Sorriso, Cruz

Alta and Teresina. This included (i) various planting date using an official data window, with an interval of 5 days between; (ii) rainfed versus full-irrigated (non-limiting water conditions) with irrigation triggered at 60% soil water available in the top 0.30 m of the soil profile (see Chapter 2), and (iii) N-fertilizer rates at 0, 300, and 600 kg N ha^{-1}; these fertilizer rates were chosen based on our findings presented in Chapter 3. We conducted these simulations to investigate the cropping system-imposed yield gap by N fertilization on soybean, which we defined as the difference in crop yield between non- or N-fertilized soybean. The simulations were repeated for 30 seasons using long-term historical weather data from 1989 to 2020. The long-term scenarios were evaluated for their response to crop yield, N volatilization, planting date, and total seasonal water applied during the growing season.

4.3. Long-term simulations for crop yield potential, water-limited crop yield potential, and yield gap under tropical and subtropical conditions

We used the official statistical data on soybean production and area in Brazil provided by the Brazilian Institute of Geography and Statistics (IBGE, 2021) under five last seasons (2016-2021). We considered only counties where there was an average sowing area greater than 400 ha as criteria to select consolidated production area (total of 34.3 Mha). Following the protocol described by Van Wart *et al*. (2013), we defined 16 agroclimatic zones (CZs) for representing the production area in the county (Fig. 4.1). Such classification was based on three factors: (i) crop degree days, calculated using basal temperature fixed at 0°C; (ii) annual dryness index, calculated by the ratio between annual average total rainfall and the yearly average of potential crop evapotranspiration; and (iii) seasonality of air temperature (Van Wart *et al*, 2013). The methodology developed by Van Wart *et al.* (2013) was widely used in yield potential studies (Van Ittersum *et al*., 2013; Grassini *et al*. 2015; Pradahan *et al.*, 2015; Jaenisch *et al*., 2021, Assefa *et al.*, 2020).

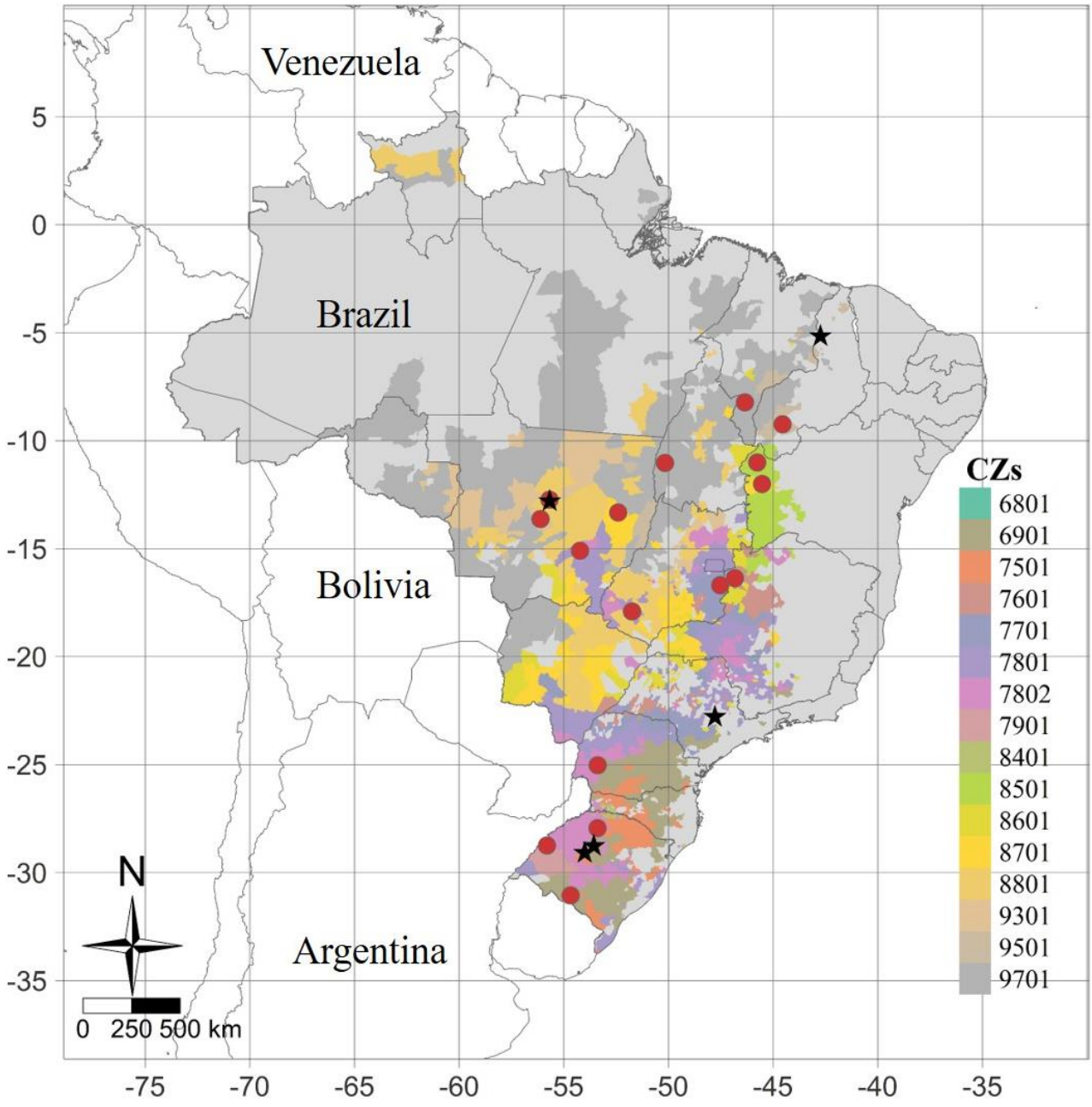

Fig.4.1. Spatial distribution of 16 agroclimatic zones (CZs) that represents all soybean production municipalities in Brazil. Red circles indicate weather stations, and black stars indicate field experiments. Source: Silva *et al*. (2021) (adapted).

The climatic dataset was obtained from the NASA [Sparks *et al*., 2018 (see Appendix V)]. Defining the dominant soil type for each CZs was performed by soil extraction data from the Brazilian Soil Map (EMBRAPA, 2014) and crossed it with each CZs. Soils were filtered by their relative presence in a given zone and by selecting the soil with the highest coverage for each CZs (Table 4.1). To represent the Brazilian soybean cropping systems, we conducted the

simulations using planting date from officially planting date recommended by the Ministry of Agriculture in Brazil (*Ministério da Agricultura, Pecuária e Abastecimento*, 2020) over 5-day intervals (Table 4.1).

Table 4.1. Name of the weather station used from each agroclimatic zones (CZs), official planting window, soil, long-term annual average temperature and total annual rainfall, and cultivar used for CROPGRO-Soybean simulations.

CZ	Weather Station	Planting date window		Soil profile	Average temperature and annual rainfall	Cultivar
6801	Cascavel- PR	Set 8	Dec 31	Ultisols	18.2°C 1822 mm	TMG 7062
6901	Dom Pedrito- RS	Set 17	Dec 31	Entisols	18.5°C 1313 mm	65i65 RSF
7501	Unaí-MG	Oct 7	Dec 31	Oxisols	23.5°C 1275 mm	NS 7901
7601	Cristalina - GO	Sep 27	Dec 31	Oxisols	20.1°C 1422 mm	NS 7901
7701	Jataí-GO	Sep 27	Dec 31	Oxisols	23.3°C 1541 mm	NS 7901
7801	Primavera do Leste-MT	Sep 27	Dec 31	Ultisols	22.0°C 1784 mm	NS 7901
7802	São Borja-RS	Oct 27	Dec 31	Oxisols	20.5°C 1567 mm	65i65 RSF
7901	Palmeira das Missões - RS	Sep 17	Dec 31	Oxisols	18.7°C 1838 mm	65i65 RSF
8401	Formosa do Rio Preto-BA	Oct 17	Jan 31	Oxisols	24.3°C 902 mm	NS 7901
8501	Barreiras-BA	Oct 17	Jan 31	Entisols	24.9°C 1045 mm	NS 7901
8601	Canarana-MT	Sep 30	Dec 25	Oxisols	24.8°C 1541 mm	NS 7901
8701	Sorriso-MT	Sep 30	Dec 25	Oxisols	25.0°C 1883 mm	NS 7901
8801	Nova Mutum-MT	Sep 30	Dec 25	Entisols	24.6°C 934 mm	NS 7901
9301	Bom Jesus-PI	Nov 6	Feb 9	Entisols	26.7°C 1002 mm	NS 7901
9501	Balsas-MA	Oct17	Jan 20	Entisols	26.4°C 1190 mm	NS 7901
9701	Lagoa da Confusão-TO	Oct 8	Mar 1	Inceptisols	27.2°C 1882 mm	NS 7901

The Y_P and $Y_{P\text{-}W}$ simulations were conducted for each CZ (Table 4.1) using (i) the FAO-56 Penman-Monteith potential evapotranspiration method (Allen *et al*., 1998) combined with the Ritchie Two-Stage soil water evaporation method (Ritchie, 1972) (see more details in Chapter 2), (ii) Century (Parton *et al*., 1992; Gijsman *et al*., 2002) as the soil organic matter method, (iii) 50% of available soil water to establish the soil-water balance of the model 30 days prior to sowing, (iv) soil profile data obtained from the Wise database from the International Soil Reference and Information Centre (Batjes, 2002) (see Appendix N), and (iv) all cultivars calibrated in Chapters 2 and 3 (BRS 399, TMG 7062, TMG 7063, NS 7901, 65i65RSF, and 8579RSF), after simulations we selected the cultivar that obtained the highest crop yield for each CZs (Table 4.1). For Y_P, we turned off the water and nitrogen options to

reach simulated yield potential, and for Y_{P-W} we only kept the water options on to simulate the effects of water on crop yield. The Y_G was computed as the difference between average Y_P and actual crop yield (Y_A). YA was computed as the average of soybean yield obtained for each county obtained by IBGE (2021), for the last five seasons (2016–2021). IBGE considers a sample of the mean yield from a farm in each county regarding multiple soils, cultivars, and planting dates.

Altogether, we generated approximately 19,200 simulations to obtain Y_P and Y_{P-W}. Based on these simulations, we estimated the long-term scenarios for (i) average Y_P and Y_{P-W}; (ii) lower limits of Y_P and Y_{P-W} (here defined as average less standard deviation); (iii) upper limits of Y_P and Y_{P-W} (here defined as average plus standard deviation); (iv) Y_G, (v) climate efficiency (E_C, %), here defined as the ratio between Y_{P-W} and Y_P; and (vi) agricultural efficiency (E_A, %) here defined as the ratio between Y_{P-W} and Y_A.

4.3.1. Simulation of long-term of water management scenarios

Following the simulation of Y_{P-W} and Y_P, we conducted a seasonal analysis based on what-if scenarios to explore water management practices for each CZ with an obtained E_C <95%. We conducted virtual simulation experiments with (i) conventional tillage practices with the original soil root growth factor [SRGF, (CT)]; (ii) no-tillage practices with 8,500 kg ha^{-1} of crop surface residue (maize) under the initial conditions, with the original SRGF (NT); (iii) no-tillage practices with 8,500 kg ha^{-1} of crop surface residue (maize) under the initial conditions, and soil root growth factor (SRGF) changed (NT+SRGF) (Appendix N); and (iv) irrigation application under treatments “i”, “ii,” and “iii”. The SRGF is an important soil-plant parameter in DSSAT because it affects the potential amount of soil water that can be extracted by roots (Calmon *et al*., 1999; Ma *et al*., 2009). We used SRGF obtained by Battisti and Sentelhas (2017) using proportional soybean root length density distribution observed in high-yield fields (>7,200 kg ha^{-1}) in Brazil. The irrigation amount was applied using irrigation triggered at 60% soil water availability in the top 0.30 m of the soil profile (see Chapter 2). The objective of these what-if scenarios was to seek water management strategies to increase the E_C and water use efficiency. Finally, the seasonal irrigation applied was multiplied per total soybean harvest area [county level, using the average of the last five seasons (2016–2021) provided by IBGE (2021)].

4.4. Results and Discussion

4.4.1. Long-term scenarios for agricultural practices

The irrigated without N-fertilization long-term simulations over 30 years of weather (see irrigation amounts in Annex O) for soybean yield showed the highest crop yield on early planting dates, and the differences between the lowest and highest crop yields were (i) 2,554 kg ha^{-1} for PI-1, (ii) 916 kg ha^{-1} for SO-1, (iii) 1,621 kg ha^{-1} for SO-2, (iv) 2,578 kg ha^{-1} for CA-1, and (v) 471 kg ha^{-1} for TE-1 (Table 4.2, and see more details in Appendix Q to U). Hence, our results showed that planting date was the important factor in reaching the maximum crop yield; this was directly related to crop cycle length: late planting date showed a shorter crop cycle than early planting date (Appendix P). Furthermore, sites at higher latitudes [Cruz Alta (28º38′S) and Piracicaba (22°43′S)] were more sensitive to the planting date than those at low latitudes [Sorriso (12º42′S) and Teresina (05º02′S)]. Other authors described that lower soybean yields observed on late planting may be associated with a short vegetative period caused by high initial temperatures and shorter grain filling period (Ball *et al*., 2000; Board and Harville, 1996; Bastidas *et al*., 2008) as influenced by the photoperiod (Kantolic and Slafer, 2001; Major *et al*., 1975).

However, rainfed conditions conducted in PI-1, SO-2, and CA-1 did not get highest crop yield for planting date close to the optimum because of adverse weather (Table 4.2). On average, the crop yield difference between irrigated and rainfed long-term scenarios were (i) 1,150 kg ha^{-1} for PI-1, (ii) 166 kg ha^{-1} for SO-1, (iii) 77 kg ha^{-1} for SO-2, (iv) 1,987 kg ha^{-1} for CA-1, and (v) 267 kg ha^{-1} for TE-1 (Table 4.2, and see more details in Appendix O to S). The small difference in crop yield between rainfed and irrigated conditions observed in Sorriso and Teresina was due to the characterization of this region by a rainy season from October to April with good distribution and regularity of rainfall (Cesarin *et al*., 2008; Dallcort *et al*., 2010; Bastos and Andrade Junior, 2012; Marco *et al*., 2016). We also observed that the cultivars TMG 7063 [earlier cultivar (SO-1)] and NS 7900 [later cultivar (SO-2)] resulted in different optimum planting date: September 30 for SO-1 and October 25 for SO-2. Thus, early cultivars showed the best performance in late planting, while late cultivars showed the best performance in early planting (Table 4.2, Appendix P and Q). This agrees with the discussion point in section 3.3.1 of Chapter 3 that, for the Southern Hemisphere,

Table 4.2. Average soybean yield for long-term simulation (1989–2020) is shown as minimum, maximum, and mean crop yield under different planting dates; rainfed and irrigated conditions; and N-fertilization doses of 0, 300 and 600 kg N ha^{-1}.

Exp.	Rainfed 0N		Rainfed 300N		Rainfed 600N		Irrigated 0N		Irrigated 300N		Irrigated 600N	
	Yield (kg ha^{-1})	Planting Date	Yield (kg ha^{-1})	Planting Date	Yield (kg ha^{-1})	Planting Date	Yield (kg ha^{-1})	Planting Date	Yield (kg ha^{-1})	Planting Date	Yield (kg ha^{-1})	Planting Date
PI-1												
Minimum	3,324	Sep 8	3,592	Sep 8	3,740	Sep 8	3,994	Dec 27	4,256	Dec 27	4,550	Dec 27
Maximum	5,065	Oct 23	5,330	Oct 23	5,357	Oct 23	6,548	Set 8	6,621	Set 8	6,795	Set 8
Mean	4,410	–	4,667	–	4,796	–	5,560	–	5,773	–	5,883	–
SO-1												
Minimum	2,990	Dec 24	3,008	Dec 24	3,050	Dec 24	3,116	Dec 24	3,210	Dec 24	3,137	Dec 24
Maximum	3,863	Oct 25	3,930	Oct 25	3,957	Oct 25	4,032	Oct 25	4,122	Oct 25	4,134	Oct 25
Mean	3,566	–	3,631	–	3,633	–	3,732	–	3,817	–	3,796	–
SO-2												
Minimum	3,787	Dec 24	3,841	Dec 24	3,890	Dec 24	3,787	Dec 24	3,840	Dec 24	3,890	Dec 24
Maximum	5,129	Oct 10	5,202	Oct 10	5,240	Oct 10	5,408	Sep 30	5,481	Sep 30	5,515	Sep 30
Mean	4,660	–	4,724	–	4,768	–	4,737	–	4,791	–	4,834	–
CA-1												
Minimum	3,407	Dec 26	3,628	Dec 26	4,557	Dec 26	4,218	Dec 26	4,487	Dec 26	4,672	Dec 26
Maximum	4,441	Oct 17	4,507	Oct 17	4,706	Oct 17	6,796	Oct 2	6,871	Oct 2	6,996	Oct 2
Mean	4,153	–	4,270	–	4,320	–	5,975	–	6,140	–	6,275	–
TE-1												
Minimum	2,393	Dec 30	2,778	Feb 18	2,657	Nov 30	2,662	Feb 28	3,067	Feb 28	3,071	Feb 28
Maximum	2,856	Nov 30	3,034	Dec 10	3,131	Dec 30	3,133	Dec 5	3,326	Nov 30	3,340	Dec 10
Mean	2,734	–	2,908	–	2,990	–	3,004	–	3,188	–	3,198	–

planting between late September (late cultivars) and mid-October (early cultivars) may be more ideal for the soybean crop to reach its peak of development (between R3 and R6) in December, when there is the greatest solar energy availability.

In section 3.3.1 of Chapter 3, we hypothesized that earlier planting dates could require N-fertilization to reach a higher crop yield. Our results did not support this hypothesis, because we found again a modest increase in crop yield in 300N or 600N treatments. On average, for all simulations, the 300N treatment showed an increase of 138 kg ha^{-1}, and the 600N treatment, 196 kg ha^{-1}. This reinforces the point discussed earlier: N-fertilization provided marginal or no effect on soybean yield under tropical conditions. Consequently, the crop yield obtained with the best planting date may be met by N fixation.

4.4.2. Long-term simulations for crop yield potential, water-limited crop yield potential, and yield gap under tropical and subtropical conditions

The diversity of simulated planting date, cultivars, and soil types resulted in an average Y_P of 5,441 kg ha^{-1} and 4,684 kg ha^{-1} for $Y_{P\text{-}W}$, with an average Y_A of 3,092 kg ha^{-1} under 16 CZs (Fig. 4.2 a, b). These results are close to those obtained by Sentelhas *et al*. (2015) for Y_P (5,332 kg ha^{-1}), but our $Y_{P\text{-}W}$ estimation was greater than theirs: they found 3,866 kg ha^{-1} with a higher penalty for water stress, 27% on average. Sentelhas *et al*. (2015) used the FAO model to estimate Y_P and $Y_{P\text{-}W}$; that model only requires total soil holding capacity (Battisti *et al*., 2017), while CROPGRO-Soybean simulates soil water movement using a tipping bucket and curve number approach that defines soil water redistribution, infiltration, and runoff (see Chapter 2). Thus, the different methods to simulate soil water balance may have contributed to differences between $Y_{P\text{-}W}$ estimates. By contrast, Battisti *et al*. (2018), using a database from soybean contest areas, found that Y_P ranged from 7,595 to 13,378 kg ha^{-1}, and $Y_{P\text{-}W}$ ranged from 5,442 to 11,296 kg ha^{-1}. Santos *et al*. (2021) estimated Y_P (range from 11,075 to 12,078 kg ha^{-1}) and $Y_{P\text{-}W}$ (range from 5,552 to 8,271 kg ha^{-1}) for the Cerrado biome in Brazil. The estimates of $Y_{P\text{-}W}$ and Y_P obtained by Battisti *et al*. (2018) and Santos (2021) seem very overrated even when compared with those of other studies conducted in areas of higher yield potential (greatest solar energy availability and non-limiting temperatures), such as USA (Grassini *et al*., 2015, Zang *et al*., 2016, Cafaro La Menza *et al*., 2017), Argentina (Merlos *et al*., 2015; Di Mauro *et al*., 2018), and Uruguay (Rizzo *et al*., 2021).

Findings from the present study showed climate efficiency ranging from 67% to 97%, with E_C <95% for 6801, 6901, 7501, 7802, 7901, 8401, 8501, and 9301 CZs (Fig. 4.2). For 74% (or 25.4

Mha) of soybean production areas under tropical and subtropical conditions, the degree of water limitation was less than 5% for average Y_P. The long-term scenarios pointed out that Y_P was penalized by drought stress from 3% to 32% (14% on average) in all CZs. In general, soybean sown in Brazil presented a good average $Y_{P\text{-}W}$ with relatively low losses due to drought in most of the soybean area, when compared with studies conducted in other countries, where the Y_P depletion by drought stress (i) ranged from 170 kg ha^{-1} to 3,350 kg ha^{-1} (with Y_P ranging from 4,470 to 6,510 kg ha^{-1}) in Mississippi, USA (Zhang *et al*., 2016); (ii) ranged from 43% to 50% for single soybean systems in Uruguay (Rizzo *et al*., 2021); and (iii) it was 28% of soybean potential yield, on average, penalized by drought stress in India (Bhatia *et al*., 2008). Nonetheless, improvements in agricultural water management are required in 26% of the soybean area in Brazil to increase the yield level.

This study documented strong associations between Y_P (or $Y_{P\text{-}W}$) and the planting date. The long-term scenarios for the lower limit (Fig. 4.3 a, b) revealed that the worst planting dates could result in a $Y_{P\text{-}W}$ of 4,353 kg ha^{-1} (331 kg ha^{-1} lower than the average $Y_{P\text{-}W}$) and a Y_P of 4,800 kg ha^{-1} (641 kg ha^{-1} lower than the average Y_P), whereas in the long-term scenarios for the upper limit shown for the best planting dates (Fig. 4.3 d, c), the $Y_{P\text{-}W}$ could reach 5,186 kg ha^{-1} (502 kg ha^{-1} greater than the average $Y_{P\text{-}W}$) and 5,854 kg ha^{-1} for Y_P (413 kg ha^{-1} greater than the average Y_P). The planting dates influence the Y_P through the crop cycle duration, which is in turn influenced by solar radiation and air temperature; this was also observed for soybean sown in the USA by Grassini *et al*. (2014) and Edreira *et al*. (2017), and in Argentina (Vitantonio-Mazzinia, 2021). For soybean sown under rainfed systems (*i.e*., $Y_{P\text{-}W}$ when there are drought losses) the prediction of the best planting date is more difficult because of the need to equate losses due to water stress vs. lower availability of energy (solar radiation). In rainfed systems, the water supply comes from stored soil water at planting and from in-season rainfall. As long-term rainfall forecasting is still challenging because it has many factors that lead to uncertainty (Asnaashari *et al*., 2015; Ni *et al*., 2020; Raval *et al*., 2021), soybeans grown under a well-managed irrigated system will be able to obtain an additional yield increase (beyond avoiding drought stress) through appropriate choice of the planting date.

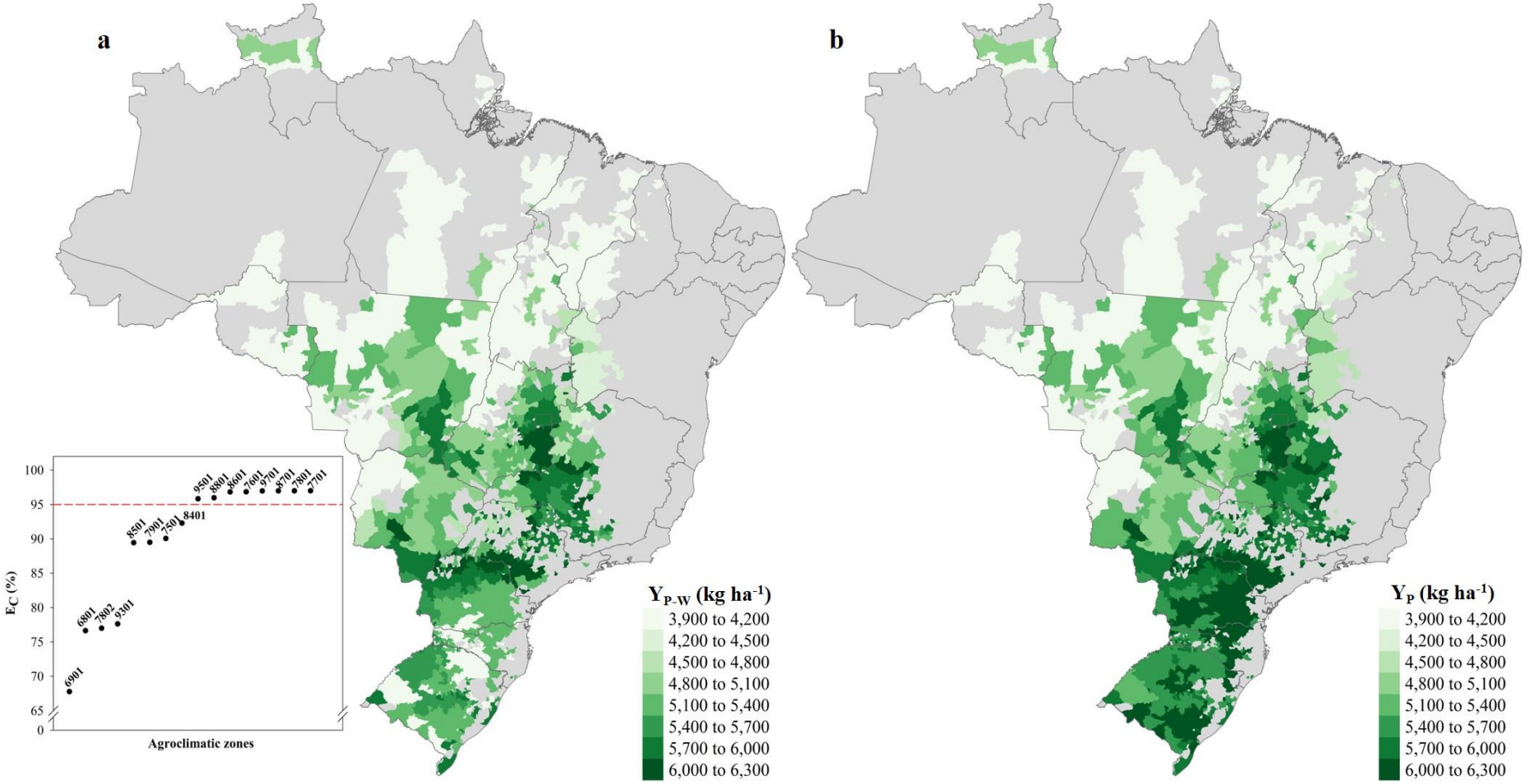

Fig. 4.2. Average of long-term simulations (1989–2020) for water-limited crop yield potential [Y_{P-W} (a)] and crop yield potential [Y_P (b)] in Brazil. Climate efficiency (ratio between Y_{P-W} and Y_P) under agroclimatic zones. Inset shows the climate efficiency (E_C) defined as the ratio between crop yield potential and water-limited crop yield potential under agroclimatic zones. Dashed red line shows the 95% climate efficiency limit.

The Y_G ranged from 589 to 4,401 kg ha^{-1}, with an average of 2,349 kg ha^{-1} (Fig. 4.4 a), which was greater than reported by Nóia Júnior and Sentelhas (2020) (Y_G=1,641 kg ha^{-1}) in Brazil. However, those authors used only one cultivar (BRS 284-maturity group 6.5) calibrated by Battisti et al. (2017) from experiments conducted in Southern Brazil for simulating Y_P and $Y_{P\text{-}W}$. One single maturity group is not adequate to represent the soybean crop system in Brazil from a realistic viewpoint and this over-simplification may be related with the underestimated Y_G obtained by Nóia Júnior and Sentelhas (2020) compared with our results. Tagliapietra *et al*. (2020) analyzed the soybean yield gap for the state of Rio Grande do Sul (RS) (the southernmost state of Brazil) and found Y_G ranging from 4,150 to 4,800 kg ha^{-1}, while our estimates of Y_G ranged from 1,628 to 4,157 kg ha^{-1} for RS. We observed that Y_G for the southern region is higher than Y_G estimated for northern Brazil due to the greater losses caused by water deficit in Southern Brazil (Fig. 4.2 and Fig. 4.4 a).

We computed the E_A ranging from 26.4% to 87.6%, with an average of 50.2% (Fig. 4.4 b). This means that, on average 49.8% of rainfed soybean production in Brazil, have been lost by suboptimal crop management [planting date, seeding rate, cultivar, tillage method, limitation of nutrients, biotic stress control (insect pests, diseases, and weeds)]. The highest values of E_A were obtained in some regions of Brazilian Amazon areas (states of Amazonas, Pará, and Rondônia, with average E_A = 77.1%), where soybean fields were usually sown on pastures converted from natural vegetation for cattle production (Song *et al*., 2021) with a relatively low average Y_P (*c.a*. 4,010 kg ha^{-1}, Fig. 4.2a). The lowest E_A values (57.3%) were obtained in São Paulo state, in which soybean is generally sown in replanting sugarcane fields without with low inputs applied (Souza and Seabra, 2013; Cortez *et al*., 2014; Longati *et al*., 2020).

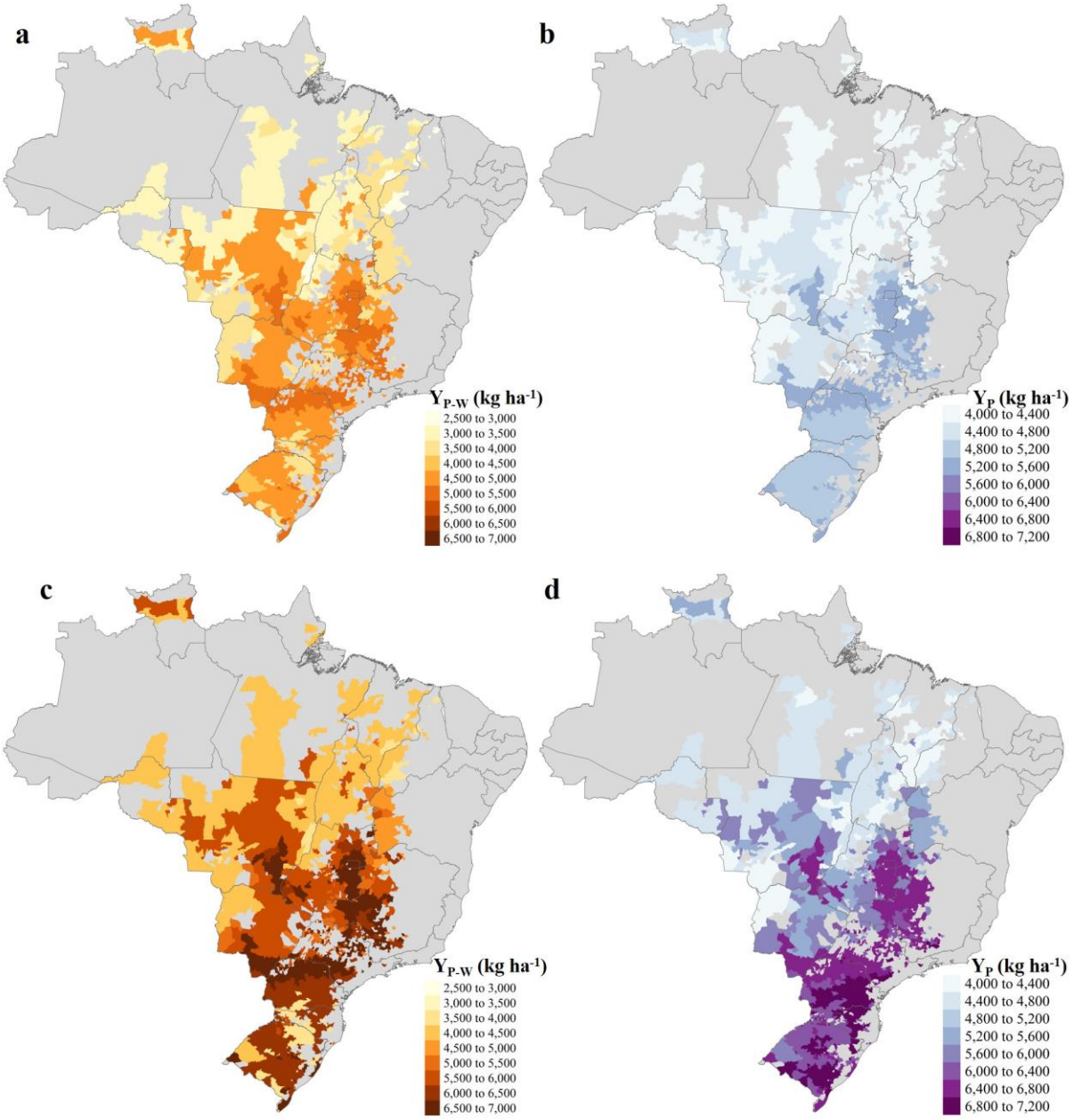

Fig. 4.3. Simulated long-term scenarios (1989–2020) for water-limited crop yield potential (Y_{P-W}) lower limit (a) and upper limit (c), and for yield potential (Y_P) lower limit (b) and upper limit (d) in Brazil.

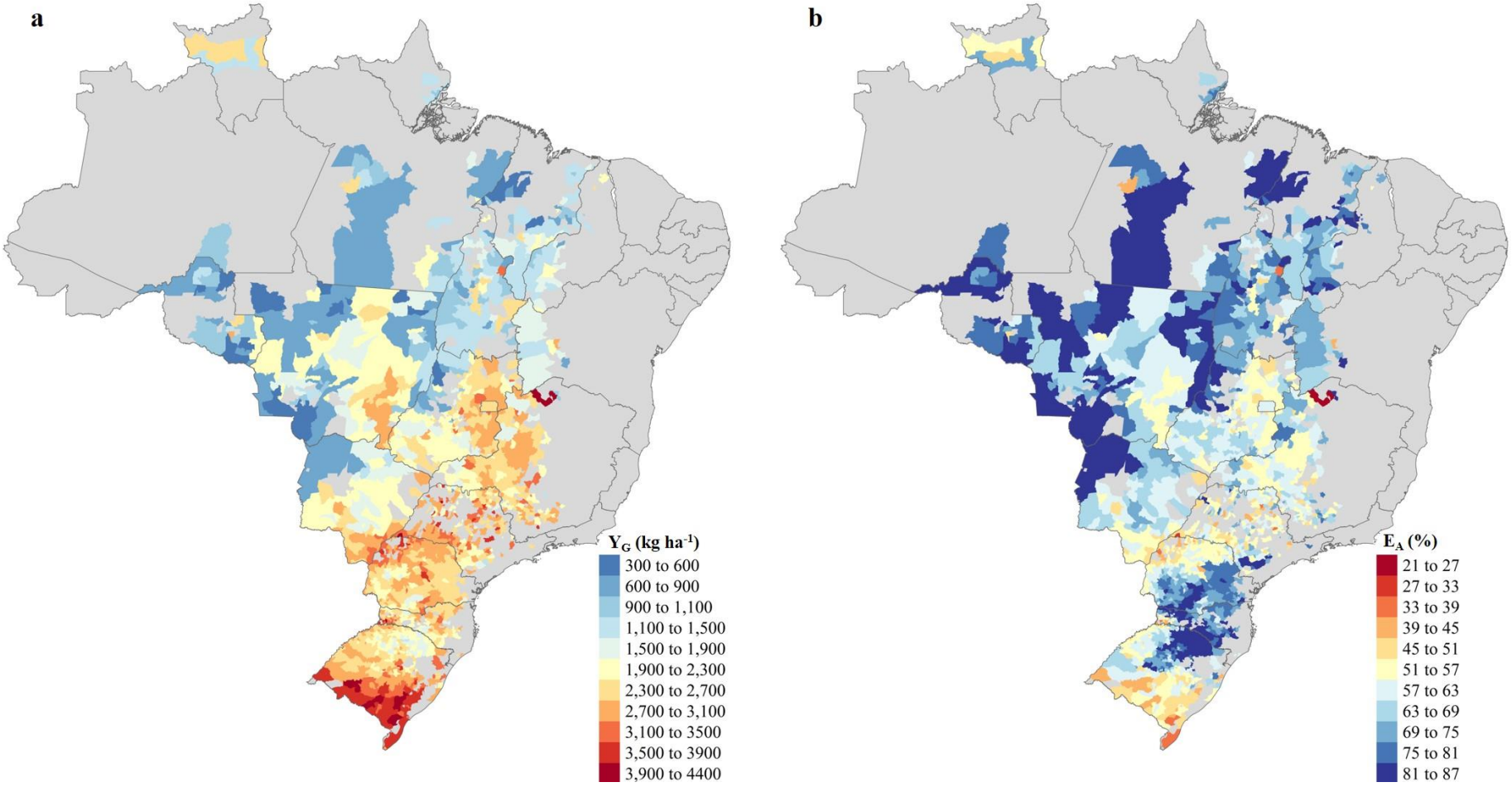

Fig. 4.4. Soybean yield gap (Y_G), computed as average yield potential (1989–2020) subtracted from the average actual soybean crop yield (2015–2020) in Brazil, and (b) agricultural efficiency (E_A) is the ratio between the actual yield and the water-limited yield potential.

4.4.3. Application of seasonal analyses of crop water management

We conducted long-term simulations based on different crop water management for CZs that obtained E_C <95%. The variation in E_C ranged from 0 to 1% between CT and NT practices, and from 2% to 5% between the CT and NT + SRGF parameters. The SRGF changes represented the improvement of crop and soil management to better root growth for high fields (Sako *et al*., 2015; Battisti and Sentelhas, 2017). Although the simulated treatments did not present a significant increase in E_C, we obtained considerable water savings between conventional tillage and no-tillage with SRGF changes (Fig. 4.5). The water savings between CT and NT+SRGF ranged from 16% to 30% (average of 20%). We obtained a small difference between conventional tillage and no-tillage practices, ranging from 1% to 5%. In all irrigated simulations under non-limiting water conditions, we reached yield values similar to the average Y_P (Fig. 4.2); the total water amount required is shown in Fig. 4.6.

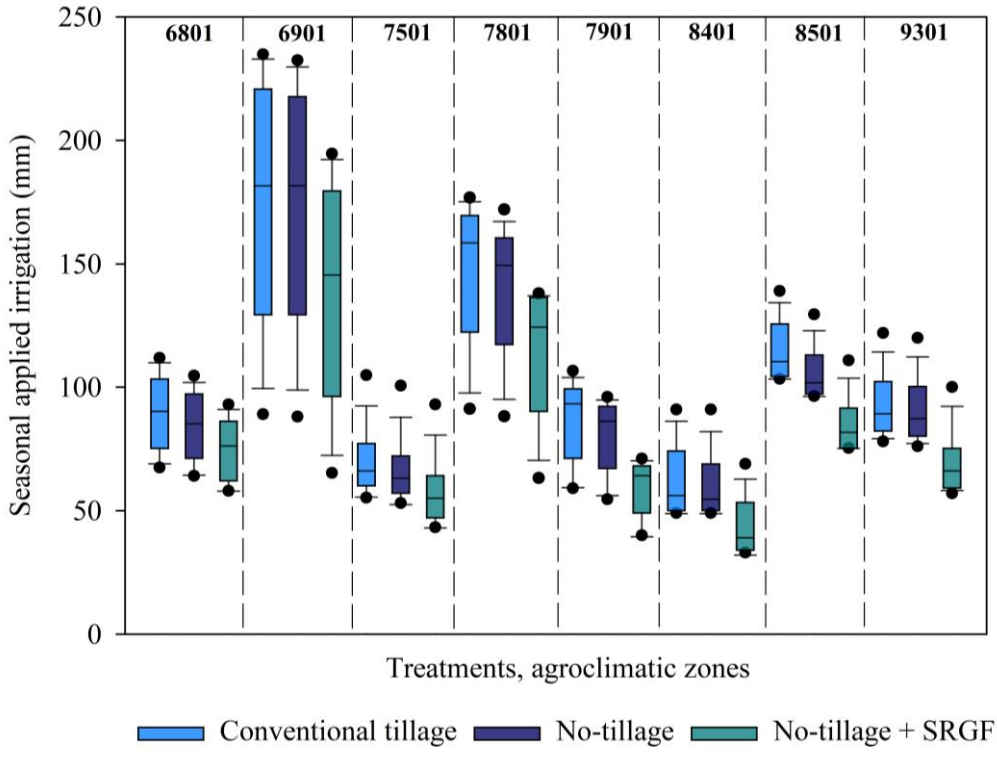

Fig. 4.5. Simulated long-term scenarios (1989–2020) for seasonally applied irrigation under conventional tillage, no-tillage, and no-tillage practices with changes in the SRGF (soil root growth factor) parameter.

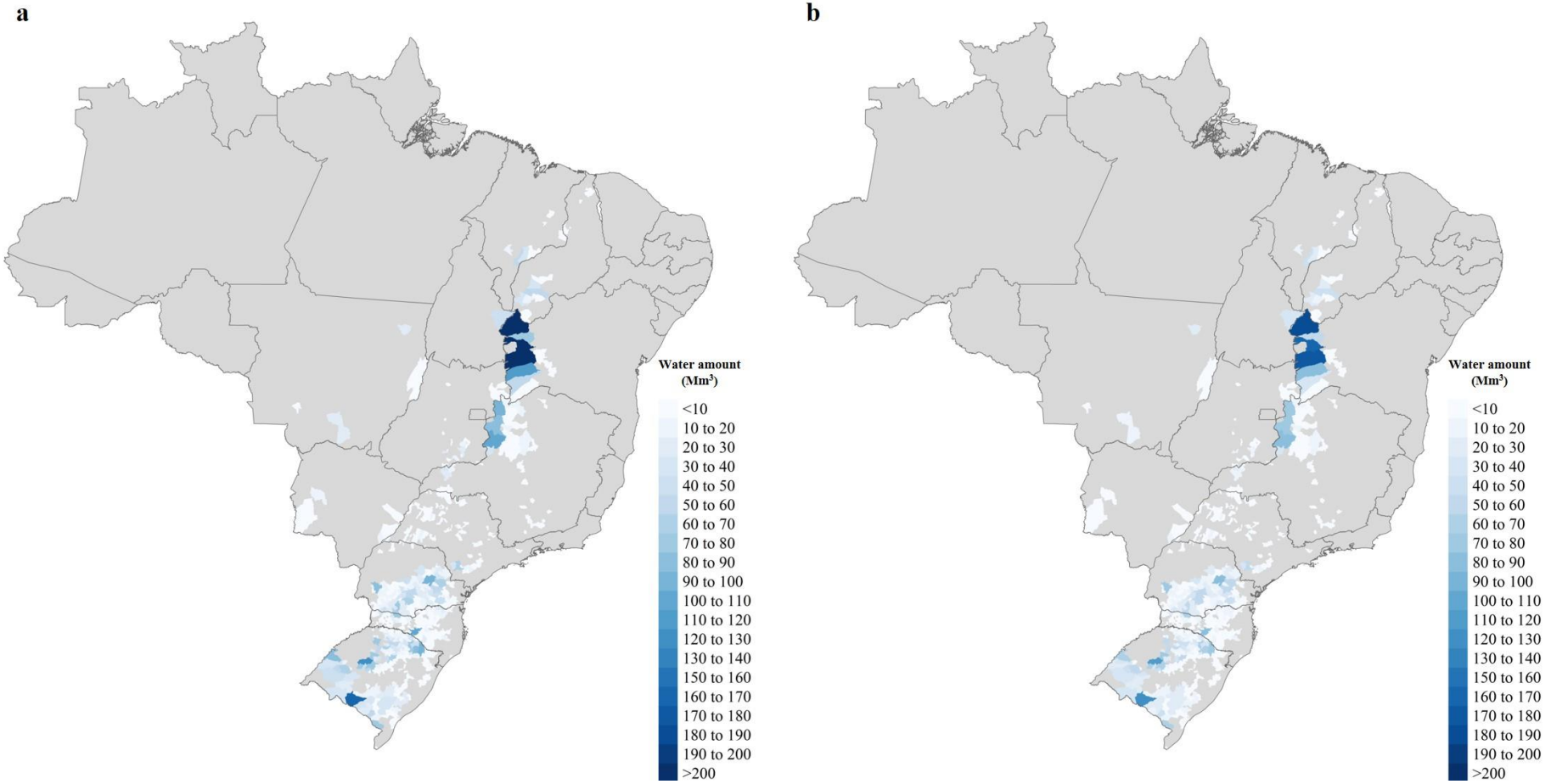

Fig. 4.6. Long-term scenarios for seasonal irrigation applied under treatments with conventional tillage (a), and no-tillage with changes in the SRGF (soil root growth factor) parameter.

We investigated options for agricultural water management to decrease the total water required for soybean $Y_{P\text{-}W}$ to reach Y_P values. For conventional tillage, the total water amount needed in Brazilian soybean areas was 9,597.94 Mm^3 (considering only areas with E_C <95%). When we ran the simulation with conservative soil practices such as no-tillage with better conditions for root growth, the total water amount required decreased to 7,665.36 Mm^3, which is 20.14% less than soybean conducted under conventional practices (Fig. 4.6). Soil management with maintenance of soil mulch can contribute to a reduction in the amount of water required for supplemental irrigation because the model simulates reduction of soil water evaporation (see Chapter 2). The most favorable conditions for root elongation and rooting depth to enhance water uptake at greater depths have been demonstrated by several researchers (Rellán-Álvarez *et al*., 2016; He *et al*., 2019; Bertollo *et al*., 2021; Bossolani *et al*., 2021). The model is structured to compute water uptake according to the soil depth and conditions, and the potential root water uptake from each soil layer is computed from the fraction of water that can be taken up from a given soil layer and the SRGF (Calmon *et al*., 1999).

The long-term simulations of the CROPGRO-Soybean conducted under tropical and subtropical conditions with early planting dates reached a higher Y_P. As shown before, our simulations revealed that agricultural management is the most important factor in the soybean yield gap (34%) in Brazil, and losses due to drought stress represent 14% of the total yield gap. Soil conservation practices were not able to increase the E_C but may contribute for saving around of 20% of the supplementary irrigation. N-fertilization proved to be inefficient for increasing soybean yield and inconsistent with sustainable agricultural intensification practices under a tropical and subtropical environment.

4.5. Conclusion

This study showed that early planting dates achieved higher soybean yields under non-limiting water conditions. The planting date did not impact on crop yield response to N-fertilization on crop yield. The long-term scenarios of N-fertilization rates 300 and 600 kg N ha^{-1} under rainfed and irrigated conditions showed marginal or no response on soybean yield. We estimated $Y_{P\text{-}W}$ (range from 4,353 to 5,186 kg ha^{-1}) and Y_P (range from 4,800 to 5,854 kg ha^{-1}) for the lower limit, average, and upper limit for all CZs. We also simulated average Y_G = 3,092, E_C = 14%, and E_A = 50.2% and concluded that the improvements in soybean crop systems could contribute to a 49.8% increase in the soybean yield under rainfed conditions. We

found that 26% soybean production areas in Brazil the supplementary irrigation was required, the average water amount required was 9,597.94 Mm^3 with conventional soil practices and 7,665.36 Mm^3 for conservative soil practices, such as no-tillage, and through improvements in the soil root growth.

References

Allen, R. G., Pereira, L. S., Raes, D., Smith, M., 1998. Crop evapotranspiration - Guidelines for computing crop water requirements-FAO Irrigation and drainage paper 56. FAO, Rome, 300(9), D05109.

Asnaashari, A., Gharabaghi, B., McBean, E. D., Mahboubi, A. A., 2015. Reservoir management under predictable climate variability and change. Journal of Water and Climate Change, 6(3), 472-485.

Assefa, B. T., Chamberlin, J., Reidsma, P., Silva, J. V., van Ittersum, M. K., 2020. Unravelling the variability and causes of smallholder maize yield gaps in Ethiopia. Food Security, 12(1), 83-103.

Armengot, L., Beltrán-Muñoz, M. J., Schneider, M., Simón, X., Pérez-Neira, D., 2021. Food-energy-water nexus of different cacao production systems from a LCA approach. Journal of Cleaner Production, 126941.

Batjes, N. H., 2002. A homogenized soil profile data set for global and regional environmental research (No. 2002/01). ISRIC-World Soil Information.

Ball, R. A., Purcell, L. C., Vories, E. D., 2000. Optimizing soybean plant population for a short-season production system in the southern USA. Crop Science, 40(3), 757-764.

Bastos, E. A., Andrade Júnior, A. S., 2013. Boletim agrometeorológico de 2012 para o Município de Teresina, Piauí. Embrapa Meio-Norte-Documentos (INFOTECA-E).

Bastidas, A. M., Setiyono, T. D., Dobermann, A., Cassman, K. G., Elmore, R. W., Graef, G. L., Specht, J. E., 2008. Soybean sowing date: The vegetative, reproductive, and agronomic impacts. Crop Science, 48(2), 727-740.

Battisti, R., Sentelhas, P. C., 2017. Improvement of soybean resilience to drought through deep root system in Brazil. Agronomy Journal, 109(4), 1612-1622.

Battisti, R., Sentelhas, P. C., Boote, K. J., 2017. Inter-comparison of performance of soybean crop simulation models and their ensemble in southern Brazil. Field crops research, 200, 28-37.

Battisti, R., Sentelhas, P. C., Pascoalino, J. A. L., Sako, H., de Sá Dantas, J. P., Moraes, M. F., 2018. Soybean yield gap in the areas of yield contest in Brazil. International Journal of Plant Production, 12(3), 159-168.

Beta, T., Isaak, C., 2016. Grain production and consumption: Overview. In: p. 349-428 [C. Wrigley, H. Corke, K. Seetharaman, J. Faubion (Eds.)], Encyclopedia of Food Grains – the World of Food Grains, V.1, Elsevier, Oxford, United Kingdom.

Bertollo, A. M., de Moraes, M. T., Franchini, J. C., Soltangheisi, A., Junior, A. A. B., Levien, R., Debiasi, H., 2021. Precrops alleviate soil physical limitations for soybean root growth in an Oxisol from southern Brazil. Soil and Tillage Research, 206, 104820.

Bhatia, V. S., Singh, P., Wani, S. P., Chauhan, G. S., Rao, A. K., Mishra, A. K., Srinivas, K., 2008. Analysis of potential yields and yield gaps of rainfed soybean in India using CROPGRO-Soybean model. Agricultural and Forest Meteorology, 148(8-9), 1252-1265.

Board, J. E., Harville, B. G., 1996. Growth dynamics during the vegetative period affects yield of narrow-row, late-planted soybean. Agronomy Journal, 88(4), 567-572.

Bossolani, J. W., Crusciol, C. A. C., Portugal, J. R., Moretti, L. G., Garcia, A., Rodrigues, V. A., Fonseca, M.C., Bernart, L., Vilela, R.G., Mendonça, P.L., dos Reis, A. R., 2021. Long-term liming improves soil fertility and soybean root growth, reflecting improvements in leaf gas exchange and grain yield. European Journal of Agronomy, 128, 126308.

Cafaro La Menza, N., Monzon, J. P., Specht, J. E., Grassini, P., 2017. Is soybean yield limited by nitrogen supply?. Field Crops Research, 213, 204-212.

Calmon, M. A., Jones, J. W., Shinde, D., Specht, J. E., 1999. Estimating parameters for soil water balance models using adaptive simulated annealing. Applied Engineering in Agriculture, 15(6), 703.

Cassman, K. G., Grassini, P. 2020. A global perspective on sustainable intensification research. Nature Sustainability, 3(4), 262-268.

Casarin, R., da Silva Neves, S. M. A., Neves, R. J. 2008. Uso da terra e qualidade da água da bacia hidrográfica Paraguai/Jauquara-MT. Revista Geográfica Acadêmica, 2(1), 33-43.

Cassman, K. G., Grassini, P., 2020. A global perspective on sustainable intensification research. Nature Sustainability, 3(4), 262-268.

Cortez, L.A.B, Leal, M. R. L.V., Nassar, A. M, Moreira, M.M.R, Feldman, S., Taube-Netto, M.; Silva, A. Land requirements for producing ethanol in Brazil, Sugarcane bioethanol R&D, 301-318. for Productivity and Sustainability, São Paulo: Editora Edgard Blücher, 2014. http://dx.doi.org/10.5151/BlucherOA-Sugarcane-SUGARCANEBIOETHANOL_30

Dallacort, R., Moreira, P. S. P., Inoue, M. H., Silva, D. J., Carvalho, I. F., Santos, C., 2010. Caracterização da velocidade e da direção dos ventos em Tangará da Serra, Mato Grosso, Brasil. Revista Brasileira de Meteorologia, 25(3), 359-364.

De Marco, K., Dias, V. R. M., Dallacort, R., Alves, E. D. L., Tieppo, R. C., de Araújo, D. V., Barbieri, J. D., 2016. Spatial variability of the ten-day rainfall in the months in which the sowing of soybean and winter corn begins in the state of Mato Grosso. Científica, 44(4), 477-484.

Di Mauro, G., Cipriotti, P. A., Gallo, S., Rotundo, J. L., 2018. Environmental and management variables explain soybean yield gap variability in Central Argentina. European Journal of Agronomy, 99, 186-194.

Duarte, Y. C., Sentelhas, P. C., 2020. NASA/POWER and DailyGridded weather datasets—how good they are for estimating maize yields in Brazil?. International Journal of Biometeorology, 64(3), 319-329.

Edreira, J. I. R., Mourtzinis, S., Conley, S. P., Roth, A. C., Ciampitti, I. A., Licht, M. A., Kandel, H., Kyveryga, P. M., Lindsey, L.E., Muller, D.S., Naeve, S.L., Nafziger, E., Specht, J., Stanley, J., Staton, Grassini, P., 2017. Assessing causes of yield gaps in agricultural areas with diversity in climate and soils. Agricultural and Forest Meteorology, 247, 170-180.

Erisman, J. W., Sutton, M. A., Galloway, J., Klimont, Z., Winiwarter, W., 2008. How a century of ammonia synthesis changed the world. Nature Geoscience, 1(10), 636-639.

Gijsman, A. J., Hoogenboom, G., Parton, W. J., Kerridge, P. C., 2002. Modifying DSSAT crop models for low-input agricultural systems using a soil organic matter–residue module from CENTURY. Agronomy Journal, 94(3), 462-474.

Grassini, P., Torrion, J. A., Cassman, K. G., Yang, H. S., Specht, J. E., 2014. Drivers of spatial and temporal variation in soybean yield and irrigation requirements in the western US Corn Belt. Field Crops Research, 163, 32-46.

Grassini, P., van Bussel, L. G., Van Wart, J., Wolf, J., Claessens, L., Yang, H., Boogard, H., Groot, H., van Ittersum, M.K., Cassman, K. G., 2015. How good is good enough? Data requirements for reliable crop yield simulations and yield-gap analysis. Field Crops Research, 177, 49-63.

He, J., Jin, Y. I., Turner, N. C., Chen, Z., Liu, H. Y., Wang, X. L., Siddique, K.H.M., Li, F. M., 2019. Phosphorus application increases root growth, improves daily water use during the reproductive stage, and increases grain yield in soybean subjected to water shortage. Environmental and Experimental Botany, 166, 103816.

Hoogeveen, J., Faurès, J. M., Van de Giessen, N., 2009. Increased biofuel production in the coming decade: to what extent will it affect global freshwater resources? Irrigation and Drainage, 58(S1), S148-S160.

IBGE, 2021. Área plantada, área colhida, quantidade produzida e rendimento médio de soja [WWW Document]. URL. https://sidra.ibge.gov.br/ (accessed 2.21.21).

Jaenisch, B. R., Munaro, L. B., Bastos, L. M., Moraes, M., Lin, X., Lollato, R. P., 2021. On-farm data-rich analysis explains yield and quantifies yield gaps of winter wheat in the US central Great Plains. Field Crops Research, 272, 108287.

Longati, A. A., Batista, G., Cruz, A. J. G., 2020. Brazilian integrated sugarcane-soybean biorefinery: Trends and opportunities. Current Opinion in Green and Sustainable Chemistry, 100400.

Kantolic, A. G., Slafer, G. A., 2001. Photoperiod sensitivity after flowering and seed number determination in indeterminate soybean cultivars. Field Crops Research, 72(2), 109-118.

Ma, L., Hoogenboom, G., Saseendran, S. A., Bartling, P. N. S., Ahuja, L. R., Green, T. R., 2009. Effects of estimating soil hydraulic properties and root growth factor on soil water balance and crop production. Agronomy Journal, 101(3), 572-583.

Major, D. J., Johnson, D. R., Tanner, J. W., Anderson, I. C. 1975., Effects of daylength and temperature on soybean development 1. Crop Science, 15(2), 174-179.

Marco, K., Dias, V. R. M., Dallacort, R., Alves, E. D. L., Tieppo, R. C., de ARAÚJO, D. V., Barbieri, J. D., 2016. Spatial variability of the ten-day rainfall in the months in which the sowing of soybean and winter corn begins in the state of Mato Grosso. Científica, 44(4), 477-484.

Mercau, J. L., Dardanelli, J. L., Collino, D. J., Andriani, J. M., Irigoyen, A., Satorre, E. H., 2007. Predicting on-farm soybean yields in the pampas using CROPGRO-soybean. Field Crops Research, 100, 200– 209.

Merlos, F. A., Monzon, J. P., Mercau, J. L., Taboada, M., Andrade, F. H., Hall, A. J., Jobbagy, E., Cassaman, K.G., Grassini, P., 2015. Potential for crop production increase in Argentina through closure of existing yield gaps. Field Crops Research, 184, 145-154.

Monteiro, L. A., Sentelhas, P. C., Pedra, G. U., 2018. Assessment of NASA/POWER satellite-based weather system for Brazilian conditions and its impact on sugarcane yield simulation. International Journal of Climatology, 38(3), 1571-1581.

Monzon, J. P., Sadras, V. O., Abbate, P. A., Caviglia, O. P., 2007. Modelling management strategies for wheat–soybean double crops in the south-eastern Pampas. Field Crops Research, 101, 44–52.

Ni, L., Wang, D., Singh, V. P., Wu, J., Wang, Y., Tao, Y., Zhang, J., 2020. Streamflow and rainfall forecasting by two long short-term memory-based models. Journal of Hydrology, 583, 124296.

Nóia Júnior, R.S., Sentelhas, P. C., 2020. Yield gap of the double-crop system of main-season soybean with off-season maize in Brazil. Crop and Pasture Science, 71(5), 445-458.

Parisi, G., Tulli, F., Fortina, R., Marino, R., Bani, P., Dalle Zotte, A., Angelis, A., Piccolo, G., Pinotti, L., Schiavone, A., Terova, G., Prandini, A., Gasco, L., Roncarati, A., Danieli, P. P., 2020. Protein hunger of the feed sector: the alternatives offered by the plant world. Italian Journal of Animal Science, 19(1), 1204-1225.

Parton, W. J., McKeown, B., Kirchner, V., Ojima, D., 1992. Century users manual. Natural Resource Ecology Laboratory, Colorado State University, Fort Collins, Colorado, USA.

Pradhan, P., Fischer, G., van Velthuizen, H., Reusser, D. E., Kropp, J. P., 2015. Closing yield gaps: how sustainable can we be?. PloS one, 10(6), e0129487.

Raval, M., Sivashanmugam, P., Pham, V., Gohel, H., Kaushik, A., Wan, Y., 2021. Automated predictive analytics tool for rainfall forecasting. Scientific Reports, 11(1), 1-13.

Rellán-Álvarez, R., Lobet, G., Dinneny, J. R., 2016. Environmental control of root system biology. Annual review of plant biology, 67, 619-642.

Ritchie, J. T., 1972. Model for predicting evaporation from a row crop with incomplete cover. Water Resources Research, 8(5), 1204–1213.

Rizzo, G., Monzon, J. P., Ernst, O., 2021. Cropping system-imposed yield gap: Proof of concept on soybean cropping systems in Uruguay. Field Crops Research, 260, 107944.

Santos, T. G., Battisti, R., Casaroli, D., Alves, J., Evangelista, A. W. P., 2021. Assessment of agricultural efficiency and yield gap for soybean in the Brazilian Central Cerrado biome. Bragantia, 80.

Sentelhas, P. C., Battisti, R., Câmara, G. M. S., Farias, J. R. B., Hampf, A. C., Nendel, C., 2015. The soybean yield gap in Brazil–magnitude, causes and possible solutions for sustainable production. The journal of agricultural science, 153(8), 1394-1411.

Silva, E. H. F. M., Antolin, L. A. S., Zanon, A. J., Junior, A. S. A., de Souza, H. A., dos Santos Carvalho, K., Vieria Júnior, N. A., Marin, F. R., 2021. Impact assessment of soybean yield and water productivity in Brazil due to climate change. European Journal of Agronomy, 129, 126329.

Siyal, A. W., Gerbens-Leenes, P. W., Nonhebel, S., 2021. Energy and carbon footprints for irrigation water in the lower Indus basin in Pakistan, comparing water supply by gravity fed canal networks and groundwater pumping. Journal of Cleaner Production, 286, 125489.

Souza, S. P., Seabra, J. E., 2013. Environmental benefits of the integrated production of ethanol and biodiesel. Applied energy, 102, 5-12.

Smárason, B. Ö., Alriksson, B., Jóhannsson, R., 2019. Safe and sustainable protein sources from the forest industry–the case of fish feed. Trends in Food Science & Technology, 84, 12-14.

Tagliapietra, E. L., Zanon, A. J., Streck, N. A., Balest, D. S., da Rosa, S. L., Bexaira, K. P., Richter, G.L., Ribas, G.G., da Silva, M. R., 2021. Biophysical and management factors causing yield gap in soybean in the subtropics of Brazil. Agronomy Journal, 113(2), 1882-1894.

USDA., 2020. World agricultural production. December 2020 WASDE report, U.S. Department of Agriculture, Washington, DC, USA.

Valeriano, T. T. B., de Souza Rolim, G., Bispo, R. C., de Oliveira Aparecido, L. E., 2019. Evaluation of air temperature and rainfall from ECMWF and NASA gridded data for southeastern Brazil. Theoretical and applied climatology, 137(3), 1925-1938.

Van Ittersum, M. K., Cassman, K. G., Grassini, P., Wolf, J., Tittonell, P., Hochman, Z., 2013. Yield gap analysis with local to global relevance—a review. Field Crops Research, 143, 4-17.

Van Vugt, D., Franke, A. C., Giller, K. E., 2017. Participatory research to close the soybean yield gap on smallholder farms in Malawi. Experimental Agriculture, 53(3), 396-415.

Van Wart, J., van Bussel, L.G.J., Wolf, J., Licker, R., Grassini, P., Nelson, A., Boogaard, H., Gerber, J., Mueller, N.D., Claessens, L., 2013. Use of agro-climatic zones to upscale simulated crop yield potential. Field Crop Research. 143, 44–55.

Vitantonio-Mazzini, L. N., Gómez, D., Gambin, B. L., Di Mauro, G., Iglesias, R., Costanzi, J., Jobbágy, E. G., Borrás, L., 2021. Sowing date, genotype choice, and water environment control soybean yields in central Argentina. Crop Science, 61(1), 715-728.

Wajid, A. L. I., Ahmad, M. M., İftakhar, F., Qureshi, M., Ceyhan, A., 2020. Nutritive potentials of Soybean and its significance for humans health and animal production: A Review. Eurasian Journal of Food Science and Technology, 4(1), 41-53.

Zhang, B., Feng, G., Kong, X., Lal, R., Ouyang, Y., Adeli, A., Jenkins, J. N., 2016. Simulating yield potential by irrigation and yield gap of rainfed soybean using APEX model in a humid region. Agricultural Water Management, 177, 440-453.

Zalles, V., Hansen, M. C., Potapov, P. V, Stehman, S. V, Tyukavina, A., Pickens, A., Song X.P, Adusei, B., Okpa, C., Aguilar, R., John, N., Chavez, S., 2019. Near doubling of Brazil's intensive row crop area since 2000. Proceedings of the National Academy of Sciences, 116(2), 428–435.

5. CONCLUSION AND FUTURE WORK

This Ph.D. thesis was devoted to investigating the yield gap in current management adopted soybean farmers in Brazil under tropical and subtropical environments. To accomplish this objective, we first conducted well-managed experiments in five strategically selected locations (Piracicaba-SP, Sorriso-MT, Cruz Alta-RS, Tupanciretã-RS, and Teresina-PI), totalizing 10 seasons, under water-limited or non-limiting water conditions, and with N-fertilization using 0 (only indigenous soil N sources) or 1,000 kg N ha^{-1}. Second, we tackled the problem of water management and nitrogen on soybean production areas. Finally, we estimated crop yield potential (Y_P), water-limited crop yield potential (Y_{P-W}), crop yield gap (Y_G), climate efficiency (E_C), and agricultural efficiency (E_A).

In the following, we summarize our contributions and highlight tangible outcomes, resulting questions and open problems. We will then conclude with a broader discussion of future research for sustainable agricultural intensification in tropical and subtropical environments.

5.1. Contributions and open problems

In Chapter 2, we investigated evapotranspiration and soil water evaporation methods, soil water balance, and crop water productivity; using field experiments and crop modeling. We further applied the CROPGRO-Soybean to explore water and tillage practices. Our findings indicated that the FAO- 56 Penman-Monteith method for evapotranspiration and Ritchie Two-Stage method for soil water evaporation were the most suitable for CROPGRO-Soybean simulations in a tropical and subtropical environment. The CROPGRO-Soybean model presented an excellent capacity for predicting evapotranspiration, soil water content, and crop water productivity, with great potential to be used as a tool of crop management. The long-term scenarios revealed that the crop water productivity could be increased by no-tillage practices; therefore, no-tillage practices may reduce the amount of required irrigation for soybean crops. However, our model evaluation only exploited the soil water evaporation and evapotranspiration methods for a single environment and soil water content for two environments. An interesting direction for future work is to conduct field experiments in a wide variety of tropical and subtropical soils and environments for a deeper understanding about how

methods of soil water evaporation and evapotranspiration can influence crop modeling and water management.

Chapter 3 presented the effects of high N-fertilization doses applied in soybean compared to soybean grown with only indigenous soil N sources. This study was influenced by many scientific papers that raised the debate on N-fertilization in soybean, mainly in temperate environments. These reported studies were not conclusive and were sometimes contradictory to each other. Furthermore, we identified a scarcity of well-conducted experiments with N-fertilization on soybean in tropical and subtropical environments. We conducted 13 experiments with a single protocol for N-fertilization on soybean under tropical and subtropical conditions. These experiments were useful to evaluate the N-fertilization effects in soybean growth and development and to calibrate and evaluate CROPGRO-Soybean. An immediate result of this research was that N-fertilization on soybean had marginal or no effect on crop yield, but increased seed protein concentration. Another relevant finding was that the CROPGRO-Soybean showed an excellent predictive capacity of soybean across tropical and subtropical environments for N-fertilization cases, and therefore it is a potential tool for predicting effects of N-fertilization. A direction for future research is to investigate the best combination of N sources (with minimal volatilization loss) and application rates to increasing seed protein concentration. This knowledge will be important when the commodity-based pricing system starts to pricing soybean based on oil and protein concentration. However, this research revealed that Brazilian farmers should not consider very high doses of fertilizer N (mainly urea) as field experiments and crop model simulations showed that these practices being not so consistent with principles of sustainable intensification.

A primary contribution of Chapter 4 was the estimates of Y_P, $Y_{P\text{-}W}$, Y_G, E_C, and E_A after a labor-intensive activity in field experimentation and crop model calibration. The Chapter 4 started by investigating an additional hypothesis raised in Chapter 3: the marginal or no N-fertilization effect on crop yield occurred because of the late sowing dates. We rejected this hypothesis based on long-term scenarios simulation, which pointed to a modest increase in crop yield under several N-fertilization rates and various sowing dates. Next step, we generated long-term simulations for yield (water-limited and potential) and efficiency ratios (climate and agricultural). The average $Y_{P\text{-}W}$ (considering lower and upper limits) across all agroclimatic zones (CZs) ranged from 2,985 to 5,369 kg ha^{-1} (with average E_C = 85%), Y_P ranged from 3,402 to 6,999 kg ha^{-1}, and Y_G ranged from 589 to 4,400 kg ha^{-1}. Our E_A projections estimated that closing a portion of the yield gap (to 50.2% of yields from fields conducted under rain fed conditions) would require fairly substantial improvements in agricultural management for

tropical and subtropical conditions. An extension to this work is deeping yield gap analyses at the on-farm level to prospect the major causes of yield losses and, based on that, propose alternative cropping systems to sustainably intensify the soybean crops.

5.2. Concluding Remarks

In this Ph.D. thesis, we conducted well-managed soybean experiments to achieve Y_{P-W} and Y_P. We used datasets from these field experiments to calibrate and evaluate CROPGRO-Soybean, focusing on water and nitrogen management under tropical and subtropical conditions. The crop model showed excellent performance for predicting soybean growth and development under tropical and subtropical conditions, being an excellent tool for research and for decision-making. The crop modelling tools were used to estimate Y_P, Y_{P-W}, Y_P, E_C, and E_A. Finally, we hope that the analyses presented here are useful for scientists, policymakers, and practitioners to improve soybean cropping systems across tropical and subtropical regions of the world.

APPENDICES

Appendix A - Weather versus day after planting for Piracicaba during seasons 2016/2017 (A) and 2017/2018 (B). Rainfall; TMAX, mean maximum air temperature; TMIN, mean minimum air temperature; SRAD, solar radiation.

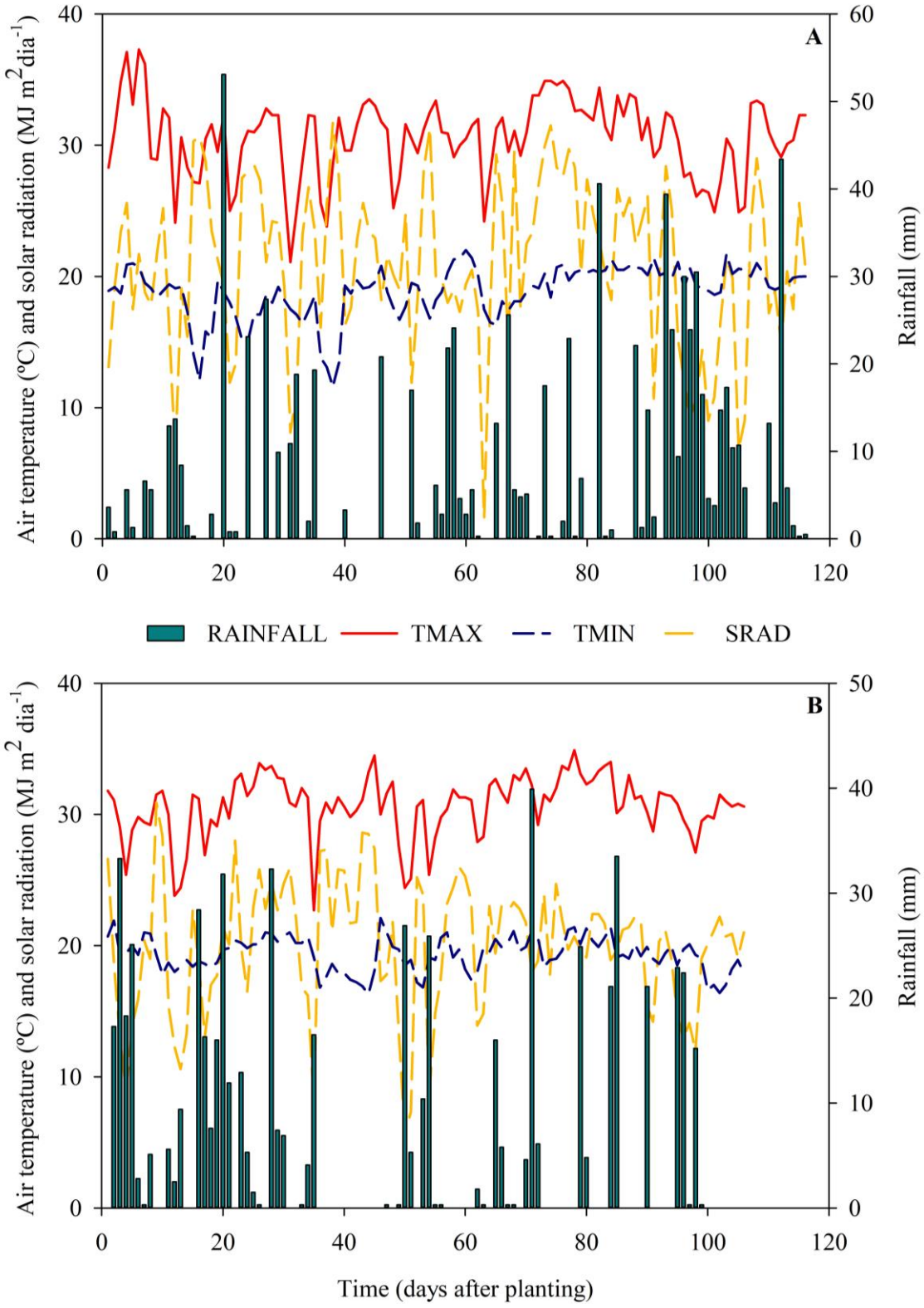

Appendix B - Weather by day after planting for Teresina [(A) TE-1, water-limited conditions (or TE-50); (B) non-limiting water conditions (or TE-100), season 2019]. SRAD, solar radiation; TMIN, mean minimum air temperature; TMAX, mean maximum air temperature; Rainfall; Irrigation.

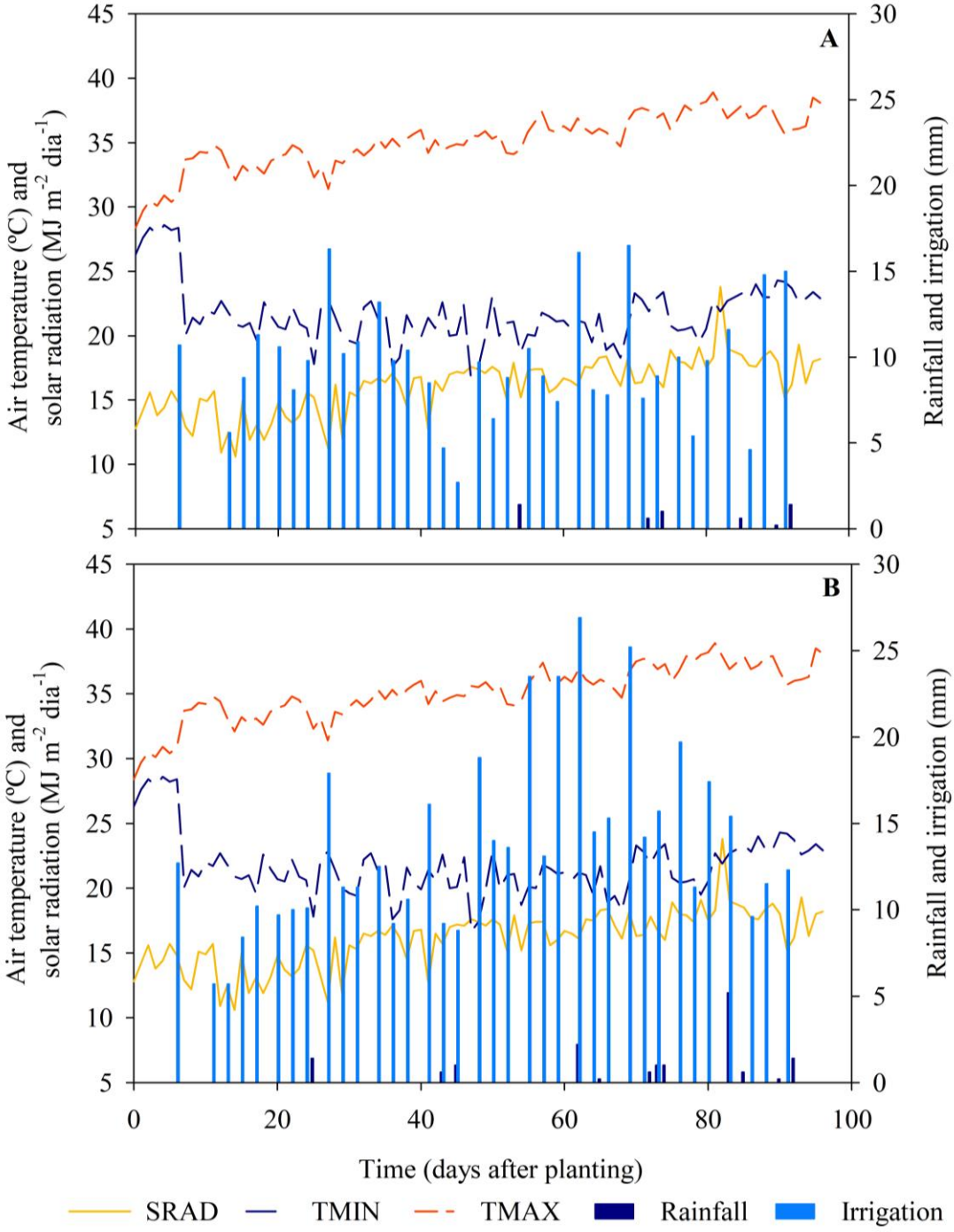

Appendix C - Description of the schedule of spraying of experiments conducted in Piracicaba (PI1-100, PI2-100, PI-1, PI-2, PI-3), Sorriso (SO-1, SO-2), Cruz Alta (CA-1), Tupanciretã (TU-1), and Teresina (TE-100 and TE-50 or TE-1 and TE-2).

(continued)

Active ingredient	Commercial pesticide	Dose ($g\ L^{-1}$ a.i)	Dose ($L\ ha^{-1}$)	Applications (phenological stages)
	PI_1-100			
Glyphosate	Roundap, Monsanto	480	3.0	V4
Flubendiamide	Belt, Bayer	480	0.7	V3, R1, R4
Thiamethoxam and Cypermethrin	Engeo Pleno, Syngenta	220	0.2	R2, R5
	PI_2-100			
Glyphosate	Roundap, Monsanto	480	3.0	Before sowing, V3
Flubendiamide	Belt, Bayer	480	0.7	V3, V8, R3
Fluxapiroxade and pyraclostrobin	Orkestra, BASF	167 + 333	0.3	V5, R3
Chlorfenapyr	Pirate, BASF	240	0.6	R3, R6
	PI-1			
Teflubenzurom	Nomolt, BASF	150	0.1	V2, V5, R3
Chlorfenapyr	Pirate, BASF	240	0.6	V2, R5, R6
Copper oxychloride	Status, BASF	588	1	V5, R1
Fluxapiroxade and pyraclostrobin	Orkestra, BASF	167 + 333	0.3	V5
Epoxiconazol, fluxapiroxade and pyraclostrobin	Ativum, BASF	50 + 50 + 81	1	R1
Fenpropimorph	Versatilis, BASF	750	0.5	R6
Acetamiprid and alpha-cypermethrin	Fastac Duo, BASF	100 + 200	0.5	R1, R5, R6
	PI-2			
Teflubenzurom	Nomolt, BASF	150	0.1	V2, V5
Chlorfenapyr	Pirate, BASF	240	0.6	R5, R6
Copper oxychloride	Status, BASF	588	1	R1

Appendix C - Description of the schedule of spraying of experiments conducted in Piracicaba (PI_1-100, PI_2-100, PI-1, PI-2, PI-3), Sorriso (SO-1, SO-2), Cruz Alta (CA-1), Tupanciretã (TU-1), and Teresina (TE-100 and TE-50 or TE-1 and TE-2).

(continuation)

Active ingredient	Commercial pesticide	Dose ($g\ L^{-1}$ a.i)	Dose ($L\ ha^{-1}$)	Applications (phenological stages)
Fluxapiroxade and pyraclostrobin	Orkestra, BASF	167 + 333	0.3	V5
Epoxiconazol, fluxapiroxade and pyraclostrobin	Ativum, BASF	50 + 50 + 81	1	R1
Fenpropimorph	Versatilis, BASF	750	0.5	R5
Acetamiprid and alpha-cypermethrin	Fastac Duo, BASF	100 + 200	0.5	R3, R5, R6
	PI-3			
Teflubenzurom	Nomolt, BASF	150	0.1	V2, V5
Chlorfenapyr	Pirate, BASF	240	0.6	R2, R5, R6
Copper oxychloride	Status, BASF	588	1	R1
Fluxapiroxade and pyraclostrobin	Orkestra, BASF	167 + 333	0.3	V5
Epoxiconazol, fluxapiroxade and pyraclostrobin	Ativum, BASF	50 + 50 + 81	1	R1
Fenpropimorph	Versatilis, BASF	750	0.5	R5
Acetamiprid and alpha-cypermethrin	Fastac Duo, BASF	100 + 200	0.5	R3, R5, R6
	SO-1			
Teflubenzurom	Nomolt, BASF	150	0.1	V2, V5
Chlorfenapyr	Pirate, BASF	240	0.6	R3, R5, R6
Copper oxychloride	Status, BASF	588	1	R1
Fluxapiroxade and pyraclostrobin	Orkestra, BASF	167 + 333	0.3	V5
Epoxiconazol, fluxapiroxade and pyraclostrobin	Ativum, BASF	50 + 50 + 81	1	R1
Fenpropimorph	Versatilis, BASF	750	0.5	R3, R5
Acetamiprid and alpha-cypermethrin	Fastac Duo, BASF	100 + 200	0.5	R3, R5, R6

Appendix C - Description of the schedule of spraying of experiments conducted in Piracicaba (PI_1-100, PI_2-100, PI-1, PI-2, PI-3), Sorriso (SO-1, SO-2), Cruz Alta (CA-1), Tupanciretã (TU-1), and Teresina (TE-100 and TE-50 or TE-1 and TE-2).

(continuation)

Active ingredient	Commercial pesticide	Dose ($g\ L^{-1}$ a.i)	Dose ($L\ ha^{-1}$)	Applications (phenological stages)
	SO-2			
Teflubenzurom	Nomolt, BASF	150	0.1	V2, V5, R5
Chlorfenapyr	Pirate, BASF	240	0.6	R1, R6
Copper oxychloride	Status, BASF	588	1	V3
Fluxapiroxade and pyraclostrobin	Orkestra, BASF	167 + 333	0.3	V5
Epoxiconazol, fluxapiroxade and pyraclostrobin	Ativum, BASF	50 + 50 + 81	1	R1
Fenpropimorph	Versatilis, BASF	750	0.5	R3, R5
Acetamiprid and alpha-cypermethrin	Fastac Duo, BASF	100 + 200	0.5	R5, R6
	CA-1			
Teflubenzurom	Nomolt, BASF	150	0.1	V2, V5
Chlorfenapyr	Pirate, BASF	240	0.6	R1, R6
Copper oxychloride	Status, BASF	588	1	V3
Fluxapiroxade and pyraclostrobin	Orkestra, BASF	167 + 333	0.3	V7
Epoxiconazol, fluxapiroxade and pyraclostrobin	Ativum, BASF	50 + 50 + 81	1	R1
Fenpropimorph	Versatilis, BASF	750	0.5	R3, R5
Acetamiprid and alpha-cypermethrin	Fastac Duo, BASF	100 + 200	0.5	R3, R5, R6
	TU-1			
Teflubenzurom	Nomolt, BASF	150	0.1	V2, V5
Chlorfenapyr	Pirate, BASF	240	0.6	R1, R6
Copper oxychloride	Status, BASF	588	1	V3
Fluxapiroxade and pyraclostrobin	Orkestra, BASF	167 + 333	0.3	V7

Appendix C - Description of the schedule of spraying of experiments conducted in Piracicaba (PI_1-100, PI_2-100, PI-1, PI-2, PI-3), Sorriso (SO-1, SO-2), Cruz Alta (CA-1), Tupanciretã (TU-1), and Teresina (TE-100 and TE-50 or TE-1 and TE-2).

(conclusion)

Active ingredient	Commercial pesticide	Dose ($g\ L^{-1}$ a.i)	Dose ($L\ ha^{-1}$)	Applications (phenological stages)
TE-100 and TE-50 or TE-1 and TE-2				
Epoxiconazol, fluxapiroxade and pyraclostrobin	Ativum, BASF	50 + 50 + 81	1	R1, R5
Fenpropimorph	Versatilis, BASF	750	0.5	R5
Acetamiprid and alpha-cypermethrin	Fastac Duo, BASF	100 + 200	0.5	R1, R4, R6
Teflubenzurom	Nomolt, BASF	150	0.1	V2, R2
Chlorfenapyr	Pirate, BASF	240	0.6	V3, R3, R6
Copper oxychloride	Status, BASF	588	1	V3, R1
Fluxapiroxade and pyraclostrobin	Orkestra, BASF	167 + 333	0.3	V4
Epoxiconazol, fluxapiroxade and pyraclostrobin	Ativum, BASF	50 + 50 + 81	1	R1
Fenpropimorph	Versatilis, BASF	750	0.5	R1, R6
Acetamiprid and alpha-cypermethrin	Fastac Duo, BASF	100 + 200	0.5	R1, R5, R6

Appendix D - Soil analysis from Piracicaba (PI_1-100, PI_2-100, PI-1, PI-2, PI-3), Sorriso (SO-1, SO-2), Cruz Alta (CA-1), Tupanciretã (TU-1), Teresina (TE-1, TE-2 or TE-100, TE-50).

Exp.	Depth	pH	O.M	CEC	V	P	S	K	Ca	Mg
	m	H_2O	%	mmolc dm^{-3}	%	mg dm^{-3}		mmolc dm^{-3}		
PI_1-100	0.0-0.2	5.2	2.2	58.6	65.2	20.0	9.0	3.2	40.2	15.0
	0.2-0.4	5.5	2.2	65.2	64.0	16.0	10.0	3.4	40.0	17.0
PI_2-100	0.0-0.2	5.5	2.2	57.2	67.3	20.0	22.0	5.4	41.0	11.0
	0.2-0.4	5.7	2.3	63.4	65.0	23.0	36.0	6.2	43.0	13.0
PI-1	0.0-0.2	5.4	2.1	59.0	65.8	18.0	11.0	3.8	24.0	11.0
	0.2-0.4	5.5	2.1	65.0	69.5	22.0	14.0	4.2	28.0	13.0
PI-2	0.0-0.2	5.2	2.3	71.0	60.7	15.0	10.0	5.1	27.0	11.0
	0.2-0.4	5.4	2.5	72.0	65.8	16.0	10.0	5.4	30.0	12.0
PI-3	0.0-0.2	5.5	2.6	70.0	67.8	27.0	12.0	2.8	36.0	19.0
	0.2-0.4	5.7	2.8	71.0	68.3	21.0	15.0	2.0	33.0	18.0
SO-1	0.0-0.2	4.5	2.7	70.0	38.6	1.1	3.0	0.8	18.3	7.9
	0.2-0.4	4.7	2.1	44.0	35.0	1.0	4.0	0.8	10.6	4.0
SO-2	0.0-0.2	5.3	3.1	62.0	38.5	4.0	7.0	1.3	20.3	10.8
	0.2-0.4	4.6	2.3	48.0	25.8	0.7	5.0	0.5	12.2	4.3
CA-1	0.0-0.2	6.1	2.5	67.0	65.0	17.0	15.0	1.3	30.0	15.0
	0.2-0.4	4.8	3.0	68.0	65.0	20.0	6.0	0.8	30.0	12.0
TU-1	0.0-0.2	5.8	2.2	66.0	65.1	7.7	13.0	0.5	44.2	16.3
	0.2-0.4	5.4	1.6	52.0	49.5	4.5	3.1	0.2	31.4	14.4
TE-1	0.0-0.2	5.7	1.1	44.8	62.0	20.7	10.0	0.5	14.3	6.4
TE-2	0.2-0.4	5.4	0.9	46.6	48.0	14.9	8.0	0.6	10.8	6.0
TE-100	0.0-0.2	5.7	1.1	44.8	62.0	20.7	10.0	0.5	14.3	6.4
TE-50	0.2-0.4	5.4	0.9	46.6	48.0	14.9	8.0	0.6	10.8	6.0

Appendix E - Description of the schedule of fertilization of experiments conducted in Piracicaba (PI_1-100, PI_2-100, PI-1, PI-2, PI-3), Sorriso (SO-1, SO-2), Cruz Alta (CA-1), Tupanciretã (TU-1), and Teresina (TE-100 and TE-50 or TE-1 and TE-2).

(continued)

Nutrient	Commercial fertilizer	Dose (kg ha^{-1})	Applications (phenological stages)	Total (kg ha^{-1})
		PI_1-100		
P	single superphosphate (18% P_2O_5, 16% Ca, 12% S, Yara)	2.00 10^2	sowing	2.00 10^2
B	boric superphosphate Bortrac (99.9 % H_3BO_3, Quiroborax)	0.40 10	sowing	0.40 10
Mg	Magnesium sulfate heptahydrate (9% Mg, 11% S, Quiriros)	0.80 10	V6	0.80 10
		PI_2-100		
P	single superphosphate (18% P_2O_5, 16% Ca, 12% S, Yara)	2.00 10^2	sowing	2.00 10^2
B	boric superphosphate Bortrac (99.9 % H_3BO_3, Quiroborax)	0.40 10	sowing	0.40 10
Mg	Magnesium sulfate heptahydrate (9% Mg, 11% S, Quiriros)	0.80 10	V6	0.80 10
K	potassium chloride (58% K_2O, Yara)	5.00 10	V7	5.00 10
		PI-1		
P	single superphosphate (18% P_2O_5, 16% Ca, 12% S, Yara)	4.00 10^2	sowing	4.00 10^2
K	potassium chloride (58% K_2O, Yara)	5.00 10	V7	5.00 10
Mn	Mantrac Pro (50% Mn, Yara)	7.50 10^{-2}	V3, R3	3.00 10^{-1}
		1.50 10^{-1}	V7, R1	
Zn	Zintrac (40% Zn, Yara)	4.00 10^{-3}	V3	1.64
		8.00 10^{-2}	V7, R1	
Ni	nickel sulfate (20% Ni, 10% S, Produquimica)	4.00 10^{-3}	V3	4.00 10^{-3}

Appendix E - Description of the schedule of fertilization of experiments conducted in Piracicaba (PI_1-100, PI_2-100, PI-1, PI-2, PI-3), Sorriso (SO-1, SO-2), Cruz Alta (CA-1), Tupanciretã (TU-1), and Teresina (TE-100 and TE-50 or TE-1 and TE-2).

(continuation)

Nutrient	Commercial fertilizer	Dose (kg ha^{-1})	Applications (phenological stages)	Total (kg ha^{-1})
Co	Teprosyn (14.25% Co, Yara)	$4.00\ 10^{-3}$	V3	$4.00\ 10^{-3}$
Mo	Teprosyn (1.43% Mo, Yara)	$4.00\ 10^{-2}$	V3	$4.00\ 10^{-2}$
Cu	Croptrac (0.5% Cu, Yara)	$2.50\ 10^{-2}$	V7, R1	$5.00\ 10^{-2}$
B	Bortrac (10.9 % B, Yara)	$5.00\ 10^{-2}$	V7, R1, R3	$1.50\ 10^{-1}$
Mg	Magtrac (20% Mg, Yara)	$3.00\ 10^{-1}$	V7, R3	$6.00\ 10^{-1}$
	PI-2			
P	single superphosphate (18% P_2O_5, 16% Ca, 12% S, Yara)	$6.00\ 10^{2}$	sowing	$6.00\ 10^{2}$
K	potassium chloride (58% K_2O, Yara)	5.00 10	V7	5.00 10
Mn	Mantrac Pro (50% Mn, Yara)	$7.50\ 10^{-2}$	V3, R3	$4.50\ 10^{-1}$
		$1.50\ 10^{-1}$	V7, R1	
Zn	Zintrac (40% Zn, Yara)	$4.00\ 10^{-3}$	V3	1.64
		$8.00\ 10^{-2}$	V7, R1	
Ni	nickel sulfate (20% Ni, 10% S, Produquimica)	$4.00\ 10^{-3}$	V3	$4.0\ 10^{-3}$
Co	Teprosyn (14.25% Co, Yara)	$4.00\ 10^{-3}$	V3	$4.0\ 10^{-3}$
Mo	Teprosyn (1.43% Mo, Yara)	$4.00\ 10^{-2}$	V3	$4.0\ 10^{-2}$
Cu	Croptrac (0.5% Cu, Yara)	$2.50\ 10^{-2}$	V7, R1	$5.0\ 10^{-2}$
B	Bortrac (10.9 % B, Yara)	$5.00\ 10^{-2}$	V7, R1, R3	$1.5\ 10^{-1}$
Mg	Magtrac (20% Mg, Yara)	$3.00\ 10^{-1}$	V7, R3	$6.0\ 10^{-1}$
	PI-3			
P	single superphosphate (18% P_2O_5, 16% Ca, 12% S, Yara)	$3.50\ 10^{2}$	sowing	$3.50\ 10^{2}$

Appendix E - Description of the schedule of fertilization of experiments conducted in Piracicaba (PI_1-100, PI_2-100, PI-1, PI-2, PI-3), Sorriso (SO-1, SO-2), Cruz Alta (CA-1), Tupanciretã (TU-1), and Teresina (TE-100 and TE-50 or TE-1 and TE-2).

(continuation)

Nutrient	Commercial fertilizer	Dose (kg ha^{-1})	Applications (phenological stages)	Total (kg ha^{-1})
K	potassium chloride (58% K_2O, Yara)	5.00 10	V7	5.00 10
Mn	Mantrac Pro (50% Mn, Yara)	7.50 10^{-2}	V3, R3	4.50 10^{-1}
		1.50 10^{-1}	V7, R1	
Zn	Zintrac (40% Zn, Yara)	4.00 10^{-3}	V3	1.64
		8.00 10^{-2}	V7, R1	
Ni	nickel sulfate (20% Ni, 10% S, Produquimica)	4.00 10^{-3}	V3	4.0 10^{-3}
Co	Teprosyn (14.25% Co, Yara)	4.00 10^{-3}	V3	4.0 10^{-3}
Mo	Teprosyn (1.43% Mo, Yara)	4.00 10^{-2}	V3	4.0 10^{-2}
Cu	Croptrac (0.5% Cu, Yara)	2.50 10^{-2}	V7, R1	5.0 10^{-2}
B	Bortrac (10.9 % B, Yara)	5.00 10^{-2}	V7, R1, R3	1.5 10^{-1}
Mg	Magtrac (20% Mg, Yara)	3.00 10^{-1}	V7, R3	6.0 10^{-1}
	SO-1			
Ca, Mg	calcareous (30% CaO; 15% MgO; PRNT = 80%, Kraemer)	2.70 10^3	before sowing	2.70 10^3
S	gypsum (20% Ca^{2+}, 15% SO_4^{2-}, Tapajós)	1.32 10^3	before sowing	1.32 10^3
P	single superphosphate (18% P_2O_5, 16% Ca, 12% S, Yara)	1.05 10^3	before sowing	1.05 10^2
P	single superphosphate (18% P_2O_5, 16% Ca, 12% S, Yara)	5.00 10^2	sowing	5.90 10^2
K	potassium chloride (58% K_2O, Yara)	5.00 10	sowing	5.00 10

Appendix E - Description of the schedule of fertilization of experiments conducted in Piracicaba (PI_1-100, PI_2-100, PI-1, PI-2, PI-3), Sorriso (SO-1, SO-2), Cruz Alta (CA-1), Tupanciretã (TU-1), and Teresina (TE-100 and TE-50 or TE-1 and TE-2).

(continuation)

Nutrient	Commercial fertilizer	Dose (kg ha^{-1})	Applications (phenological stages)	Total (kg ha^{-1})
Mn	Mantrac Pro (50% Mn, Yara)	$1.50\ 10^{-1}$	V4, V8, R2	$4.50\ 10^{-1}$
Zn	Zintrac (40% Zn, Yara)	$6.50\ 10^{-2}$	V4, V8	$2.00\ 10^{-2}$
		$7.00\ 10^{-2}$	R2	
Ni	nickel sulfate (20% Ni, 10% S, Produquimica)	$4.00\ 10^{-3}$	V4	$4.00\ 10^{-3}$
Co	Teprosyn (14.25% Co, Yara)	$4.00\ 10^{-3}$	V4	$4.00\ 10^{-3}$
Mo	Teprosyn (1.43% Mo, Yara)	$4.00\ 10^{-2}$	V3	$4.00\ 10^{-2}$
Cu	Croptrac (0.5% Cu, Yara)	$2.50\ 10^{-2}$	V8, R2	$5.00\ 10^{-2}$
B	Bortrac (10.9 % B, Yara)	$5.00\ 10^{-2}$	V8, R2	$1.00\ 10^{-1}$
Mg	Magtrac (20% Mg, Yara)	$2.50\ 10^{-1}$	V7, R3	$5.00\ 10^{-1}$
	SO-2			
Ca, Mg	calcareous (30% CaO; 15% MgO; PRNT = 80%, Kraemer)	$1.63\ 10^{3}$	before sowing	$1.63\ 10^{3}$
S	gypsum (20% Ca^{2+}, 15% SO_4^{2-}, Tapajós)	$2.50\ 10^{3}$	before sowing	$2.50\ 10^{2}$
P	Calcined thermophosphate (23% P_2O_5, Phosfaz)	$1.50\ 10^{3}$	before sowing	$1.05\ 10^{2}$
P	single superphosphate (18% P_2O_5, 16% Ca, 12% S, Yara)	$2.00\ 10^{2}$	sowing	$5.90\ 10^{2}$
K	potassium chloride (58% K_2O, Yara)	5.00 10	sowing	5.00 10
Mn	Mantrac Pro (50% Mn, Yara)	$1.50\ 10^{-1}$	V4, V8, R2	$4.50\ 10^{-1}$
Zn	Zintrac (40% Zn, Yara)	$6.50\ 10^{-2}$	V4, V8	$2.00\ 10^{-2}$

Appendix E - Description of the schedule of fertilization of experiments conducted in Piracicaba (PI_1-100, PI_2-100, PI-1, PI-2, PI-3), Sorriso (SO-1, SO-2), Cruz Alta (CA-1), Tupanciretã (TU-1), and Teresina (TE-100 and TE-50 or TE-1 and TE-2).

(continuation)

Nutrient	Commercial fertilizer	Dose (kg ha^{-1})	Applications (phenological stages)	Total (kg ha^{-1})
Zn	Zintrac (40% Zn, Yara)	$7.00\ 10^{-2}$	R2	
Ni	nickel sulfate (20% Ni, 10% S, Produquimica)	$4.00\ 10^{-3}$	V4	$4.00\ 10^{-3}$
Co	Teprosyn (14.25% Co, Yara)	$4.00\ 10^{-3}$	V4	$4.00\ 10^{-3}$
Mo	Teprosyn (1.43% Mo, Yara)	$4.00\ 10^{-2}$	V3	$4.00\ 10^{-2}$
Cu	Croptrac (0.5% Cu, Yara)	$2.50\ 10^{-2}$	V8, R2	$5.00\ 10^{-2}$
B	Bortrac (10.9 % B, Yara)	$5.00\ 10^{-2}$	V8, R2	$1.00\ 10^{-1}$
Mg	Magtrac (20% Mg, Yara)	$2.50\ 10^{-1}$	V7, R3	$5.00\ 10^{-1}$
	CA-1			
Ca, Mg	calcareous (30% CaO; 15% MgO; PRNT = 80%, Fida)	$4.20\ 10^{2}$	before sowing	$4.20\ 10^{2}$
P	single superphosphate (18% P_2O_5, 16% Ca, 12% S, Yara)	$4.70\ 10^{2}$	sowing	$4.70\ 10^{2}$
K	potassium chloride (58% K_2O, Yara)	5.00 10	sowing	5.00 10
Mn	Mantrac Pro (50% Mn, Yara)	$7.50\ 10^{-2}$	V3, R3	$4.50\ 10^{-1}$
		$1.50\ 10^{-1}$	V7, R1	
Zn	Zintrac (40% Zn, Yara)	$4.00\ 10^{-2}$	V3	$1.20\ 10^{-1}$
		$8.00\ 10^{-2}$	V7, R1	
Ni	nickel sulfate (20% Ni, 10% S, Produquimica)	$4.00\ 10^{-3}$	V3	$4.00\ 10^{-3}$
Co	Teprosyn (14.25% Co, Yara)	$4.00\ 10^{-3}$	V3	$4.00\ 10^{-3}$

Appendix E - Description of the schedule of fertilization of experiments conducted in Piracicaba (PI_1-100, PI_2-100, PI-1, PI-2, PI-3), Sorriso (SO-1, SO-2), Cruz Alta (CA-1), Tupanciretã (TU-1), and Teresina (TE-100 and TE-50 or TE-1 and TE-2).

(continuation)

Nutrient	Commercial fertilizer	Dose (kg ha^{-1})	Applications (phenological stages)	Total (kg ha^{-1})
Mo	Teprosyn (1.43% Mo, Yara)	$4.00\ 10^{-2}$	V3	$4.00\ 10^{-2}$
Cu	Croptrac (0.5% Cu, Yara)	$2.50\ 10^{-2}$	V7, R1	$5.00\ 10^{-2}$
B	Bortrac (10.9 % B, Yara)	$5.00\ 10^{-2}$	V7, R1, R3	$1.5\ 10^{-1}$
Mg	Magtrac (20% Mg, Yara)	$3.00\ 10^{-1}$	V7, R3	$6.0\ 10^{-1}$
	TU-1			
S	gypsum (20% Ca^{2+}, 15% SO_4^{2-}, Fida)	5.20 10	before sowing	5.20 10
P	single superphosphate (18% P_2O_5, 16% Ca, 12% S, Yara)	$8.20\ 10^{2}$	sowing	$8.20\ 10^{2}$
K	potassium chloride (58% K_2O, Yara)	5.00 10	V7	5.00 10
Mn	Mantrac Pro (50% Mn, Yara)	$7.50\ 10^{-2}$	V3, R3	$1.50\ 10^{-1}$
		$1.50\ 10^{-1}$	V7, R1	
Zn	Zintrac (40% Zn, Yara)	$4.00\ 10^{-2}$	V3	$1.2\ 10^{-1}$
		$8.00\ 10^{-2}$	V7, R1	
Ni	nickel sulfate (20% Ni, 10% S, Produquimica)	$4.00\ 10^{-3}$	V3	$4.00\ 10^{-3}$
Co	Teprosyn (14.25% Co, Yara)	$4.00\ 10^{-3}$	V3	$4.00\ 10^{-3}$
Mo	Teprosyn (1.43% Mo, Yara)	$4.00\ 10^{-2}$	V3	$4.00\ 10^{-2}$
Cu	Croptrac (0.5% Cu, Yara)	$2.50\ 10^{-2}$	V7, R1	$5.00\ 10^{-2}$
B	Bortrac (10.9 % B, Yara)	$5.00\ 10^{-2}$	V7, R1, R3	$1.50\ 10^{-1}$

Appendix E - Description of the schedule of fertilization of experiments conducted in Piracicaba (PI_1-100, PI_2-100, PI-1, PI-2, PI-3), Sorriso (SO-1, SO-2), Cruz Alta (CA-1), Tupanciretã (TU-1), and Teresina (TE-100 and TE-50 or TE-1 and TE-2).

(conclusion)

Nutrient	Commercial fertilizer	Dose (kg ha^{-1})	Applications (phenological stages)	Total (kg ha^{-1})
Mg	Magtrac (20% Mg, Yara)	$3.00\ 10^{-1}$	V7, R3	$6.00\ 10^{-1}$
	TE-100 and TE-50 or TE-1 and TE-2			
Ca, Mg	calcareous (30% CaO; 15% MgO; PRNT = 80%, MinerSul)	$4.48\ 10^{2}$	before sowing	$4.48\ 10^{2}$
S	gypsum (20% Ca^{2+}, 15% SO_4^{2-}, Nutrigesso)	$1.86\ 10^{2}$	before sowing	$1.86\ 10^{2}$
P	single superphosphate (18% P_2O_5, 16% Ca, 12% S, Yara)	$3.50\ 10^{2}$	sowing	$3.50\ 10^{2}$
K	potassium chloride (58% K_2O, Yara)	5.00 10	V3	5.00 10
Mn	Mantrac Pro (50% Mn, Yara)	$1.50\ 10^{-1}$	V4, V8, R2	$4.50\ 10^{-1}$
Zn	Zintrac (40% Zn, Yara)	$6.50\ 10^{-2}$	V4, V8	$1.35\ 10^{-1}$
		$7.00\ 10^{-2}$	R2	
Ni	nickel sulfate (20% Ni, 10% S, Produquimica)	$4.00\ 10^{-3}$	V4	$4.00\ 10^{-3}$
Co	Teprosyn (14.25% Co, Yara)	$4.00\ 10^{-3}$	V4	$4.00\ 10^{-3}$
Mo	Teprosyn (1.43% Mo, Yara)	$4.00\ 10^{-2}$	V3	$4.00\ 10^{-2}$
Cu	Croptrac (0.5% Cu, Yara)	$2.50\ 10^{-2}$	V8, R2	$5.00\ 10^{-2}$
B	Bortrac (10.9 % B, Yara)	$5.00\ 10^{-2}$	V8, R2	$1.00\ 10^{-1}$
Mg	Magtrac (20% Mg, Yara)	$2.50\ 10^{-1}$	V7, R3	$5.00\ 10^{-1}$

Appendix F - Properties of the Eutric Rhodic Ferralic Nitisol soil profile from Piracicaba, Dystrophic Red Yellow Ferrosol soil profile from Sorriso, Dystrophic Red Acrisol soil profile from Cruz Alta, Dystrophic Red Acrisol soil profile from Tupanciretã and the Dystrophic Red Yellow Acrisol soil profile from Teresina.

(continued)

Site	Depth (m)	Bulk Density (g cm^{-1})	Clay (%)	Silt (%)	Soil			
					SRGF[a]	Lower limit	Drained upper limit	Saturated upper limit
						(cm^3 cm^{-3})		
Piracicaba	0.1	1.31	46	21	1.000	0.235	0.363	0.508
	0.2	1.31	46	21	1.000	0.235	0.363	0.508
	0.3	1.31	46	21	0.800	0.235	0.342	0.508
	0.4	1.32	57	18	0.800	0.264	0.432	0.534
	0.5	1.32	57	18	0.600	0.264	0.432	0.534
	0.6	1.35	56	19	0.500	0.304	0.432	0.520
	1.2	1.35	56	19	0.300	0.304	0.432	0.520
	1.5	1.37	53	20	0.080	0.283	0.422	0.526
Sorriso	0.1	1.55	50	38	1.000	0.290	0.445	0.501
	0.2	1.55	50	38	1.000	0.290	0.445	0.501
	0.3	1.55	50	38	0.800	0.290	0.445	0.501
	0.4	1.43	44	11	0.800	0.251	0.413	0.534
	0.5	1.43	44	11	0.600	0.251	0.413	0.534
	0.6	1.39	38	10	0.500	0.212	0.362	0.540
	1.2	1.39	38	10	0.300	0.212	0.362	0.540
	1.5	1.39	38	10	0.080	0.212	0.362	0.540
Cruz Alta	0.1	1.59	17	8	1.000	0.117	0.202	0.377
	0.2	1.59	17	8	1.000	0.117	0.202	0.377
	0.3	1.60	19	6	0.900	0.126	0.208	0.373
	0.4	1.60	19	6	0.800	0.126	0.208	0.373
	0.5	1.60	19	6	0.700	0.127	0.209	0.373
	0.6	1.60	19	6	0.600	0.127	0.209	0.373
	1.2	1.57	23	11	0.200	0.144	0.233	0.384
	1.5	1.57	23	11	0.067	0.144	0.233	0.384
Tupanciretã	0.1	1.56	32	9	1.000	0.181	0.374	0.487
	0.2	1.56	32	9	1.000	0.181	0.374	0.487
	0.3	1.56	32	9	0.900	0.181	0.374	0.487
	0.4	1.56	36	8	0.800	0.199	0.393	0.487
	0.5	1.56	36	8	0.700	0.199	0.393	0.487
	0.6	1.56	36	8	0.600	0.199	0.393	0.487
	1.2	1.56	38	7	0.200	0.209	0.302	0.487
	1.5	1.56	38	7	0.067	0.209	0.302	0.487

[a] Soil root growth factor.

Appendix F - Properties of the Eutric Rhodic Ferralic Nitisol soil profile from Piracicaba, Dystrophic Red Yellow Ferrosol soil profile from Sorriso, Dystrophic Red Acrisol soil profile from Cruz Alta, Dystrophic Red Acrisol soil profile from Tupanciretã and the Dystrophic Red Yellow Acrisol soil profile from Teresina.

(conclusion)

Site	Depth (m)	Bulk Density (g cm^{-1})	Clay (%)	Silt (%)	Soil			
					SRGF[a]	Lower limit	Drained upper limit	Saturated upper limit
						(cm^3 cm^{-3})		
Teresina	0.1	1.51	11	20	1.000	0.081	0.173	0.355
	0.2	1.51	11	20	1.000	0.081	0.173	0.368
	0.3	1.51	11	20	0.900	0.081	0.183	0.368
	0.4	1.49	26	26	0.800	0.090	0.183	0.370
	0.5	1.49	26	26	0.700	0.090	0.193	0.370
	0.6	1.49	26	26	0.600	0.080	0.193	0.370
	1.2	1.49	26	26	0.200	0.080	0.193	0.370
	1.5	1.50	25	24	0.080	0.070	0.203	0.370
	1.8	1.50	25	24	0.080	0.070	0.203	0.370

Appendix G - Final values of the calibrated cultivar coefficients for BRS 399 (MG 6.0), TMG 7062 (MG 6.0), TMG 7063 (MG 7.0), NS7901 (MG 8.0), 65i65RSF (MG 6.0) and 8579RSF (MG 8.0).

(continued)

Traits	Definition	Unit	BRS 399	TMG 7062	TMG 7063	NS7901	65i65RSF	8579RSF
CSDL	Critical short-day length	hour	12.58	12.58	12.33	12.07	12.58	12.07
PPSEN	Slope of the relative response of development to photoperiod	$hour^{-1}$	0.311	0.311	0.320	0.330	0.311	0.001
EM-FL	Time between VE and R1	photothermal days	20.4	25.5	20.5	26.7	25.1	19.7
FL-SH	Time between R1 and R3	photothermal days	8.2	11.5	9.8	10.5	8.0	9.1
FL-SD	Time between R1 and R5	photothermal days	13.7	15.3	15.2	16.3	13.5	14.9
SD-PM	Time between R5 and R7	photothermal days	28.7	33.0	36.2	34.2	36.6	32.1
FL-LF	Time between R1 and end of leaf expansion	photothermal days	18.0	18.8	18.0	18.0	18.8	34.0
LFMAX	Maximum leaf photosynthesis rate at 30ºC, 350 vpm CO_2, and high light	mg CO_2 m^{-2} s^{-1}	1.03	1.30	1.03	1.03	1.30	1.40
SLAVR	Specific leaf area of cultivar under standard growth conditions	cm^2 g^{-1}	335	400	495	435	400	400
SIZLF	Maximum size of full leaf (three leaflets)	cm^2	180	180	210	180	180	190
XFRT	Maximum fraction of daily growth that is partitioned to seed + shell	g g^{-1}	1	1	1	1	1	1
WTPSD	Maximum weight per seed	g	0.19	0.18	0.18	0.18	0.18	0.19

Appendix G - Final values of the calibrated cultivar coefficients for BRS 399 (MG 6.0), TMG 7062 (MG 6.0), TMG 7063 (MG 7.0), NS7901 (MG 8.0), 65i65RSF (MG 6.0) and 8579RSF (MG 8.0).

(conclusion)

Traits	Definition	Unit	BRS 399	TMG 7062	TMG 7063	NS7901	65i65RSF	8579RSF
SFDUR	Seed filling duration for pod cohort at standard growth conditions	photothermal days	23.0	26	23	23	26	21
SDPDV	Average seed per pod under standard growing conditions	# pod^{-1}	2.4	2.40	2.05	2.05	2.4	2.30
PODUR	Time required for cultivar to reach final pod load under optimal conditions	photothermal days	10	10	10	10	10	10
THRSH	Threshing percentage	seed (seed+shell) $^{-1}$	78	78	78	78	78	77
SDPRO	Fraction protein in seeds	g(protein) g(seed) $^{-1}$	0.4	0.408	0.400	0.400	0.360	0.315
SDLIP	Fraction oil in seeds	g(oil) g(seed) $^{-1}$	0.2	0.180	0.200	0.200	0.170	0.210

Appendix H - Climatology by month from 1989 to 2020 for Piracicaba (A), Teresina (B), Sorriso (C), and Cruz Alta (D). Rainfall; TMAX, mean maximum air temperature; TMIN, mean minimum air temperature; SRAD, solar radiation.

(continued)

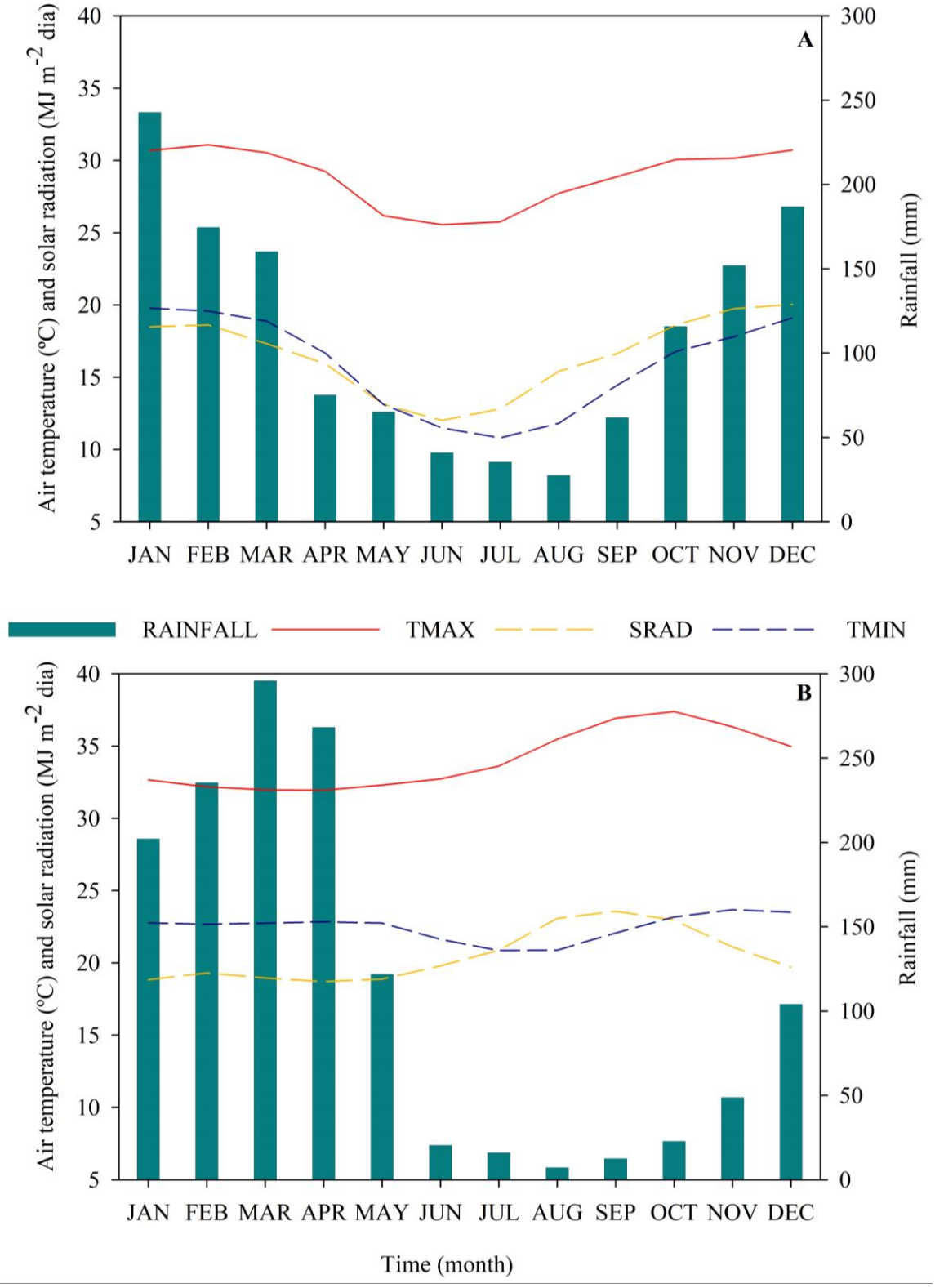

Appendix H - Climatology by month from 1989 to 2020 for Piracicaba (A), Teresina (B), Sorriso (C), and Cruz Alta (D). Rainfall; TMAX, mean maximum air temperature; TMIN, mean minimum air temperature; SRAD, solar radiation.

(conclusion)

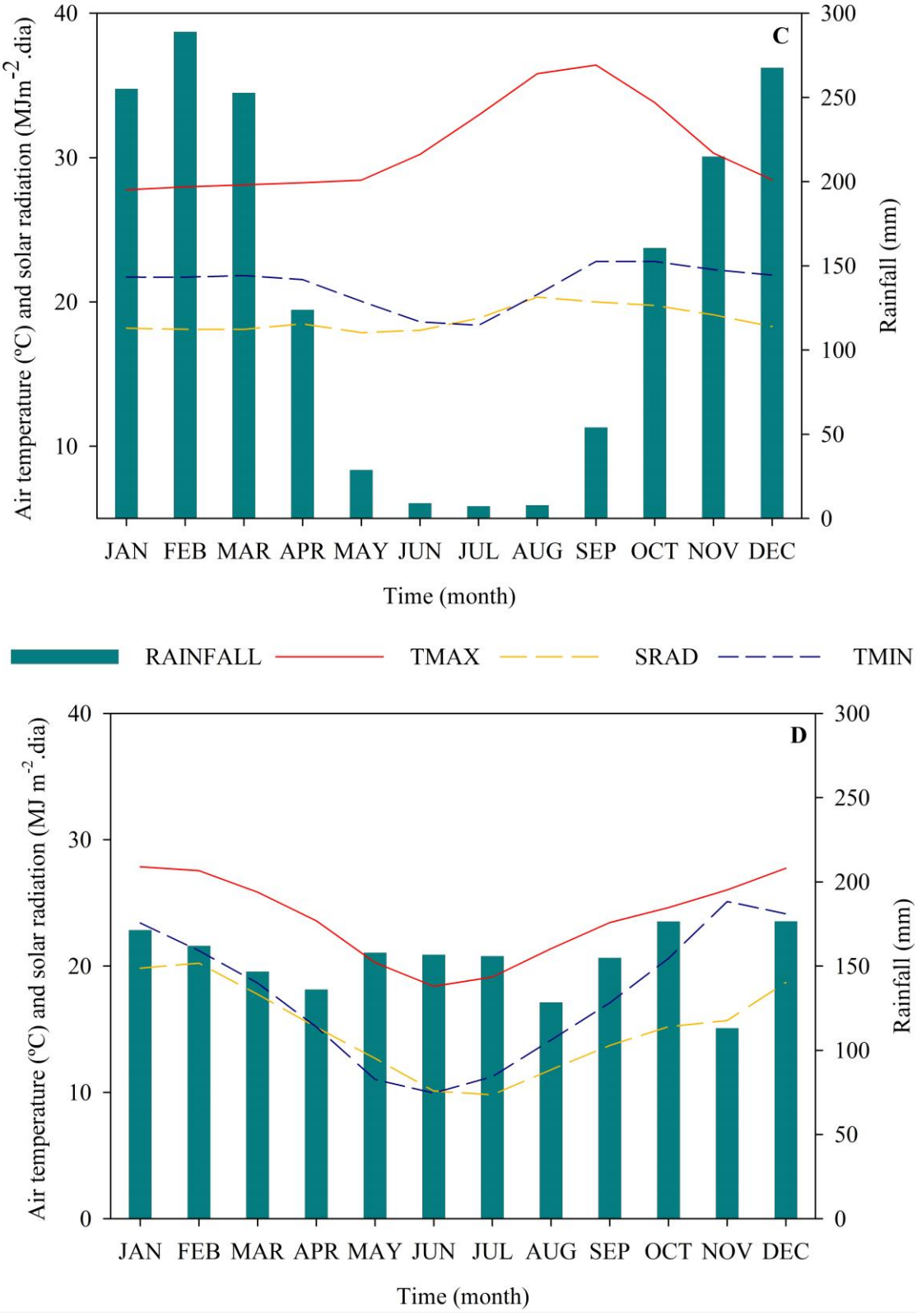

Appendix I – Weather by day after planting for Piracicaba [(A), PI-1, season 2017/2018); (B), PI-2, season 2018/2019; (C), PI-3, season 2019/2020]. SRAD, solar radiation; TMIN, mean minimum air temperature; TMAX, mean maximum air temperature; Rainfall; Irrigation.

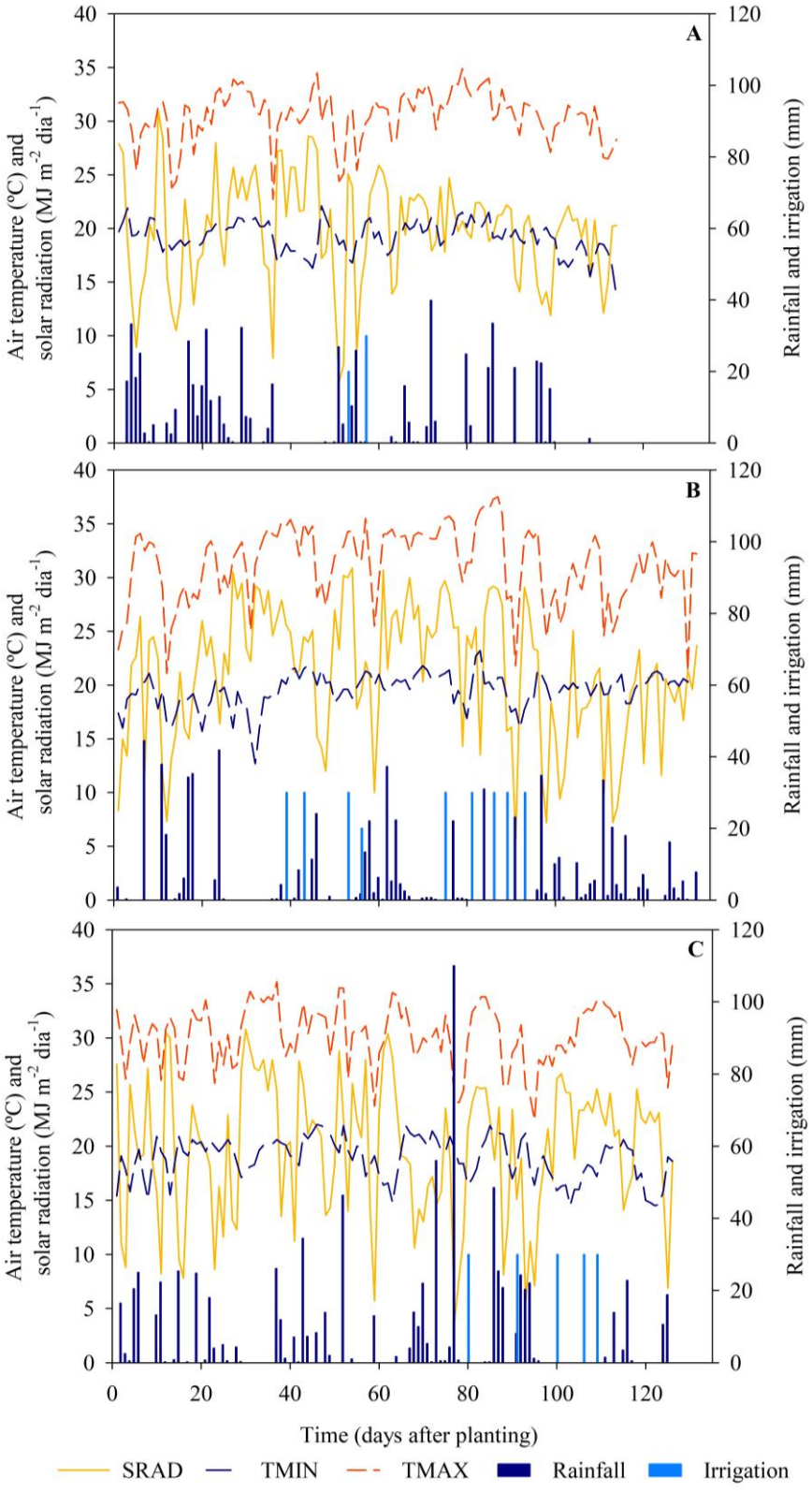

Appendix J – Weather by day after planting for Sorriso [(A), SO-1, season 2018/2019); (B), SO-2, season 2019/2020]. SRAD, solar radiation; TMIN, mean minimum air temperature; TMAX, mean maximum air temperature; Rainfall; Irrigation.

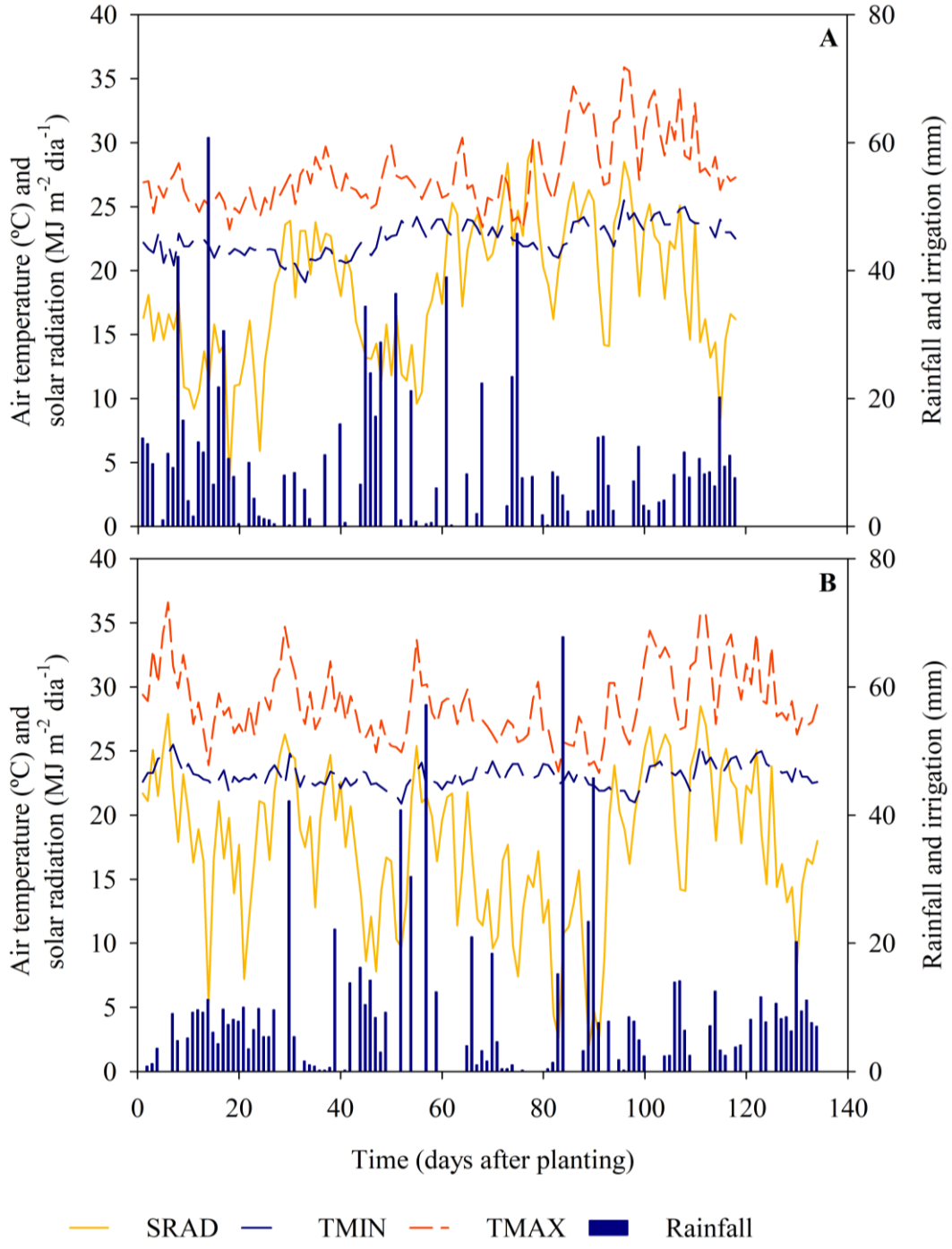

Appendix K – Weather by day after planting for Cruz Alta (CA-1, season 2018/2019). SRAD, solar radiation; TMIN, mean minimum air temperature; TMAX, mean maximum air temperature; Rainfall; Irrigation.

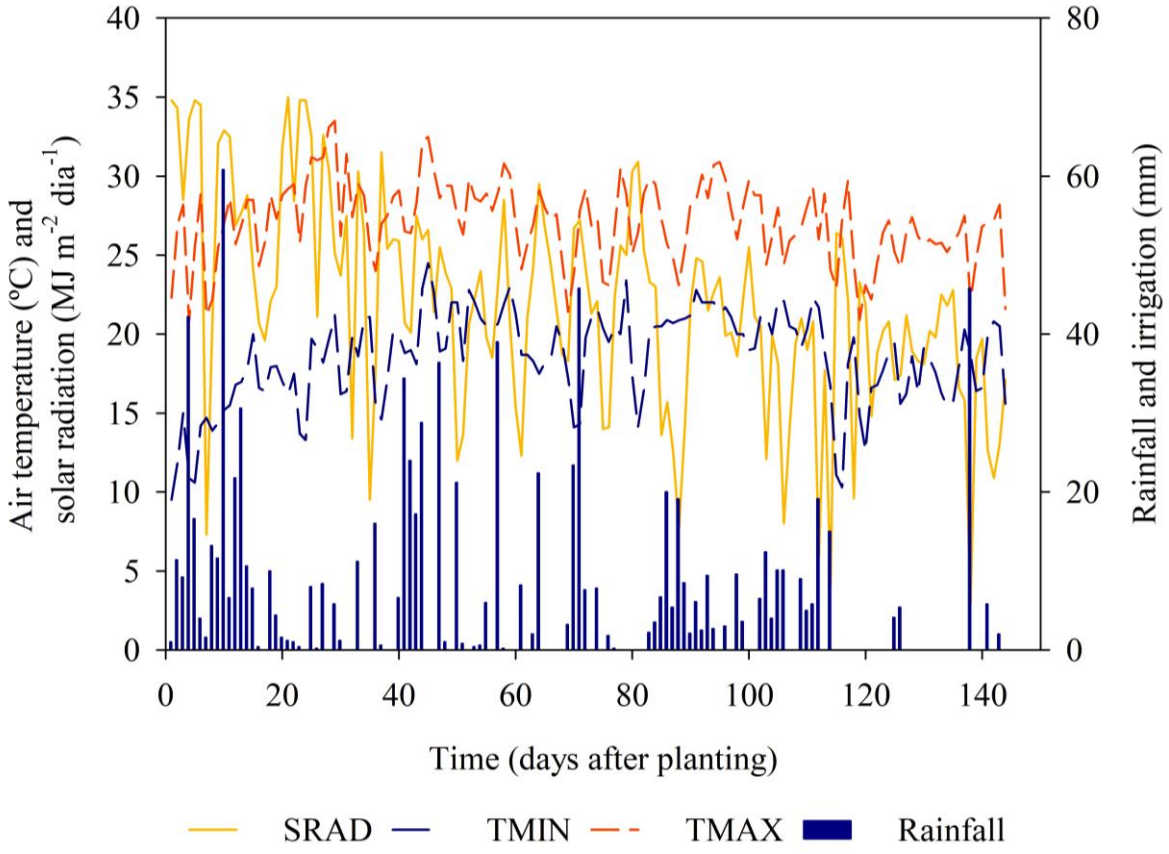

Appendix L – Weather by day after planting for Tupanciretã (TU-1, season 2019/2020). SRAD, solar radiation; TMIN, mean minimum air temperature; TMAX, mean maximum air temperature; Rainfall; Irrigation.

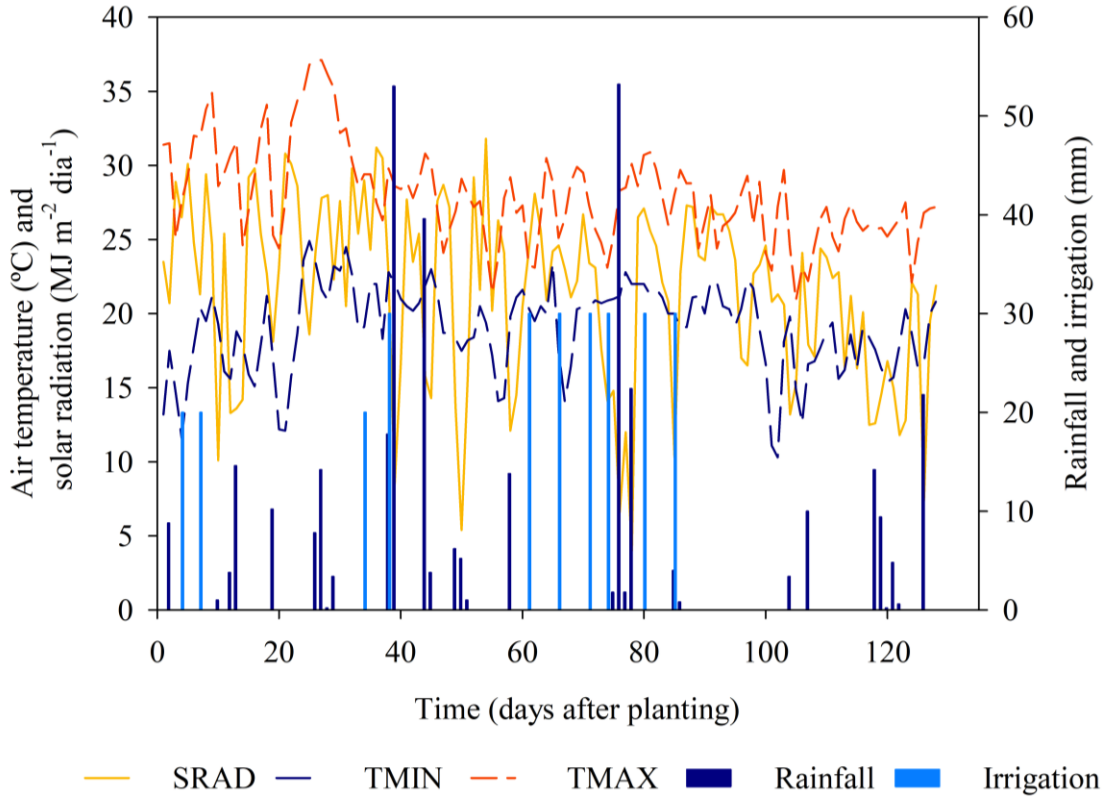

Appendix M – Measured soil N concentration for initial conditions in Piracicaba (PI-1, PI-2, PI-3), Sorriso (SO-1, SO-1), Cruz Alta (CA-1), Tupanciretã (TU-1), and Teresina (TE-1).

Experiment	Layer (m)	NH_4	NO_3
		g[N] $Mg[soil]^{-1}$	
PI-1	0.1-0.2	0.6	0.2
	0.2-0.4	0.4	0.1
	0.4-0.6	0.5	0.2
PI-2	0.1-0.2	0.5	0.2
	0.2-0.4	0.3	0.1
	0.4-0.6	0.4	0.1
PI-3	0.1-0.2	0.5	0.1
	0.2-0.4	0.4	0.1
	0.4-0.6	0.4	0.1
SO-1	0.1-0.2	2.1	1.8
	0.2-0.4	2.0	1.8
	0.4-0.6	1.8	1.8
SO-2	0.1-0.2	2.1	1.8
	0.2-0.4	2.1	1.8
	0.4-0.6	2.0	1.8
CA-1	0.1-0.2	0.6	0.2
	0.2-0.4	0.4	0.1
	0.4-0.6	0.5	0.2
TU-1	0.1-0.2	0.7	0.3
	0.2-0.4	0.4	0.1
	0.4-0.6	0.3	0.1
TE-1	0.1-0.2	0.6	0.1
	0.2-0.4	0.6	0.1
	0.4-0.6	0.5	0.1

Appendix N - Properties of the Ultisols, Entisols, Oxisols, Inceptisols soil profile from WISE Global Soil Profile Database.

Site	Depth (m)	Bulk Density (g cm^{-1})	Clay (%)	Silt (%)	Soil				
					SRGF[a]	SRGF[b]	Lower limit	Drained upper limit	Saturated upper limit
					(cm^3 cm^{-3})				
Ultisols	0.10	1.33	16	24	1.00	1.00	0.082	0.234	0.452
	0.20	1.43	23	24	0.74	0.98	0.129	0.241	0.429
	0.40	1.46	36	22	0.55	0.85	0.204	0.324	0.432
	0.75	1.45	45	16	0.32	0.70	0.213	0.336	0.434
	1.10	1.39	53	17	0.16	0.53	0.224	0.343	0.460
Entisols	0.05	1.18	26	67	1.00	1.00	0.148	0.337	0.513
	0.15	1.29	29	60	1.00	1.00	0.124	0.271	0.491
	0.40	1.36	38	53	0.58	0.85	0.223	0.348	0.470
	1.10	1.39	46	47	0.22	0.70	0.259	0.362	0.460
	1.40	1.38	59	36	0.08	0.35	0.211	0.353	0.462
	1.70	1.40	56	39	0.05	0.20	0.225	0.359	0.455
Oxisols	0.10	1.23	56	16	1.00	1.00	0.235	0.392	0.509
	0.20	1.23	56	16	0.82	0.98	0.235	0.392	0.509
	0.40	1.26	60	20	0.55	0.85	0.235	0.377	0.502
	0.60	1.27	65	17	0.37	0.78	0.236	0.388	0.500
	1.20	1.32	58	19	0.17	0.48	0.214	0.358	0.483
	1.30	1.49	35	21	0.08	0.30	0.236	0.310	0.422
Inceptisols	0.10	1.43	19	10	1.00	1.00	0.040	0.177	0.418
	0.20	1.43	19	10	0.82	0.74	0.040	0.177	0.418
	0.50	1.54	23	19	0.50	0.65	0.192	0.289	0.396
	0.70	1.55	26	16	0.30	0.60	0.215	0.299	0.390
	1.00	1.53	26	21	0.18	0.52	0.215	0.299	0.399
	1.40	1.52	27	23	0.09	0.35	0.225	0.299	0.402
	1.70	1.57	34	13	0.05	0.20	0.240	0.309	0.386

[a] Soil root growth factor original.

[a] Soil root growth factor adjusted based on curve R200 obtained by Battisti *et al*. (2017).

REFERENCE

Battisti, R., Sentelhas, P. C., 2017. Improvement of soybean resilience to drought through deep root system in Brazil. Agronomy Journal, 109(4), 1612-1622.

Appendix O – Simulated long-term scenarios (1989 to 2020) for season applied irrigation for TMG 7062 in Piracicaba (PI-1), TMG 7063 in Sorriso (SO-1), NS 7901 (SO-2) in Sorriso, 65i65RSF in Cruz Alta (CA-1), and 8579RSF in Teresina (TE-1) under rainfed and irrigated conditions. Boxplots were set at 90th (the upper whisker) and 75th (the upper quartile), outliers are shown as black dots.

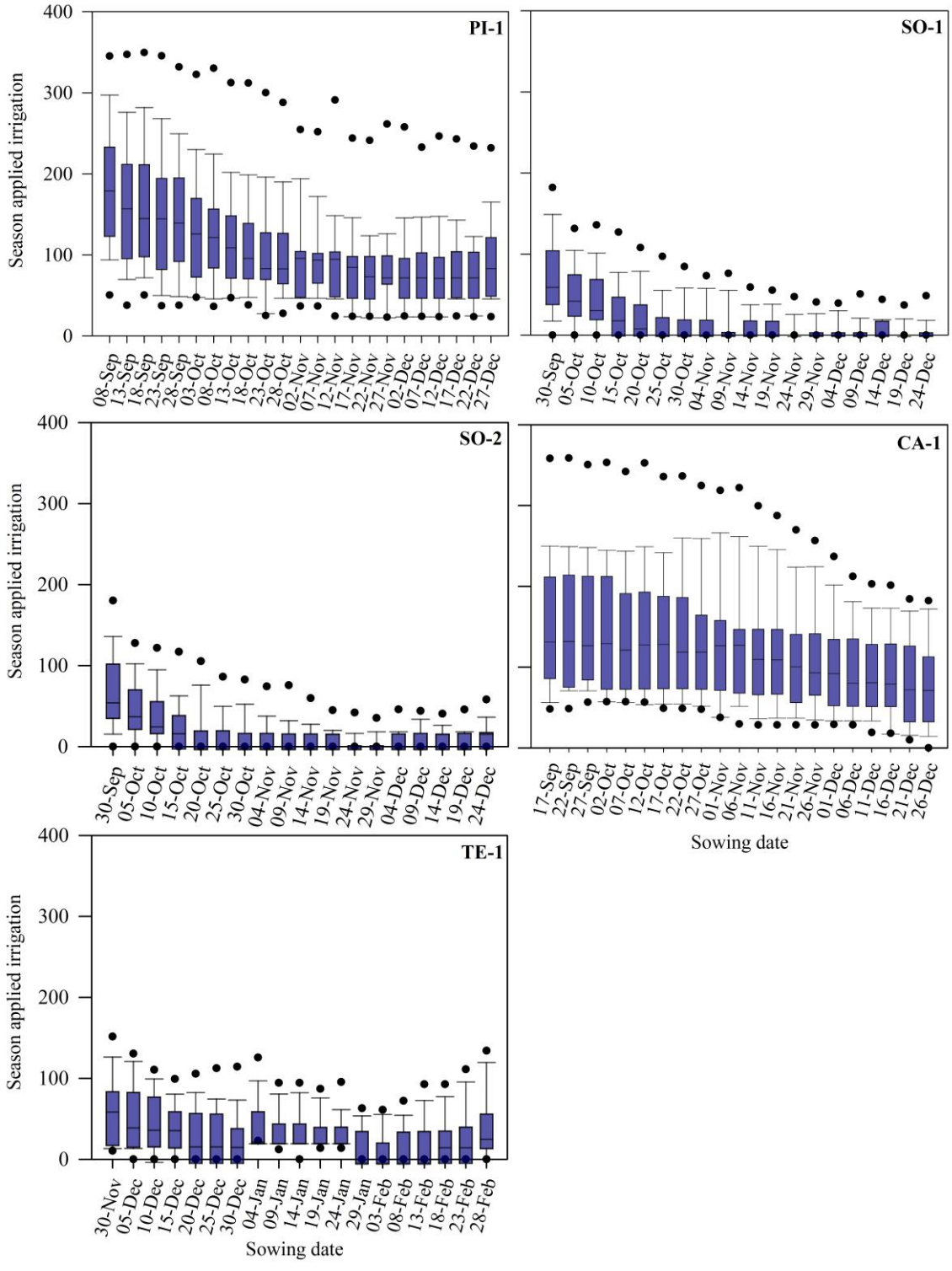

Appendix P – Simulated long-term scenarios (1989 to 2020) for soybean crop cycle for TMG 7062 in Piracicaba (PI-1), TMG 7063 in Sorriso (SO-1), NS 7901 (SO-2) in Sorriso, 65i65RSF in Cruz Alta (CA-1), and 8579RSF in Teresina (TE-1) under rainfed and irrigated conditions. Boxplots were set at 90th (the upper whisker) and 75th (the upper quartile), outliers are shown as black dots.

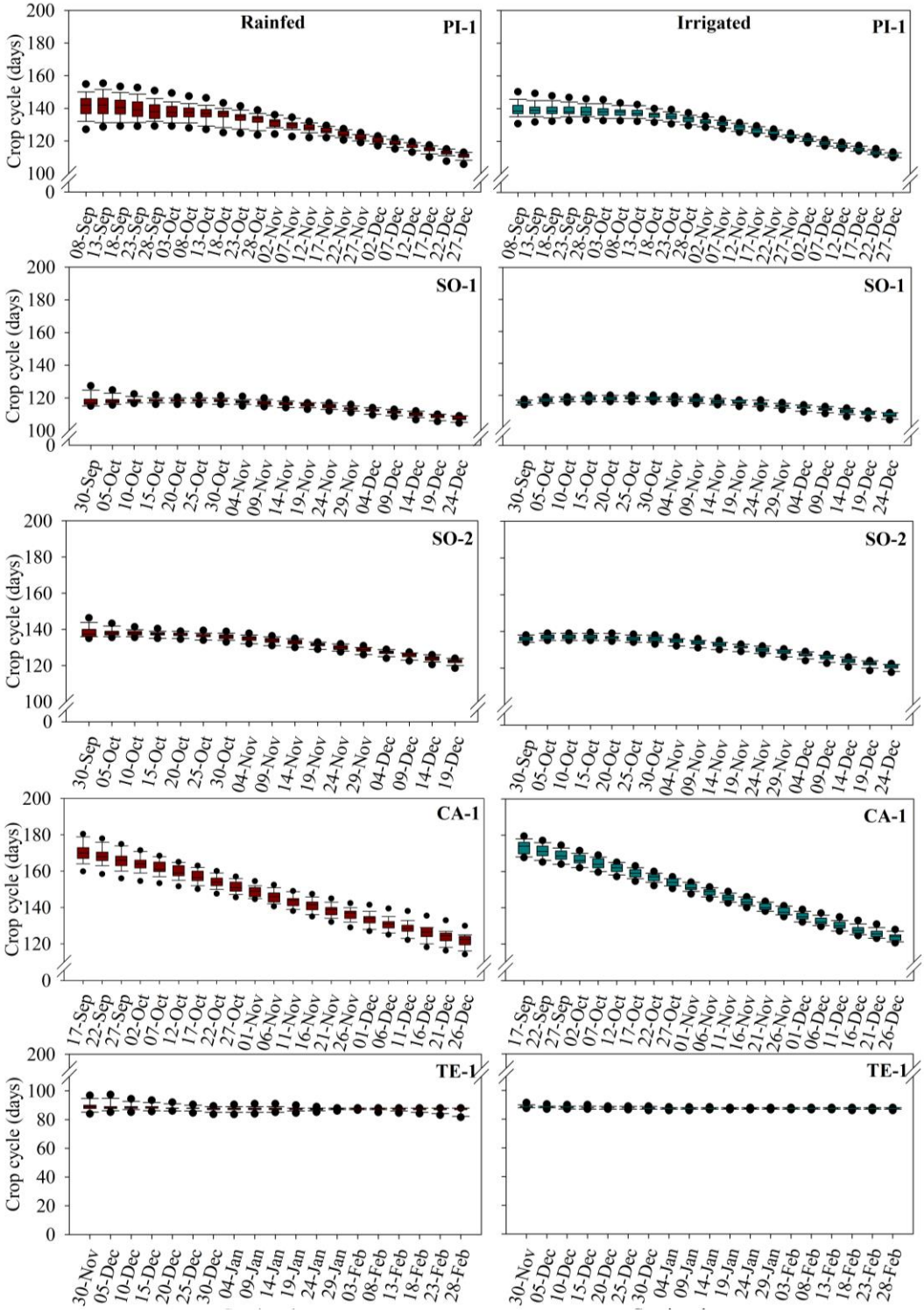

Appendix Q – Simulated long-term scenarios (1989 to 2020) for crop yield for TMG 7062 in Piracicaba (PI-1) under rainfed and irrigated conditions with N-fertilizer doses of 0, 300, and 600 kg ha^{-1}.

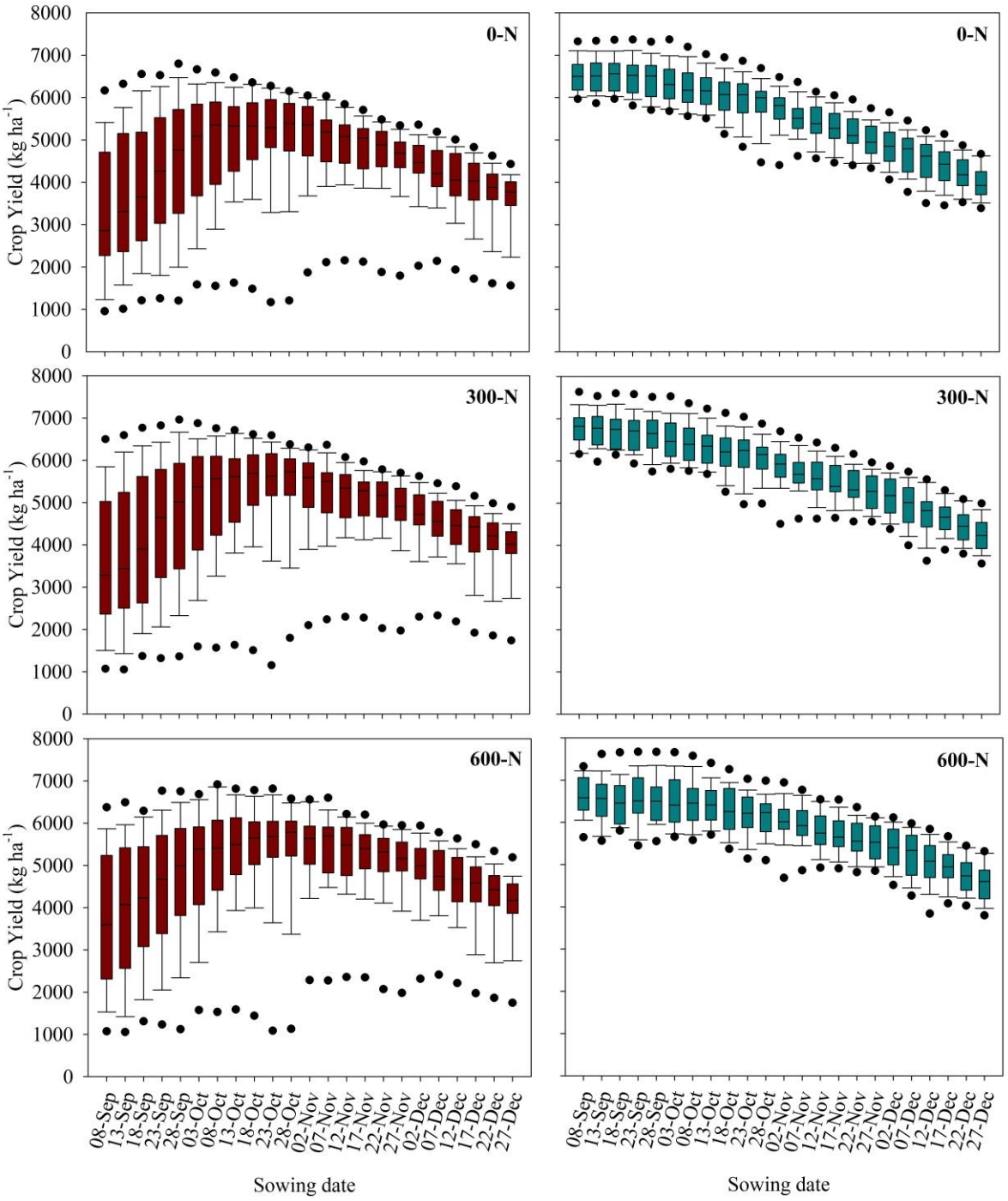

Appendix R – Simulated long-term scenarios (1989 to 2020) for crop yield for TMG 7063 in Sorriso (SO-1) under rainfed and irrigated conditions with N-fertilizer doses of 0, 300, and 600 kg ha^{-1}.

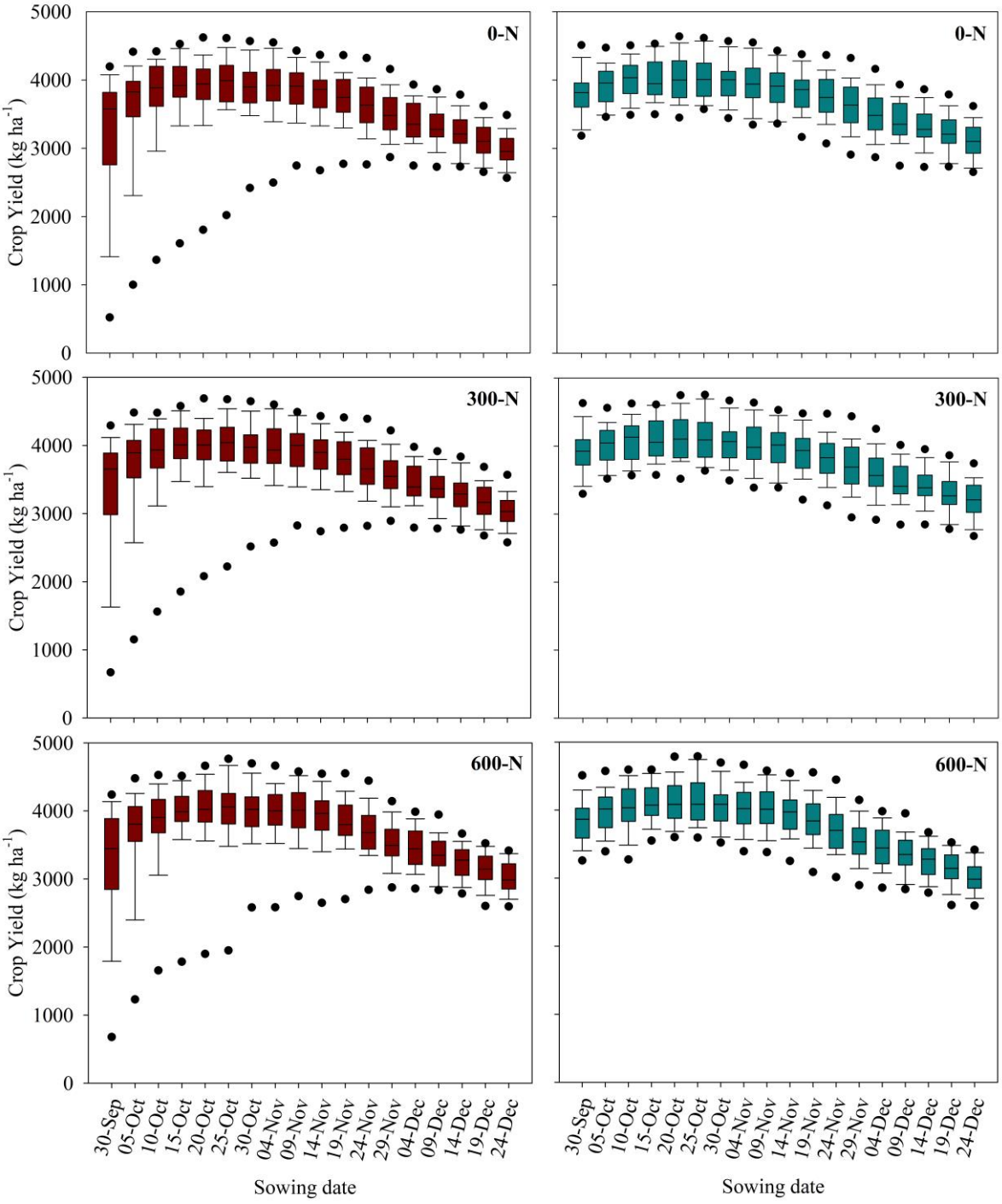

Appendix S – Simulated long-term scenarios (1989 to 2020) for crop yield for NS 7901 in Sorriso (SO-2) under rainfed and irrigated conditions with N-fertilizer doses of 0, 300, and 600 kg ha^{-1}.

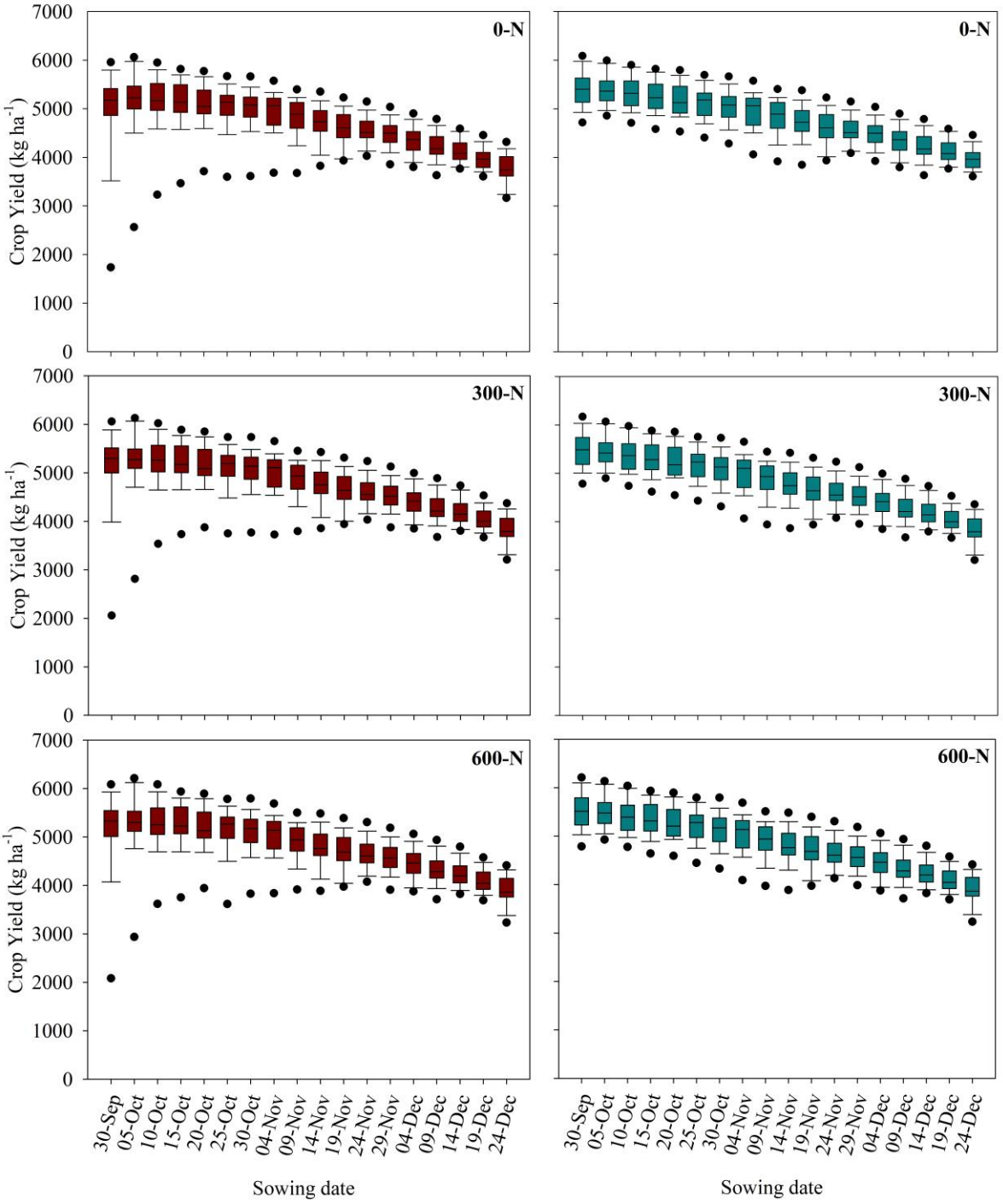

Appendix T – Simulated long-term scenarios (1989 to 2020) for crop yield for 65i65RSF in Cruz Alta (CA-1) under rainfed and irrigated conditions with N-fertilizer doses of 0, 300, and 600 kg ha^{-1}.

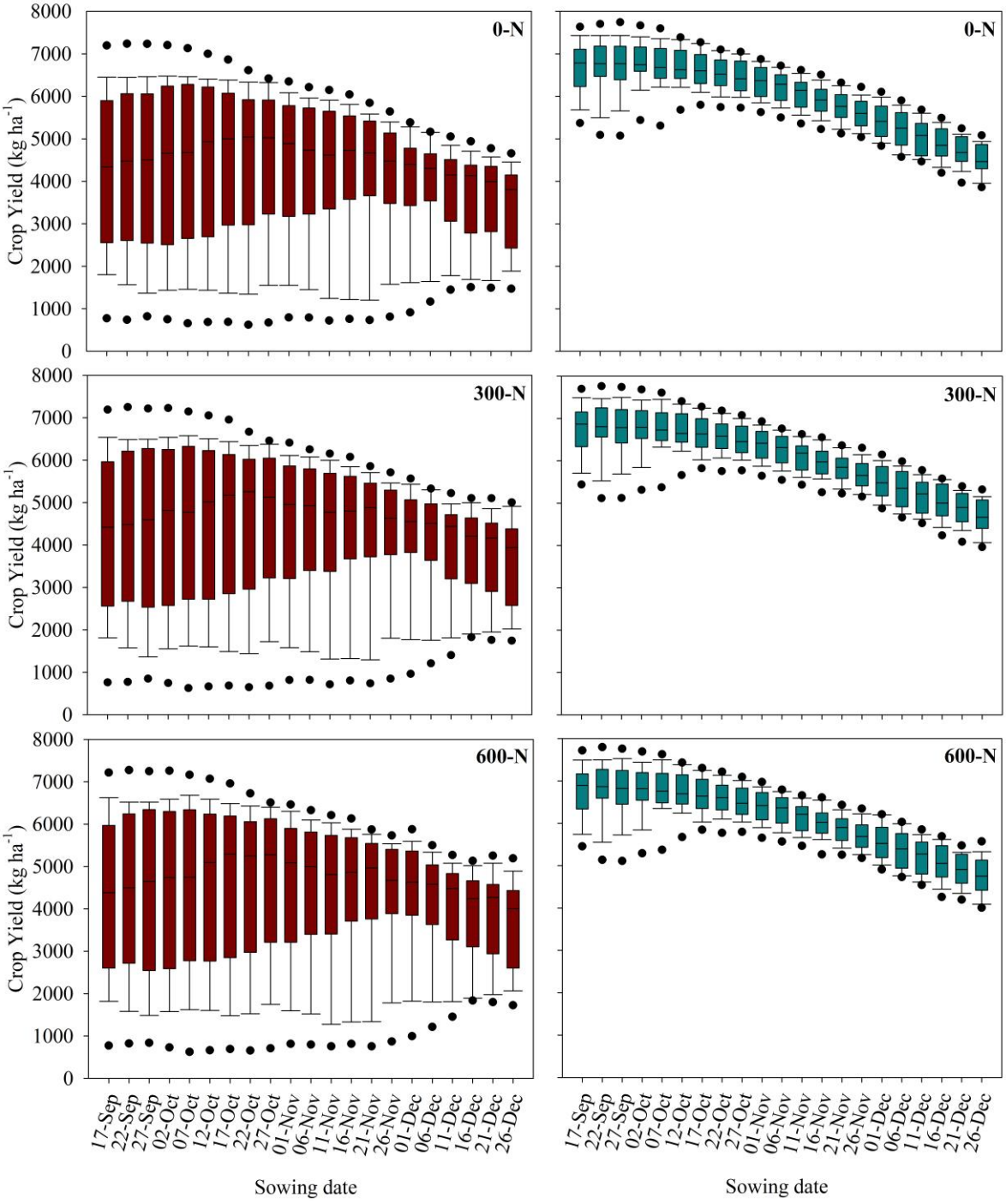

Appendix U – Simulated long-term scenarios (1989 to 2020) for crop yield for 8579RSF in Teresina (TE-1) under rainfed and irrigated conditions with N-fertilizer doses of 0, 300, and 600 kg ha^{-1}.

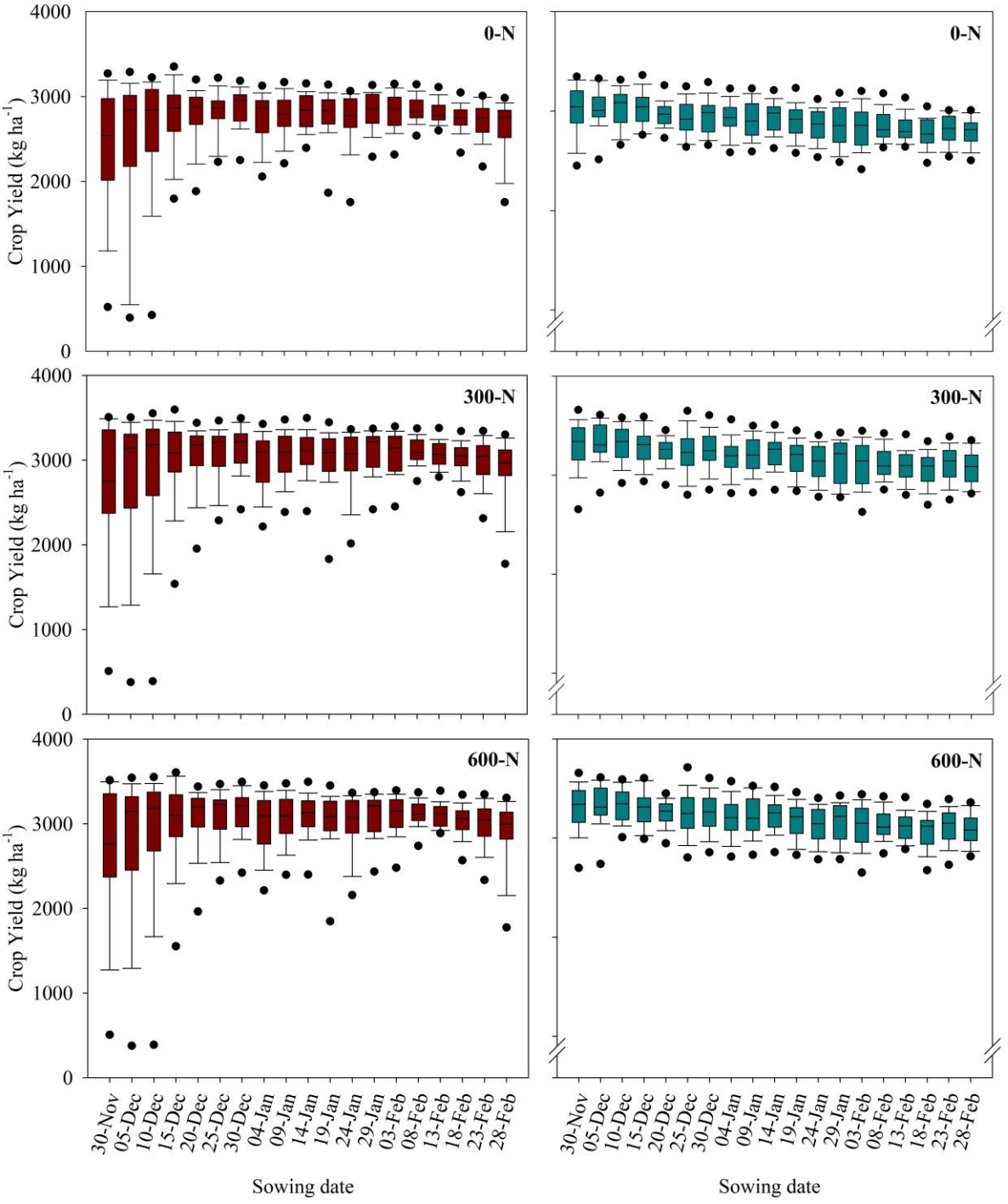

Appendix V - Climatology by month from 1989 to 2020 for Cascavel (6801), Dom Pedrito (6901), Unaí (7501), Cristalina (7601), Jatai (7701), Primavera do Leste (7801), São Borja (7802), Palmeira do Leste (7801), São Borja (7802), Palmeira das Missões (7901), Formosa do Rio Preto (8401), Barreiras (8501), Canarana (8601), Sorriso (8701), Nova Mutum (8801), Bom Jesus (9301), Balsas (9501), Lagoa da Confusão (9701). Rainfall; TMAX, mean maximum air temperature; TMIN, mean minimum air temperature; SRAD, solar radiation.

(continued)

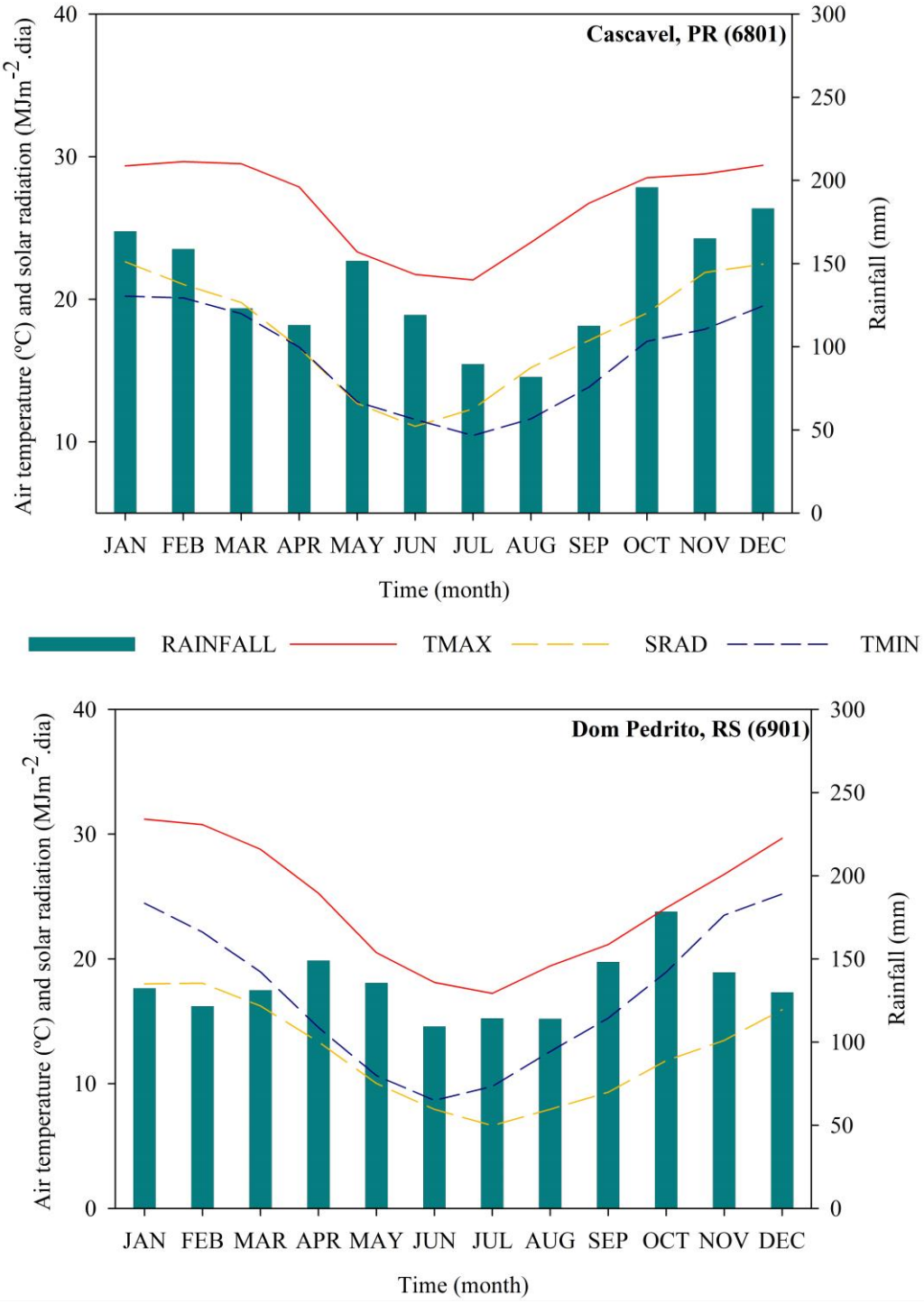

Appendix V - Climatology by month from 1989 to 2020 for Cascavel (6801), Dom Pedrito (6901), Unaí (7501), Cristalina (7601), Jatai (7701), Primavera do Leste (7801), São Borja (7802), Palmeira do Leste (7801), São Borja (7802), Palmeira das Missões (7901), Formosa do Rio Preto (8401), Barreiras (8501), Canarana (8601), Sorriso (8701), Nova Mutum (8801), Bom Jesus (9301), Balsas (9501), Lagoa da Confusão (9701). Rainfall; TMAX, mean maximum air temperature; TMIN, mean minimum air temperature; SRAD, solar radiation.

(continuation)

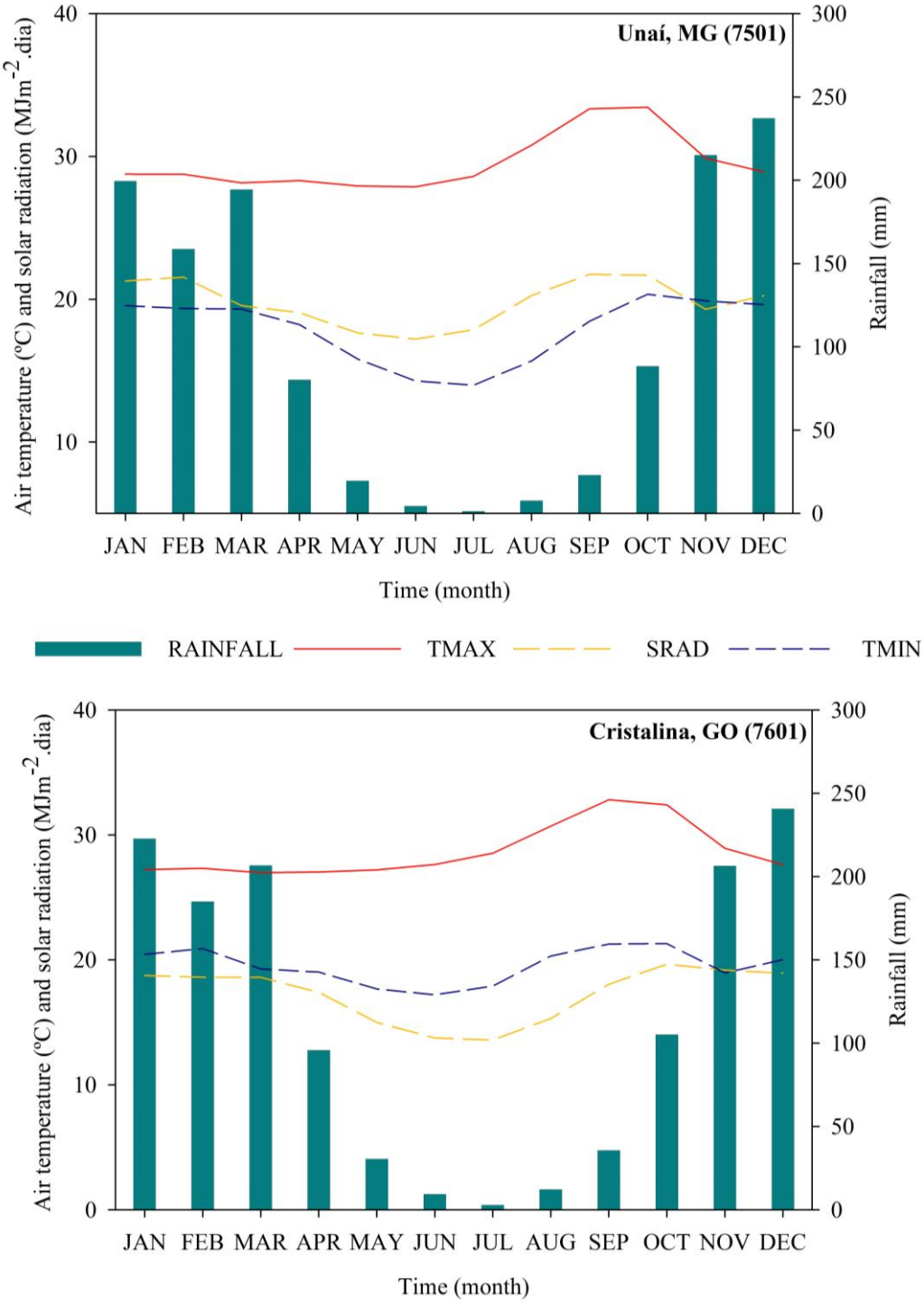

Appendix V - Climatology by month from 1989 to 2020 for Cascavel (6801), Dom Pedrito (6901), Unaí (7501), Cristalina (7601), Jatai (7701), Primavera do Leste (7801), São Borja (7802), Palmeira do Leste (7801), São Borja (7802), Palmeira das Missões (7901), Formosa do Rio Preto (8401), Barreiras (8501), Canarana (8601), Sorriso (8701), Nova Mutum (8801), Bom Jesus (9301), Balsas (9501), Lagoa da Confusão (9701). Rainfall; TMAX, mean maximum air temperature; TMIN, mean minimum air temperature; SRAD, solar radiation.

(continuation)

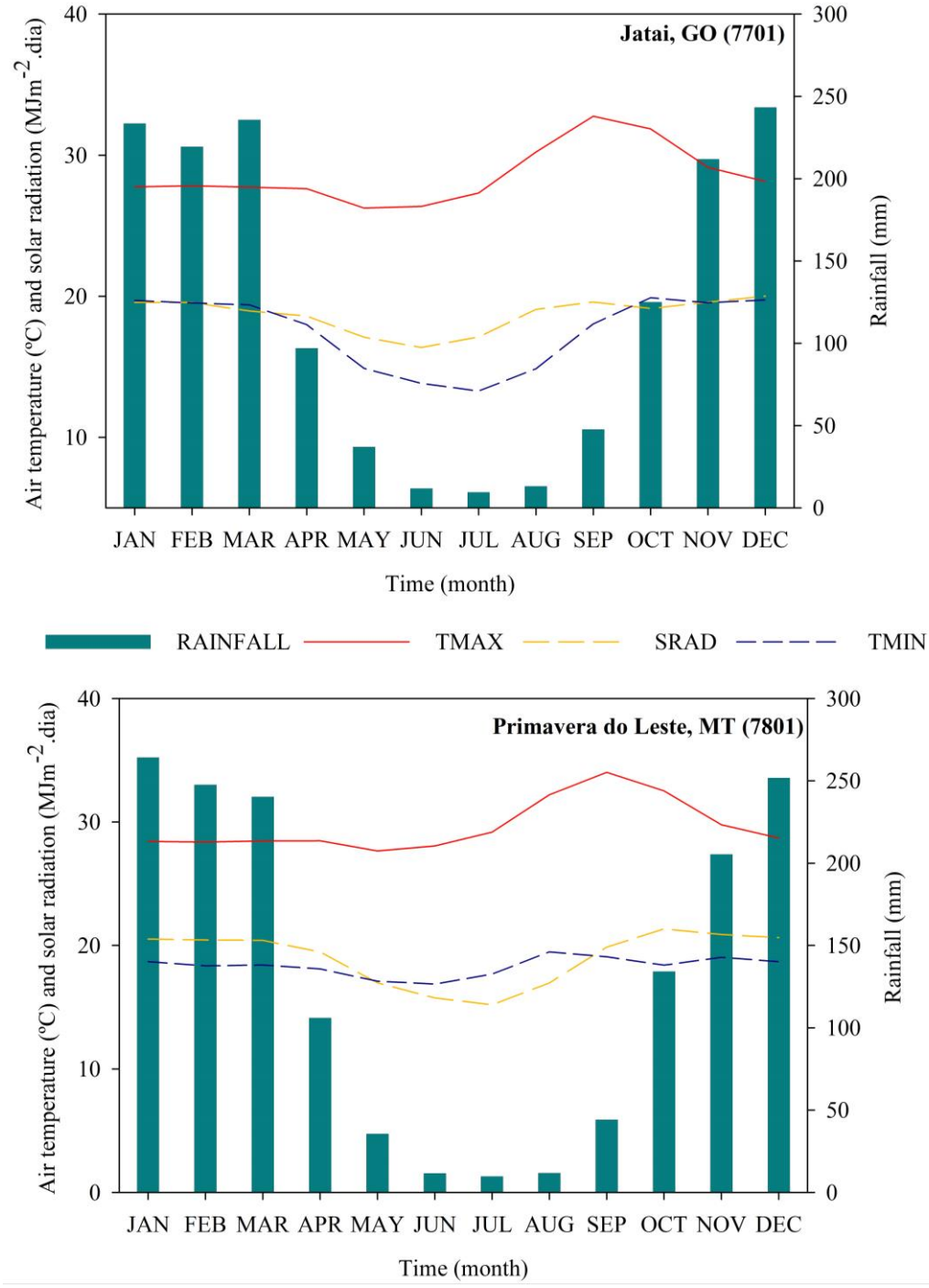

Appendix V - Climatology by month from 1989 to 2020 for Cascavel (6801), Dom Pedrito (6901), Unaí (7501), Cristalina (7601), Jatai (7701), Primavera do Leste (7801), São Borja (7802), Palmeira do Leste (7801), São Borja (7802), Palmeira das Missões (7901), Formosa do Rio Preto (8401), Barreiras (8501), Canarana (8601), Sorriso (8701), Nova Mutum (8801), Bom Jesus (9301), Balsas (9501), Lagoa da Confusão (9701). Rainfall; TMAX, mean maximum air temperature; TMIN, mean minimum air temperature; SRAD, solar radiation.

(continuation)

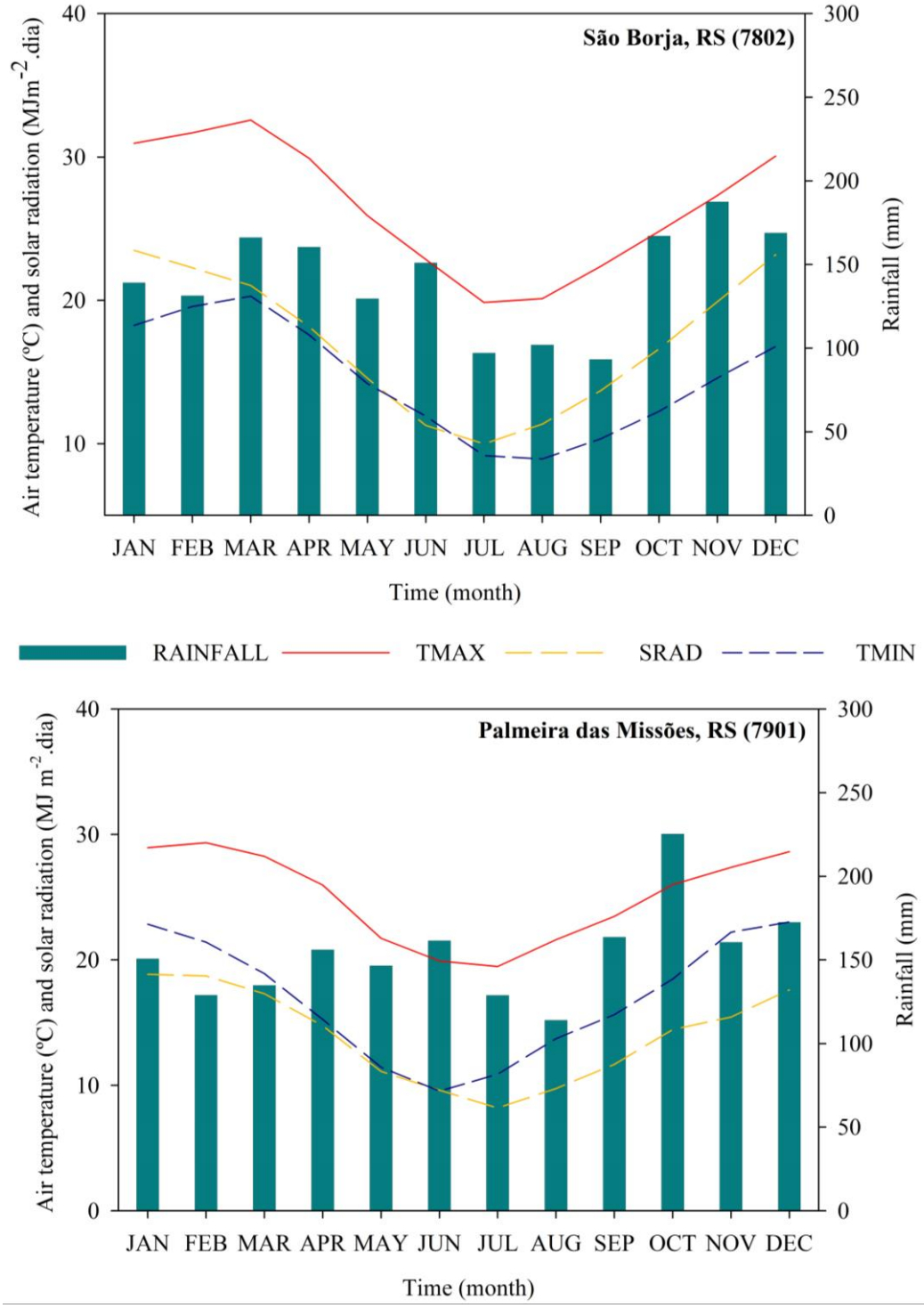

Appendix V - Climatology by month from 1989 to 2020 for Cascavel (6801), Dom Pedrito (6901), Unaí (7501), Cristalina (7601), Jatai (7701), Primavera do Leste (7801), São Borja (7802), Palmeira do Leste (7801), São Borja (7802), Palmeira das Missões (7901), Formosa do Rio Preto (8401), Barreiras (8501), Canarana (8601), Sorriso (8701), Nova Mutum (8801), Bom Jesus (9301), Balsas (9501), Lagoa da Confusão (9701). Rainfall; TMAX, mean maximum air temperature; TMIN, mean minimum air temperature; SRAD, solar radiation.

(continuation)

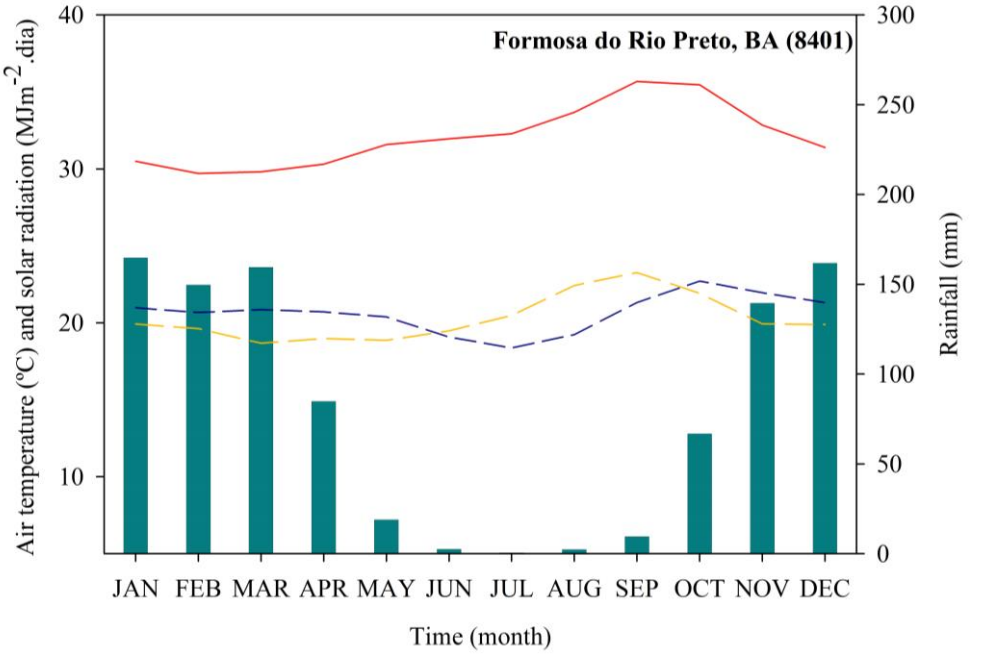

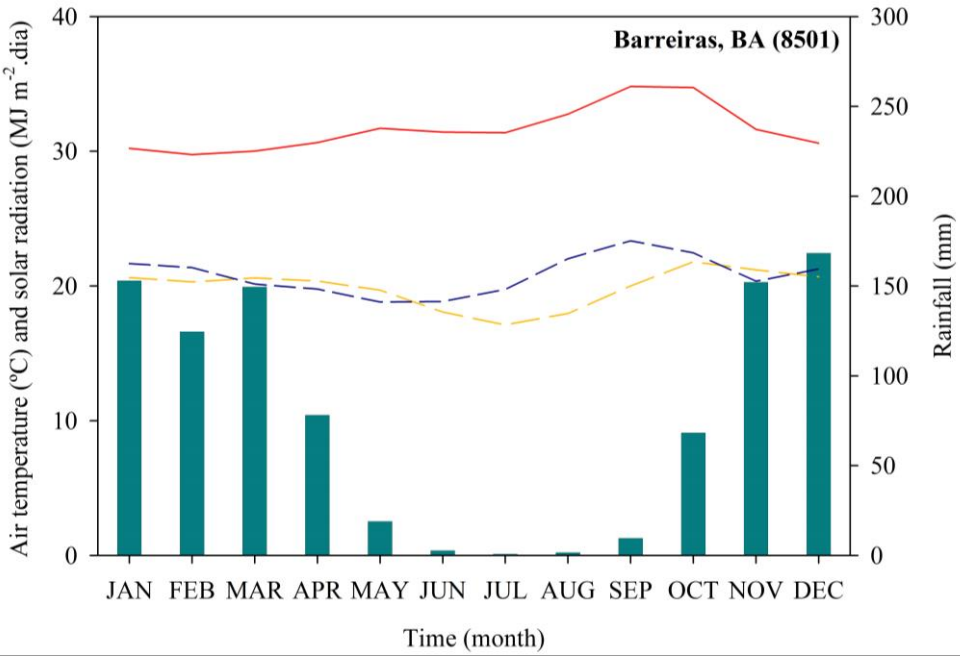

Appendix V - Climatology by month from 1989 to 2020 for Cascavel (6801), Dom Pedrito (6901), Unaí (7501), Cristalina (7601), Jatai (7701), Primavera do Leste (7801), São Borja (7802), Palmeira do Leste (7801), São Borja (7802), Palmeira das Missões (7901), Formosa do Rio Preto (8401), Barreiras (8501), Canarana (8601), Sorriso (8701), Nova Mutum (8801), Bom Jesus (9301), Balsas (9501), Lagoa da Confusão (9701). Rainfall; TMAX, mean maximum air temperature; TMIN, mean minimum air temperature; SRAD, solar radiation.

(continuation)

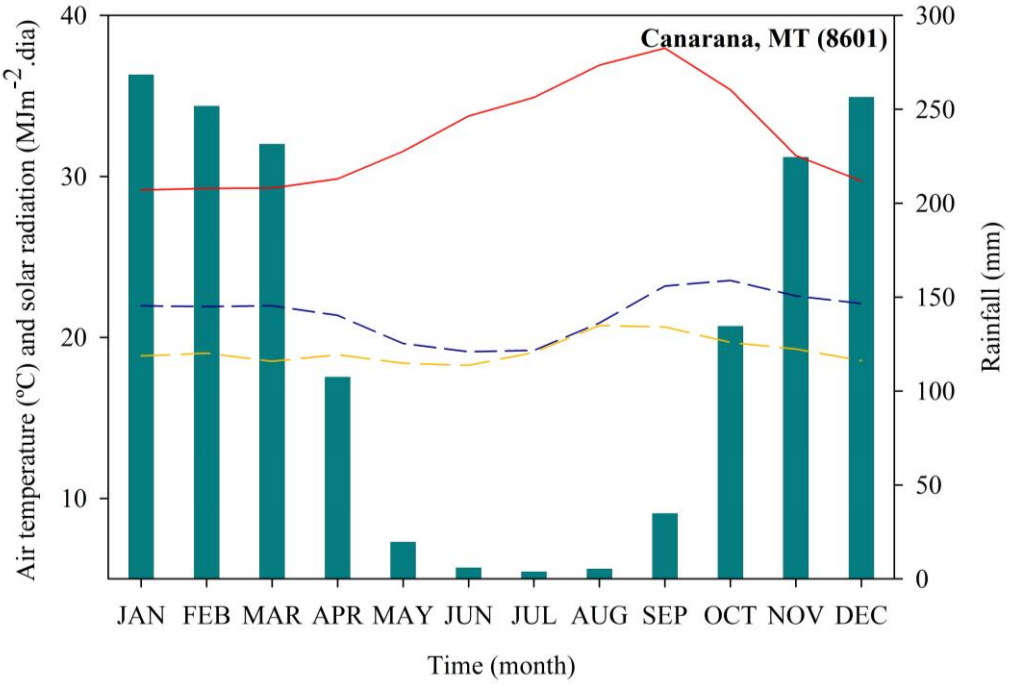

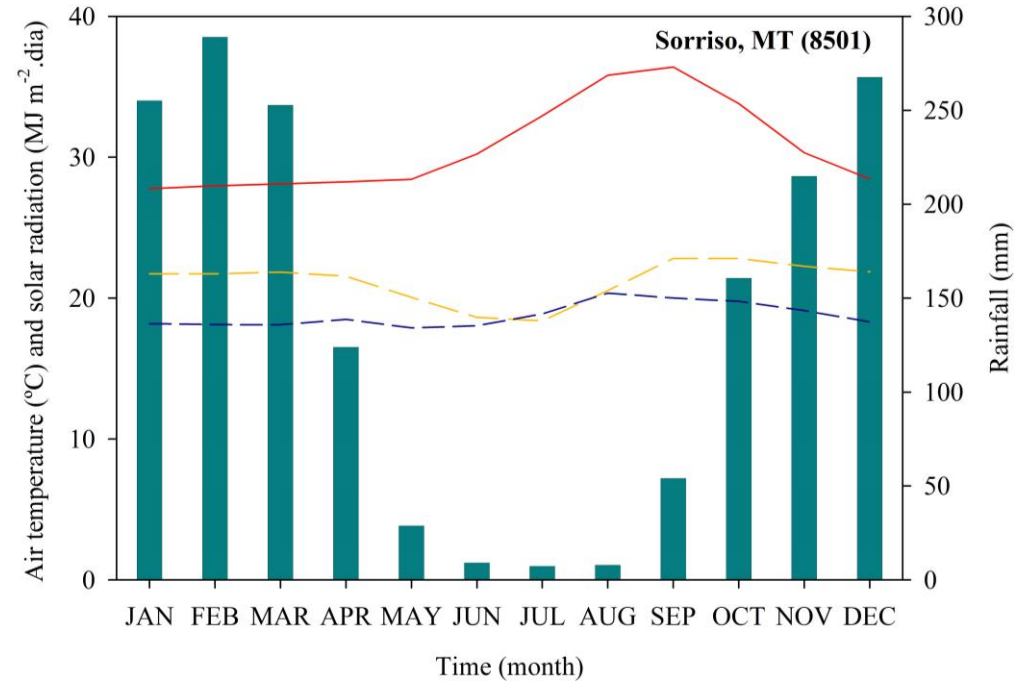

Appendix V - Climatology by month from 1989 to 2020 for Cascavel (6801), Dom Pedrito (6901), Unaí (7501), Cristalina (7601), Jatai (7701), Primavera do Leste (7801), São Borja (7802), Palmeira do Leste (7801), São Borja (7802), Palmeira das Missões (7901), Formosa do Rio Preto (8401), Barreiras (8501), Canarana (8601), Sorriso (8701), Nova Mutum (8801), Bom Jesus (9301), Balsas (9501), Lagoa da Confusão (9701). Rainfall; TMAX, mean maximum air temperature; TMIN, mean minimum air temperature; SRAD, solar radiation.

(continuation)

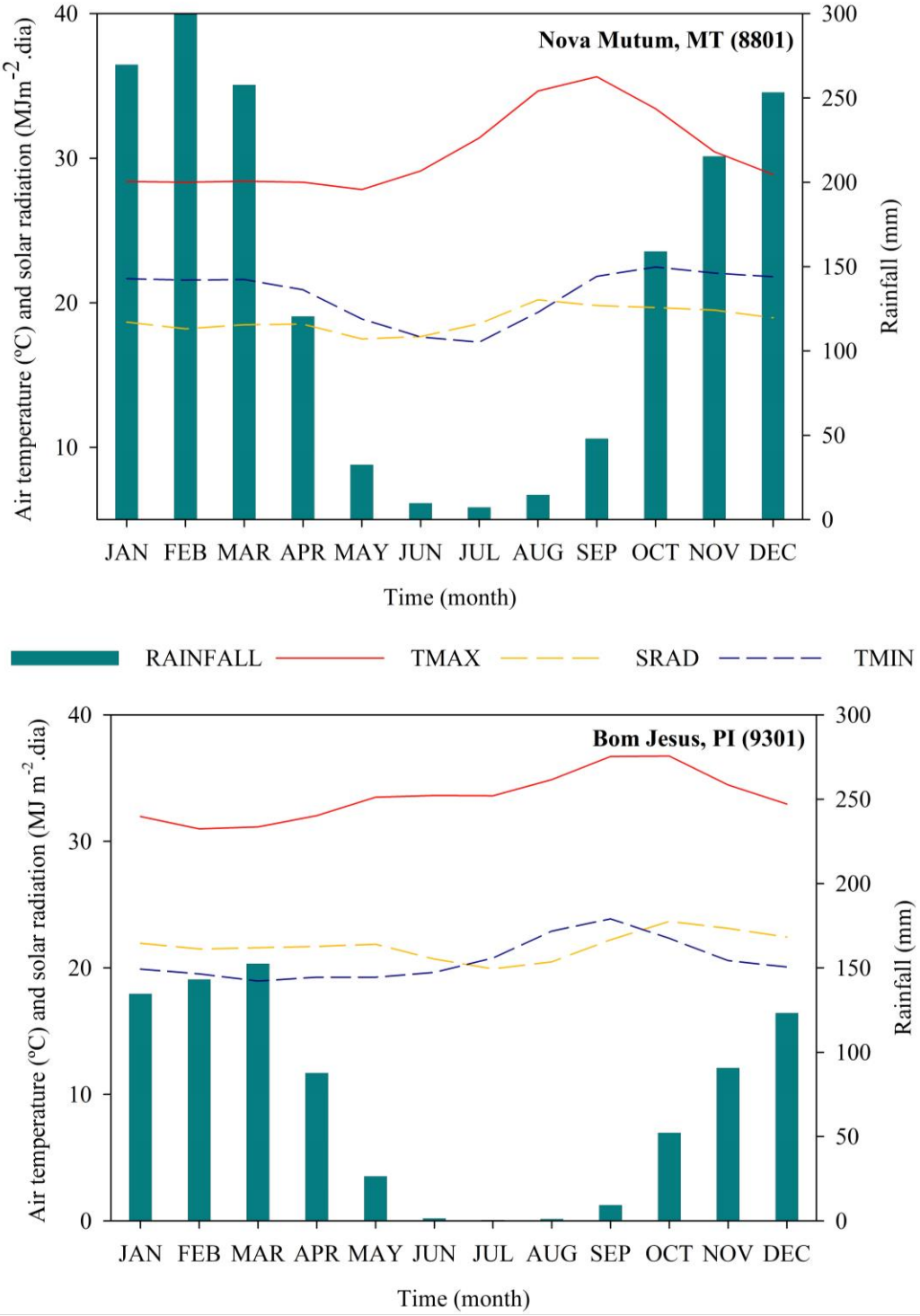

Appendix V - Climatology by month from 1989 to 2020 for Cascavel (6801), Dom Pedrito (6901), Unaí (7501), Cristalina (7601), Jatai (7701), Primavera do Leste (7801), São Borja (7802), Palmeira do Leste (7801), São Borja (7802), Palmeira das Missões (7901), Formosa do Rio Preto (8401), Barreiras (8501), Canarana (8601), Sorriso (8701), Nova Mutum (8801), Bom Jesus (9301), Balsas (9501), Lagoa da Confusão (9701). Rainfall; TMAX, mean maximum air temperature; TMIN, mean minimum air temperature; SRAD, solar radiation.

(conclusion)